J. Bangladesh Acad. Sci. Volume 46, Issue 1, June 2022

ISSN 2224-7270 (Online), 0378-8121 (Print)

Journal of Bangladesh Academy of Sciences is published twice a year (June and December comprising one volume) in English. Original research articles, review articles, and short communications of all branches of Science and Technology are considered for publication in this journal. Review articles are generally by invitation.

Disclaimer
The opinions, analysis and conclusions expressed or implied in this journal are those of the authors and do not represent the views of Bangladesh Academy of Sciences.

Submission
All correspondence regarding contributions for publication in the journal should be addressed to the *Editor, Journal of Bangladesh Academy of Sciences* <office@bas.org.bd>. Authors should consult the contributor's guideline at the back of the journal before submitting their manuscripts.

Published by
Bangladesh Academy of Sciences, National Museum of Science and Technology Agargaon, Dhaka-1207.

Design and Printed by
Sucharu Desktop Publishing, 1/E/1, Paribagh, Dhaka-1000, Bangladesh

Annual Subscription: Tk. 500.00 (Bangladesh); US $ 60.00; £ 21.50 plus postage.
Single Copy: Tk. 250.00 (Bangladesh); US $ 30.00; £ 11.25 plus postage.

COUNCIL OF
THE BANGLADESH ACADEMY OF SCIENCES
(July 2019 - June 2022)

Emeritus Prof. Dr. AK Azad Chowdhury	-	President
Prof. Dr. Zahurul Karim	-	Vice-President
Prof. Dr. Choudhury Mahmood Hasan	-	Vice-President
Prof. Dr. Z N Tahmida Begum	-	Treasurer
Prof. Dr. Haseena Khan	-	Secretary
Prof. Dr. Yearul Kabir	-	Associate Secretary
Prof. Dr. Mesbahuddin Ahmed	-	Immediate Past Secretary (Ex-officio)
Dr. M. Idris Ali	-	Member
Prof. Dr. Md. Anwar Hossain	-	Member
Prof. Dr. Liaquat Ali	-	Member
Maj Gen. Prof. Dr. ASM Matiur Rahman (Retd)	-	Member
Prof. Dr. Zia Uddin Ahmed	-	Member
Dr. Firdausi Qadri	-	Member

JOURNAL OF
BANGLADESH ACADEMY OF SCIENCES

EDITORIAL BOARD

Obituary

Prof. Hironmoy Sen Gupta
(1934-2022)

Prof. Hironmoy Sen Gupta, an illustrious son of the soil and a reputed nuclear physicist of the world is no more. He breathed his last on 07 January 2022 at the age of 88. He did his M.Sc. in Physics from Dhaka University in 1954 and Ph.D. in Nuclear Physics from University of London, England. His Ph.D. Thesis was supervised by Nobel Laureate Professor J. Rotblat.

I was one of his earliest and most favorite students in the University of Dhaka. I feel greatly obliged to write a few lines about this great scholar. When I joined the Dhaka University as a 1st year Honours student in the department of Physics in 1956, I had him as a teacher. He taught us geometrical optics. One of the books that he used on this subject was titled Geometrical Optics by Flint. Dhaka University had only one copy of this book and it was with him. However, although we did not have direct access to the book in the beginning, it posed no problem to us. He explained things very slowly and clearly. In the class, he used to address us, his students as "Apni" and not "Tumi". This caused a little embracement to us as we were used to hearing "Tumi" from our teachers from the very school days. He held class examinations to find out whether what he taught registered in our minds or went over our heads. I remember that in the very first class examination in 1956, he gave me 92 marks out of 100. There was a brilliant female student named Saqeba Khan (the only female student of the class). She got around 80 marks. She rushed to Hironmoy Sir and wanted to find why she got lower marks than I did. Hironmoy Sir asked for the presentation of both the answers scripts of Saqeba and myself. He asked Saqeba to find out for herself what was missing in her script. Saqeba understood the marking and smiled. I must say Professor Hironmoy Sen Gupta was one of the very successful teachers that the Physics Dept. of Dhaka University ever had. He also taught us the Gravitation forces between objects. The Book he was following was of Byerley. Again although we had problems in finding the book we faced no difficulty: he was explaining things very clearly. In 1959, when I appeared in the Honours practical exam I was a little upset because although all my measurements were completed and I wrote down the formula to be used in the answer scripts, I could not complete the calculation of the final result because of the lack of time. I was not sure if the results of the calculations would turn up to be right. After a day or two of this practical examination, Hironmoy Sir said to me "Don't get upset at all. I put all of your experiment numbers in the formula and the result was very good". On hearing this, I breathed a sigh of relief.

A few days after the Honours examination, we had to give a farewell to Hironmoy Sir on the eve of his departure for England for his Ph.D studies. Incidentally, only two years later in 1961 I proceeded to Manchester University for Ph.D. studies in theoretical Nuclear Physics. While in England we met a couple of times. Fortunately, at that point in time he did address me as "Tumi" instead of "Apni". I was very glad at this

change of address. On our return home, Dr. Sen Gupta resumed teaching at the Dhaka University and I started working in the Atomic Energy Center in Dhaka. Dr. Sen Gupta was associated with the research projects at the Van de graaff Accelerator of the Atomic Energy Center, Dhaka for a long time since it was set up in 1965. When I become Director of the Atomic Energy Center, Dhaka in 1970, it was a great pleasure for me to have him as a research colleague. An interesting fact to be mentioned here is that there was a very good research interaction between the Atomic Energy Center in Dhaka and the Physics Department of the Dhaka University. I cannot help mentioning a memorable fact of my life wherein Professor Hironmoy Sen Gupta played an important part. In 1973, a special committee was constituted by the Syndicate of the Dhaka University consisting of the members Dr. Qudrat-e-Khuda, Prof. M Innas Ali, Prof. Kabir Chowdhury, Prof. Abu Hena Mostafa Kamal and Prof. Hironmoy Sen Gupta along with Prof. Motin Chowdhury as the Chair. On the basis of the recommendation of the committee, the University of Dhaka in its Syndicate resolution recognized me (in view of my career and original contribution to Nuclear Physics) as Honorary Professor of Physics of the University of Dhaka. This lifelong recognition has been a matter of great honor for me. This had been a rare and unique event in the University of Dhaka. Prof. H Sen Gupta had been associated with this event and I remember this with great joy and delight.

Prof. Sen Gupta has interacted with many scholars at home and abroad. People with whom he worked remembered him for his talent and good disposition. His supervisor Professor J. Rotblat who was associated with the Pagwash Movement for science and world affairs and was awarded Nobel Prize, often asked me at Pagwash Conferences on Science and World Affairs about Prof. Sen Gupta's health and work. Prof. Sen Gupta built a strong collaboration with the researchers at the Atomic Energy Center, Dhaka and also with other universities of which the Physics Dept. of Rajshahi University deserves a special mention. Prof. Arun Kumar Basak, one of the most pioneering nuclear researcher of Bangladesh had a good collaboration with Prof. Sen Gupta as a valuable member of his team. Incidentally, my interaction with Prof. Arun Kumar Basak has also been very intense. When I propounded my Folding Model Theory of the Nuclear Reactions to Professor Basak, he kindly tried the same in a number of reactions between nuclei involving alpha clusters. The results were pretty satisfactory in many cases and a matter of delight was that Professor H Sen Gupta along with Prof. Fazlay Bari Malik were participants of the research team which Arun Kumar Basak had organized. Like me, Arun also had great respect for Prof. Sen Gupta who will be missed by us for all times to come.

Prof. Sen Gupta was associated with the Bangladesh Academy of Sciences as a Senior Fellow, almost from the very beginning. We invited him to chair the selection committees for awards of gold medals both in the senior and junior groups. He participated in these meetings almost till the very end of his life. Interestingly enough, his home work for selection almost coincided with that of me and other members of the committee.

Prof. H Sen Gupta married rather late. He has left behind two sons and his wife Suchorita Sen Gupta who was till recently been the Assistant Attorney General at Dhaka High Court. The Bangladesh Academy of Sciences has always held Prof. H Sen Gupta in high esteem for his research contributions and for his wonderful disposition as a fine gentleman. Prof. H Sen Gupta was highly religious in his personal life.

We pray to the Almighty for the salvation of his soul and for a sound and peaceful living of his family members.

- M. Shamsher Ali

J. Bangladesh Acad. Sci. 46(1); 1-8: June 2022 DOI: 10.3329/jbas.v46i1.56864

Journal of Bangladesh Academy of Sciences

Journal homepage: http://www.bas.org.bd/publications/jbas.html

Research Article

Mathematical comparison of defuzzification of fuzzy logic controller for smart washing machine

Md. Azharul Islam* and Md. Sahadat Hossain

Department of Mathematics, University of Rajshahi, Rajshahi, Bangladesh

ARTICLE INFO

Article History

Received: 5 December 2021
Revised: 2 March 2022
Accepted: 10 May 2022

Keywords: Fuzzy number, Fuzzy logic controller, Defuzzication method, Fuzzy rule base, MATLAB simulation.

ABSTRACT

This is the age of modern science where different kinds of gadgets are used for the betterment of humanity. Various electronic, intelligence systems are invented via modern technology where FLC (Fuzzy Logic Controller) is used to develop their intelligence systems. Nowadays, FLC is widely used in uncertainty and robust development systems. Two inputs and one output have been used in this paper. Also, various defuzzification methods are used to determine the washing time of a smart washing machine. Finally, the performance of the various defuzzification methods has been compared mathematically. This work has been simulated by using the MATLAB toolbox.

Introduction

The fundamental concept of Fuzzy Logic was first introduced by Zadeh in 1965 (Zadeh, 1965). After that, for the first time, Mamdani (Mamdani, 1974) demonstrated its application in 1974. Fuzzy logic helps to monitor nonlinear systems that are difficult to solve mathematically. Fuzzy logic and fuzzy set theory mention the non-probabilistic logic theory now augments substitute paths to solve automatic control problems (Mamdani and Assilian, 1975). According to fuzzy logic's basic ideas, Mamdani and Assilian submitted fuzzy controllers that describe human control in linguistic form. Therefore, the first applications of a fuzzy control replaced a human operator (Kilr and Yuan, 1965). Moreover, several researchers, namely Lohani and Hasan (2009), Aggarwal (2011), Alhanjouri and Alhaddad (2013), Akram et al. (2014), and Soparkar (2015), calculated wash time for the washing machine.

Further, many researchers, namely Amin et al. (2020), Mahbub et al. (2019), Amin and Rana (2018), Roshmi and Hossain (2019) and Khatun Fand Hossain (2022) are also working on fuzzy set.

The paper aims to develop a fuzzy logic Control System to make it automated by using triangular and trapezoidal fuzzy numbers. Here, we demonstrated a little bit about FIS in the introductory section, while the simulation results and graphical representation obtained by using MATLAB, are discussed afterward.

Proposed Design of an FLC of Washing Machine

In this paper, the Mamdani, the Center of Gravity (Centroid method), the Bisector, and the Mean of Maxima (MOM) methods are used to design and develop a washing machine. This FLC for consists of two linguistic inputs i.e.

(1) Present degree of dirt on the clothes.

(2) Present amount of grease on the clothes.

These two linguistic variables are used to achieve the wash time as an output. For all linguistic inputs and linguistic outputs, triangular and trapezoidal MF are used. Fuzzy arithmetic and criterion terms are applied to these variables and the outcome is a defuzzified term to get the following crisp results, as described by Ahmed and Toki (2016).

*Corresponding author: <azislam14math.ru@gmail.com>

Fuzzy Logic Controller (FLC)

If-Then rules-based format is solved by the fuzzy logic controller in four steps as follows in Fig. 1.

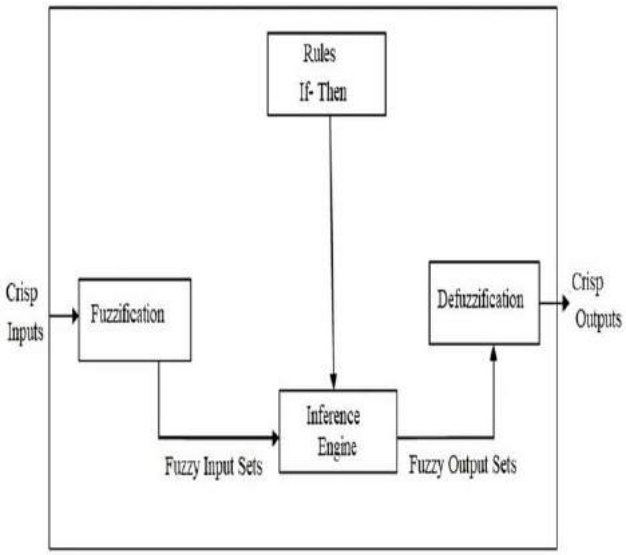

Fig. 1. Fuzzy logic controller system

Input Variables: Firstly, a set of MF of linguistic variables are taken as inputs where input variables are words or sentences. To take any fuzzy or crisp output by fuzzification is defuzzification respectably, fuzzy MF is used.

Fuzzification: Fuzzification is a process that provide a fuzzy output. Here, crisp values are fuzzified for fuzzy output.

Fuzzy Inference System: Fuzzy rule-based is applied here. For each antecedent, there is a consequent which is the resued output for every rule-base. Several operators like or, and, else, are not being used in rule-based system to connect multiple linguistic variables so that target output is obtained inside the inference system.

Defuzzification: The crisp output is obtained from a fuzzy set in the defuzzification process. Hardware applications are greatly dependent on defuzzification systems.

Defuzzification Techniques

Centroid Method

The "Centroid method", also known as the "Center of Gravity" or "Center of Area" method, is a technique that is most commonly employed and most familiar for defuzzification. It reduces the area to smaller regions, and a combined operation is performed to obtain the final output. It is stated by the expression below (Islam and Hossain, 2021).

$$x = \frac{\sum_{i=1}^{n} x_i \cdot \mu(x_i)}{\sum_{i=1}^{n} \mu(x_i)}$$

Here, n represents the number of elements in the sample, i.e., x_i are the elements and $\mu(x_i)$ are their corresponding membership functions.

Bisector Method

The Bisector method or Bisector of area splits the area into two states with the corresponding area, which can coincide or not with the centroid line of the particular area.

Mean of Maxima (MOM) method

The easiest way of defuzzification is to take the nearby crisp value with the highest MF. The arithmetic average of all mean values of the intervals containing fuzzy sets, including zero-length intervals, is the mean of the maxima method. The general equation of this method is given by Islam and Hossain (2021).

$$x = \frac{\sum_{x_i \in M} x_i}{|M|}$$

Where M = height of the fuzzy set and $|M|$ = cardinality of the fuzzy set M.

Fuzzy Membership Functions

The membership function (MF) represents a fuzzy set graphically. Triangular and trapezoidal MF is used in FIS. This paper uses triangular and trapezoidal MF to develop a Fuzzy Logic Controller (FLC). Each input, and output, including their linguistic variable, are discussed below.

Fuzzy Input Variables

Usually, crisp inputs can be converted into fuzzy inputs in fuzzy mathematics, where MF represents crisp inputs based on their linguistic terms and ranges. Here, three

linguistic terms such as small (SD), medium (MD), and large (LD) for the present degree of dirt on the cloth are taken. Secondly, the present amount of grease on the clothes with three linguistic variables such as- amount of no grease (NG), medium amount of grease (MG) and a large amount of grease (LG) are taken. The universe of discourse for the present degree of dirt and the present amount of grease is [0, 100]. The MFs. Corresponding to the linguistic values are represented by the following TFN and TrFN The membership value and range are shown in Table 1 below.

Table 1. Show the membership value of input variables

Linguistic Value	Notation	Numerical Range (Normalized)
Linguistic Input Variable: Dirtiness of Clothes (Dirt)		
Small Dirt	SD	[0, 0, 20, 50]
Medium Dirt	MD	[0, 50, 100]
Large Dirt	LD	[50, 80, 100, 100]
Linguistic Input Variable: Type of Dirt (Grease)		
No Grease	NG	[0, 0, 20, 50]
Medium Grease	MG	[0, 50, 100]
Large Grease	LG	[50, 80, 100, 100]

Fuzzy Output Variable

The primary reason for this washing machine is to study the wash time of those inputs and additionally divide them into five linguistic variables consisting of very short time (VS), Short time (S), medium time (M), large time (L) and very large time (VL) that belong to the universe [0, 60]. The membership value and range are shown in Table 2 below.

Table 2. Show the membership value of output variables

Linguistic Output Variable: Wash-Time		
Linguistic Value	**Notation**	**Numerical Range (Normalized)**
Very Short	VS	[0, 0, 5, 10]
Short	S	[0, 10, 25]
Medium	M	[10, 20, 30, 40]
Large	L	[25, 40, 60]
Very Large	VL	[40, 50, 60, 60]

Here in Figs. 2 to 4, FLC inputs and output membership functions are shown.

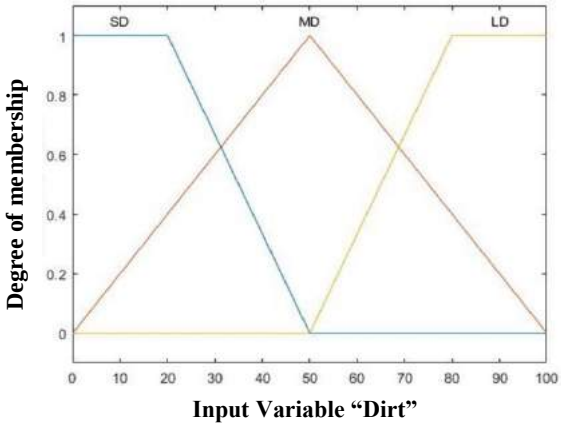

Fig. 2. Input variable of FLC "Dirt"

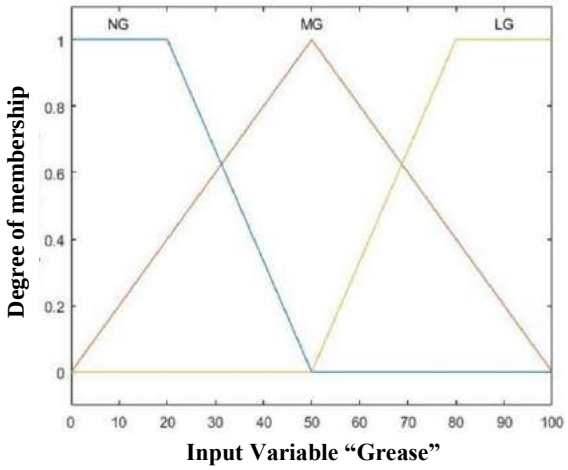

Fig. 3. Input variable of FLC "Grease"

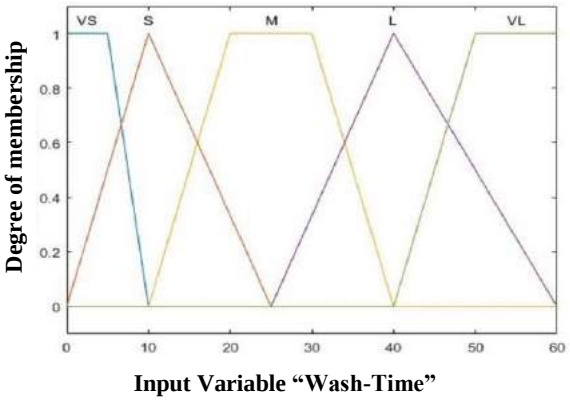

Fig. 4. Output variable of FLC "Wash-Time"

Fuzzy Rule Base

Fuzzy Rules-based are applied in the FLC by selecting the appropriate sequence in the If-Then rules, which are based on natural language. It is designed to make any automated decision, and formed by keeping the relationship between input and output in mind. The input variables (Dirt, Grease) make a total of 3*3=9 rules, as shown in the followings:

Rule 1: If (Type-Dirt is SD) and (Amount-Grease is NG), then (Wash-Time is VS).

Rule 2: If (Type-Dirt is SD) and (Amount-Grease is MG), then (Wash-Time is S).

Rule 3: If (Type-Dirt is SD) and (Amount-Grease is LG), then (Wash-Time is M).

Rule 4: If (Type-Dirt is MD) and (Amount-Grease is NG), then (Wash-Time is S).

Rule 5: If (Type-Dirt is MD) and (Amount-Grease is MG), then (Wash-Time is M).

Rule 6: If (Type-Dirt is MD) and (Amount-Grease is LG), then (Wash-Time is L).

Rule 7: If (Type-Dirt is LD) and (Amount-Grease is NG), then (Wash-Time is M).

Rule 8: If (Type-Dirt is LD) and (Amount-Grease is MG), then (Wash-Time is L).

Rule 9: If (Type-Dirt is LD) and (Amount-Grease is LG), then (Wash-Time is VL).

Fuzzy Logic Controller (FLC) Implementation in Smart Washing Machine

Fuzzy Base Class

Mamdani method is used to create system control rules obtained from experienced human operators (Kilr and Yuan, 1995). This paper uses the Mamdani method to illustrate, and the centroid method for defuzzification. Here, FIS editor FIS Editor defines the Fuzzy Base Class, the various inputs, i.e., dirt and grease, and the output variable like wash time (Zadeh and Berkeley, 1995), as shown in Fig. 5.

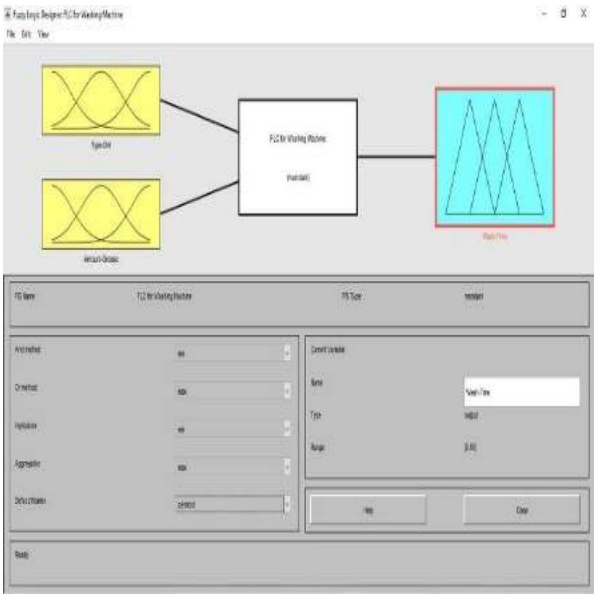

Fig. 5. Show the simulated washing machine on MATLAB

Fuzzy Rule Base

The users can design Fuzzy rules automatically or manually, i.e., some rules produced by the rules Editor for all combinations of selected input variables and a user fills consequent fuzzy term. The fuzzy outputs subsequently come from inputs (Zadeh and Berkeley, 1995), as shown in Fig. 6.

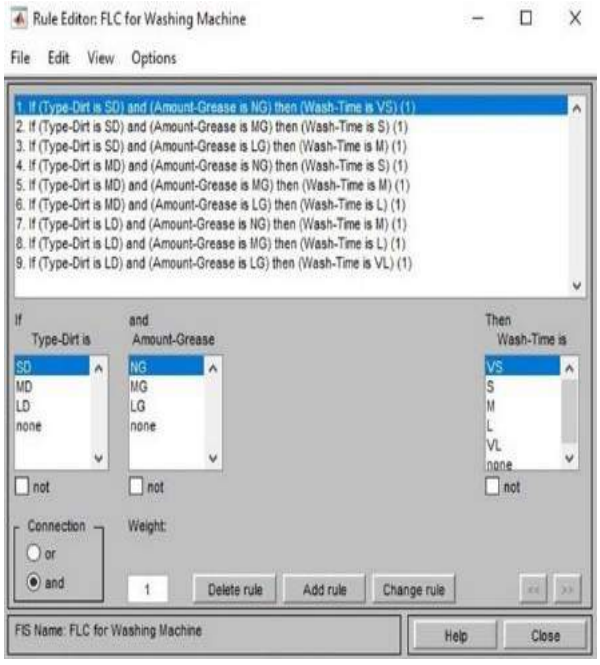

Fig. 6. Fuzzy base rules

Surface Plots

By applying three defuzzification methods like-COG, bisector, and MOM methods. We get the surface plots shown in Figs. 7 to 9 based on the above effectuation (Naaz et al., 2011).

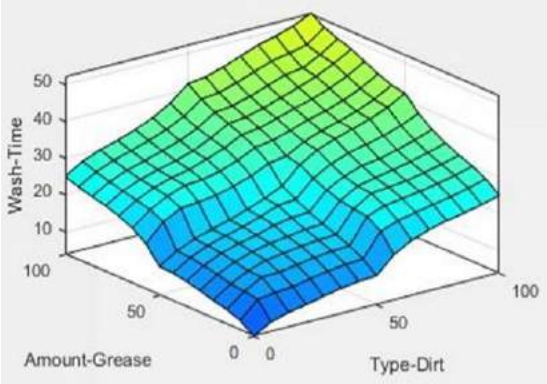

Fig. 7. Input/Output response surface for FLC using COG method

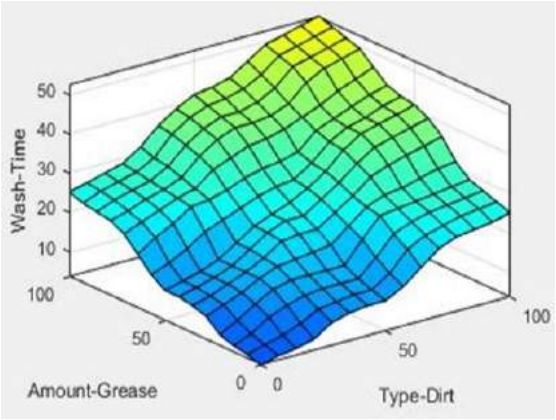

Fig. 8. Input/Output response surface for FLC using bisector method

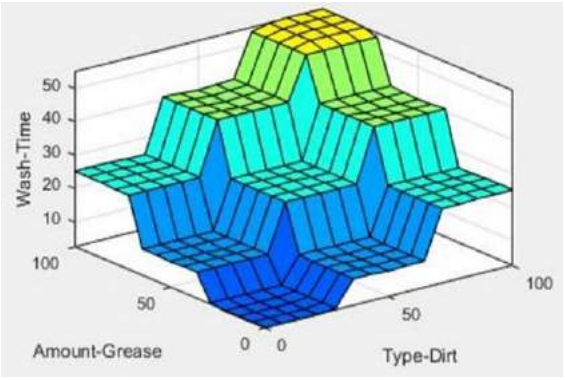

Fig. 9. Input/Output response surface for FLC using the MOM method

Result and Discussion

Based on the present degree of dirt and the present amount of grease on the clothes, it can be said that this method will have a different wash time. Here, a large number of values for dirt and grease can be used to evaluate the difference between these methods. Clearly, it can be said that these three techniques are shown in Table 3, which is used for comparison and provide wash time as an output. Hence, by using "If-Then" rules during the defuzzification of the washing machine, its output can be modified and verified simultaneously. Any amendment in the guidelines of the thumb base version would require you to alter the "If-Then" regulations to get the accurate output.

Table 3. Wash-Time output for varying input parameters

Type-Dirt (%)	Amount-Grease (%)	Wash-Time		
		COG	Bisector	MOM
25	40	18.3	16.8	10.5
30	50	19.7	19.2	11.1
40	60	27.8	27	24.9
50	50	25	25.2	25.2
60	70	34.9	35.4	40.8
70	90	41.6	43.2	53.4
90	40	33.9	37.2	40.5
80	50	35.9	37.8	40.2
60	20	25.4	22.8	10.5
40	30	19.2	19.2	11.1

Table 3 shows how the machine will respond to different situations. For example, if the type of dirt and the amount of grease are 60 and 70, respectively, according to the quality of the fabric, then the washing time for the models of COG, bisection, and MOM is equal to 34.30 minutes, 35.40 minutes, and 40.08 minutes respectively. It is quite believable and justifiable.

Mathematicians use the most effective triangular or trapezoidal fuzzy number in the models used to

locate the wash time of the washing machine. In our mathematical research, we have calculated the wash time using the Center of Gravity (COG), the Bisector, and the Mean of Maxima (MOM) models with the assistance of triangular and trapezoidal fuzzy numbers and mentioned their comparison.

The results in Figs 10 to 12 shows that when dirt and grease increase, the wash time of the washing machine for the COG method increases a bit slower than the bisector method and MOM method. Hence, if we use centroid, it will decrease the cost of electricity. So, it is more logical to use the COG method for our preferable

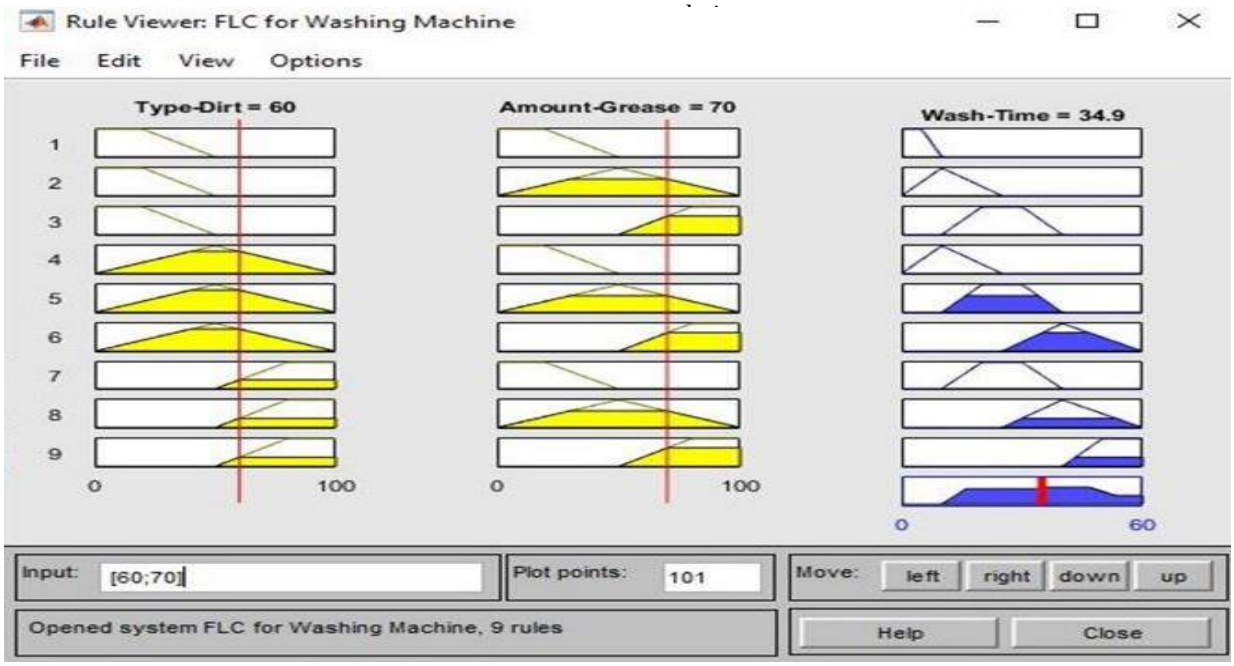

Fig. 10. Rule viewer of wash-time for FLC using the centroid method

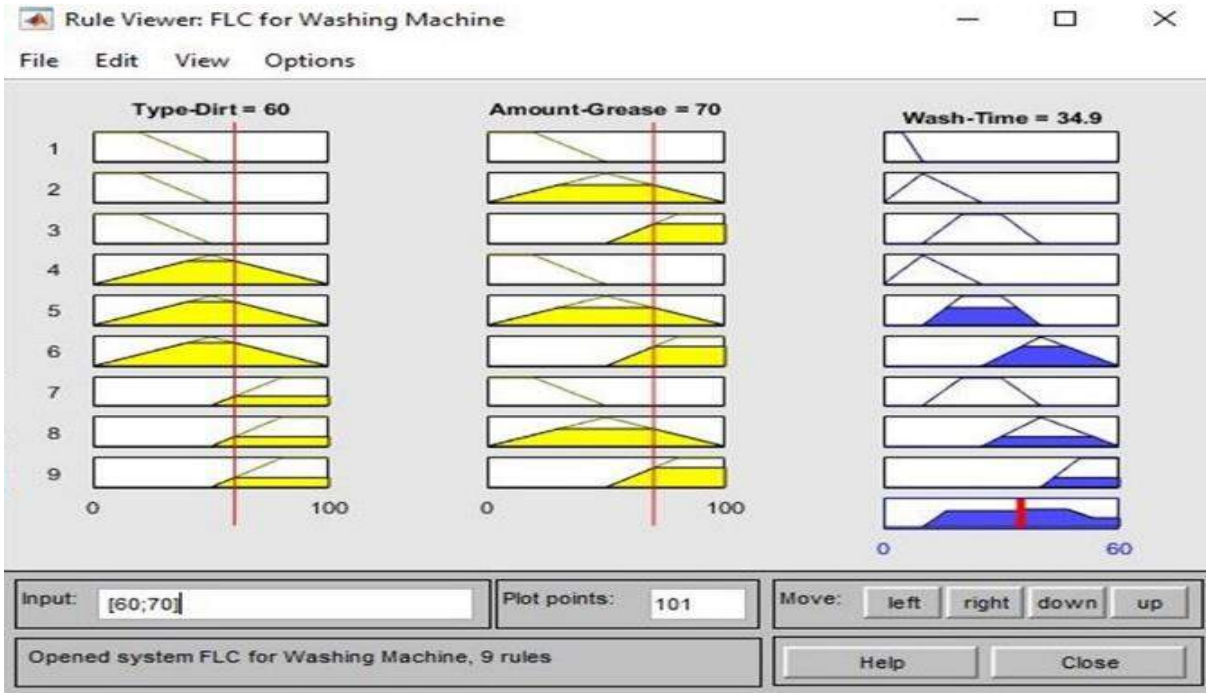

Fig. 11. Rule viewer of wash-time for FLC using the bisector method

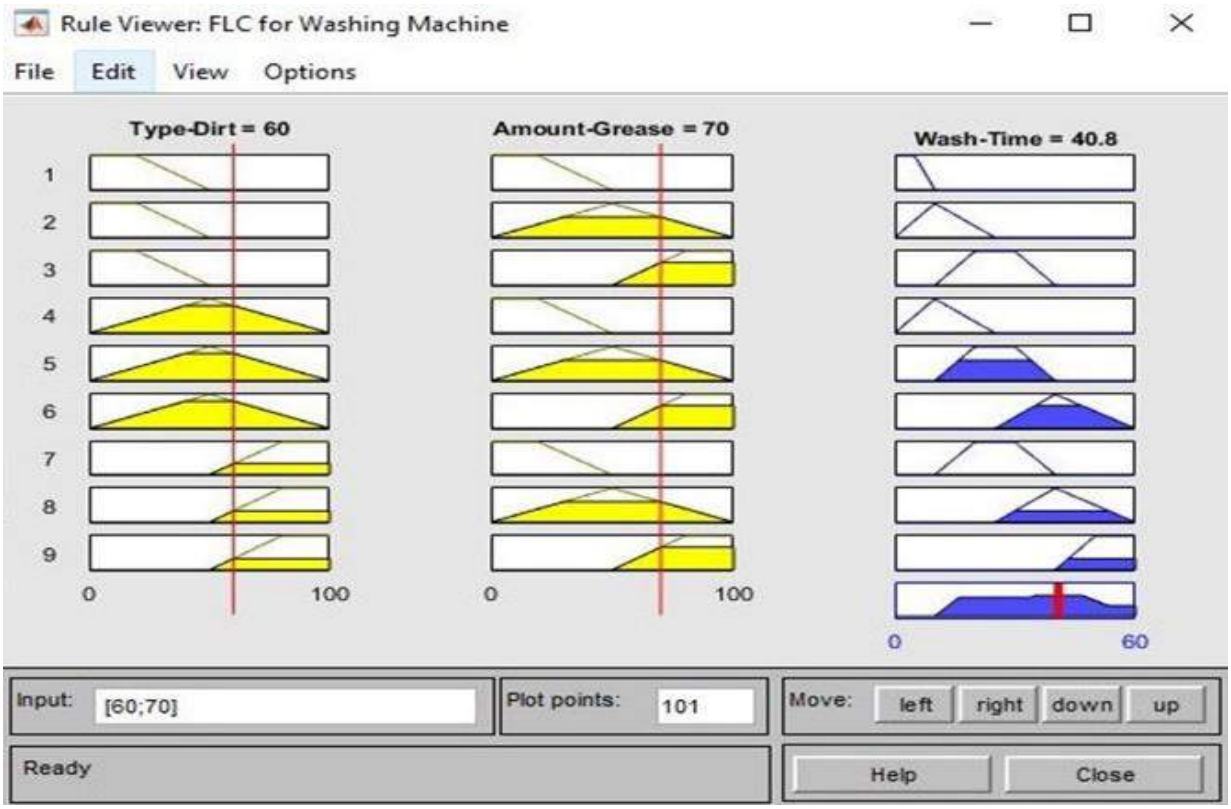

Fig. 12. Rule viewer of wash-time for FLC using the MOM method

The above work is done only mathematically using a Fuzzy Logic Controller. This model has not been used in the washing machine yet but has been successfully MATLAB simulated with the fuzzy toolbox. Hopefully, future researchers will get the same result if they use the above model in the washing machine.

Acknowledgments

The authors of this paper are thankful to other authors whose names are included in the references section for their suggestions, which helped us modify this paper. Besides, we are also grateful to the Department of Mathematics, Faculty of Science, and the University of Rajshahi for their unconditional the support and cooperation.

Conflicts of Interest

The authors declare that they have no conflicts of interest regarding the publication of this article.

References

Aggarwal M. Fuzzy logic controller for washing machine. *Roll No. 00ME1011, Department of Mechanical Engineering, India Institute of Technology, Kharagpur*. 2011; p. 1-5.

Ahmed T and Toki A. A review on washing machine using fuzzy logic controller. *Int. J. Emerg. Trends Eng. Dev.* 2016; 4(7): 64-67.

Akram M, Habib S and Javed I. Intuitionistic fuzzy logic control for washing machines. *Indian J. Sci. Technol*. 2014; 7(5): 654-661.

Alhanjouri MA and Alhaddad A. Optimize wash time of washing machine using fuzzy logic. *In: The 7th International Conference on Information and Communication Technology and Systems (ICTS 2013).* Institut Teknologi Sepuluh Nopember Sukolilo, Surabaya, Indonesia, 2013.

Amin MR, Hossain MS and Miah SS. Fuzzy pairwise regular bitopological spaces in quasi-coincidence sense. *J. Bangladesh Acad. Sci.* 2020; 44(2): 139-143.

Amin R and Rana S. Certain Properties of fuzzy path connectedness and maximal fuzzy path connectedness. *J. Bangladesh Acad. Sci.* 2018; 42(1): 67-71.

Kilr JG and Yuan B. Fuzzy sets and fuzzy logic, theory and applications. *Prentice Hall of India Private Ltd. New Delhi, India*, 1995.

Islam MA and Hossain MS. Optimizing the wash time of the washing machine using several types of fuzzy numbers. *J. Bangladesh Acad. Sci.* 2021; 45(1): 105-116.

Khatun F and Hossain MS. Mathematically forecasting for generalized business by using fuzzy trapezoidal numbers. *J. Bangladesh Acad. Sci*. 2022; 45(2): 147-154.

Lohani P and Hasan SR. Design of an improved controller microchip for washing machine. In: *16th Annual Electronics New Zealand Conference*. Dunedin: Otago University 2009, p. 20-26.

Mahbub MA, Hossain MS and Hossain MA. On Q-compactness in intuitionistic fuzzy topological spaces. *J. Bangladesh Acad. Sci.* 2019; 43(2): 197-203.

Mamdani EH and Assilian S. An experiment in linguistic synthesis with a fuzzy logic controller. *Int. J. Man-Mach. Stud.* 1975; 7(1): 1-13.

Mamdani EH. Application of fuzzy algorithms for control of simple dynamic plant; In: *Proceedings of the Institution of Electrical Engineers. IET*. 1974; 121: 1585-1588.

Naaz S, Alam A and Biswas R. Effect of different defuzzification methods in a fuzzy based load balancing application. *Int. J. Comput. Sci.* 2011; 8(5): 261-267.

Roshmi R and Hossain MS. Properties of separation axioms in bitopological spaces. *J. Bangladesh Acad. Sci*. 2019; 43(2): 191-195.

Soparkar B. Defuzzification in a fuzzy logic controller: Automatic washing machine. *IJCA Proceedings on International Conference on Computer Technology ICCT 2015;* 2015(5): 16-19.

Zadeh LA. Fuzzy sets. *Inf. Control.* 1965; 8(3): 338- 353.

Zadeh LA and Berkeley C. Fuzzy Logic Toolbox User's Guide Version 2. *The Math Works, Inc;* 1995.

J. Bangladesh Acad. Sci. 46(1); 9-18: June 2022 DOI: 10.3329/jbas.v46i1.60344

Journal of Bangladesh Academy of Sciences

Journal homepage: http://www.bas.org.bd/publications/jbas.html

Research Article

Prevalence and distribution of antimicrobial resistance profile of *Escherichia coli* isolated from various local fish markets in Dhaka city, Bangladesh

Mahmuda Akter*, Minhajul Abedin[1], Md. Parvez Mosharaf[1], Mohammad Ariful Islam[1] and Zahid Hassan

Department of Genetic Engineering and Biotechnology, Jagannath University, Dhaka, Bangladesh

ARTICLE INFO

Article History

Received: 20 February 2022
Revised: 9 May 2022
Accepted: 10 May 2022

Keywords: TVBC, TCC, TFCC, *E. coli*, Antibiotic susceptibility test, MAR index

ABSTRACT

Considering the importance of the fish and fish products as a vital part of the human diet in Bangladesh, the study aimed to estimate the microbial load, identify the *E. coli* and observe the isolates antibiogram pattern. Standard plate count technique, as well as the 3-tube most probable number (MPN) method, were applied to estimate the total viable bacteria (TVB) and total coliforms (TC), total fecal coliforms (TFC), and *E. coli*, respectively. Approximately 61.91% of samples fell into the marginally acceptable limit for TVB count, while 66.67% and 95.25% of examined species exceeded the threshold limit for TC and TFC, respectively ($p<0.05$). Around 90% of samples were contaminated with *E. coli*. A culture sensitivity test revealed that cent percent strains harbored resistance to penicillin, rifampicin, and erythromycin. Multiple antibiotic resistance (MAR) index above 0.2 may indicate the misuse or overuse of antibiotics. The findings highlight the potential food safety hazards associated with fish concerning the random use of antibiotics.

Introduction

Fish and all the fish items are the primary sources of their protein, and there is a growing recognition of their nutritional and health-promoting qualities. The products of fish are also considered a major source of earning and livelihood for numerous communities worldwide (Nowsad et al., 2015). Bangladesh is recognized as the world's foremost fish-producing country, where people also depend on fishing, fish farming, processing, and trading for their earnings (DoF, 2018). Comparatively, Bangladeshi people eat more fish as a source of animal protein which covers 60% of their demand, than meat products (DoF, 2018). From CDC (USA) data, it has been known that 3% people of United States acquired foodborne illnesses from contaminated fish (Barrett et al., 2017). So, consuming more fish may be a great concern for food security. FAO reported that each year nearly 30 million people are affected by food-borne diseases in Bangladesh (FAO, 2012). Though the involvement of fish causing food-borne illness is not clear in this tropic, several microorganisms that are normal inhabitants in the aquatic environment may cause contamination (Dutta et al., 2018).

Due to the dense population and poor sanitation facilities, the people of Bangladesh are more susceptible to microbial attacks and face the challenges of fecal contamination (Singh et al., 2020). A large group of the population involved in unhygienic sanitary practices mostly live beside the haor, baor, beel, pond, and river. Open defecation and inadequately treated or untreated domestic sewage disposal may contaminate these natural water bodies with several human pathogenic microbes (Dutta, 2016). In most cases, domestic local markets' surroundings remain soggy, filthy, and unhealthy

*Corresponding author: <mahmudaakter.geb.jun@gmail.com>

[1]Department of Microbiology, Jagannath University, Dhaka, Bangladesh

(Begum et al., 2015). Unhygienic landing sites, poor handling, transport, storage, display, and packaging process may increase the risk of microbial contamination of fish (Costa, 2013).

Consequently, consumers may develop infection or intoxication (Assefa et al., 2019). Besides food safety issues, intake of contaminated fish may increase the risk of developing antimicrobial resistance (Ng et al., 2018). The extensive, random, and misuse of antibiotics for therapeutic purposes or as growth promoters in livestock or as feed additives in fish farms caused a genetic selection of more harmful bacteria, a matter of great public health concern (Founou et al., 2016). A member of the coliform group, *Escherichia coli* is found in the intestinal tract of the animals, humans, and fish microbiota (Cardozo et al., 2018). It is a widely accepted fecal contamination indicator organism of fish and water (Price and Wildeboer, 2017). It can be easily propagated in various living ecosystems and interchange genetic material with other bacterial communities that may lead to the emergence of resistant bacteria, ultimately causing the disease in humans (Ryu et al., 2012). A higher frequency of resistant *E. coli* strains has been noticed in fish and seafood in India (Kumar et al., 2005) and Korea (Ryu et al., 2012), indicating the urgency of monitoring the presence of the bacteria in our region (Boss et al., 2016). Limited studies were performed in our country regarding this point. The specific objectives of the study were: 1) to get insight into the microbial status in fresh fish samples 2) identification of the major fecal coliform *E. coli*, and 3) to determine the antibiogram profiles of *E. coli*, and observe their multidrug-resistant nature.

Materials and Methods

Field sampling

Between March and August 2019, a total of 21 fish samples were purchased from three different local fish markets (Karwan bazar, Khilgaon bazar, and Shyambazar) located at three zones in the city of Dhaka, Bangladesh (Fig. 1). The samples included in this study were the following seven different categories: Koi (*Anabas testudineus*), Poa (*Otolithoides pama*), Loitta (*Harpadon nehereus*), Sorputi (*Puntius sarana*), Rupchanda (*Pampus chinensis*), Bhata (*Labeo bata*) and Taki (*Channa punctate*). Each type of fish sample was aseptically collected after a one-week interval into sterile plastic boxes, afterward placed in a cool box, and immediately transported to the laboratory. The samples were processed as early as possible for microbiological analysis, i.e., total viable bacterial count (TVBC), total coliform count (TCC), and total fecal coliform count (TFCC).

Sample processing and media preparation

About 20 g of the muscle of individual fish samples were weighed aseptically in an analytical balance (Shimadzu, Japan) in a triplicate fashion. After that, samples were crushed for 2 minutes in a pre-sterile blender containing 180 mL of sterilized normal saline at room temperature to make proper homogenization. Various nutrient broths and agar used in this study were nutrient agar, lauryl tryptose broth (LTB), 2% brilliant green bile broth (BGBB) and MacConkey broth. All of these media were prepared according to Cheesbrough (1984) and autoclaved at 121°C for 15 min before use.

Quantitative analysis of total viable bacteria

The aerobic plate count (APC) method enumerated the total microbial load (FAO, 1992). Nutrient agar was used in this method. Each sample was serially diluted up to 10^{-4} dilutions with 9 mL of sterile 0.85% NaCl solution. An aliquot of 0.1 mL diluted fish sample was placed on the agar plates (Hi-Media, India) using a spread plate technique. Plates were incubated at 37 °C for 18-24 hours, followed by cell counting.

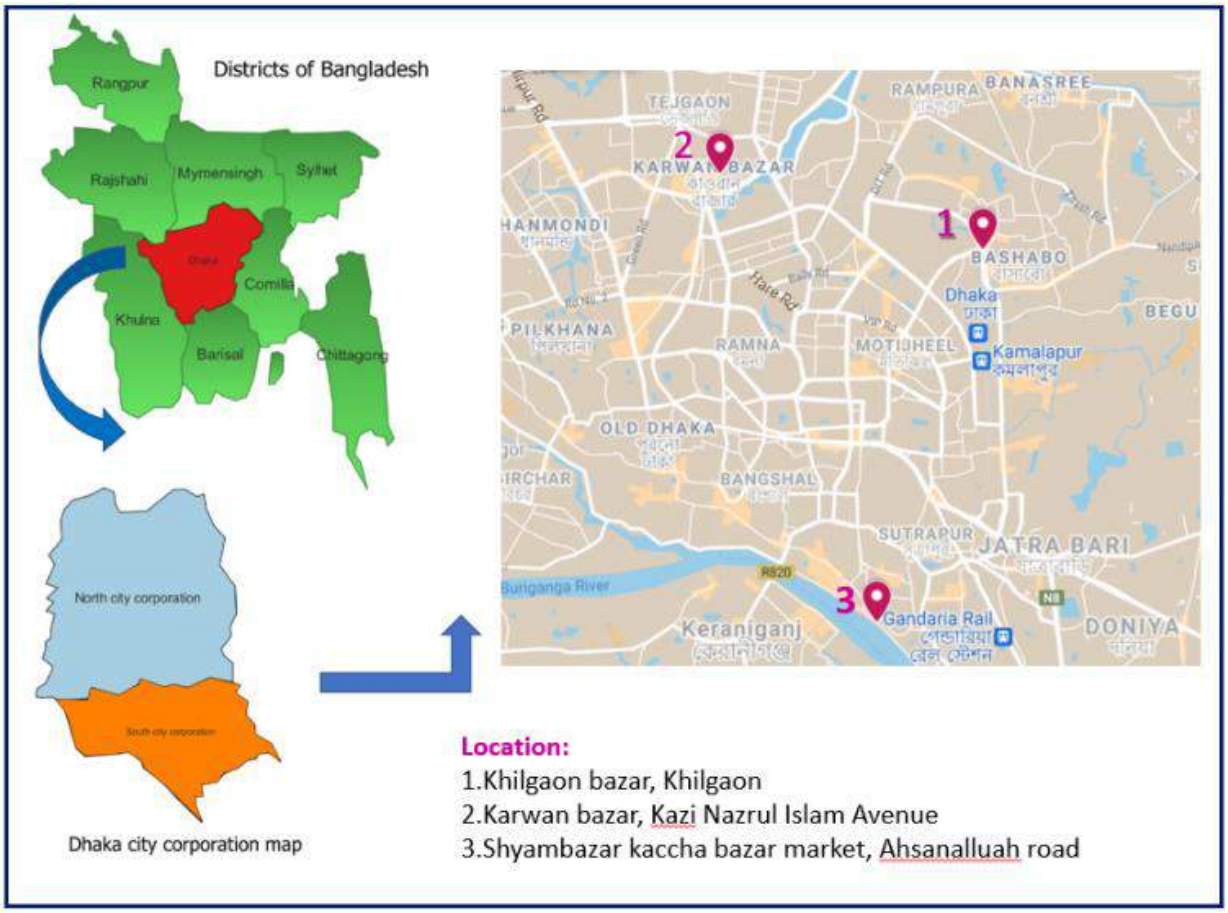

Fig. 1. The map of Dhaka city indicates the area of sampling sites

Estimation of total coliforms and fecal coliforms

Lauryl tryptose broth (LTB), 2% brilliant green bile broth (BGBB), and MacConkey broth were used to estimate the number of total coliforms and fecal coliforms. According to standard protocol, the most probable number (MPN), the most conventional 3-tube method, was employed here (FAO, 1992). A similar decimal serial dilution series for each sample was performed here (i.e., 9 mL LTB plus one 1 mL crushed fish sample). A triplicate set of three test tubes filled with 9 ml LTB (Hi-Media, India) were sterilized. A one ml of ten-fold serial dilutions (up to 10^{-3}) were inoculated into triplicate sets, respectively and incubated at 37 ^{0}C for 24-48 hours. Gas and acid produced from lactose fermentation point out the presumptive heterofermentative metabolism of coliforms (FAO, 1992). To confirm the presence of total coliforms and fecal coliforms bacteria, approximately one-loopful inoculum of each gas positive LTBs were placed in the pre-sterilized test tube containing BGBB (Oxoid, UK) at 37 ^{0}C for 48 hours and MacConkey broth (Oxoid, Uk) at 44.5±0.5 ^{0}C for 48 hours respectively. After incubation, the gas produced in the tubes was recorded and compared with the MPN chart to count the total coliforms and total fecal coliforms number.

Isolation and Identification of E. coli

From each gas positive MacConkey broth, one loopful fecal coliforms sample was streaked on an eosin methylene blue (EMB) agar (Scharlau, Spain) plate. The plates were incubated at 37 ^{0}C and examined after 24-48 hours for bacterial growth and any change of color in the media. Black colonies with a metallic green sheen were observed on the EMB agar plate, indicating the presence of *E. coli*. After Gram's staining of suspected bacterial

colonies, several biochemical tests such as indole production, methyl-red, Voges-Proskauer and citrate utilization (IMViC) tests were performed according to standard microbiological guidelines for the identification of *E. coli* (FAO, 1992).

Antimicrobial susceptibility testing

The bacterial isolates were subjected to a culture sensitivity test on a Mueller-Hinton agar (MHA) (Hi-Media, India) plate according to the Kirby-Bauer disc diffusion method (Bauer et al., 1966). A total of twelve panels of commercial antibiotic disks (Oxoid, UK) were used at different concentrations. The discs strength were: Cefixime, Rifampicin and Ciprofloxacin at 5 µg/mL; Gentamicin, Ampicillin, Penicillin, Streptomycin and Norfloxacin at 10 µg/mL; Erythromycin at 15 µg/mL and Tetracycline, Chloramphenicol and Neomycin at 30 µg/mL. A suspension of *E. coli* isolates was prepared equivalent to 0.5 McFarland standards and was made as lawn cultures onto sterile Mueller Hinton agar plates. The antibiotic discs were placed on the surface of the plates using sterile forceps and were incubated at 37 ^{0}C for 18-24 hours. Criteria for the sensitivity, intermediate, and resistance were recorded as per Clinical Laboratory Standards Institute (CLSl) guidelines, 2012. Multidrug-resistant (MDR) *E. coli* was defined according to the international expert proposal for interim standard definitions for acquired resistance. Further multiple antibiotic resistance (MAR) index of only multiple drug-resistant (MDR) *E. coli* isolates was calculated. Krumperman (1983) represents the MAR index, calculated by the ratio of the digit of antibiotics to which the isolate was resistant (a) and the digit of antibiotics to which the isolate was subjected (b).

Statistical analysis

All the data were analyzed and filtered in Microsoft Excel version 2012. The APC data were converted to $\log_{10}$ formed for ease of calculation. Descriptive statistics (graphs) were applied to visualize the outcome, and a p-value ≤ 0.05 was considered as significant for mean values.

Results and Discussion

All samples' average total viable bacterial count (TVBC) was 6.30 $\log_{10}$ cfu/g, ranging from 4.08-6.47 $\log_{10}$ cfu/g. The mean value of the total viable bacterial count belonging to seven different fish species was varied (Fig. 2). The highest mean of TVBC was found in Rupchanda (6.57±0.66 $\log_{10}$ cfu/g), whereas the lowest mean count (4.80±0.62 $\log_{10}$ cfu/g) was observed in the Taki.

The current study reported the microbiological quality of the fishes following the ICMSF, 1986 criteria into three categories: good (>5×10^5 cfu/g), marginally acceptable (5×10^5 cfu/g to 10^7), and unacceptable (<10^7). Based on the criteria, 100% of samples of Taki were good microbiological limits. In contrast, cent percent of Loitta and Poa fishes and 66.67% of Rupchanda fishes were marginally acceptable quality (Fig. 3). Notably, 33.33% of Rupchanda fishes with unacceptable limits were noticed. Overall, the TVB count of the 33.33% samples was within the range of good quality, whereas 61.91% and 4.76% samples fell into marginally acceptable ($p<0.05$) and unacceptable limits, respectively. Hence, statistically significant percentages of the samples, 66.67%, were beyond the good quality limit ($p<0.05$).

Several previous investigations performed on various fishes from retail shops also reflect the same scenario. The TVBC ranges from 6×10^4 to 1.6×10^6 cfu/g (Sarkar et al., 2020), 2.89×10^5 to 2.98×10^7 cfu/g (Begum et al., 2015), and 3.3×10^5 cfu/g to 1.9×10^8 cfu/g (Begum et al., 2010) comply with the outcomes of the present study. So, the fish samples of domestic markets contain a high bacterial load that may be transmitted to the consumers and the people associated with the transportation, handling, and processing through contact (Ribeiro et al., 2016). The outcomes provide an initial alarm to safeguard fish consumers from the chance of infection and demand an urgent step to uplift the quality control systems of the local shops.

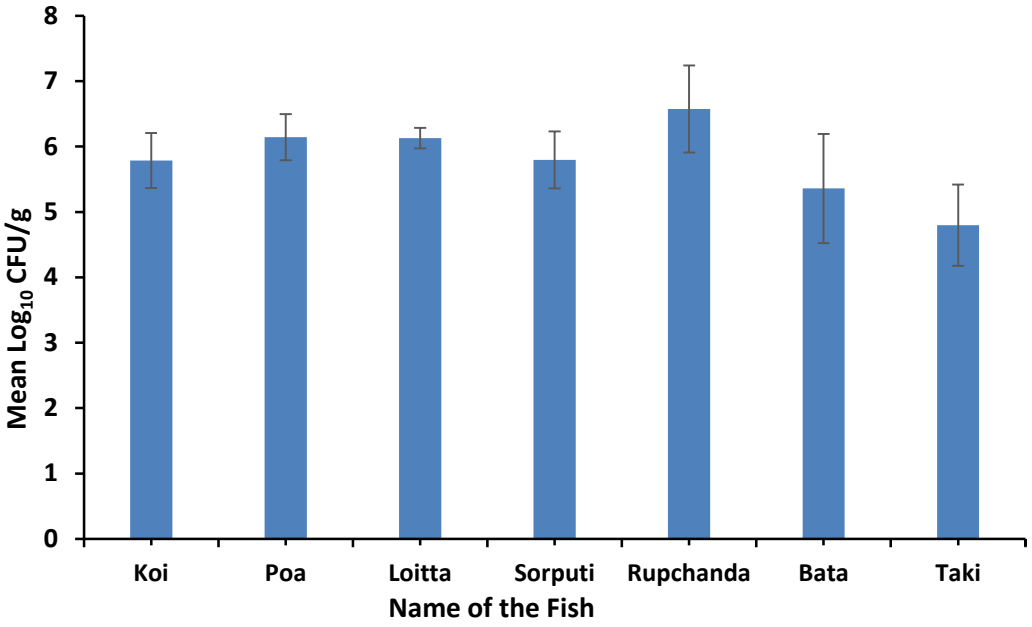

Fig. 2. Total viable bacterial count (log_{10} cfu/g) of the raw fish samples collected from local markets. The values were represented with mean ± SD.

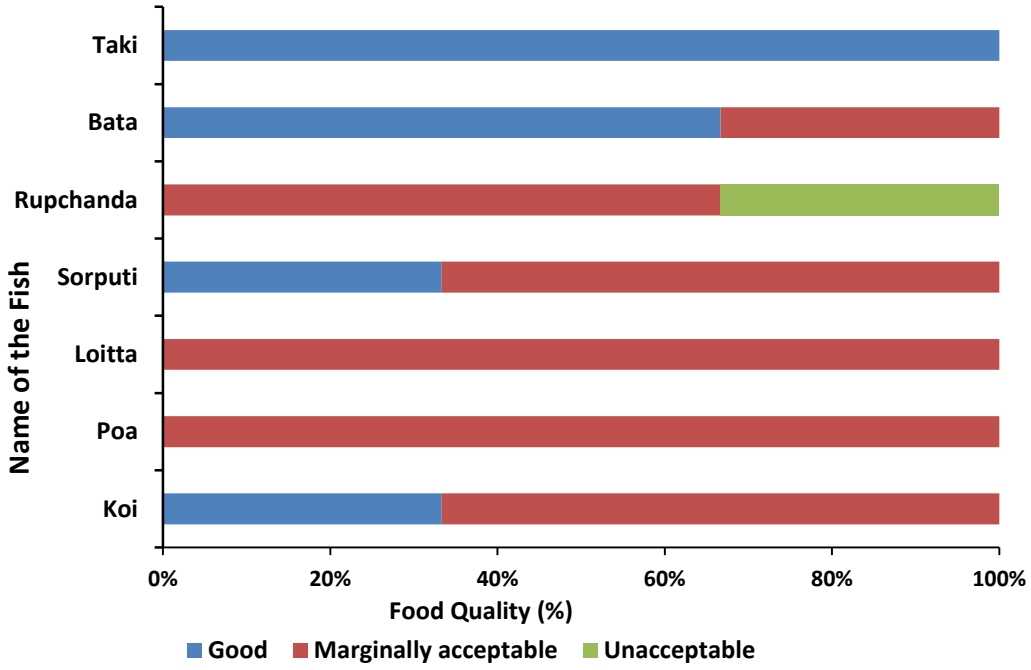

Fig. 3. Microbiological quality of the fishes according to the International Commission on Microbiological Specifications for Food (ICMSF).

Nearly all the representative fish samples were contaminated with coliforms and fecal coliforms bacteria. The bacteriological qualities of the fish samples brought from the local markets are summarized in Table 1. In the present research work, the total coliforms count (TCC) ranged between 2.1 and >1100 MPN/g, and the total fecal coliforms count (TFCC) was in the range of 3.6 MPN/g to >1100 MPN/g. The maximum TCC and TFCC count was found on Koi and Poa fish (>1100 MPN/g) from Shyambazar and the Taki fish from Khilgaon Bazar. The lowest TCC count was present in Loitta fish (2.1 MPN/g) of Shyambazar, while the Taki fish (3.6 MPN/g) of Karwan bazar exhibited the least TFCC count. ICMSF establishes the standard acceptance limits of total coliforms (TCC) and fecal coliforms (TFCC) for fresh fish that are <100 MPN/g and <10 MPN/g, respectively. The present study found that almost 66.67% and 95.25% of examined species exceeded the acceptance limit significantly ($p<0.05$) for coliforms, and fecal coliforms, respectively.

Table 1. The total coliform (TC) and total faecal coliform (TFC) count assessment of raw fish samples.

Sampling Sites	Microbial Load (MPN/g)	Name of the Fish						
		Koi	Poa	Loitta	Sorputi	Rupchanda	Bata	Taki
LM-1	TCC	>1100	>1100	2.1	35	210	1100	210
	TFCC	>1100	>1100	210	20	28	150	28
LM-2	TCC	210	150	21	210	210	21	>1100
	TFCC	460	210	28	28	1100	23	3.6
LM-3	TCC	28	28	150	43	240	460	>1100
	TFCC	28	460	240	93	240	150	>1100

LM-1= Shyambazar, LM-2= Karwan bazar, LM-3=Khilgaon bazar, TCC= Total Coliform Count, TFCC=Total Faecal Coliform Count. MPN=Most Probable Number.

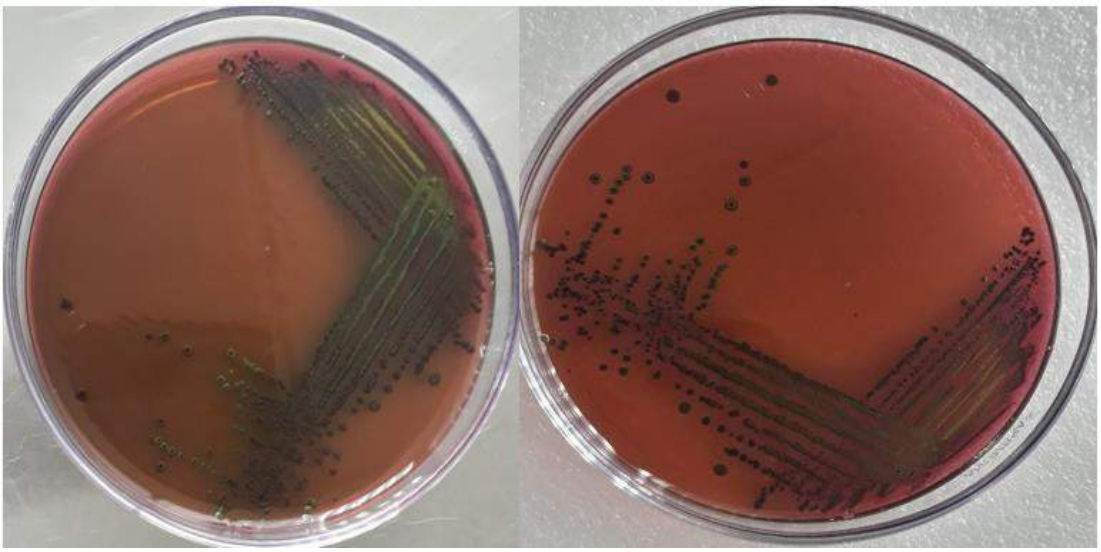

Fig. 4. Growth of *E. coli* colonies on EMB agar plate

Following the conventional culture technique, 19 out of 21 samples displayed black colonies with a metallic green sheen on the EMB agar plate (Fig. 4). All the gram-negative samples that were subjected to IMViC tests also confirmed the identification of *E. coli* strains (Table 2). In the present research finding, the overall prevalence of *E. coli* was more than 90%. The presence of the organism in the fish was 100% in the two sampling sites Shyambazar and Karwan bazar. Moreover, a lower contamination rate was reported in the Khilgaon bazar, which was 71.4%. The percentages may indicate the probability of the presence of these bacteria in higher density in freshwater. High *E. coli* load like 80.70%, 46.6% and 80% was also found in India (Dutta, 2016), Kenya (Onyuka et al. 2011), and Switzerland (Boss et al., 2016), respectively. The prevalence of coliforms and fecal coliforms at higher ranges may indicate sewage contamination. Untreated sewage is already identified as one of the principal reasons for the deterioration of water quality in the capital city of Bangladesh (Bashar and Fung, 2020).

Table 2. The results of biochemical characterization of *E. coli.*

E. coli isolates	Indole production	Methyl red	Voges-Proskauer	Citrate utilization test
19	+	+	-	-

Where + = positive and - = negative

The antibiotic disk diffusion method examined the antimicrobial sensitivity pattern of *E. coli* isolates. Following the test result, *E. coli* isolated from fish samples were entirely (100%) resistant to rifampicin, penicillin and erythromycin. In contrast, gentamycin and norfloxacin effectively suppress the growth of 94.74% of the isolates. More than 80% sensitivity was also observed in chloramphenicol and ciprofloxacin. The susceptibility percentage of candidate isolates was displayed in Fig. 5.

The antibiotic susceptibility tests revealed that all *E. coli* strains were multidrug-resistant (MDR). Isolates in this investigation were resistant to at least 3 antibiotics and at most 9 antibiotics (Table 3). The antibiogram patterns of the strains of *E. coli* are displayed in Table 3.

This observation was nearly concordant with the investigations of Pinu et al. (2007), and Ahmed et al. (2013), where strains of *E. coli* harvested from different

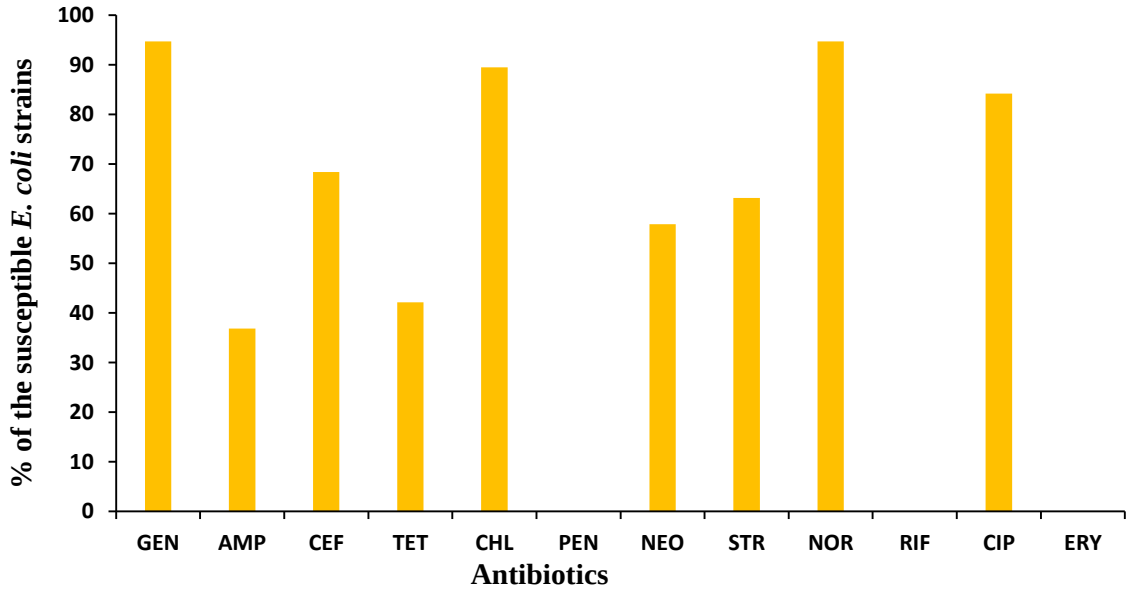

Fig. 5. The percentages of susceptible *E. coli* isolates to multiple antibiotics. The isolated strains were highly susceptible to GEN and NOR while resistant to PEN, RIF and ERY. Here, GEN= Gentamicin, Ampicillin, AMP= CEF= Cefixime, TET= Tetracycline, CHL= Chloramphenicol, PEN= Penicillin, NEO= Neomycin, STR= Streptomycin, NOR= Norfloxacin, RIF= Rifampicin, CIP= Ciprofloxacin, ERY= Erythromycin.

Table 3. The pattern of *E. coli* isolates harboring multiple antibiotic resistance

Sample No.	Source	Drug resistance patterns
1, 2, 8,12	Koi (LM-2), Poa (LM-2), Koi (LM-3), Rupchanda (LM-3)	PEN, RIF, ERY
9	Poa (LM-3)	TET, PEN, RIF, ERY
21	Taki (LM-1)	AMP PEN, RIF, ERY
5, 19	Rupchanda (LM-2) (LM-1)	AMP, TET, PEN, RIF, ERY
7	Taki (LM-2)	AMP, CEF, PEN, RIF, ERY
20	Bhata (LM-1)	TET, PEN, STR, RIF, ERY
3	Loitta (LM-2)	AMP, TET, PEN, STR, RIF, ERY
6, 10	Bhata (LM-2), Loitta (LM-3)	AMP, CEF, TET, PEN, RIF, ERY
11	Sorputi (LM-3)	AMP, TET, PEN, RIF, CIP, ERY
13	Bhata (LM-3)	CEF, NOR, CIP, PEN, RIF, ERY
14	Taki (LM-3)	GEN, AMP, NEO, PEN, RIF, ERY
4	Sorputi (LM-2)	AMP, CEF, TET, PEN, NEO, RIF, ERY
18	Sorputi (LM-1)	AMP, TET, PEN, NEO, RIF, ERY, CHL, CIP
17	Loitta (LM-1)	AMP, CEF, TET, PEN, NEO, RIF, ERY, CHL, STR

LM-1= Shyambazar, LM-2= Karwan bazar, LM-3=Khilgaon bazar. GEN= Gentamicin, AMP= Ampicillin, CEF= Cefixime, TET= Tetracycline, CHL= Chloramphenicol, PEN= Penicillin, NEO= Neomycin, STR= Streptomycin, NOR= Norfloxacin, RIF= Rifampicin, CIP= Ciprofloxacin, ERY= Erythromycin.

fish species exhibited resistance to penicillin G and erythromycin, respectively. The origins of these drug-resistant *E. coli* isolates might come from the hospital or veterinary sources. However, the data concerning the prevalence of antibiotic-resistant *E. coli* strains either in clinical or environmental sources is unavailable in Bangladesh. Moreover, antibiotics are indiscriminately used in agriculture and the animal industry in our country. Adeleke and Omafuvbe (2011) calculated a MAR index value that clarifies the potential health risk among the population and whether the distribution of resistant bacteria in a particular population is high or low. Table 4 depicts the summary of the MAR index value, which varied within the range of 0.25 to 0.75. Maximum 31.58% of strains exhibited resistance to six different antibiotics, and 5.26% showed resistance to seven, eight or nine different antibiotics. All of the *E. coli* isolates scores with MAR index above 0.2

Table 4. Multiple Antibiotic Resistance Index (MAR Index) of resistant *E. coli* isolates

No. of isolates	% of isolates	No. of the antibiotics to which the isolates were resistant	MAR Index
4	21.05	3	0.25
2	10.53	4	0.33
4	21.05	5	0.42
6	31.58	6	0.50
1	5.26	7	0.58
1	5.26	8	0.67
1	5.26	9	0.75

indicate resistance to six different antibiotics, and 5.26% showed resistance to seven, eight, or nine different antibiotics. All of the *E. coli* isolate scores with a MAR index above 0.2 indicate that the strain of a particular bacteria evolved from such an environment where multiple antibiotics are frequently used. Somehow there is a misuse or overuse of antibiotics in fish farms and related water bodies. It is hard to predict the source and routes of contamination until extensive surveillance is conducted to determine the presence and dissemination of antibiotic-resistant *E. coli.* The involvement of raw or frozen fishes in the epidemiological pathways for foodborne disease transmission has already been reported (Fleming et al., 2018). Foodborne illness related to fresh fish consumption has not yet been traced in our region, or data on this issue is still lacking. In this respect, the bacteriological assessment of local fishes appears to be the foremost issue. This kind of study generates scientific facts that would help the authority to take proper steps to maintain the microbial quality of the fishes and the hygiene of fish markets and aquatic environments.

Conclusion

In conclusion, this comprehensive study reported the poor hygiene status of our domestic markets and the pitiable quality of fish by examining the microbial levels of candidate fishes that are higher than acceptable limits. The outcomes of the research highlight the potential food safety hazards associated with fish as well as also concern about the random use of antibiotics. Since there is a limitation of sample size, the study warrants the attention of authorities for further large-scale studies to continuously monitor the microbiological quality and safety of the fishes. Besides, finding out the source of contamination and routine examination of other foodborne pathogens related to fish shall focus on future research.

Acknowledgment

All the financial support for the research work was provided by the University Grant Commission (UGC) and the research cell of Jagannath University. The authors expressed their gratitude and thanks for the grant.

References

Adeleke EO and Omafuvbe BO. Antibiotic resistance of aerobic mesophilic bacteria isolated from poultry faeces. *Res. J. Microbiol.* 2011; 6(4): 356-365.

Ahmed T, Baidya S, Sharma BC, Malek M, Das KK, Acharjee M, Munshi SK and Noor R. Identification of drug-resistant bacteria Among Export quality shrimp samples in Bangladesh. *Asian J. Microbiol. Biotechnol. Environ. Sci.* 2013; 15(4): 655-660.

Assefa A, Regassa F, Ayana D, Amenu K and Abunna F. Prevalence and antibiotic susceptibility pattern of *Escherichia coli* O157: H7 isolated from harvested fish at Lake Hayq and Tekeze dam, Northern Ethiopia. *Heliyon.* 2019; 5(12): e02996.

Barrett KA, Nakao JH, Taylor EV, Eggers C and Gould LH. Fish-associated foodborne disease outbreaks: United States, 1998-2015. *Foodborne Pathog. Dis.* 2017; 14(9): 537-543.

Bashar T and Fung IWH. Water pollution in a densely populated megapolis, Dhaka. *Water*. 2020; 12(8): 1-13.

Bauer AW, Kirby WMM, Sherris JC and Turck AM. Antibiotic Susceptibility Testing by a Standardized Single Disk Method. *Am. J. Clin. Pathol.* 1966; 45(3): 493-496.

Begum M, Tweb A, Ahmed A, Das M, Parveen S. A comparative microbiological assessment of five types of selected fishes collected from two different Market. *Adv. Biol. Res*. 2010; 4(5): 259-265.

Begum MK, Chowdhury MM, Haque W and Nasrin T. Comparative microbiological assessment of export oriented fishes and locally marketed fishes of Bangladesh. *IOSR J. Pharm. Biol. Sci.* 2015; 10(3): 17-23.

Boss R, Overesch G and Baumgartner A. Antimicrobial resistance of *Escherichia coli*, Enterococci, *Pseudomonas aeruginosa,* and *Staphylococcus aureus* from raw fish and seafood imported into Switzerland. *J. Food Prot.* 2016; 79(7): 1240-1246.

Cardozo MV, Borges CA, Beraldo LG, Maluta RP, Pollo AS, Borzi MM, Santos LFD, Kariyawasam S and de Avila FA. Shigatoxigenic and atypical enteropathogenic *Escherichia coli* in fish for human consumption. *Braz J. Microbiol.* 2018; 49(4): 936-941.

Cheesbrough M. *Medical Laboratory Manual for Tropical Countries Vol. II*. 1st ed.; London: Tropical Health Technology, 1984.

Clinical and Laboratory Standards Institute (CLSI). *Performance standards for antimicrobial susceptibility testing*: 22nd informational supplement, M100-S22. Wayne, PA: CLSI; 2012.

Costa RA. *Escherichia coli* in seafood: A brief overview. *Adv. Biosci. Biotechnol.* 2013; 4(3): 450-454.

DoF. *Yearbook of Fisheries Statistics of Bangladesh*, 2017-2018. Fisheries Resources Survey System (FRSS), Department of Fisheries. Ministry of Fisheries, Govt. of Bangladesh. 2018, Vol. 35, P. 129.

Dutta C, Manna SK, Panigrahi AK and Sengupta C. Microbiological quality of fish and shellfish with special reference to Vibrio parahaemolyticus in domestic markets of West Bengal, India. *Int. J. Curr. Microbiol. Appl. Sci.* 2018; 7(10): 2772-2783.

Dutta C. Prevalence of *Escherichia coli* in fish and shrimps obtained from retail fish markets in & around Kolkata, India. *Front. Environ. Microbiol.* 2016; 2(1): 1-5.

FAO, WFP and IFAD. The State of Food Insecurity in the World 2012. Economic growth is necessary but not sufficient to accelerate reduction of hunger and malnutrition. Rome, 2012.

FAO. Microbiological analysis, Chapter 4. In: *Manuals of food quality control*, Rome, 1992.

Fleming LE, Katz D, Bean JA and Hammond R. Epidemiology of seafood poisoning. In: *Foodborne Disease Handbook*. CRC Press; 2018. P. 287-310.

Founou LL, Founou RC and Essack SY. Antibiotic resistance in the food chain: A developing country-perspective. *Front. Microbiol.* 2016; 7: 1-19.

Krumperman PH. Multiple antibiotic resistance indexing of *Escherichia coli* to identify high-risk sources of fecal contamination of foods. *Appl. Environ. Microbiol.* 1983; 46(1): 165-170.

Kumar HS, Parvathi A and Karunasagar I. Prevalence and antibiotic resistance of *Escherichia coli* in tropical seafood. *World J. Microbiol. Biotechnol.* 2005; 21(5): 619-623.

Ng C, Chen H, Goh SG, Haller L, Wu Z, Charles FR, Trottet A and Gin Karina. Microbial water quality and the detection of multidrug resistant *E. coli* and antibiotic resistance genes in aquaculture sites of Singapore. *Mar Pollut Bull.* 2018; 135: 475-480.

Nowsad AAKM, Hossain MM, Hassan MN, Sayem SM and Polanco JF. Assessment of post harvest loss of wet fish: a novel approach based on sensory indicator assessment. *SAARC J. Agric.* 2015; 13(1): 75-89.

Onyuka J, Kakai R, Onyango D, Arama P, Gichuki J and Ofulla AVO. Prevalence and antimicrobial susceptibility patterns of enteric bacteria isolated from water and fish in lake Victoria Basin of Western Kenya. *World Acad. Sci. Eng. Technol.* 2011; 51: 761-768.

Pinu FR, Yeasmin S, Bari ML and Rahman MM. Microbiological conditions of frozen shrimp in different food market of Dhaka city. *Food Sci. Technol. Res.* 2007; 13(4): 362-365.

Price RG and Wildeboer D. *E. coli* as an indicator of contamination and health risk in environmental waters, Chapter 7. In: *Escherichia coli - Recent Advances on Physiology, Pathogenesis and Biotechnological Applications.* Intech, 2017; P.125-139

Ribeiro LF, Barbosa MMC, de Rezende Pinto F, Guariz CSL, Maluta RP, Rossi JR, Rossi GAM, Lemos MVF and do Amaral LA. Shiga toxigenic and enteropathogenic *Escherichia coli* in water and fish from pay-to-fish ponds. *Lett. Appl. Microbiol.* 2016; 62(3): 216-220.

Ryu SH, Park SG, Choi SM, Hwang YO, Ham HJ, Kim SU, Lee YK, Kim MS, Park GY, Kim KS and Chae YJ. Antimicrobial resistance and resistance genes in *Escherichia coli* strains isolated from commercial fish and seafood. *Int. J. Food Microbiol.* 2012; 152(1-2): 14-18.

Sarkar S, Dey SK, Nipu MAI, Brishti PS and Billah MB. Microbiological assessment of Nile tilapia *Oreochromis niloticus* collected from different super shops and local market in Dhaka, Bangladesh. *J. Fish.* 2020; 8(2): 782-791.

Singh AS, Nayak BB and Kumar SH. High prevalence of multiple antibiotic-resistant, Extended-Spectrum β-Lactamase (ESBL)-producing *Escherichia coli* in fresh seafood sold in retail markets of Mumbai, India. *Vet. Sci.* 2020; 7(2): 46.

J. Bangladesh Acad. Sci. 46(1); 19-29: June 2022 DOI: 10.3329/jbas.v46i1.59052

Journal of Bangladesh Academy of Sciences

Journal homepage: http://www.bas.org.bd/publications/jbas.html

Research Article

Recycling of waste or crude lubricating oil by vacuum distillation to produce reusable lubricants and its economic viability evaluation

Md. Rajibul Akanda*, Md. Hasan and Md. Abdur Rouf[1]

Department of Chemistry, Jagannath University, Dhaka, Bangladesh

ARTICLE INFO

Article History

Received: 7 April 2022
Revised: 25 May 2022
Accepted: 12 June 2022

Keywords: Lubricant oil, Recycling, Vacuum distillation, Economic viability, Reusable.

ABSTRACT

Recycling waste or crude lubricant oil is the best alternative to incineration. This article used the vacuum distillation method to recycle of waste lubricant oil. About 90% of lubricating oil was recovered from waste oil within the temperature range of 60-360 ^{0}C. Every measured property like density, viscosity, flash point, pour point, sulfur content, carbon residue, ash content, and water content were investigated and compared with fresh oil. Pour point was found not to improve through vacuum distillation but rather decreased. Similarly, vacuum distillation could not improve the viscosity and density of recycled material but rather decreased. Adding 2% EPDM, SPO ESPRENE V0141, and pellet form of rubber as additives increased those two properties significantly. Finally, 0.1% $NaNO_3$ was also added as an antioxidant. So, lastly, it can be concluded that the vacuum distillation process can effectively recycle waste lubricant oil in an economical and environmentally friendly manner.

Introduction

Global industrialization, urbanization, and mechanization of agriculture increase the volume of used lubricating oil produced each year. The used lubricant oil contains water, salt, broken down additive components, varnish, gum, and other materials (Durrani et al., 2011). Waste lubricating oil refers to the engine oil, transmission oil, hydraulic, and cutting oil after use. It is also referred to as the degradation of the fresh lubricating components that are contaminated by metals, ash, carbon residue, water, varnish, gums, and other contaminating materials, in addition to asphaltic compounds which result from the bearing surface of the engines (Riyanto et al., 2018). This waste engine oil may harm the environment when dumped into the ground or water streams, including sewers, resulting in soil and groundwater contamination (Udonne and Onwuma, 2014). Recycling such contaminated waste oil and reuse of recycled lubricant is highly beneficial not only in reducing engine oil costs and has a significant positive impact on the environment (Lolos et al., 2010; Boughton and Horvath, 2004).

A large amount of waste engine oils have a significant impact on the economy and the environment. They cost millions of dollars to manufacture and represent a high pollutant material when disposed of. If discharged into the land, water, or even burnt as a low-grade fuel, this may cause serious pollution problems because they release harmful metals and other pollutants into the environment (Martins, 2019). Also, due to oxidation or thermal degradation, many impurities are generated in lubricating oil during its application in internal combustion engines. These impurities contain unsaturates, aldehydes, phenolic compounds, alcohols, acidic compounds, and unsafe hydrocarbons products. In addition, used oil absorbs nitrogen oxides and exhaust gases from acidic fuel combustion. Besides, dust, fuel, lubricating oil additives degradation products, and fuel additives regularly decrease the

*Corresponding author: <rhakanda@gmail.com, rhakanda@chem.jnu.ac.bd>

[1]Institute of Fuel Research & Development (IFRD), BCSIR, Dhaka, Bangladesh

lubricating oil performance. Moreover, the viscosity increases by producing of an asphalt-like sludge, in which metallic scrapings act as catalysts at the high operating temperature and oxygen vicinity (Bridjanian and Sattarin, 2006). This used oil needs proper management to make it a valuable product by minimizing the quality of oil being improperly disposed of and reducing the waste oils environmental burden. Therefore, many studies have been done on the recycling of used oil, its management, and its economic viability worldwide, and still going on (Sánchez-Alvarracín et al., 2021; Jafiri and Hasanpour, 2015; Pinheiro et al., 2021).

The used oil was burned initially to produce energy, and later this oil was re-blended to engine oil after treatment.

Recycling of used oil has been carried out by several methods. Oil re-refining is one of the most important recycling technologies used so far. During oil re-refining, the mechanical, physical, and chemical contaminations are removed with the following processes: distillation, clay treatment, and hydrogenation (Kamal and Khan, 2009; Josiah and Ikiensikimama, 2010), acidic refining (Kamal and Khan, 2009; Abdel-Jabbar et al., 2010), solvent refining (Durrani et al., 2012; Ogbeide, 2010) or combinations of the formers. These processes have different yield and product properties, construction, and operational cost. In Bangladesh, yearly lube oil consumption increases by 12% against a 3.42% global rate (Islam et al., 2021). About 23.62 thousand barrels of crude oil are imported per day (Source: The United States Energy Information Administration). Proper recycling can minimize the cost of importing. A recommended solution for this issue is recovering the lubricating oil from the waste oil. Recycling processes using nontoxic and cost-effective materials can be an optimum solution. Acid clay has been used as a recycling method for used engine oil for a long time. This method has many disadvantages, it also produces many pollutants, is unable to treat modern multi-grade oils, and is difficult to remove asphaltic impurities (Fox, 2007). Solvent extraction has replaced acid treatment as the method of choice for improving the oxidative stability and viscosity/ temperature characteristics of base oils. The solvent selectively dissolves the undesired aromatic components (the extract), leaving the desirable saturated components, especially alkanes, as a separate phase (the raffinate) (Rincon et al., 2005a). In another study, a mixture of methyl ethyl ketone (MEK) and 2-propanol was used as an extracting material for recycling used engine oils (Rincon et al., 2005b).

Although the acid clay method produces comparable oil to that of fresh one but is highly expensive. Expensive solvents and vacuum distillation are required to carry out this method (Shakirullah et al., 2006; Udonne, 2001). Recently propane was used as a solvent (Ghosh et al., 2011). Propane can dissolve paraffinic or waxy material and immediately dissolves oxygenated material. Asphaltenes, which contain heavy condensed aromatic compounds and particulate matter, are insoluble in liquid propane. These properties make propane ideal for recycling the used engine oil, but many other issues must be considered. Propane is hazardous and flammable; therefore, this process is regarded as a hazardous process. Also, the extraction involves solvent losses and highly skilled operating maintenance.

In addition, extraction occurs at higher pressures and requires high pressure sealing systems, making solvent extraction plants expensive to construct and operate. The method also produces remarkable amounts of hazardous by-products (Rincón et al., 2003). Membrane technology is another method for the regeneration of used lubricating oils. The process is a continuous operation as it removes metal particles and dust from used engine oil and improves the liquidity and flashpoint of the recovered oils. Despite the above-mentioned advantages, the expensive membranes may get damaged and fouled by large particles (Dang, 1997). It was found that distillation/clay and activated/charcoal could be recovered from 80% lubricant oil and acid/clay method to about 50%

(Abdulkareem et al., 2014). Vacuum distillation and hydrogenation are two other methods that can be used for recycling used engine oil (Vasiliadou, 2021). The Kinetics Technology International (KTI) process combines vacuum distillation and hydro-finishing. This method removes most of the contaminants from the waste oil. The process starts with atmospheric distillation to eliminate water and light hydrocarbons. This is then followed by vacuum distillation at a temperature of 250 °C. The final stage is the hydrogenation of the products to eliminate the sulfur, nitrogen, and oxygenated compounds. This stage is also used to improve the color and odor of the oil. The product can be of quality standard (Gp.I) with a yield of approximately 82% and minimized polluting by-products (Vasiliadou, 2021, Sinağ et al., 2010). This article investigated the impact of vacuum distillation on recycling waste and crude lubricant oil to find optimum recycling.

Material and Apparatus

Waste lubricant oil from local market of Dholaikhal, old Dhaka, crude oil from the garage of Dholaikhal, old Dhaka, 2% EPDM, SPO ESPRENE V0141 rubber pellet from Sumitomo chemical company of japan, $NaNO_3$ from sigma USA. Fuller's earth powder from Neel Kanth Minechem India, Electric balance from Unilab pharmaceutical and chemical Pvt Ltd India, Cloud And Pour Point Apparatus from Hamco, India, Abels Flash Point Apparatus from alfa engineering solution, Maharastra, India, Bomb calorimeter from Advance research instrument company, Oune India, Vacuum distillation plant (ASTM D1160) from India, Distilled water plant (model: Basic/PH4 Pure-HIT still) was purchased from Glasco Company Ltd., UK, viscometer and pycnometer from Indiamart, Centrifuge machine (model no. PSM-LE018), Uttar Pradesh, India.

Experimental methods

Collection of waste lubricating oil

To recycle, two waste oil samples are collected. One is collected from the Market after being used in small machinery and another (crude) from the garage after being used in vehicles. Then preliminary these two waste oil properties were analysed.

Analysis of properties: The different properties like density (by pycnometer), viscosity (by viscometer), pour point (by Cloud And Pour Point Apparatus), flash point (by Abels Flashpoint Apparatus), sulfur content (by bomb calorimeter), water content, carbon content and ash content of the waste and crude lubricant oil has been evaluated through traditional methodologies.

Vacuum distillation process: In vacuum distillation, the samples (the waste oil and crude oil) were not subjected to temperatures above 370 to 380 °C because the high molecular weight components in the crude oil will undergo thermal cracking and form petroleum coke at temperatures above that. A vacuum pressure of about 6 mm Hg was maintained in each vessel. After the vacuum distillation, 2% EPDM, SPO ESPRENE V0141 rubber pellet was added as additives or viscosity modified, and 1% of Fuller's earth was used as the bleaching agent. Then 0.1% $NaNO_3$ was used as an anti-oxidant and stirred very well. The retention time in each vessel was maintained about 30 to 40 minutes. A filtration centrifuge of 6000 rpm was used to sediment or sludge out. The whole recycling process by vacuum distillation is schematically represented in Fig. 1.

Result and discussion

Properties investigation of lubricant oils: The properties of waste lubricant oils (market waste oil and crude oil) were evaluated and a vacuum distillation process was carried out to refine the oil. After that, the properties were evaluated and compared with the standard. All the measured properties are included in Table-1. The effect of the vacuum distillation on lubricant oil has been visualized from their values before and after vacuum distillation. Moreover, the effect of temperature has also been investigated, and the density and viscosity were found to decrease with temperature (Fig. 2-A,B).

Table 1. Properties of Market waste oil and crude oil before and after vacuum distillation compared to standard

Properties	Market waste oil		Crude oil		Standard value
	Before vacuum distillation	After vacuum distilled	before vacuum distillation	After vacuum distilled	
Density (g/ml)	0.880 (15°C),	0.877 (15°C),	0.8496 (15°C),	0.794 (15°C),	0.90 (15.5°C)
	0.876 (20°C),	0.867 (20°C),	0.8467 (20°C),	0.792 (20°C),	
	0.873 (25°C),	0.859 (25°C),	0.8435 (25°C),	0.790 (25°C),	
	0.870 (30°C),	0.851 (30°C),	0.8407 (30°C),	0.788 (30°C),	
	0.865 (40°C),	0.839 (40°C),	0.8354 (40°C),	0.787 (40°C),	
	0.860 (50°C)	0.787 (50°C)	0.8294 (50°C)	0.785 (50°C)	
Viscosity (cSt)	342.3405 (15°C),	316.29 (15 °C),	108.8503 (15 °C)	81.694 (15 °C),	Up to 210 (40 °C)
	284.9523 (20°C),	261.37 (20 °C),	85.5414 (20 °C),	68.342 (20 °C),	
	211.0863 (25°C),	230.59 (25 °C),	70.6056 (25 °C),	60.109 (25 °C),	
	147.6384 (30°C),	178.98 (30 °C),	60.1958 (30 °C),	54.085 (30 °C),	
	100.0032 (40°C),	92.332 (40 °C),	39.8288 (40 °C),	36.208 (40 °C),	
	57.9564 (50°C),	43.088 (50 °C)	29.1927 (50 °C),	27.156 (50 °C),	
	25.8640 (100 °C)	25.095 (100 °C)	8.3731 (100 °C)	7.920 (100 °C)	
Pour point	-14 °C	-16 °C	-15 °C	-20 °C	-9 °C
Flash and Fire point	66 °C and 70°C	152 °C and 154 °C	34 °C and 37 °C	130 °C and 134 °C	>188 °C
Sulphur content (wt %)	1.02 %	0.46 %	2.25 %	0.67 %	nil
Water Content (v/v)	Trace amount	Nil	2 %	Nil	< 0.20
Carbon residue (wt %)	2 %	1 %	2.99 %	0.2 %	nil
Ash content (wt %)	1 %	0.5 %	1.159 %	0.13 %	0.01 %
Range	IBP (100 °C),	IBP (70 °C),	IBP (70 °C),	IBP (60 °C),	
	5 % (236 °C),	5 % (210 °C),	240 °C (5 %),	5 % (200 °C),	
	10 % (242 °C),	10 % (223 °C),	260 °C (10 %)	10 % (212 °C),	
	15 % (254 °C),	15 % (241 °C),	268 °C (15 %),	15 % (230 °C),	
	20 % (270 °C),	20 % (260 °C),	275 °C (20 %),	20 % (243 °C),	
	30 % (312 °C),	30 % (280 °C),	280 °C (30 %),	30 % (260 °C),	
	40 % (314 °C),	40 % (301 °C),	286 °C (40 %),	40 % (266 °C),	
	50 % (344 °C),	50 % (309 °C),	291 °C (50 %),	50 % (280 °C),	
	60 % (344 °C),	60 % (319 °C),	310 °C (60 %),	60 % (300 °C),	
	70 % (344 °C) ,	70 % (333 °C),	330 °C (70 %),	70 % (315 °C),	
	80 % (360 °C)	80 % (348 °C)	341 °C (80 %),	80 % (338 °C)	
		90 % (360°C)	360 °C (90 %)	90 % (360 °C)	

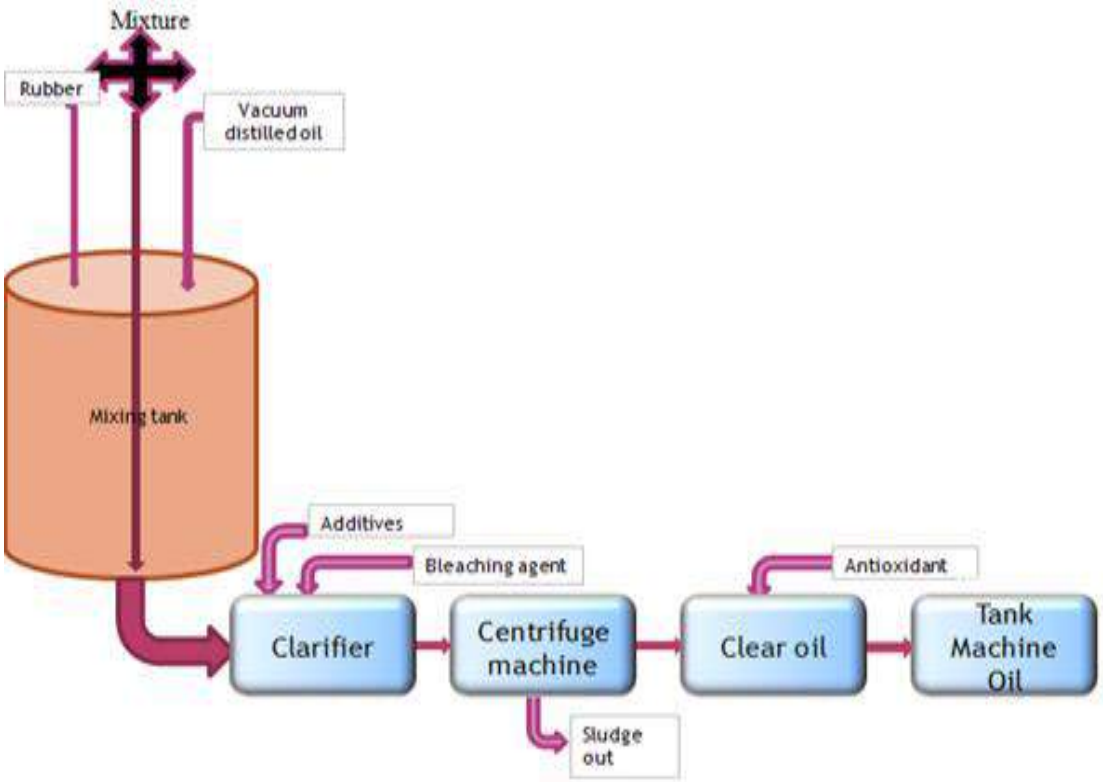

Fig. 1. Pictorial representation of the recycling plant for the preparation of lubricating oil from waste oil by vacuum distillation.

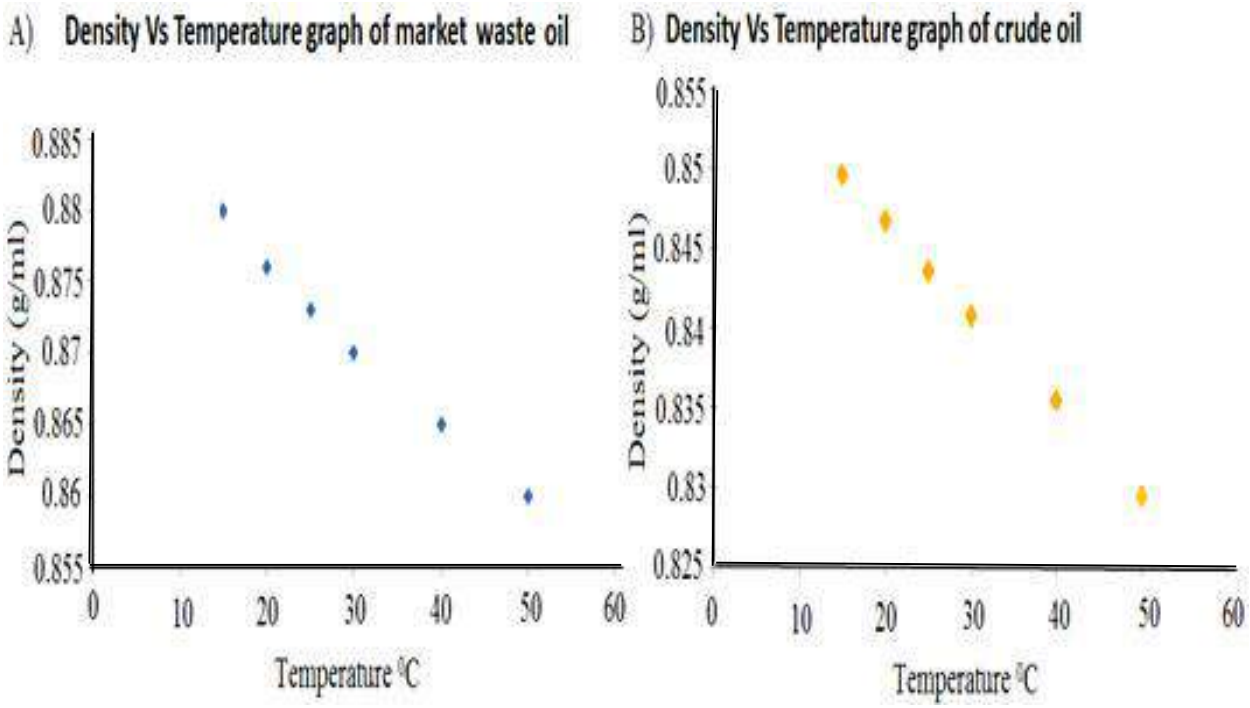

Fig. 2. Effect of temperature on the density of A) Market waste lubricating oil and Crude oil.

Investigation of the effect of rubber on density and viscosity: All properties except density and viscosity are improved after vacuum distillation. Therefore rubber pellets were used as additives or a viscosity modifier. And it has been found to significant improve of the viscosity and density of the lubricant oils after the rubber is added, as shown in Table 2 and Fig. 3 and Fig. 4, respectively.

Overall comparison of the lubricant oils: Finally, the effect of vacuum distillation and rubber addition on the properties in terms of density (Fig. 5A) and viscosity (Fig. 5B) with fresh oil, non distilled market waste oil and crude oil, and vacuum distilled market waste oil and crude oil respectively. It has been found from the study that density values when rubber is added to vacuum distilled oil are comparable to the fresh oil, and viscosity values when rubber is added to vacuum distilled oil are superior to the fresh oil. The impact of vacuum distillation on flash points and pour points, have also been evaluated. From the experimental data, it can be clearly said that vacuum distillation can improve the flash point value of crude oil and is close to fresh oil (Fig. 6A), but the pour point value is significantly decreased (Fig. 6B).

Moreover, it has been found that market waste oil and crude have a significant amount of sulphur content though vacuum distillation can cause a lowering of sulphur content but not that much (Fig. 7A). Interestingly, carbon residue could be significantly decreased and comparable to fresh oil (Fig. 7B). Besides, ash content could also be significantly decreased by vacuum distillation compared to non-distilled market waste oil and crude oil (Fig. 8A). Finally, water content was found significant in crude oil only compared to fresh oil and market waste oil. But vacuum distillation could remove water content almost completely (Fig. 8B).

Table 2. Rubber Added oil density and Viscosity

Properties	Market Waste oil	Crude oil	Standard value
Density (g/ml)	0.890 (15°C),	0.886 (15°C),	0.90 (15.5°C)
	0.881 (20°C),	0.875 (20°C),	
	0.876 (25°C),	0.865 (25°C),	
	0.872 (30°C),	0.854 (30°C),	
	0.866 (40°C),	0.843 (40°C),	
	0.861 (50°C)	0.830 (50°C)	
Viscosity (cSt)	720.8051 (15°C),	360.0021 (15°C),	Up to 210 (40°C)
	588.0870 (20°C),	295.1073 (20°C),	
	452.6661 (25°C),	224.6521 (25°C),	
	355.1250 (30°C),	191.0543 (30°C),	
	223.4923 (40°C),	160.9630 (40°C),	
	157.6782 (50°C),	127.0503 (50°C),	
	89.3412 (100°C)	60.6412 (100°C)	

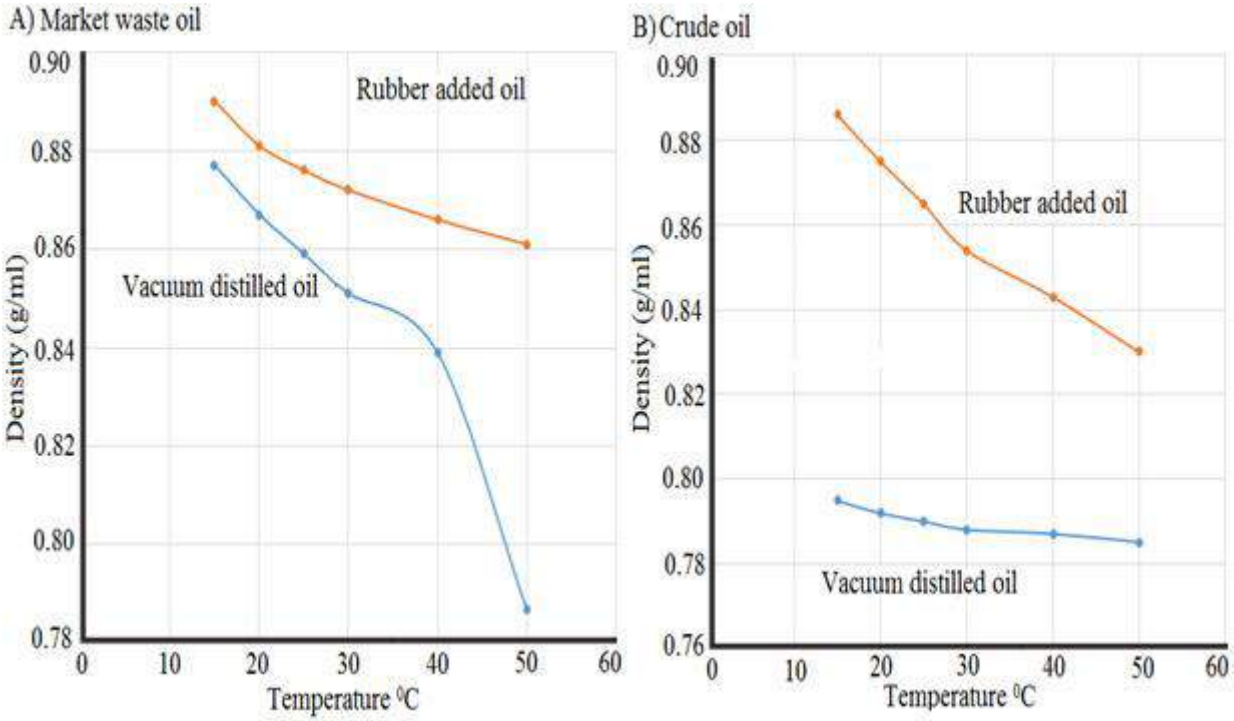

Fig. 3. Effect of temperature on the density of vacuum distilled (A) Market waste lubricating oil and (B) crude oil and after adding rubber, respectively

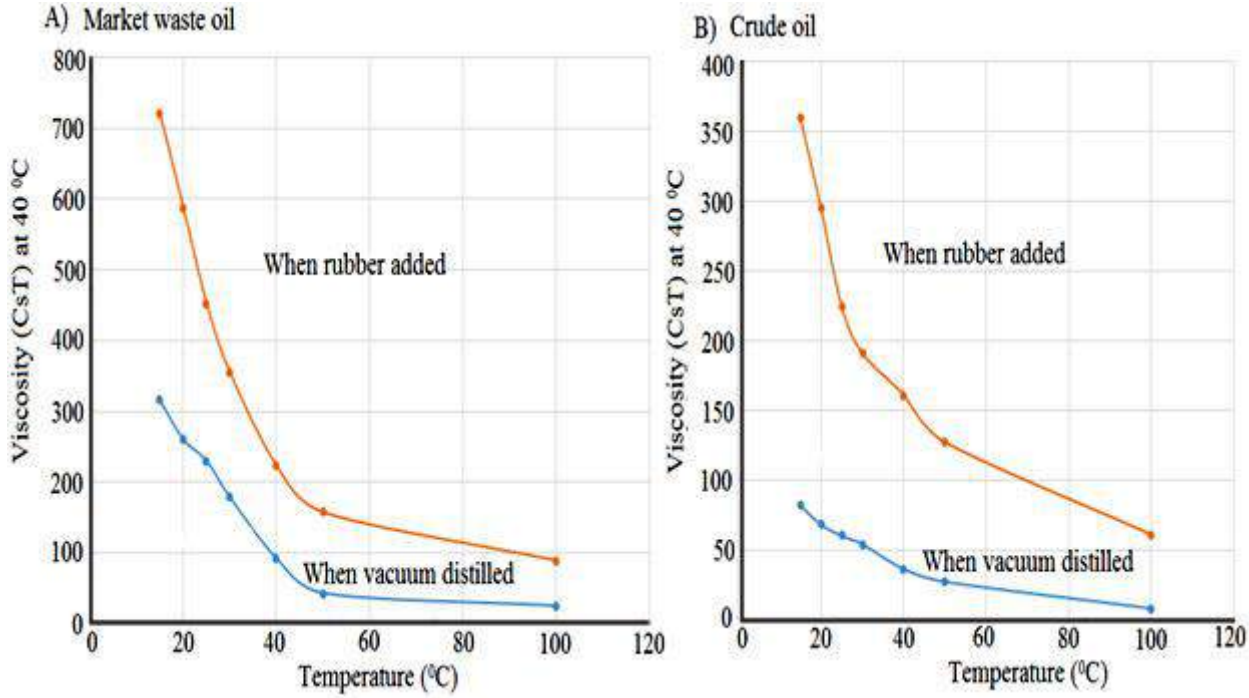

Fig. 4. The effect of temperature on the viscosity of vacuum distilled A) Market waste lubricating oil and crude oil and after adding rubber, respectively.

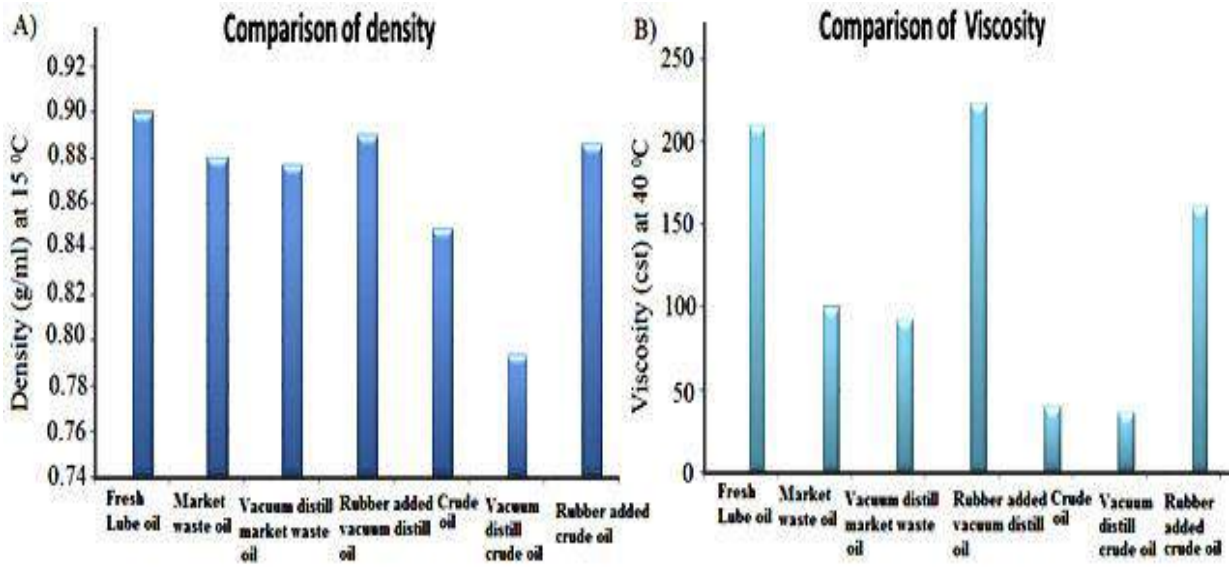

Fig. 5. Comparison of (A) the density and (B) the viscosity of rubber added market waste oil and crude oil with vacuum distilled oil, non-distilled oil and fresh oil, respectively.

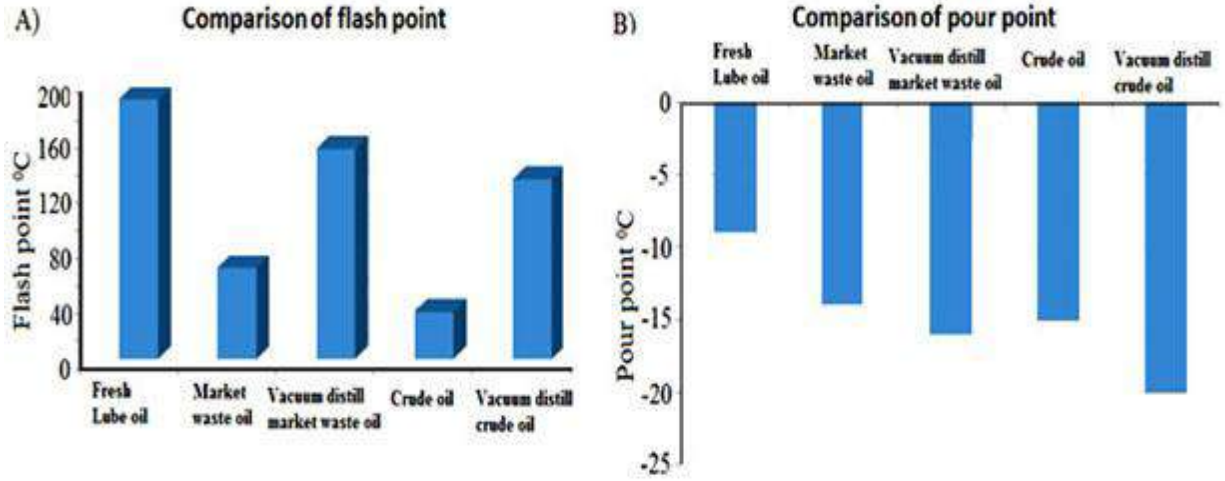

Fig. 6. Comparison of the (A) flash point and (B) pour point of market waste oil and crude oil with vacuum distilled oil and fresh oil, respectively

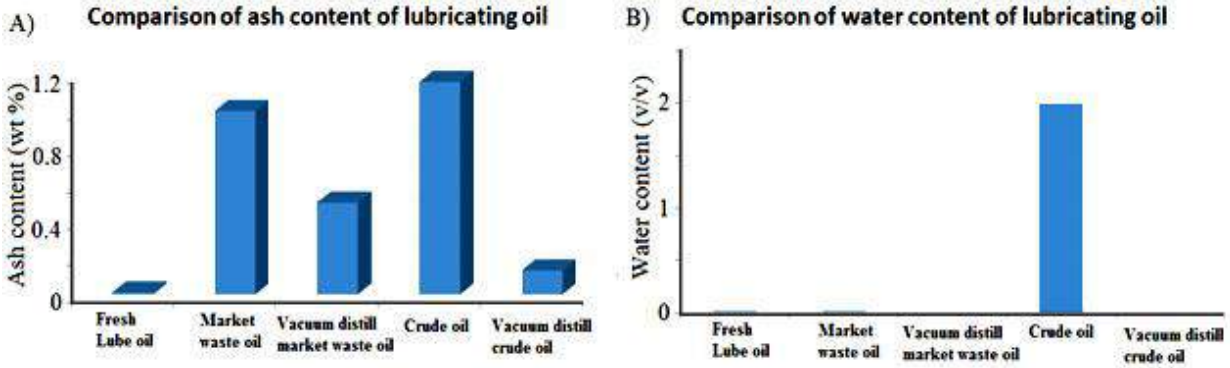

Fig. 7. Comparison of the sulphur content and carbon residue content of market waste oil and crude oil with vacuum distilled oil and fresh oil, respectively.

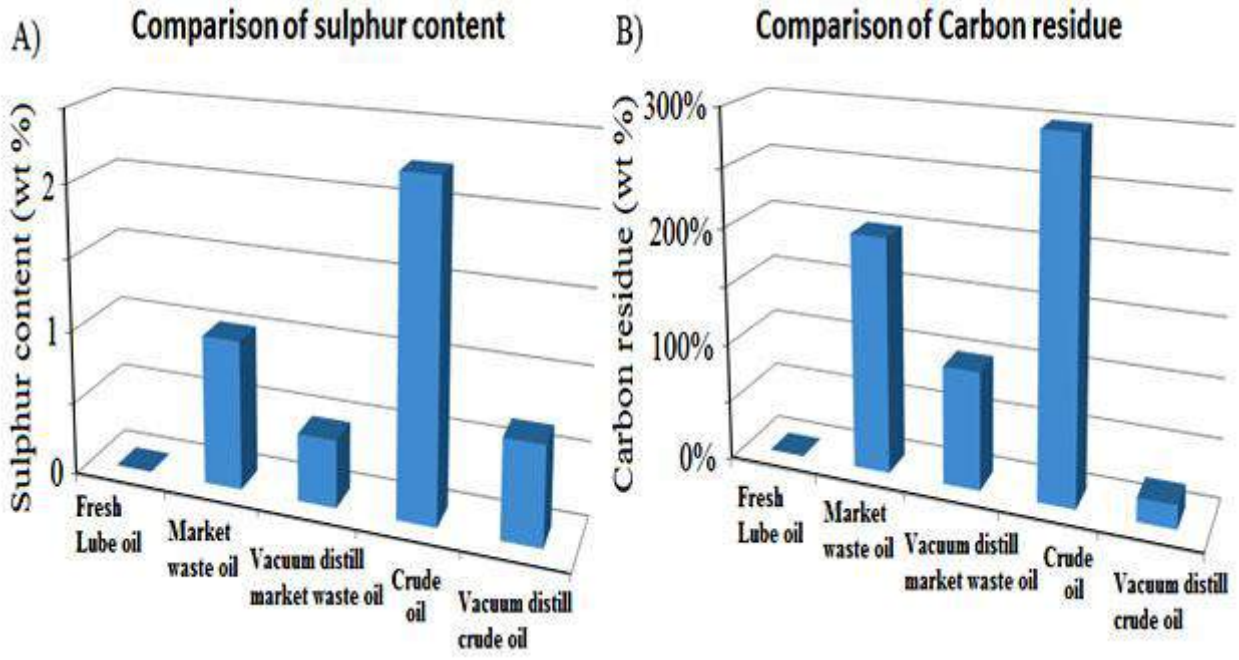

Fig. 8. Comparison of the ash content and water content of market waste oil and crude oil with vac distilled oil, and fresh oil, respectively.

Economic viability investigation

After analyzing all the data, it was noticed that the vacuum distillation process was found to be the best method to improve the properties of waste lubricant oil to lubricant. A large amount of waste oils is generated every day, and a vacuum distillation-based small-scale recycling plant can be an excellent and cost-effective option for oil Recovery. The total production cost of preparing lubricating oil is 100 taka per liter, whereas, in comparison to the market, its cost is above 300 takas. That means it is economical to use and profitable for business purposes. An economic analysis of the recycling of lubricant oil from waste and crude lubricant oil-based small-scale batch plants is described below in Table 3.

Table 3. The total production cost of lubricating oil from waste oil in a small scale-batch plant.

Raw materials	Amount	Cost (Taka)
Waste lube oil	1000 ml	45.00
Rubber	20 gm	10.00
Fuller Earth	10 gm	20.00
Colour	0.125 gm	0.50
Container	1 liter per piece with cap	18.00
Label	1 liter pack	1.50
Outer carton	1 liter pack (24 piece)	1.46
Sealing	1 liter pack	0.30
Other cost		4.24

Total production cost per liter = 100.00

Conclusion

In this research, recycling lubricating oil from waste lubricating oil has successfully done by vacuum distillation method. By this method, 90% of lubricating oil has recovered from waste oil much better than the reported one, about 62 to 66% (Rahman et al., 2008). Every measured property like density, viscosity, flash point, water content, carbon residue, ash content, and sulphur content has developed, which are close to standard value. But the pour point has decreased. However, the vacuum distillation viscosity and density of recycled oil have decreased by the using of 2% EPDM, SPO ESPRENE V0141, pellet form, Mooney viscosity of

OCP as viscosity modifier, viscosity and density has increased before that by the centrifugation sludge have removed. After that, 0.1% $NaNO_3$ was added as an antioxidant. So, finally, it can be said by the vacuum distillation process that waste oil can be effectively recycle, and it is so much economical to use and environmentally friendly.

Acknowledgment

We would like to thank BCSIR, Dhaka, Bangladesh, for the instrumental support.

Conflict of Interest

The authors declared that they have no conflict of interest.

Author's contribution

M.R. Akanda contributes to conceptualization, supervision, and manuscript drafting, M. Hasan contributes to carrying out the whole experiment, and M.A. Rouf contributes to conceptualization, supervision, and instrumental support from BCSIR.

References

Abdel-Jabbar NM, Al Zubaidy EAH and Mehrvar M. Waste lubricating oil treatment by adsorption process using different adsorbents. Int. J. Chem. Mol. Eng. 2010; 4(2): 141-144.

Abdulkareem AS, Afolabi AS, Ahanonu SO and Mokrani T. Effect of treatment methods on used lubricating oil for recycling purposes. *Energ. Source Part A* 2014; 36: 966-973.

Boughton B and Horvath A. Environmental assessment of waste oil management methods. *Environ. Sci. Technol.* 2004; 38: 353-358.

Bridjanian H and Sattarin M. Modern recovery methods in used oil re-refining. *Pet. Coal* 2006; 48(1): 40-43.

Dang CS. Re-refining of used oils- A review of commercial processes. *Tribotest* 1997; 3: 445-457.

Durrani HA, Panhwar MI and Kazi RA. Re-refining of waste lubricating oil by solvent extraction. *Mehran Univ. Res. J. Eng. Technol.* 2011; 30(2): 237-246.

Durrani HA, Panhwar MI and Kazi RA. Determining an efficient solvent extraction parameters for re-refining of waste lubricating oils. *Mehran Univ. Res. J. Eng. Technol.* 2012; 31(2): 265-270.

Fox MF. Sustainability and environmental aspects of lubricants. In: *Handbook of Lubrication and Tribology*, George ED, Totten E, eds.; Taylor and Francis: New York, USA, 2007.

Ghosh P, Das T and Nandi D. Synthesis characterization and viscosity studies of homopolymer of methyl methacrylate and copolymer of methyl methacrylate and styrene. *J. Solut. Chem.* 2011; 40: 67-78.

Islam MS, Sanzida N, Rahman MM and Alam MD. From the value chain to environmental management of used lube oil: A baseline study in Bangladesh. *Case Stud. Chem. Environ. Eng.* 2021; 4: 100159.

Jafiri AJ and Hasanpour M. Analysis and comparison of used lubricants, regenerative technologies in the world. *Resour. Conserv. Recycl.* 2015; 103: 179- 191.

Josiah PN and Ikiensikimama SS. Effect of desludging and absorption ratios on recovery of low pour fuel oil (LPFO) from spent engine oil. *Chem. Eng. Res. Bull.* 2010; 14: 24-28.

Kamal A and Khan F. Effect of extraction and adsorption on re-refining of used lubricating oil. *Oil Gas Sci. Technol.* 2009; 64(2): 191-197.

Lolos TH, Raptis CG, Lolos G, Tsompanidis C and Fragkakis P. The waste oil management plan of cyprus republic: technical and financial aspects of the proposed strategy. The *2nd International Conference on Hazardous and Industrial Waste Management Chania*, Greece, 2010.

Martins JP. The extraction-flocculation re-refining lubricating oil process using ternary organic solvents. *Ind. Eng. Chem. Res.* 1997; 36: 3854-3858.

Ogbeide SO. An investigation to the recycling of spent engine oil. *J. Eng. Sci. Technol.* 2010; 3(1): 32-35.

Pinheiro CT, Quina MJ and Gando-Ferreira LM. Management of waste lubricant oil in Europe: A circular economy approach. *Crit. Rev. Environ. Sci. Technol.* 2021; 18: 2015–2050.

Rahman MM, Siddiquee TA, Samdani S and Kabir KB. Effect of operating variables on regeration of base-oil from waste oil by conventional acid-clay method. *Chem. Eng. Res. Bull.* 2008; 12: 24-27.

Rincón J, Cañizares P and García MT and Garcia I. Regeneration of used lubricant oil by propane extraction. *Ind. Eng. Chem. Res.* 2003; 42: 4867-4873.

Rincón J, Cañizares P and García MT. Regeneration of used lubricating oil by polar solvent extraction. *Ind. Eng. Chem. Res.* 2005a; 44: 43-73.

Rincón J, Cañizares P and García MT. Waste oil recycling using mixtures of polar solvents. *Ind. Eng. Chem. Res.* 2005b; 44: 7854-7859.

Riyanto, Ramadhan B and Wiyanti D. Treatment of waste lubricating oil by chemical and adsorption process using butanol and kaolin. *IOP Conf. Ser.: Mater. Sci. Eng.* 2018; 349: 012054.

Sánchez-Alvarracín C, Criollo-Bravo J, Albuja-Arias D, García-Ávila F and Pelaez-Samaniego MR. Characterization of used lubricant oil in a latin-american medium-size city and analysis of options for its regeneration. *Recycling* 2021; 6(10): 1-22.

Shakirullah M, Ahmed I, Saeed M, Khan MA, Rehman H, Ishaq M and Shah AA. Environmentally friendly recovery and characterization of oil from used engine lubricants. *J. Chin. Chem. Soc.* 2006; 53: 335-342.

Sinağ A, Gülbay S, Uskan B, Uçar S and Özgürler SB. Production and characterization of pyrolytic oils by pyrolysis of waste machinery oil. *J. Hazard. Mater*. 2010; 173: 420-426.

Udonne JD. A comparative study of recycling of used lubrication oils using distillation, acid and activated charcoal with clay methods. *J. Pet. Sci. Eng.* 2001; 2(2): 12-19.

Udonne JD and Onwuma HO. A study of the effects of waste lubricating oil on the physical/ chemical properties of soil and the possible remedies. *J. Petroleum Gas Eng.* 2014; 5(1): 9-14.

Vasiliadou I. Waste engine oil recycling. *Adv. Recycling Waste Manag.* 2021; 6: 6.

J. Bangladesh Acad. Sci. 46(1); 31-43: June 2022 DOI: 10.3329/jbas.v46i1.60345

Journal of Bangladesh Academy of Sciences

Journal homepage: http://www.bas.org.bd/publications/jbas.html

Research Article

Protease from jute endophyte *Micrococcus luteus* MBL-Bac7 functions as a potential bating agent for the leather industry

Md. Enayet Ullah, Farhana Tasnim Chowdhury, Sharaf Aroni, Al Amin, Maqsud Hossain[1], Haseena Khan and Mohammad Riazul Islam[*]

Molecular Biology Laboratory, Department of Biochemistry and Molecular Biology, University of Dhaka, Dhaka, Bangladesh

ARTICLE INFO

Article History

Received: 17 April 2022
Revised: 29 May 2022
Accepted: 12 June 2022

Keywords: Jute endophytes, *Micrococcus luteus* MBL-Bac7, protease, bating agent.

ABSTRACT

Ever since the discovery of jute endophytes, testing their potential for commercial uses has been a matter of interest. Considering the same, jute endophyte *Micrococcus luteus* MBL-Bac7, capable of producing extracellular proteases, was selected for *in vitro* and *in silico* analysis to assess its role as a bating agent required in rawhide processing. The presence of extracellular protease was confirmed from the plate assay. As the enzyme is tested for commercial use, the effect of various metal ions and reaction conditions (pH, temperature) have been optimized. The protease activity appears to be retained even at 85°C. It also showed significant activity in a wide range of pH (pH 3.0-8.5). Metal ion Mn^{2+} increased the protease activity significantly, but Fe^{2+}, $Zn^{2+,}$ and Co^{2+} ions showed the opposite effect. Molecular identification of the protease was done from the whole genome sequence data. Using PSORTb v.3.0.2, SecretomeP-1.0, TMHMM-2.0, and protein molecular weight software, the physicochemical properties of the protease were predicted. The isolated protease shared a strong evolutionary link with Micrococcus species' S8 family serine peptidase. Finally, in the bating of cowhide, effects similar to that of commercial agents were obtained during finger prick, lastometer, and tensile tests. The findings of this study corroborate the possibility of using this protease as a potential bating agent. However, further studies are necessary to reduce the production cost for higher yield and commercialization.

Introduction

Endophytic bacteria are omnipresent in plants, residing either latently or actively colonising plant tissues both systematically and locally, without having any harmful effect on the plant. Reports say plants may harbour both Gram-positive and Gram-negative bacteria. However, many Gram-positive bacteria have biological control activities, such as *Bacillus*, *Brevibacteria*, and *Micrococcus* species are found inhabiting plants (Kobayashi and Palumbo, 2000). The jute (*Corchorus olitorius*) plant is home to a large number of endophytes, including both bacteria and fungi. Various biochemical and physiological tests suggest that these microbes may provide their host a wide range of benefits (Najnin et al., 2015). Among the significant benefits of endophytic bacteria, observed up to now, are growth stimulation in soya beans (Kuklinsky-Sobral et al., 2004), increasing nitrogen fixation in sugarcane (Boddey et al., 2003), assisting plants in obtaining nutrients, enhancing systemic resistance to pathogens and growth

[*]Corresponding author: <mriazulislam@du.ac.bd>

[1]Department of Biochemistry and Microbiology, School of Health and Life Sciences, North South University, Dhaka, Bangladesh.

promotion in rice (Madhaiyan et al., 2004), regulating phytohormones resulting in stress relief and increased root growth (Hardoim, 2011). Endophytes generate extracellular enzymes such as amylase, lipase, protease, xylanase, and esterases to hydrolyze different components and initiate resistance against plant invasions (Tan and Zou, 2001). Over the years, the use of bio-based chemicals has increased. New bio-products are being developed that can reduce the dependency on mineral fuels and provide a more reliable energy source (Carole, 2004). Efficient catalytic properties of enzymes have already promoted their use in various industrial processes (Beilen and Li, 2002). Selected microorganisms, including bacteria and fungi, have been explored globally for the biosynthesis of commercially viable preparations of enzymes for industrial uses (Saxena and Singh, 2011). Protease represents one of the largest groups among commercially important enzymes (Srilakshmi et al., 2015). Proteases can hydrolyze peptide bonds. Given its many applications, it has been employed in different industries. It is used in detergent industries to remove protein stains, in food industries, in the pulp and paper industries to remove biofilm, and especially in leather industries (Kirk et al., 2002). According to the commercial standing of Bangladesh, protease's largest market is the leather industry. One of the wet blue processing steps in the leather process is bating. To prepare leather with a certain degree of softness and pliable feel and a high-quality grain, the unhaired pelts must be subjected to bating following liming and de-liming. Protease is utilised in such processes. Since bating is a crucial stage in leather processing, and there is a large market for a protease that is currently occupied by the importation of protease, this study aims to establish protease from jute endophytic bacteria *Micrococcus luteus* MBL-Bac-7 as a compatible bating agent.

Methods and materials

Bacterial strain

Bacterial strain *Micrococcus luteus* MBL-Bac7 was taken from the jute endophytic bacterial library of the Molecular Biology Laboratory, Department of Biochemistry and Molecular Biology, University of Dhaka. This was previously isolated from jute in the same lab and stored in both LB agar and 30% glycerol stocks at -80°C.

Morphological analysis

MBL-Bac7 was cultured on a plate containing tryptic soy agar (TSA). A drop of water along with a loopful of bacteria was placed on a clear slide and spread very thinly. After the thin film dried, crystal violet was applied to the stain for 30 s and rinsed with water. Then it was covered with gram's iodine for another 30 s and again washed with water. Decolourisation was done with 90% ethanol for 30 s, which was later washed with water followed by staining with safranin. Further, it was stained for the 30s, washed with water, and allowed to dry. A coverslip was fixed on the stained bacteria with 60% glycerol. Finally, the slide was observed under a microscope.

Production of enzyme

The enzyme was produced by fermentation with bacteria in the presence of substrate, which is specific to the enzyme. For submerged fermentation media was prepared with glucose (1.0%), peptone (0.5%), yeast extract (0.5%), salt solution (5.0%). Salt solution was prepared with $MgSO_4.7H_2O$ (0.5%), KH_2PO_4 (0.5%), $FeSO_4.7H_2O$ (0.01%), and NaCl (0.01%). The components were mixed in Erlenmeyer flasks with distilled water, and pH was fixed around 7.0-7.2 and autoclaved to sterilise at 121ºC for 20 min. Then a loop of the bacterial colony was inoculated in liquid media and incubated at 37ºC with 2×g relative centrifugal force (RCF) for 24 h.

Isolation of enzyme

After incubation, the culture medium was centrifuged at 3920×g RCF for 10 min, and the supernatant was collected. The collected supernatant was measured in a measuring cylinder, and a required amount of ammonium sulphate for 80% saturation was

calculated. Ammonium sulphate was mixed with the collected supernatant and was aliquoted in different falcon tubes. After overnight incubation at 4ºC, they were centrifuged at 10000×g for 30 min, the supernatant was discarded, and the precipitated protein was dissolved in phosphate buffer.

Qualitative screening of the enzyme

The qualitative screening of the enzyme was carried out on the medium containing gelatin (1%), peptone (0.5%), yeast extract (0.5%), salt solution (5%) $MgSO_4.7H_2O$, (0.5%), KH_2PO_4, (0.5%), $FeSO_4.7H_2O$ (0.01%) NaCl) (0.01%) and agar (1.5%). Inoculation was done using 10.0 µL of an overnight liquid bacterial culture and incubated for one day. After one day of incubation, the plate was flooded with a saturated solution of ammonium sulphate [$(NH_4)_2SO_4$]. The gelatin unutilised by the bacteria was precipitated by $(NH_4)_2SO_4$, which created a clear zone around the bacterial colony.

Protease activity assay

Protease activity was measured by a slightly modified method of Cupp-Enyard. The reaction mixture was prepared by mixing 100.0 µL enzyme with 5 mL of 0.65% casein (Nacalai Tesque Inc., Japan) solution dissolved in phosphate buffer and incubated at 37ºC in a water bath for 10 min. The reaction was stopped with 5.0 mL of 110 mM trichloroacetic acid (TCA), which precipitated the proteins interrupting their activities, and incubated again under the same condition for 30 min. After incubation, 2 mL of supernatant was collected by centrifuging the mixture at 10000×g for 10 min. Meanwhile, standard samples were prepared with different amounts of L-tyrosine, making the volume up to 2.0 mL with distilled water where the concentration of a stock solution L-tyrosine (for use as a standard) was 1.1 mM. 5.0 mL 500 mM sodium carbonate and 1.0 mL Folin and Ciocalteu's phenol reagent (Sigma-Aldrich, USA) were added. Again, all the tubes were incubated at 37ºC for 30 min. Readings were taken in a spectrophotometer at 660 nm. A standard curve was prepared using the absorbance against different concentrations of tyrosine. Each µmole of tyrosine released by protease per min per mL was defined as one unit of protease.

Quantitation of protein content

The Bradford method was used to calculate protein content in the culture supernatant using bovine serum albumin (BSA) as a reference. The absorbance was taken at 595 nm, and the specific activity was measured in units per mg of protein.

Characterization of the protease

Effect of temperature on protease activity

To study the effect of various temperatures, crude protein extracts were taken in different falcon tubes and incubated at 37ºC, 45ºC, 60ºC, and 85ºC. The activity of protease was measured according to the procedure described above.

Effect of pH on protease activity

To study the effect of different pHs on protease, gelatin was used as a substrate instead of casein, as casein does not dissolve at a pH lower than 6.0. Gelatin was dissolved in pH 3.0, 4.0, 5.5, 6.5, 7.5, 8.5, and the activity of protease was measured according to the protocol explained before.

Effect of metal ions on protease activity

The effects of metal ions were studied by incubating 100.0 µL crude protease enzyme with 900.0 µL of 10 mM salt solutions for an hour, then the activity was measured following the method explained above. Metal salts such as $FeCl_2$, $CaCl_2$, $MnCl_2$, $CuSO_2$, NaH_2PO_4, Na_2HPO_4, and $ZnSO_4$ were used as sources of Fe, Ca, Mn, Cu, Na, Zn ions to study their effects, if any, on the protease enzyme.

Genome analysis of bacteria to identify secreted protease

Molecular identification of the bacteria through PCR amplification of 16S rRNA gene

For amplification of the 16S rRNA gene, PCR was done directly from the bacterial genomic DNA (gDNA) isolated from the glycerol stock. Specific forward primer

27F (5'-ACGCTTACCTTGTTACGACTT-3') and reverse primer 1492R (5'-AGAGTTTGATCACT GGCTCAG-3') were used in 0.5 µL of each 10mM concentration in a 35-cycle PCR reaction on ProFlex PCR system (Thermo Fisher Scientific, UK). The thermocycler was set as follows: an initial denaturation of 5 min at 95°C, template denaturation at 95°C for 30s, primer annealing and extension at 68°C for 20s, and 72°C for 1 min, respectively. The final extension step was set for 5 min at 72°C.

Whole-genome sequencing of the bacteria

Whole-genome sequencing of the *Micrococcus luteus* MBL-Bac7 strain was performed using the isolated DNA of high quality at the National Institute of Biotechnology, Bangladesh, using the Sanger sequencing platform.

Sequence analysis

Sequence identity and resemblance were performed through BLASTn analysis. The genome assembly data of the bacteria were analysed with RAST (Rapid Annotation using Subsystem Technology) (https://rast.nmpdr.org/) annotation server to predict the genes and protein models along with their functions. Proteins that were predicted as proteases were short-listed for further analysis.

Subcellular localization and physicochemical property

PSORTb v.3.0.2 (https://www.psort.org/psortb/) was used to determine the subcellular location of the predicted proteases. Since the screening of protease activity was carried out on extracellular extracts, finding the extracellular proteases were important. Proteins were also investigated for secretory properties by SecretomeP-1.0 (https://services.healthtech.dtu.dk/service.php?SecretomeP-1.0) and Transmembrane Helix Prediction 2.0 (TMHMM-2.0) (https://services.healthtech.dtu.dk/service.php?TMHMM-2.0). As these proteins are not located in the organism's genetic code, SecretomeP identifies these non-canonical secretory proteins that lack any signal peptide, and TMHMM identifies if the predicted secretory proteins have more than one transmembrane domain. Finally, molecular weights of the predicted secretory proteins were calculated with Protein Molecular Weight software (https:// www.genecorner.ugent.be/ protein_mw.html).

Multiple sequence alignment and phylogenetic analysis

Multiple sequence alignment analysis, bootstrap analysis, and neighbour-joining phylogenetic tree construction were performed using molecular evolutionary genetics analysis (MEGA) software version MEGA 11.0.8.

Prediction of secondary structure

The secondary structure of the protease was predicted with the help of two web-based tools, SWISS-MODEL (https://swissmodel.expasy.org/nteractive/9fF3Aw/models) and Phyre2 (http://www.sbg.bio.ic.ac.uk/phyre2/html/page.cgi?id=index).

Application of protease in leather processing

The final goal of this study was to apply the protease to cowhide for bating and determine its efficiency as a bating agent. Wet blue processing is a long process where the following steps are serially done soaking, pre-liming, liming, dehairing and fleshing, chemical wash, deliming and bating, pickling, and chrome tanning (Lyu and Cheng et al., 2017). The sixth step is deliming and bating. At this step 2% ammonium sulphate, 1% ammonium chloride, and 0.5% sodium metabisulphite with 80% water were mixed and the pH became 8.2-9.0, and the drum was run for an hour. Then 1% bating agent and 100% water were added and again ran for another hour. Water was drained and a finger prick test and bubble test were done. Then pickling, tanning, shaving, shamming, dying and fat liqouring were done. When the whole processing was finished, lastometer test, water vapour permeability test, and tensile and elongation tests were done. For the lastometer test, leathers were cut into a round shape of 4.5 cm diameter, placed into the lastometer, and pressure was applied. At the moment when a crack appeared on the leather, the amount of pressure was read. In the tensile strength test, leathers were cut into 14 cm long pieces where

at the middle portion, the width was 1.0 cm, then placed into a tensile test machine. Water vapour permeability was tested through the cup method (Huang and Qian, 2008).

Results

Morphology analysis of the bacteria

The bacteria from the yellowish colony when cultured in TSA plate, retain purple colour after Gram staining. Under the microscope, it appears cocci-shaped. (Fig. 1).

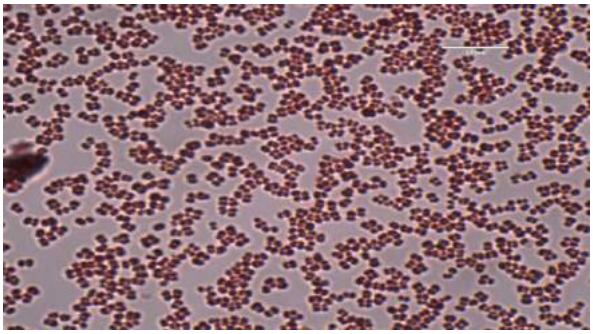

Fig. 1. Morphology analysis of *Micrococcus luteus* MBL-Bac7 under a microscope.

Qualitative screening of the protease

After 48h incubation of MBL-Bac7 in gelatin containing plate, a clear zone developed around the bacterial colony where the gelatin was hydrolyzed by extracellular enzymes (Fig. 2)

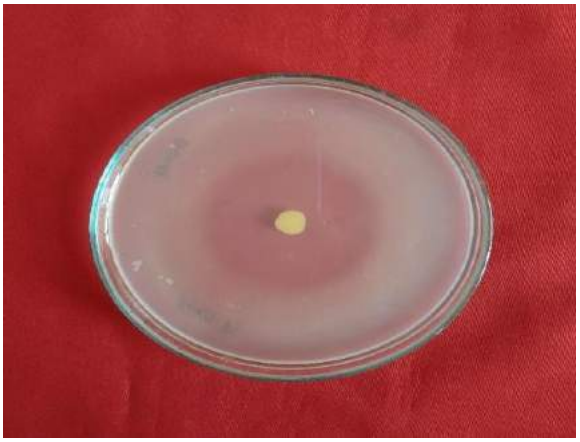

Fig. 2. Formation of a clear zone in gelatin agar plate containing *Micrococcus luteus* MBL_Bac7 indicating gelatin degradation around the bacterial colony.

Protease activity

The protease activity of 1630.3 UmL^{-1} was found in the $(NH_4)_2SO_4$ precipitated protein extract. On the other hand, the specific activity was 3702.9 UmL^{-1} with a purification fold of 7.33. In the culture supernatant, the protein remains diluted. But after precipitation, the protein concentration increases approximately 7.33 times (Table 1).

Table 1. Protease activity of cell-free supernatant and $(NH_4)_2SO_4$ precipitated protein.

Steps	Cell-free supernatant	$(NH_4)_2SO_4$ precipitated
Volume (mL)	280.0	5.0
Protein concentration (mg/mL)	0.06	0.44
Activity (U/mL)*	191.85	1630.30
Specific activity (U/mg)	3197.52	3702.70

*One-unit activity is defined as the amount of µmole tyrosine was released during assay per minute

Characterization of the protease

Effect of temperature on protease activity

Protease activity in the crude protein extract at 37º, 50º, 60º, and 85ºC was found to be 710.8, 773.8, 852.2, 465.4 UmL^{-1} respectively, where the control was 685.6 UmL^{-1} on average (Fig. 3).

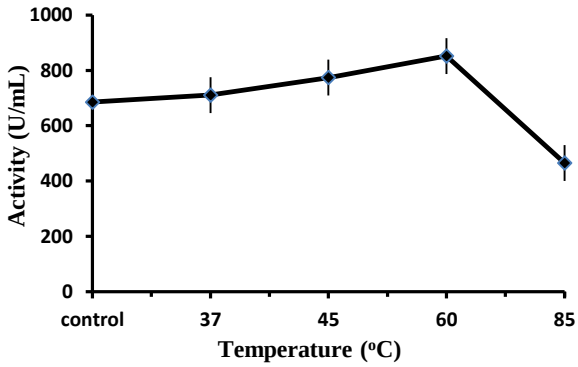

Fig. 3. Effect of temperature on the activity of the protease. Activity increases as the temperature rises and starts to decline after 60 ºC. The optimum temperature was found to be 60 ºC.

Effect of pH on protease activity

Protease activity was assessed at different pHs of 3.0, 4.0, 5.5, 6.5, 7.5, 8.5, and the activities were found to be 1164.9, 1509.1, 1253.6, 1790.4, 1565.2 and 1491.3 UmL^{-1} respectively (Fig. 4).

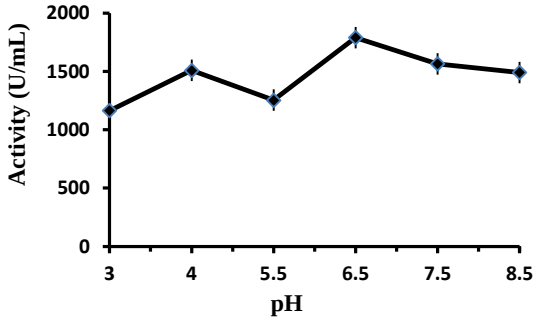

Fig. 4. Effect of pH on the activity of the protease. The protease is stable at a neutral pH range (6.5-7.5) without losing activity, and the highest activity was obtained at pH 6.5.

Effect of metal ions on protease activity

Protease treated with Na^{+}, Mn^{2+}, Fe^{2+}, Zn^{2+}, Co^{2+}, Ca^{2+} salts showed activity of 2477.95, 861.9, 7698.8, 517.4, 558.4, 577.7, 1514.3 UmL^{-1} respectively (Fig. 5).

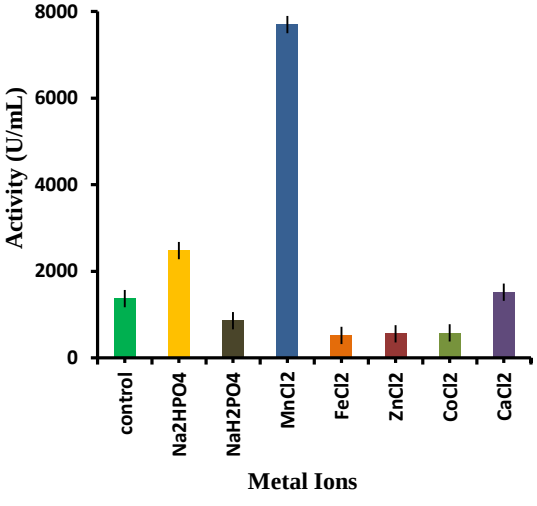

Fig. 5. Effect of metal ions on the activity of the protease. In the presence of Mn^{2+} salt, the proteolytic activity increased, while activity significantly reduced in the presence of Fe^{2+}, Zn^{2+}, and Co^{2+} salts.

Genome analysis of bacteria to identify secreted protease

Molecular identification of the protease

When the 16s rDNA sequence was retrieved from the whole genome sequence and compared using BLASTn against nucleotides, more than 99% similarity was found for *Micrococcus luteus* SA211 strain.

Sequence analysis

Whole-genome sequence of MBL-Bac7 was analysed using RAST (Rapid Annotation using Subsystem Technology), and the summary of the analysis is shown in Table 2.

Table 2. RAST analysis result: whole-genome analysis of MBL-Bac 7.

Genome size	2530185 bp
Total G-C content	72.94%
Number of genes	2501
Non-coding RNA genes	51
16s rRNA gene	1528 bp

Among all the protein-coding genes, 19 genes were found to have protease coding sequences. The identified protein-coding genes with their molecular mass and possible functions are described in Table 3.

Subcellular localization and physicochemical properties

Among all the 19 proteases, only peg. 158 had signal peptide and was found to be extracellular (Table 4). This protease (peg.158) has 641 amino acids and a molecular weight of 63.84 kDa. Others were non-canonical (peg. 1071, peg. 1968, and peg. 1089). Peg. 1968 had 6 transmembrane domains which are not likely to be secreted. Peg. 1071 is a zinc metalloprotease and peg. 1089 was found to be protease II. Peg.158 was targeted for this study and was subjected to further analysis.

Table 3. Proteases identified in the MBL-Bac7 genome.

Serial no	Protein encoding gene (peg)	No of amino acids	Molecular weight (kDa)	Functions
1	peg.37	238	25.61	SOS-response repressor and protease LexA (EC 3.4.21.88)*
2	peg.54	739	80.18	CatalaseKatE-intracellular protease (EC1.11.1.6)*
3	peg.107	851	93.49	ATP-dependent Clp protease,ATP-binding subunit ClpC
4	peg.158	641	63.84	Extracellular protease precursor (EC 3.4.21)
5	peg.256	464	50.39	Protease II (EC 3.4.21.83)
6	peg.365	432	46.94	ATP-dependent Clp protease ATP-binding subunit ClpX
7	peg.366	221	24.34	ATP-dependent Clp protease proteolytic subunit (EC 3.4.21.92)
8	peg.367	204	22.10	ATP-dependent Clp protease proteolytic subunit (EC 3.4.21.92)
9	peg.800	194	20.72	Intracellular protease
10	peg.948	138	14.29	Intracellular protease
11	peg.1071	222	24.26	Zinc metalloprotease
12	peg.1089	308	34.23	Protease II (EC 3.4.21.83)
13	peg.1268	332	33.49	Lon-like protease with PDZ domain
14	peg.1359	120	13.28	ATP-dependent Clp protease adaptor protein ClpS
15	peg.1620	184	19.86	YpfJ protein, zinc metalloprotease superfamily
16	peg.1721	227	24.27	Intracellular protease
17	peg.1932	518	56.41	ATP-dependent Zn protease
18	peg.1968	455	48.1	Membrane-associated zinc metalloprotease
19	peg.2456	158	16.05	Putative activity regulator of membrane protease YbbK

*Enzyme Commission number (EC number) is a numerical classification for enzymes given based on the chemical reactions they catalyze.

Table 4. Subcellular localization of the protease using PSORTb.

Localization	Scores
Extracellular	8.91
Cell wall	0.80
Cytoplasmic	0.24
Cytoplasmic membrane	0.05
***Final prediction: Extracellular 8.91**	

*Final prediction is done based on the localization that scores above the 7.5 cutoff value.

Phylogenetic analysis of the predicted protease

The strong similarity and tight phylogenetic connection of peg.158 with *Micrococcus luteus* serine peptidase suggest that the predicted protease is a *Micrococcus luteus* isolate and imply that the protease belongs to the serine peptidase family (Fig. 6).

Prediction of the secondary structure

Protein model of the peg. 158 was generated using both SWISS-MODEL and PHYRE2. The modeling was validated by the Ramachandran plot (Table 5, Fig. 7)

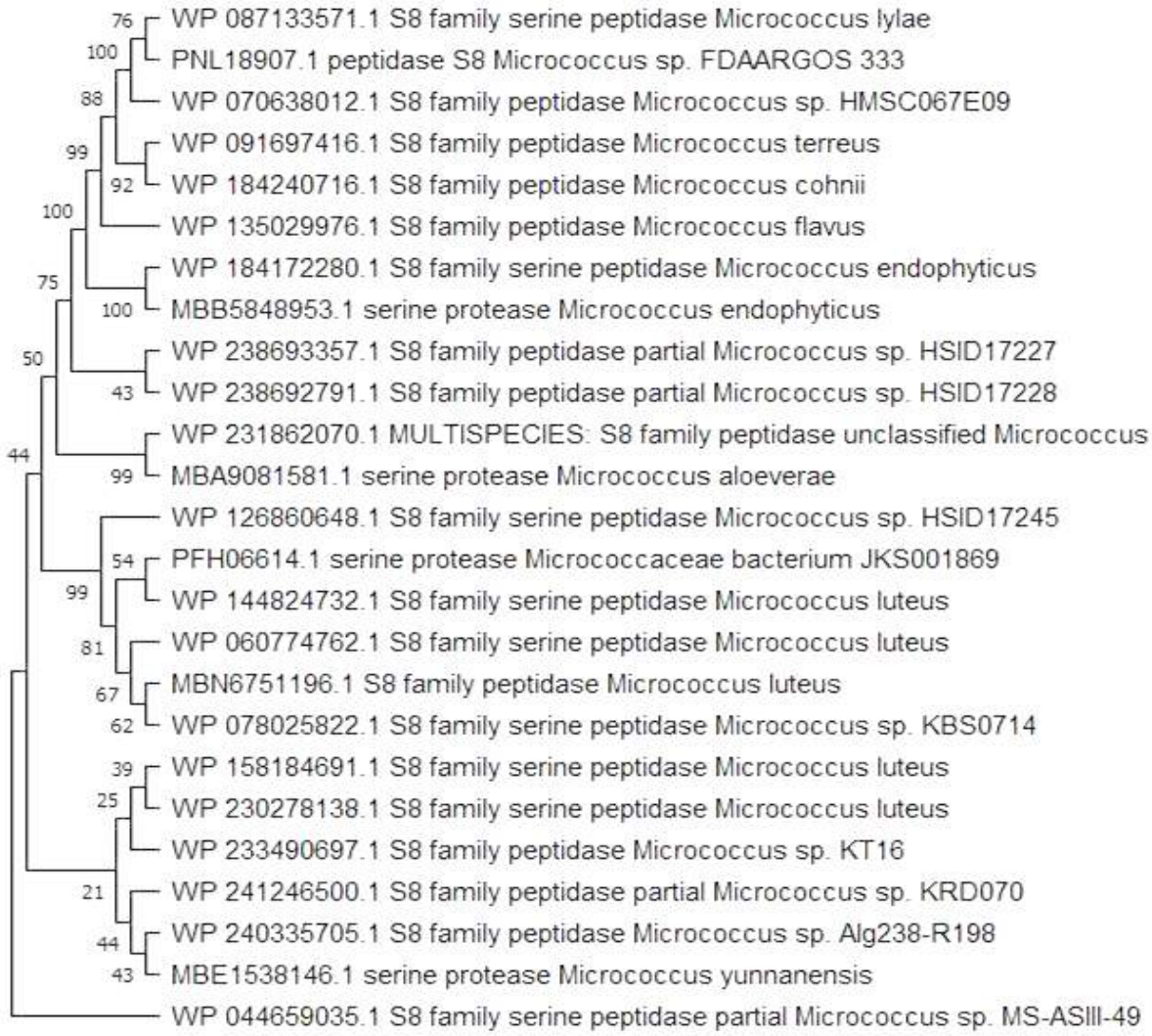

Fig. 6. Phylogenetic position of predicted protease and those from other *Micrococcus luteus* groups. The branching pattern was generated by neighbour-joining tree method.

Table 5. Summarization of Ramachandran plot for modelled structures: for validation of homology modeling.

Residues	SWISS-MODEL	PHYRE2
Most favoured regions	88.70%	80.10%
Additional allowed regions	9.70%	16.50%
Generously allowed regions	1.20%	2.00%
Disallowed regions	0.40%	1.40%

The structure of the protease was modeled using SWISS-MODEL and PHYRE2 and the structures were validated by the Ramachandran plot. This table shows that the model generated by SWISS-MODEL has a slightly better score than PHYRE2.

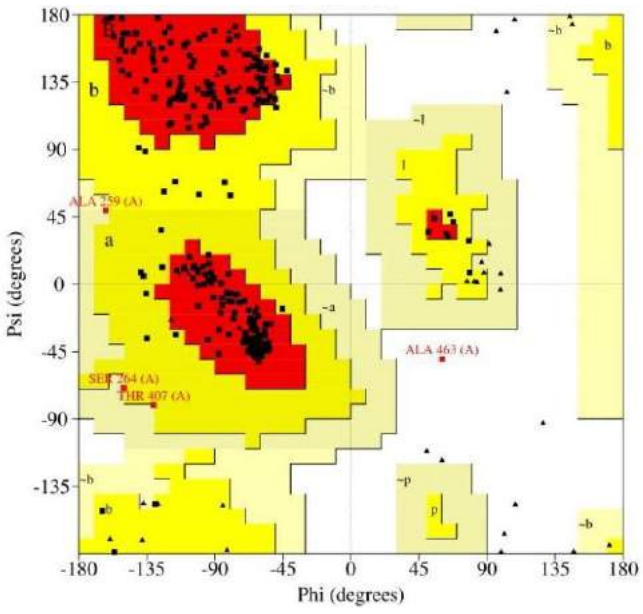

Fig. 7. Ramachandran Plot obtained from Procheck server, showing the most favored regions (red), less favored regions (dark yellow), and allowed regions but rare (light yellow). Regions in white are not possible due to strict collision.

The Swiss model server found to be the best model among the servers was used for modeling and viewed with Discovery Studio Visualizer v17.2 (Fig. 8). The model of the Swiss model server used proteases from *Pseudoalteromonas arctica* PAMC 21717 (Pro21717) (PDB ID: 5YL7) to construct Model 1. The peg.158 had a sequence identity of 56.92%. The standalone BLAST between peg.158 sequence and proteases from *Pseudoalteromonas arctica* sequence (reference protease of Swiss model resulted in an e value of $3e\text{-}10^{8}$).

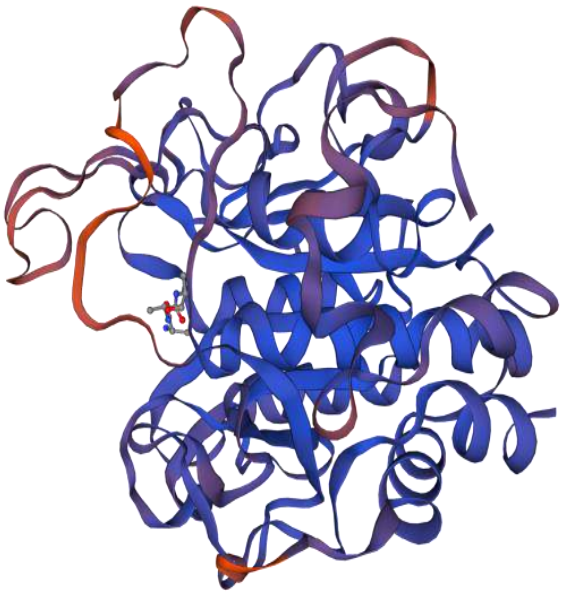

Fig. 8. Three-dimensional model of the predicted protease using Swiss model server. Purple-colored regions are well modeled, and red-colored regions are poorly modeled. This estimation of the model quality is based on the QMEAN scoring.

Bating activity of the protease

As there is no direct test to determine the strength of bating, the final states of hiding after wet blue processing and crusting were evaluated. These will indirectly provide an idea of the proper bating of a processed hide. Tensile strength, percent of elongation, water vapour permeability, and lastometer were tested for the processed hide and then compared with a commercially available bating agent (Table 6). Crude extract of Bac7 was found to be comparable with the standard commercial bating agent.

Table 6. Different test report of processed hides bated by Bac7 protease and a commercial bate.

Name of the tests	Bac7 protease	Commercial bate	Standard Value
% of Elongation Test	20.00%	22.73%	30-45%
Tensile Strength Test	212.96 kg cm^{-2}	175.44 kg cm^{-2}	200.00 kg cm^{-2}
Water Vapor Permeability Test	12.03 mg cm^{-2} hr^{-1}	11.57 mg cm^{-2} hr^{-1}	10.00 mg cm^{-2} hr^{-1}
Grain Crack Strength (Lastometer) Test	20.00 kg	22.00 kg	20.00 kg

Discussion

The present study aims to purify the extracellular protease from *Micrococcus luteus* MBL-Bac7 that can be used as a bating agent in the leather industry. Bating is the process of treating dehaired hides or skins with an enzyme to eliminate certain undesirable proteinaceous components (Thanikaivelan et al., 2004). This is a significant part of leather processing because proteases remove residues of the interfibrillar proteins. Otherwise, non-collagenous proteins cause cementing, which results in a lack of flexibility of leather (Hameed et al., 1996).

The endophytic bacteria *Micrococcus luteus* MBL-Bac7 was found to produce extracellular protease. Incubation with a drop of bacteria in a gelatin-containing plate created a clear zone when the plate was flooded with 100% ammonium sulphate solution. The clear zone indicated the presence of protease, because the gelatin on that area was utilized, and no gelatin was left for precipitation. It has been reported that *Micrococcus luteus* from water reservoirs can produce protease (Venkatesham et al., 2014). Rapid Annotation of MBL-Bac7 whole genome using Subsystem Technology (RAST) (Aziz et al., 2008) showed 2501 genes and among them, only 19 are proteases. The 19 proteases were further analysed to find the signal peptides or transmembrane helixes.

The presence of signal peptide means the protein is likely to be secreted. Only one protein was found to have a signal peptide and that was protein encoding gene, peg.158) with 641 amino acids and a predicted molecular weight of 63.84 kDa.

There were three other proteases that may follow the non-classical secretion pathway and may also be secreted extracellularly (Bendtsen et al., 2005). Nonclassical secretory proteins are independent of signal peptides and seem to follow a novel pathway to be secreted from the cytosol. However, it is reported that the non-classical secreted proteins can be distinguished from the cellular proteins by properties such as amino acid composition, secondary structure, and disorder regions.

Prediction of disorder for MBL-Bac7 reveals that the bacterial secretory proteins are more structurally disordered than their cytoplasmic counterparts (Bendtsen et al., 2005). The three non-classical extracellular proteases (peg.1071, peg.1089 and peg.1968) have 222, 308, and 455 amino acids, respectively. To evaluate all four of these proteases, transmembrane helices were compared using Transmembrane Helix Prediction (TMHMM). It can discriminate between soluble and membrane proteins with specificity and sensitivity by 99%. However, the percentage decreases in the presence of signal peptides (Krogh et al., 2001). If a protein has transmembrane helices, it may not be secreted, instead, it will translocate on the plasma membrane. One of the targeted proteases (peg.1968) had six transmembrane domains. With several transmembrane helices, the protein is expected to be

embedded in the membrane, rather than be secreted out of the cell. So, it can be concluded that peg.1968 protease is not a secretory protease. It was predicted that peg.158 might be the desired secretory protease. PSORTb also declared the protease as extracellular but not cytoplasmic as the localization score of the extracellular site exceeded the threshold score of 7.5. For further confirmation, mass spectrometry is required. To study more about the protein peg.158, homology modeling was done using the Swiss Model and PHYRE2. The 3D structure of the protease was generated. After analysing all the data achieved from the Ramachandran plot, especially the e-value, it was determined that the model constructed by the Swiss model was the best one. Again, the Swiss model created the protein model based on proteases from *Pseudoalteromonas arctica* PAMC 21717 (Pro21717) (PDB ID: 5YL7), these two protease sequences were subjected to BLAST. From the e-value of BLAST, it can be predicted that the proteins have significant sequence similarities. The proteases from *Pseudoalteromonas arctica* are serine proteases, so from the homology and sequence similarity, it can be presumed that peg.158 might be a serine protease family.

Suppose the protease isolated from Bac7 is to be used in tanneries. In that case, several ions or chemical compounds will be present in the reaction's mixture of bating, such as sodium polyphosphate and ammonium sulphate etc. Inside the drums of leather processing, the temperature may rise to 40ºC. Considering all these features, the protease's activity was measured after incubating at different temperatures, pHs, and with various metal ions. When the protease was incubated at different temperatures for one hour, it was observed that if the incubation temperature increased from 37ºC to 60ºC, the activity increased. But the activity started to decline after 60ºC, and at 85ºC, the activity was found to be ~89% compared to the control. It was reported that *Bacillus subtilis* protease had 100% stability in the temperature ranges from 35º-55ºC (Manachini et al., 1988). To study the effect of pH, the reaction mixture was set at different pHs. The general process of activity measurement is to use casein as the substrate. However, casein does not dissolve at a pH lower than 6.0. To avoid such hindrance, gelatin was taken as the substrate to demonstrate pH's effect on protease activity. A long-range of pH was chosen from acidic to alkaline. Although the protease showed high activity in alkaline conditions, it also had significant activity in an acidic environment, suggesting it was active within a large pH range. A previous report says protease isolated from *Bacillus megaterium* shows remarkable activity and stability at a large pH range of 5.5-9.0 (Asker et al., 2013).

In this study, Mn^{2+} ion increased the protease activity by about five-fold. During bating, sodium polyphosphate was used. Therefore, the enzyme activity was measured in the presence of Na_2HPO_4 and NaH_2PO_4, although NaH_2PO_4 reduced the activity of the enzyme compared to the control. In such cases, there may be an influence of HPO_4^{2-} ion on the protease that is yet to be determined. Slight inhibition of enzymatic activity was found after treatment with $CaCl_2$, $CoCl_2$, $ZnCl_2$, and $FeCl_2$.

Finally, the protease was applied to raw cowhide, simultaneously; a commercial bating powder was applied to another piece of hide as a control. There is no direct test to ensure the strength of bating. Proper completion of leather processing depends on the accuracy of bating because bating creates micropores for Cr^{3+} to enter into collagen, called tanning. So, if the processed leather meets all the characteristics of physical tests, then it can be concluded that the bating was efficient. Both pieces of leather that were bated with the protease of Bac7 and commercial bating agent were subjected to several physical tests. One test was the lastometer test, where the softness of the leather was measured. MBL-Bac7 protease treated leather could tolerate 20 kg of load, which is equal to the standard value. Tensile strength and elongation tests were also done. Tensile strength is the capacity of a material or structure to withstand loads, allowing it to elongate. The load is calculated as kg cm^{-2}. The

standard value is considered 200 kg cm^{-2}. Leather treated with MBL_Bac7 protease had a tensile strength of 212.96 kg cm^{-2}. This means that it can withstand more than the standard level of tension. Hameed et al. (1996) reported that protease of *Bacillus subtilis* K2 had a remarkable bating property considering tensile strength test and elongation at break, giving the value of 175 kg cm^{-2} and 19% respectively at 1800 UmL-1. The last physical test of processed hide was the water vapour permeability test. Water vapour permeability indicates how quickly textiles can transfer sweat from the human body during an activity involving higher metabolism into the air. Proper selection and manufacture of materials with high water vapour permeability, especially during outdoor activities, can provide comfort for the users. One of the most significant physical properties of leather is the water vapour permeability test, which greatly affects the breathability and the comfortable feeling of leather textiles and footwear. In the experiment, two types of leathers (one of which was bated with crude protein and the other bated with a commercial bating agent) were subjected to water vapour permeability tests. The results showed that the treated leather had higher water vapour permeability compared to the standard value. But among the two, leather bated with crude protease had a higher value than the one in which a commercial bating agent was used.

Conclusion

Considering all the experimental results, it can be concluded that the protease from *Micrococcus luteus* MBL_Bac7 is potential for industrial production. However, there are still some concerns regarding the use of this protease as a commercial bating agent. One of them is the production cost of the enzyme. This can be alleviated by using low-cost protein sources for bacterial culture and their optimization. Modification at the molecular level can also be undertaken to allow more protein precipitation at a lower cost.

References

Asker MM, Mahmoud MG, El Shebwy K and Abdel Aziz MS. Purification and characterization of two thermostable protease fractions from *Bacillus megaterium*. *J. Gene. Eng. Biotechnol*. 2013; 11(2): 103-109.

Aziz RK, Bartels D, Best AA, DeJongh M, Disz T, Edwards RA, Formsma K, Gerdes S, Glass EM, Kubal M and Meyer F. The RAST Server: rapid annotations using subsystems technology. *BMC Genom*. 2008; 9: 75.

Beilen JB and Li Z. Enzyme technology: an overview. *Curr. Opin. Biotechnol.* 2002; 13(4): 338-344.

Bendtsen JD, Kiemer L, Fausbøll A and Brunak S. Non-classical protein secretion in bacteria. *BMC Microbiol*. 2005; 5(1): 1-3.

Boddey RM, Urquiaga S, Alves BJ and Reis V. Endophytic nitrogen fixation in sugarcane: present knowledge and future applications. *Plant Soil*. 2003; 252(1): 139-149.

Carole TM, Pellegrino J and Paster MD. Opportunities in the industrial biobased products industry. In: Finkelstein M, McMillan JD, Davison BH, Evans B(eds). *Proceedings of the Twenty-Fifth Symposium on Biotechnology for Fuels and Chemicals.* May 4-7, 2003, in Breckenridge, CO. Humana Press, Totowa, NJ, 2004; p. 871-885.

Hameed A, Natt MA and Evans CS. Production of alkaline protease by a new Bacillus subtilis isolate for use as a bating enzyme in leather treatment. *World J. Microbiol. Biotechnol*. 1996; 12(3): 289-291.

Hardoim PR. Bacterial endophytes of rice: Their diversity, characteristics and perspectives. Ph.D. Thesis, University of Groningen, Groningen; 2011, p. 220.

Huang J and Qian X. Comparison of test methods for measuring water vapor permeability of fabrics. *Text. Res. J*. 2008; 78(4): 342-352.

Kirk O, Borchert TV and Fuglsang CC. Industrial enzyme applications. *Curr. Opin. Biotechnol*. 2002; 13(4): 345-351.

Kobayashi DY and Palumbo JD. Bacterial endophytes and their effects on plants and uses in agriculture. In: *Microbial Endophytes*. Bacon CW and White JF, eds. Marcel Dekker, New York, 2000; p.199-233.

Krogh A, Larsson B, Von Heijne G and Sonnhammer EL. Predicting transmembrane protein topology with a hidden Markov model: application to complete genomes. *J. Mol. Biol*. 2001; 305(3): 567-580.

Kuklinsky-Sobral J, Araújo WL, Mendes R, Geraldi IO, Pizzirani-Kleiner AA and Azevedo JL. Isolation and characterization of soybean-associated bacteria and their potential for plant growth promotion. *Environ. Microbiol*. 2004; 6(12): 1244-1251.

Lyu B, Cheng K, Ma J, Hou X, Gao D, Gao H, Zhang J and Qi Y. A cleaning and efficient approach to improve wet-blue sheepleather quality by enzymatic degreasing. *J. Clean. Prod*. 2017; 148: 701-708.

Madhaiyan M, Poonguzhali S, Senthilkumar M, Seshadri S, Chung H, Jinchul YA, Sundaram S and Tongmin SA. Growth promotion and induction of systemic resistance in rice cultivar Co-47 (Oryza sativa L.) by Methylobacterium spp. *Bot. Bull. Acad. Sin.* 2004; 45: 315-324.

Manachini PL, Fortina MG and Parini C. Thermostable alkaline protease produced by Bacillus thermoruber-a new species of Bacillus. *Appl. Microbiol. Biotechnol*. 1988; 28(4): 409-413.

Najnin R A, Shafrin F and Polash AH, Zaman A, Hossain A, Taha T, Ahmed R, Tuli JF, Barua R, Sajib AA, Khan H. A diverse community of jute (Corchorus spp.) endophytes reveals mutualistic host–microbe interactions. *Ann. Microbiol*. 2015; 65(3): 1615-1626.

Saxena R and Singh R. Amylase production by solid-state fermentation of agro-industrial wastes using Bacillus sp. *Braz. J. Microbiol*. 2011; 42(4): 1334-1342

Srilakshmi J, Madhavi J, Lavanya S and Ammani K. Commercial potential of fungal protease: past, present and future prospects. *J. Pharm. Chem. Biol. Sci*. 2015; 2(4): 218-234.

Tan RX and Zou WX. Endophytes: a rich source of functional metabolites. *Nat. Prod. Rep*. 2001; 18(4): 448-459.

Thanikaivelan P, Rao JR, Nair BU and Ramasami T. Progress and recent trends in biotechnological methods for leather processing. *Trends Biotechnol*. 2004; 22(4): 181-188.

Venkatesham M, Ayodhya D, Madhusudhan A, Santoshi Kumari A, Veerabhadram G and Girija Mangatayaru K. A novel green synthesis of silver nanoparticles using gum karaya: characterization, antimicrobial and catalytic activity studies. *J. Clust. Sci*. 2014; 25(2): 409-422.

J. Bangladesh Acad. Sci. 46(1); 45-55: June 2022 DOI: 10.3329/jbas.v46i1.60346

Journal of Bangladesh Academy of Sciences

Journal homepage: http://www.bas.org.bd/publications/jbas.html

Research Article

Preliminary CFD investigation for secondary coolant in molten salt reactor with alumina nanofluid considering FLiBe and FLiNaK as base fluid through a double pipe heat exchanger

Joy Surjy Deb, Md Mahidul Haque Prodhan*, Nazmul Hossain, and Golam Sarwar Rakib

Department of Nuclear Engineering, University of Dhaka, Dhaka, Bangladesh

ARTICLE INFO

Article History

Received: 22 March 2022
Revised: 29 May 2022
Accepted: 12 June 2022

Keywords: MSR, Nanofluids, Double Pipe Heat Exchanger, CFD, Nuclear Thermal Hydraulics.

ABSTRACT

This work analyzes a computational fluid dynamics (CFD) methodology based on ANSYS to investigate the 3 % and 4 % volume fraction alumina (Al_2O_3) nanofluids with base fluids FLiBe (LiF(67)-BeF_2(33) (mol%)) and FLiNaK (LiF(46.5)-NaF(11.5)-KF(42) (mol%) through a double pipe heat exchanger. The purpose of the paper is to choose better candidates as secondary coolants in molten salt reactors for better thermodynamics performances and heat transfer characteristics. Six secondary coolants with and without nanofluids and fuel salt as primary coolants are driven through the inner and outer pipe. Later overall heat transfer coefficient, outlet temperatures and pressure drops of the fluids, and LMTD are calculated. Thus, this work eventually recommends the best candidate as a secondary coolant by CFD methodology using ANSYS-FLUENT 18.1.

Introduction

The molten salt reactor is one of the advanced generation reactors that may ensure the inherent safety of a nuclear power plant due to its unique safety features like molten salt coolant and fuel. This unique feature provides a distinct advantage over the conventional BWR or PWR fuel rods which might melt over a certain temperature (Cantor et al., 1968). Currently, different researches are being carried on to improve the efficiency of the coolant and enhance the convective heat transfer coefficient and other thermodynamics properties based on their figure of merits. SAMOFAR (Safety Assessment of the Molten Salt Fast Reactor) is a project based on the molten salt fast reactor, one of the leading projects the Europeans manage to ensure the best available molten salt coolant for molten salt nuclear reactors by analyzing their thermal-hydraulic properties with substantial experiments. They have nominated FLiBe and FLiNaK till now (Aniza et al., 2017; Forsberg, 2006; Allibert et al., 2017; Doche et al., 2017; Allibert et al., 2012; Dieuaid, 2018; Marcello et al., 2008). Moreover, nanofluids are showing crucial importance as a coolant in nuclear power plants due to their enhanced material properties and sizes through real-life and simulation-based experiments. Since the last century, many experiments and research have been being contrived, and recently molten salt thermal nuclear power reactors, fast breeder reactors are also initiated in the research arena. Both solid fuels like particles and liquid fuels can be used. As a solid fuel, particles may be incorporated in to a matrix made of graphite. On the other hand, actinides in liquid fuel structure are used, which can be uniformly dispersed in the molten salt directly and kept at very high temperature, coveys inside and outside of the reactor core. In the reactor core, the fuel salt is heated up by the fission reactions of the nuclear elements, and later heat is transferred

*Corresponding author: <prodhan@du.ac.bd>

to the secondary coolant, which subsequently transfers the heat to the tertiary fluid for the power conversion cycle. Most of the previous studies were to investigate the thermal and physical properties of LiF(67)-BeF2(33) (mol%) (FLiBe) and LiF(46.5)-NaF(11.5)-KF(42) (mol%) (FLiNaK) (Aniza et al., 2017; Forsberg, 2006; Williams, 2006; Clarno et al., 2006). Bahri et al. discussed the physical properties of these two molten salts in terms of their application as coolant and fuel solvent and also stated the comparative advantages and disadvantages. Charles et al. analyzed a technology gap to initiate and understand technological challenges for developing and deploying MSRs (molten salt reactors). Williams stated that molten salts seem to be noteworthy candidates because of their strong performances in terms of high temperatures with convenience and flexibility (Williams, 2006; Clarno et al., 2006). Similarly, for the single tube, Hoffman experimentally conducted the forced convective heat transfer performance of FLiNaK salt. (Hoffman and Lones, 1955). Bang et al. (2009) experimented with FLiNaK and gas, where a double pipe heat exchanger was established using small diameter tubes. Primarily, mainly for the SAMOFAR project as a fuel salt which is also a primary coolant, two main options (LiF-ThF4-^{233}UF4) and (LiF-ThF4-^{235}UF4-(Pu-MA)F3) are strongly and significantly recommended (Allibert et al., 2017; Doche et al., 2017). Similarly, Huntly et al. (1976) investigated the forced convective heat transfer of one fuel salt LiF-BeF2-ThF4-UF4 to ensure its competence. While E. Merle investigated another fuel considering the SAMOFAR project (Allibert et al., 2012). Subsequently, CFD based research have been carried on by different academicians to improve heat exchanger as well as to investigate the thermal performances of the fuel and coolant salts, some of which are also considered to use in the SAMOFAR project as well as for future purposes; some CFD based modeling methods have been proposed too (Rubiolo et al. 2017). Cammi et al. (2019) investigated and referred to two promising technologies and also presented preliminary results on the Printed Circuit and the Helical Coil heat exchangers to improve heat transfer efficiency. Dieuaid (2018) has analyzed neutronic and thermal analyses like decay heat and re-criticality of molten salt reactors considering the SAMOFAR project using MCNPX to introduce reprocessing unit design. In addition, Marcello et al. conducted research with the help of COMSOL Multiphysics® to investigate and determine the coupled dynamics considering both nuclear and thermal parts (Marcello et al., 2008). Kasam and Shwageraus (2017) conducted CFD simulations for a single fuel tube which were performed with varying parameters to establish the relationship between the maximum fuel temperature and parameters such as fuel salt properties, tube diameter, and power density. Moreover, several CFD types of research were conducted to determine the thermal- hydraulics performances of the coolant in designed shell and tube heat exchangers and improve the heat exchangers for better heat transfer conditions (Fraas and Laverne, 1971; Bettis et al., 1967). Köse et al. (2019) investigated and proposed a heat exchanger design for SAMOFAR using ANSYS FLUENT commercial code. Chi et al. (2011) examined the thermal-hydraulic characteristics such as the Nusselt number of the molten salt LiF(46.5)-NaF(11.5)-KF(42) using Gnielinski and Hausen correlations that are considered more appropriate than Dittus- Boeltar in terms of molten salt (Gnielinski, 1976; Hausen, 1959). However, Ambrosek et al. recently re-evaluated the FLiNaK test data with an updated formula which eventually showed an improved relation according to the Dittus-Boelter correlation with a minor 15 percent error (Ambrosek et al., 2009). Apurba used Hausen and Gnielinski correlations for evaluating molten nitrate heat transfer (Anderson et al., 2015). Nanofluids are also contributing a significant part to the future nuclear industry and its research arena for safe operation and ensuring enhanced heat transfer rate. Choi et al. (2001) investigated nanofluids of different elements and observed a 40% increase that is significant in terms of thermal conductivity for Cu-containing ethylene glycol. Li and Xuan (2003)

examined the convective heat exchange and the stream highlights of Cu-water nanofluids at a -10 mm inward distance across the tube, which eventually provided a positive output. Rea (Buongiorno et al., 2012) led an investigation on the laminar convective warmth exchange and weight drop of alumina– water and zirconia-water nanofluids in a tube with a 4.5 mm inward width. Their discoveries illustrated that there is no deviation in convective heat exchange and weight drop of nanofluid spill out of customary single-stage stream hypothesis with appropriately measured nanofluid properties. Etemad et al. (2006) played out an exploratory investigation to decide that alumina nanoparticles are more beneficial than CuO nanoparticles in terms of the same volume and Reynolds number. Ding and Wen (2004) examined alumina nanoparticles and de-ionized water for heat transfer calculation and eventually concluded that heat transfer increases using nanofluid. Allahyari et al. (2011) studied laminar mixed convection of alumina water by heating the top half surface of a Cu tube horizontally. They concluded that the heat transfer coefficient rises with the increased concentration of nanoparticles. Sarma experimented with water-based alumina nanofluids and calculated the increase of convective heat transfer for different Reynolds numbers with constant wall heat flux (Sarma et al., 2009). Buongiorno proposed a mathematical model by considering nanoparticle/base fluid slip, and he showed that Brownian motion and thermophoresis are the main mechanisms for this slip mechanism (Buongiorno, 2006). On the other hand, Kleinstreuer and Koo (2004) proved that Brownian motion was the more important phenomenon. Also, the thermal conductivity of nanofluids has strong temperature dependence. Evans et al., (2006) proved that the direct influence of the Brownian motion of the nanoparticles via diffusion is negligible. Aybar et al. (2009) did experimental investigations that support the indirect influence of the Brownian motion regarding nanofluids' higher heat transfer characteristics. Choi and Jang (2007) proposed a model based on Brownian motion-induced nano-convection. The model proposed by Kumar et al. (2004) based on Brownian motion overestimated the contribution of Brownian motion to heat flow. But Das et al. (2005) improved the model proposed by Kumar et al. by incorporating the effect of micro convection due to particle movement. Trivedi (2008) found that decreasing the temperature of a component increases its performance, such as reliability. Das and Vajjha (2009) presented the dependency of thermal conductivity on both temperature and nanoparticle concentration. Hadad et al. (2013) investigated the thermal-hydraulic properties of $Al_2O_3^+$ water nanofluid as the coolant in a VVER-1000 nuclear reactor core by using a CFD code considering a finite volume method for single-phase and two-phase mixture models to find convective heat transfer coefficient and pressure drop. Similarly, in a study done by Boungiorno et al. (2017), nanofluids are used as the main reactor coolant for pressurized water reactors (PWRs), which could be used to enhance economic performance with at least 32% higher critical heat flux (CHF) and a 20% power density commensurate with current PWRs without varying the fuel assembly design and without decreasing the margin to CHF. However, to date, not many experiments have been conducted with a mixture of nanofluids with FLiBe or FLiNaK as a nuclear coolant. Therefore, this paper will analyze this promising aspect of nanofluids in molten salt reactors, considering the fuel salt and secondary coolant salt for the SAMOFAR project.

Mathematical Model Governing Equations

Before the simulation, this work assumed some significant criteria. Firstly the rate of turbulence energy ε. These two parameters k and ε can be found by solving the following equations (Choi and Jang, 2017; Aybar et al., 2009). The simulation was conducted under steady-state conditions. The vital governing equations that were used to simulate the thermal-hydraulic characteristics include the continuity, momentum, and energy equations (Li and Xuan, 2003; Li et al., 2019). Besides, the appropriate

turbulence model was integrated to conduct the simulation. For steady-state conditions. The following equation (Li et al., 2019) can be described as below:

Continuity Equation

$$\nabla.(\rho u) = 0 \quad \text{..... (3.1)}$$

Momentum Equation

$$\nabla.(\rho uu) = -\nabla.p + \nabla.\tau \quad \text{..... (3.2)}$$

τ is the stress tensor (described below),

$$\tau = \mu\,[(2\nabla.u) - \tfrac{2}{3}\nabla.u] \quad \text{..... (3.3)}$$

Energy Equation

$$\nabla \cdot (\rho uh) = \nabla \cdot \left(\left(\frac{\Gamma}{c_p}\right)\nabla.u\right) \quad \text{..... (3.4)}$$

Turbulence Model

Since the Reynolds number is greater than 2300 in pipe flow, the influence of turbulence must be considered. In the present work, a standard k-ε turbulence model is employed. The standard k-ε model includes two transport equations: turbulence kinetic energy k and dissipation rate of turbulence energy ε. These two parameters, k and ε, can be found by solving the following equations (Choi and Jang, 2007; Aybar et al., 2009).

$$\frac{\partial}{\partial x_i}(\rho k u_i) = \frac{\sigma}{\partial x_j}\left[(\mu + \mu_t/\sigma_k)\frac{\sigma_K}{\partial x_j}\right] + G_k - \rho\epsilon \quad \text{..(3.5)}$$

$$\frac{\partial}{\partial x_i}(\rho\epsilon u_i) = \frac{\partial}{\partial x_j}\left[(\mu + \mu_t/\sigma_\epsilon)\frac{\partial}{\partial x_j}\right] + C\epsilon_1(\epsilon/k)\,G_k -$$

$$C\epsilon_2(\epsilon^2/k)\,\rho \quad \text{.....(3.6)}$$

Here, turbulence viscosity, $\mu_t = \rho\, C\mu\, (k^2/\epsilon)$ G_k is the production of turbulent kinetic energy and $G_k = \rho\overline{u'_i u'_j}\frac{\partial u_j}{\partial x_i}$, $C\epsilon_1$, $C\epsilon_2$, $C\mu$, σ_k and σ_ϵ are empirical constants where, $C\epsilon_1 = 1.44$, $C\epsilon_2 = 1.92$, $C\mu = 0.9$, $\sigma_k = 1$ and $\sigma_\epsilon = 1.3$

Simulation

Geometry and Boundary Condition

This work investigates a preliminary concept of a double pipe heat exchanger. Though a double pipe heat exchanger is not considered significant in real life, it demonstrates a brief analysis of the effect of alumina nanofluids with FLiBe and FLiNaK as secondary coolants regarding the overall heat transfer coefficient, cycle efficiency, and pressure drop of the coolants. For meshing multi-zoned meshing method with Hexa mapped mesh type is used. In the meshing section also, inflation is controlled to ensure first layer thickness competence and increase meshing quality. As the standard k epsilon method is introduced, the wall Y+ value is adjusted between the value of 30-100, and thus the meshing is employed bearing that for the simulation. The SIMPLE method is employed to couple velocity and pressure here. According to different previous works, nanofluids can be treated as single-phase models for low volume fractions (Singh and Sundar, 2013; Mujumdar and Wang, 2008). As the volume fraction of 3% and 4% are considered for this work, the single-phase method is employed here. In this investigation, computational fluid dynamics (CFD) code FLUENT 18.1 is used as an analysis tool; it utilizes the continuity equation, momentum equation, energy equation, and standard K- epsilon turbulence model. A double pipe heat exchanger has been introduced to determine the better secondary coolant out of the proposed candidates above. For this simulation, t = 5 mm; D_i = 50 mm; D_o = 45 mm; L_i = 1.3 m; L_o = 1 m.

To conduct this experiment, as a fuel salt ^{7}LiF(77.5)-ThF4(20)-^{233}UF3(2.5) (%mol) is selected, which is forced to travel through the inner pipe. The inlet velocity for the fuel salt is 2.5 ms^{-1}. Similarly, for the six secondary coolant candidates, which are also forced to pass through the outer pipe, the inlet velocity is selected 5 ms^{-1}. The Inlet temperature for the inner pipe is 1023K, while for the outer pipe, it is 833K. In addition, the pressure is kept at 1-2 atm. These data are selected based on several studies and recommended operating temperature, pressure, velocity, and other operating conditions (Cammi et al., 2019; Köse et al. 2019).

Thermal Properties

For Pipe material, it has been suggested to use hastelloy-n alloy for its higher melting point, and better strength and physical since MSRs need to

operate at a higher temperature compared to conventional PWR and BWR power plants (Williams, 2006; Carno et al. 2006; Hoffman and Lones, 1955). The thermal properties of the fuel salt, secondary coolant candidates, and hastelloy-n alloy are selected by different empirical equations and data from several studies. Allibert et al. (2012) represented empirical equations to determine the thermal and physical properties of the fuel salt, which is calculated for a temperature of 1023K for this experiment. Moreover, for hastelloy-n alloy, this data is selected from another study (Kedl, 1970). In addition, the thermal and physical data of FLiBe and FLiNaK have been derived from another study for 973K (Ebner et al., 2010). According to work mentioned above, the thermal properties of FLiBe, FLiNaK, and Hastelloy-n alloy are given in Table-1 for 700°C, whereas; for alumina nanofluids, the data is considered at 25°C (Chukwu et al., 2006).

Table 1. Thermal properties of the coolant and materials

Name	Specific Heat ($JKg^{-1}K^{-1}$)	Thermal Conductivity ($Wm^{-1}K^{-1}$)	Density (kgm^{-3})	Viscosity (Pa.s)
FLiBe	2397.73	1.1163	1938.06	0.0055
FLiNaK	2011.7	0.9050	2018.9	0.0025
Hastelloy-n	578	23.6	8860	
Alumina	773	36	3880	

Similarly, for 3% and 4% alumina nanofluid with base fluid molten salt coolant (FLiBe and FLiNaK), all the thermophysical properties are derived from the following equations (Chukwu et al., 2006), where ø is the volume percentage of the nanoparticles in the base fluid, whereas; nf and bf mean nanofluid and base fluid respectively.

$$\rho_{nf} = (1-ø)\,\rho_{nf} + ø \times \rho_p \quad (4.1)$$

$$(\rho C_p)_{nf} = (1-ø)\,(\rho C_p)_{bf} + ø \times (\rho C_p)_p \quad (4.2)$$

$$\mu_{nf} = (123ø^2 + 7.3ø + 1)\mu_{bf} \quad (4.3)$$

$$k_{nf} = (4.97ø^2 + 2.72ø + 1)k_{bf} \quad (4.4)$$

Results and Discussions

The fuel salt and the six candidates are forced to be conveyed through the double pipe heat exchanger. The average overall heat transfer coefficient is found along with LMTD and pressure drop in both pipes and the outlet temperature of both fluids (inner and outer). For analyzing this data, some equations related to thermodynamics are used.

$$Qi = \dot{m}\, cph\, (t_{hi} - t_{ho}) \quad (5.1)$$

$$Qo = \dot{m}\, cpc\, (t_{co} - t_{ci}) \quad (5.2)$$

$$LMTD = (\Delta T_1/\Delta T_2)/[\ln(\Delta T_1/\Delta T_2)] \quad (5.3)$$

$$Q_{avg} = Q_i + Q_o \quad (5.4)$$

$$U = Q_{avg} / (A_s \times LMTD) \quad (5.5)$$

Where, $\Delta T_1 = t_{hi} - t_{co}$; $\Delta T_2 = th_o - t_{ci}$,
and $A_s = \pi D_o L_o$

From Fig.1 and Table 2, it can be derived that with increasing nanofluid volume percentage in base molten salt for both FLiBe and FLiNaK as secondary coolant, the pressure drop in terms of

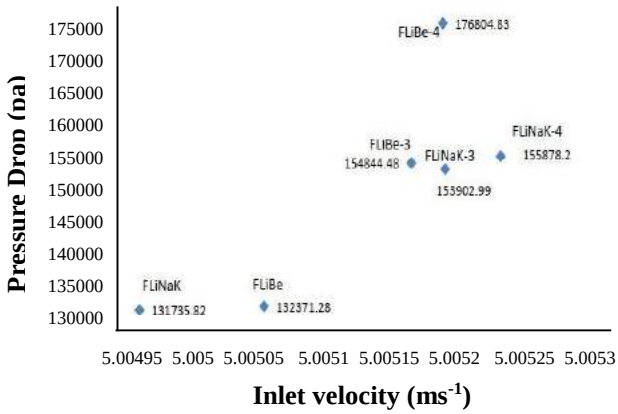

Fig. 1. Outer pipe inlet velocity vs. pressure drop for secondary coolant candidates.

Table 2. Outer Fluid' Reynolds Number and Mean Velocity

Name	Reynolds Number	Mean Velocity (ms^{-1})
FLiBe	792842.73	5.00253155
FLiBe-3	615303.55	5.00258795
FLiBe-4	553098.7317	5.0026
FLiNaK	1817010	5.00248385
FLiNaK-3	1414590.682	5.0026009
FLiNaK-4	12722979.459	5.0026221

secondary coolant has been increased, indicating that a higher power required to pump in case of a real application with nanofluids than an conventional plan without nanofluids. The explanation behind that is quite convenient and simple. According to available friction factor correlations, the friction factor will increase smooth pipe for turbulent and higher Reynolds number flow, with higher viscosity and lower Reynolds number of the fluid for the same inlet velocity. Thus the pressure drop will increase too (Srichai S). From the table, it can be seen that for both base fluids with a higher percentage of nanofluids, the Reynolds number decreases for the same inlet velocity 5 ms^{-1}. In contrast, the viscosity is increasing according to equation no. 4.3 that has been previously discussed. Physically, in turbulent flow, fluid mixing at different layers is very significant and high. Therefore, the average velocity gradient doesn't vary significantly in these regions. However, this cannot happen near the wall since the fluid follows no-slip condition. So, a large change in velocity has to occur within a very thin region (laminar sub-layer), resulting in a very high gradient. Moreover, in a given regime, the friction factor decreases with increasing Reynolds number since when Re increases, the gradient (du/dy) also increases but at a lesser rate. Moreover, with higher viscosity of the fluids means higher probabilities of collisions between fluid layers that eventually increase pressure drop. In Fig. 2, the contour image of the pressure distribution of the six secondary coolants has been shown has been developed after simulation.

From Fig. 3, it can be shown that with increasing nanofluid volume percentage in FLiBe, the outlet temperature of the fuel salt is decreased, indicating transferring a higher amount of energy to the secondary coolant. Nevertheless, in the case of FLiNaK, it demonstrates, unlike FLiBe. With

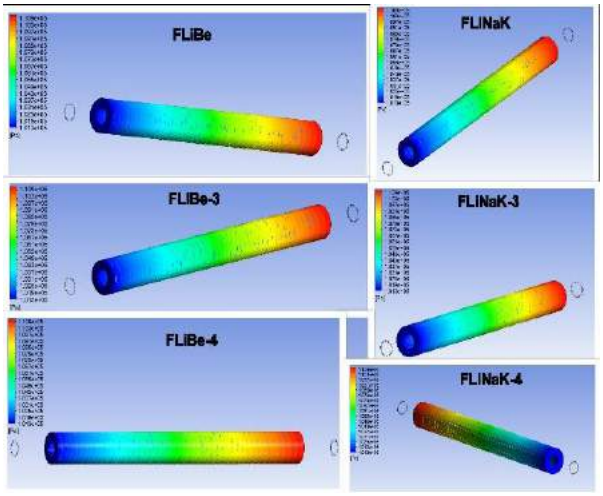

Fig. 2. Contour image of the secondary coolants' pressure distribution

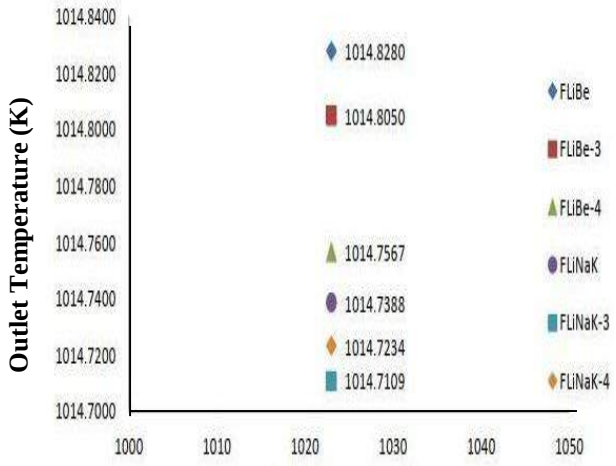

Fig. 3. Fuel salt's inlet temperature vs. outlet temperature for different secondary coolants.

FLiNaK as a secondary coolant, the fuel salt has the highest outlet temperature like FLiBe in the previous case. However, the lowest value of outlet temperature of fuel salt is in the case for FLiNaK-3 as a secondary coolant instead of FLiNaK-4 with a difference of 0.0125 K, which is a convoluted case and mysterious.

In Fig. 4, the contour image of the temperature distribution of the fuel salts in terms of the six different secondary coolants has been shown that has been developed after simulation.

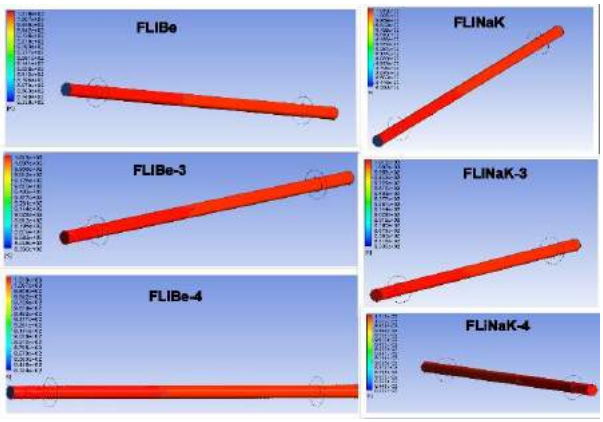

Fig. 4. Contour image of fuel salt's temperature in case of different secondary coolants.

Nonetheless, in Fig. 5, the results are as expected. In both FLiBe and FLiNaK cases, with the gradually increasing nanofluids volume percentage, the outlet temperature has also increased conveniently, and FLiBe-4 and FLiNaK-4 have come out best secondary coolants compared with their base fluids. In the following Fig. 6, the contour image of the six secondary coolants' temperature distribution has been developed after simulation.

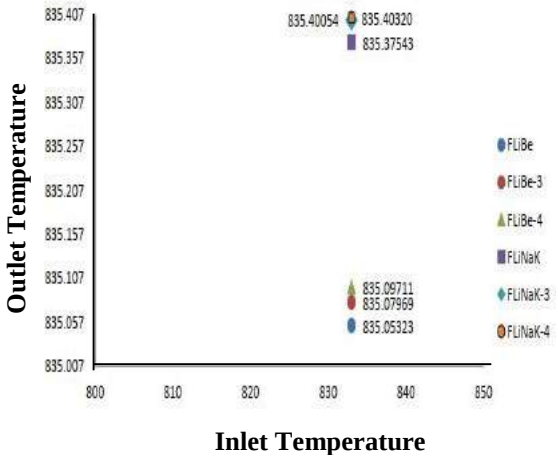

Fig. 5. Outer pipe inlet temperature vs. outlet temperature for secondary coolant candidates.

Fig. 7, illustrates that with the overall heat transfer coefficient increased with increasing Nano fluid volume percentage. At the same time, LMTD showed a decreasing trend in the case for FLiBe, whereas for the FLiNaK case, FLiNaK have been

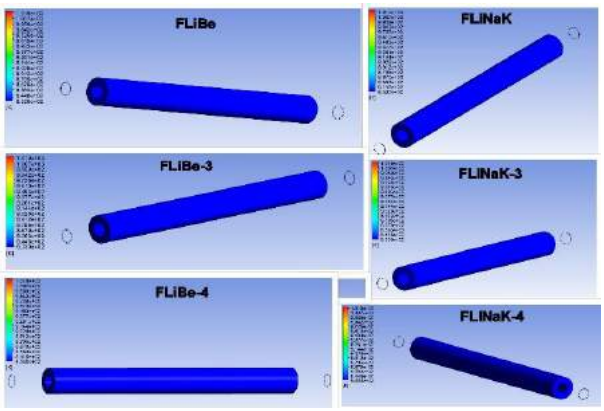

Fig. 6. Contour image of secondary coolants' temperature distribution.

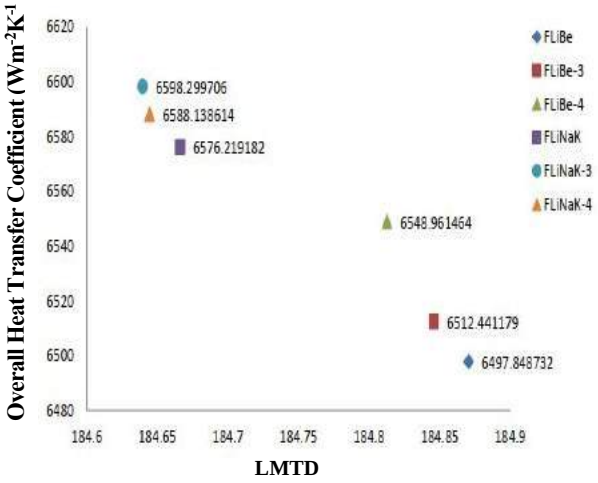

Fig. 7. LMTD vs. overall heat transfer coefficient for double pipe heat exchangers.

shown the lowest overall heat transfer coefficient and highest LMTD. However, the highest overall heat transfer coefficient and lowest LMTD have been found whenever FLiNaK-3 is used instead of FLiNaK-4 as a secondary coolant for the same fuel salt.

To summarize, it can be stated that by increasing nanofluid volume percentage gradually, the overall heat transfer coefficientand the outlet temperature of the secondary coolant have been increased for FLiBe. This indicates a positive output of the study.

Therefore, the heat exchanger area can be reduced whenever nanofluid is used, securing an economic

benefit. Because less area means less material is to be used for heat exchangers, which are expensive enough to withstand the high temperature.

The reason behind the nanofluids' positive impact can be explained by analyzing thepositive impact of nonofluids' Brownian motion and the higher wettability of the nanofluids compared to base fluids. The Brownian motion in nanofluids is significant compared to base fluids due to their nano-scale molecular presence, it transfers heat more conveniently than the base fluids. Moreover, due to its higher surface to volume ratio, it can easily create and continue contact between the solid surface of the pipe more conveniently and efficiently than the base fluid, thus increasing the heat transfer compared with the latter one. In addition, since the outlet temperature of the secondary coolant is increased, it will help enhance the efficiency of the power conversion loop later. But one distinct disadvantage of this experiment is that whenever there is an increased amount of nanofluid in FLiBe, the pressure drop pump's shows an increasing trend, which determines the power an economic setback.

For FLiNaK, it is clear that coolant with nanofluid is better than without using it in the first place, and it almost showed positive results like FLiBe. Nevertheless, there is a convoluted output. Instead of FLiNaK-4, FLiNaK-3 showed the best overall heat transfer coefficient, while FLiNaK-4 showed the best outlet temperature for coolant. The result is not as expected. The probable explanation for this matter can be about the heat exchanger dimension and less contact area to find positive feedback properly. It might also be solved with the finest meshingtechniques. Nonetheless, it is known that the temperature drop in fuel salt shouldn't exceed 100 K and for coolant, it should be around 50 K. Bearing that in mind, FLiNaK-4 may be a better candidate. However, the results difference was not significant enough. It can be overlooked due to the double pipe heat exchanger system. These results will be more significant with a more refined and rigorous shell and tube heat exchanger design.

Conclusions

Nanofluid plays a key role in enhancing heat transfer quality for nuclear reactors. This study illuminates the idea of using nanofluid in MSRs. This study has found out that, in the case of FLiBe, the outcome is satisfactory for using nanofluid and can be vouched for using it. However, in the case of FLiNaK, the study produced a convoluted outcome. Despite ensuring nanofluids superiority, the best option between FLiNaK-3 and FLiNaK-4 cannot be chosen without a doubt. In the future, with shell and tube heat changers, this proposal can be verified more providently and rigorously. Moreover, the neutronic analysis should also be conducted to ensure its criticality and maintain the safety and positive output of the reactors. Similarly, an opportunity cost may be decided between expensive heat exchanger material and a higher power pump, obviously with a detailed analysis of the findings.

Conflicts of Interest

The authors declare that they have no conflicts of interest regarding the publication of this article

Author's Contributions

Joy Surjy Deb: Concepts, Literature review, Simulation, analysis, Formatting, manuscript writing and revision.

Md. Mahidul Haque Prodhan: Concepts, Literature review, simulation, supervision, manuscript writing, analysis correction, and revision.

Nazmul Hossain: Literature review, result analysis, Formatting, and manuscript writing.

Golam Sarwar Rakib: Literature review, Formatting, and manuscript writing.

Nomenclature

u = fluid velocity

ρ = fluid density

η = stress tensor

Γ = fluid thermal conductivity

k = turbulence kinetic energy

ε = turbulence dissipation rate

μ_t = turbulence viscosity

G_k = production of turbulence kinetic energy

t = inner pipe thickness
D_i = inner pipe diameter
D_o = outer pipe diameter
L_i = inner pipe length
L_o = outer pipe length
t_{ci} = inlet temperature of fuel salt
t_{co} = outlet temperature of fuel salt
Q_i = amount of heat transfer taking place in fuel salt
Q_o = amount of heat transfer taking place in coolant salt
LMTD = logarithmic mean temperature difference
U = overall heat transfer coefficient
A_s = outer surface area of the inner pipe
k = thermal conductivity of hastelloy-nalloy

References

Allahyari S, Behzadmehr A and Sarvari SMH. Conjugate heat transfer of laminar mixed convection of a nanofluid through a horizontal tube with circumferentially non-uniform heating. *Nanoscale Res. Lett.* 2011; 6: 360.

Allibert M, Merle-Lucotte E, Heuer D, Brovchenko M and Ghetta V. Preliminary design assessment of the molten salt fast reactor. European Nuclear Conference (ENC 2012), Dec 2012, Manchester, United Kingdom. pp. 17-26. (in2p3-00766659).

Ambrosek J, Allen T, Anderson M, and Sridharan K. Current status of knowledge of the fluoride salt (FLiNaK) heat transfer. *Nucl. Tec.,* 2009; 165(2): 166-173.

Anderson MH, Clark MM, Das AK, Fiveland WA and Teigen BC. Heat transfer behavior of molten nitrate salt. In AIP Conference Proceedings, Solar, PACES. 2015; 1734(1): 040003. 1-8.

Aniza CN, Bahri CB, Al Areqi WM, Majid AAB and Ruf MIFM. Characteristic of molten fluoride salt system LiF-BeF2 (Flibe) and LiF-NaF-KF (Flinak) as coolant and fuel carrier in molten salt reactor. In: *AIP Conference Proceedings*, 2017; 1799(1): 040008.1-8.

Aybar HS, Azizian MR and Okutucu T. Effect of nanoconvection due to Brownian motion on thermal conductivity of nanofluids. In: *Proceeding of the 7th IASME/WSEAS International Conference on Heat Transfer, Thermal Engineering and Environment*, Moscow 2009; pp. 53-55

Bang KH, Choi OK, Hwang, IS, Jeong HS, and Kim KK. An experimental study on the flow and heat transfer of flinak molten salt in small channels for the application to the VHTR intermediate heat exchanger. In: *Proceedings of international congress on advances in nuclear power plants*, 2009, p. 2572.

Bettis CE, Braatz RJ, Cristy GA, Dyslin DA, Kelly OA, Pickel TW, Shobe LR, Spaller AE and Stoddart WC. Design study of a heat-exchange system for one MSBR (Molten Salt Breeder Reactor) concept, Oak Ridge National Laboratory, Tennessee, USA, 1967; Tech. Rep.TM-1545.

Boungiorno J, Forrest E, Hannink R, LW, Kim SJ and Truong B. Nanofluids for enhanced economics and safety of nuclear reactors: an evaluation of the potential features, issues, and research gaps. *Nucl. Tec.*, 2017; 162: 80-91.

Buongiorno J, Hu LW, McKrell T and Rea U. Laminar convective heat transfer and viscous pressure loss of alumina- water and zirconia-water nanofluids. *Int. J. Heat Mass Transf.* 2012; 52, 2042-2048.

Buongiorno J. Convective transport in nanofluids. *J. Heat Transf.* 2006; 128(3): 240-250.

Cammi A, Lorenzi S and Ronco A. Preliminary analysis and design of the heat exchangers for the molten salt fast reactor. *Nucl. Eng. Tec.*, 2019; 52(1): 51-58.

Cantor S, Cooke JW, Dworkin AS, Robbins GD, Thomas RE and Watson GM. Physical properties of molten-salt reactor fuel, coolant, and flush salts. Oak Ridge National Laboratory, Tennessee, USA, 1968; Tech. Rep. TM-2316.

Chi CW, Ferng YM and Kun-Yueh Lin. CFD investigating thermal-hydraulic characteristics of FLiNaK salt as a heat exchange fluid. *App. Ther. Eng., 20*12. 37: 235-240.

Choi SUS and Jang SP. Effects of various parameters on nanofluid thermal conductivity. *J. Heat Transf.* 2007; 129(5): 617-623.

Choi SUS, Eastman JA, Li S, Thompson LJ and Yu W. Anomalously increase effective thermal conductivities of ethylene glycol-based nanofluids containing copper nanoparticles. *Appl. Phy. Lett.*, 2001; 78 (6): 718-720.

Chukwu GA, Das DK and Kulkarni DP. Temperature dependent rheological property of copper oxide nanoparticles suspension (nanofluid). J. Nanosci. Nanotechnol., 2006; (4): 1150-1154.

Clarno KT, Toth LM and Williams DF. Assessment of candidate molten salt coolants for the advanced high- temperature reactor (AHTR). Oak Ridge National Laboratory, Tennessee, USA, 2006; Tech. Rep.TM-2006/12.

Das DK and Vajjha RS. Experimental determination of thermal conductivity of three nanofluids and development of new correlations. *Int. J. Heat Mass Transf.* 2009; 52(21-22): pp. 4675-4682.

Das SK, Dasgupta A, Dasgupta N, Patel HE, Sundararajan T and Pradeep T. A micro-convection model for thermal conductivity of nanofluids. *Pramana J. Phys*. 2005, 65: 863-869.

Dieuaide M. SAMOFAR molten salt fast reactor reprocessing unit design.

Ding Y and When DS. Experimental investigation into convective heat transfer of nanofluids at the entrance region under laminar flow conditions. *Int. J. Heat Mass Transf.* 2004; 47(24): 5181-5188.

Doche O, Rubiolol P and Tano M. Progress in modeling solidification in molten salt coolants. *Mod. Sim. Mat. Sci. Eng.*, 2017; 25: 074001.

Ebner MA, Sabharwall P, Sharpe P and Sohal MS. Engineering database of liquid salt thermophysical and thermochemical properties, Idaho National Laboratory, Idaho, USA, 2010; Tech. Rep. INL/EXT-10-18297.

Etemad SG, Esfahany MN and Heris SZ. Experimental investigation of oxide nanofluids laminar flow convective heat transfer. *Int. Com. Heat Mass Transf.* 2006; 33(4): 529-535.

Evans W, Fish J and Keblinski P. Role of Brownian motion hydrodynamics on nanofluid thermal conductivity. *Appl. Phy. Let.*, 2006; 88(9): 093116.

Forsberg CW. Molten-salt-reactor technlogy gapsk. In: Proceedings of ICAPP, USA, 2006; Article ID 6295: pp. 1-8.

Fraas AP and Laverne ME. Parametric survey of the effects of major parameters on the design of fuel-to-inert-salt heat mchangees for the msbr. Oak Ridge National Laboratory, Tennessee, USA, 1971; Tech. Rep. TM-2952.

Gerardin D, Allibert M, International Conference on Fast Reactors and Related Fuel Cycles: Next Generation Nuclear Systems for Sustainable Development. Yekaterinburg, Russia 2017; p. 129.

Gnielinski V. New equations for heat and mass transfer in turbulent pipe and channel flow. *Int. Chem. Eng.*, 1976; 16 (2): 359-367.

Hadad K, Rahimian A and Nematollahi M. Numerical study of single and two- phase models of water/Al2O3 nanofluid turbulent forced convection flow in VVER-1000 nuclear reactor. *Ann. Nucl. Energy*, 2013; 60: 287-294.

Hausen H. Neue gleichungen für die wärmeübertragung bei freier oder erzwungener stromüng (new equations for heat transfer in free or forced flow). *Allg. Wärmetechn*; 1959; 9: 75-79.

Hoffman HW and Lones J. Fused salt heat transfer, part II: forced convection heat transfer in circular tubes containing NaF-KF-LiF eutectic. Oak Ridge National Laboratory, Tennessee, USA, 1955; Tech. Rep.1777; Corpus ID: 137946943.

Huntley WR, Robertson HE and Silverman MD. *Heat transfer measurements in a forced convection loop with two molten-fluoride salts: LiF–BeF2-ThF4–UF4* and *EUTECTIC NaBF4–NaF*. Oak Ridge National Laboratory, Tennessee, USA, 1976; Tech. Rep. TM- 5335.

Kasam A and Shwageraus E. Approximate heat transfer solution for the breed and burn molten salt reactor. In: International Conference on Mathematics & Computational Methods Applied to Nuclear Science & Engineering, Korea, 2017; P146S02-07.

Kedl RJ. Fluid dynamic studies of the molten-salt reactor experiment (msre) core, Oak Ridge National Laboratory, Tennessee, USA, 1970; Tech. Rep. TM- 3229.

Kleinstreuer C and Koo J. A new thermal conductivity model fornanofluids. J. Nanoparticle. Res., 2004; 6(6): 577-588.

Köse U , Koç U, Erbay LB , Öğüt E and Ayhan H. Heat exchanger design studies for molten salt fast reactor. EPJ Nuclear Sci. Technol., 2019; 5: 12.

Kumar DH, Patel HE, Kumar VRR, Sundararajan T, Pradeep T and Das SK. Model for heat conduction in nanofluids. *Phy. Rev. Lett.* 2004; 93(14): 144301.

Li M, Ning B, Qiu Y and Zhang H. Numerical and experimental study on heat transfer and flow features of representative molten salts for energy applications in turbulent tube flow. *Int. J. Heat Mass Transf.* 2019; 135: 732-74.

Li Q and Xuan Y. Investigation on convective heat transfer and flow features of nanofluids. *J. Heat Transf.* 2003; 125(1): 151-155.

Marcello V, Cammi A and Luzzi L. Analysis of coupled dynamics of molten salt reactors. In: *Proceedings of the COMSOL Conference*, Hannover, Germany, Poster Presentation, 2008.

Mujumdar AS and Wang X. A Review on Nanofluids - part I: Theoretical and Numerical Investigations. *B. J. Chem. Engr.*, 2008; 25(4): 613-630.

Rubiolo PR, Retamales MT, Ghetta VE and Giraud J. High temperature thermal hydraulics modeling of a molten salt: application to a molten salt fast reactor (MSFR). In: *ESAIM: Proc. Surv.*, 2017; 58: 98-117.

Sarma PK, Sharma KV and Sundar LS. Estimation of heat transfer coefficient and friction factor in the transition flow with low volume concentration of Al_2O_3 nanofluid flowing in a circular tube and with twisted tape insert. *Int. Com. Heat Mass Transf.* 2009; 36(5): 503-507.

Singh MK and Sundar LS. Convective heat transfer and friction factor correlations of nanofluid in a tube and with inserts: A review. *Renew. Sustain. Energy Rev.*, 2013; 20: 23-35.

Srichai S. Friction factors for single phase flow in smooth and rough tubes, Thermopedia. doi: 10.1615/ A to Z.f.friction_factors_for_single_phase_flow_in_smooth _and_rough_tubes.

Trivedi A. Thermo-mechanical solutions in electronic packaging: component to system level. M.Sc. dissertation, Dept. Mechanical. Eng., The University of Texas, Arlington, Texas, USA, 2008.

Williams DF. Assessment of candidate molten salt coolants for the ngnp/hi heat transfer loop. Oak Ridge National Laboratory, Tennessee, USA, 2006; Tech. Rep. TM-2006/69.

J. Bangladesh Acad. Sci. 46(1); 57-63: June 2022 DOI: 10.3329/jbas.v46i1.60347

Journal of Bangladesh Academy of Sciences

Journal homepage: http://www.bas.org.bd/publications/jbas.html

Research Article

One nucleon pick-up reaction ^{58}Ni(p,d)^{57}Ni at 68 MeV

Sadia Afroze Sultana* and Md. Azizur Rahman[1]

Open School, Bangladesh Open University, Gazipur, Bangladesh

ARTICLE INFO

Article History

Received: 21 May 2021
Revised: 8 June 2022
Accepted: 12 June 2022

Keywords: Double-differential cross section, (p,d) reaction, DWBA analysis, Direct reaction model.

ABSTRACT

The double differential cross-section for the ^{58}Ni(p,d)^{57}Ni reaction has been studied with 68 MeV protons for the 25°, 30°, 35°, 45°, and 60° laboratory angles. The spectra have been calculated using DWBA-based cross-sections including an asymmetric form of the Lorentzian strength function containing energy-dependent spreading widths. The comparison between the measured spectra and the theoretical predictions is accomplished in the direct reaction region. The values of the calculated double differential cross-sections agree with those of the measured cross-sections as far as ~17 MeV deuteron excitation energies; the ejectile deuterons-energy for direct reactions at 68 MeV proton energy.

Introduction

Reliable nuclear structure and reaction data represent the fundamental building blocks of nuclear physics and are of importance in astrophysics research and many other applications (U.S. DEPARTMENT OF ENERGY, 2016). The development of modern nuclear technologies requires a large amount of nuclear data for the conceptual design of different fields of applications, such as the technology of radioactive waste transmutation, power production, radiotherapy, shielding problems, and so on (Grudzevich et al., 2007).

Theoretical models for producing nuclear data are always in demand both for a general understanding of the physical phenomena related to the analyzed data and to estimate the required cross-sections in cases where data are contradictory or not fully available (Ignatyuk, 2013). Ideally, nuclear data are expected to be collected experimentally for nucleons at various incident energies and all kinds of emitted particles over all the energies and the emission angles. However, it is not possible, in reality, to have all necessary nuclear data experimentally as desired for its high cost and all kinds of preparations for the experiments. So, developing a theoretical model, that can produce nuclear data is always indispensable.

Therefore, an approach by Lewis (Lewis, 1975) was suggested to be employed in parallel with the predictive models given by Crawley (Crawley, 1980); Gales et al. (Gales et al., 1988), and Matoba et al. (Matoba et al., 1995 and 1996). These authors had suggested methods using an asymmetric shape of the Lorentzian strength function having energy-dependent spreading widths multiplied by DWBA cross-sections for the theoretical calculations of double differential cross-sections. This model has been successfully applied to the (p,d) reactions (Syafarudin et al., 2002; Sultana et al., 2004; Aramaki et al., 2002; Sultana et al., 2005; Sultana et al., 2009; Sultana and Imtiaz, 2017), then applied to the (n,d) reaction (Sultana et al., 2003; Sultana et al., 2004; Sultana, 2006; Sultana et al., 2010) with a slight modification and with reasonable success.

The continuum spectra of the ^{58}Ni(p,d)^{57}Ni reaction have been analyzed in the present work by

*Corresponding author: <sadia_afroze@yahoo.com>

[1]Department of Physics, University of Dhaka, Bangladesh

the same method of calculations discussed above to ascertain the reliability of this method of calculations as a global one. This may be mentioned here that the same reaction (p,d) for the same target nucleus (^{58}Ni) and with the same method of calculation but at different incident energy (42 MeV) were studied by the author (Sultana and Hossain, 2016; Sultana, 2017). In the present work, the laboratory angles of deuterons emission are 25^o, 30^o, 35^o, 45^o, and 60^o for the incident proton energy 68.0 MeV. The experimental continuum spectra are well produced by calculation as far as ∼17 MeV deuteron excitation energies in the direct reaction region.

Experiment

The experiments were performed at the TIARA facility of JAERI. A proton beam of 68 MeV from the AVF cyclotron was led to the HB-1 beam line. The energy distribution of light ions emitted from the target was measured using a ΔE-E counter telescope, which consisted of two thin silicon ΔE-detectors and a CsI(T1) E-detector with a photo-diode readout. Details of the experimental procedure and the results have been reported in Harada et al. (2002).

Theoretical Calculations

The Glimpses of the Theoretical Basis

Generally, the spectra of the emitted particles from one nucleon transfer reactions can be divided into three types, direct, pre-equilibrium, and evaporation processes, because of different mechanisms and the time lengths of events involved. The spectrum of the evaporation process results from three processes. These are absorption of the incident particles by the target nucleus, formation of a compound nucleus and emission of nucleons, or light particles from a highly excited state of the compound nucleus, or the decay of the compound nucleus. The direct reaction process occurs with a low momentum transfer condition through interactions between the incident particles and surface nucleons in the target nucleus. Here, the energy of the emitted particles is higher, and the residual nucleus remains in lower excitation energy. A relatively flat spectrum, in the pre-equilibrium region is observed between the evaporation and direct reaction regions. The former results from multi-step, direct and/or compound nuclear reactions. The pre-equilibrium processes progress step by step through the interactions between incident nucleons and nucleons within the target nucleus.

The theoretical calculations of the double differential cross-sections, a function both of solid angle and incident energy, have been performed, considering a direct reaction model as an incoherent summation of the direct reaction components. The double differential cross-section, $\frac{d^2\sigma}{d\Omega dE}$, consists of three factors (Sultana and Rahman, 2021), a normalization constant, spin-weighted spectroscopic factor $C^2S_{l,j}(E)$, where the energy dependence is taken care of by an asymmetric Lorentzian function, $f_{l,j}(E)$ (Matoba et al., 1995 and 1996; Mahaux and Sartor, 1989 and 1991) and the $\frac{d\sigma}{d\Omega}\Big]_{i,j}^{dw}(E)$, the DWBA based cross-section calculated by the code DWUCK-4 (Kunz, unpublished). The sum rule of the spectroscopic factors of nucleon orbits for $T \pm 1/2$ isospin states is estimated with a simple shell model prescription (French and Macfarlane, 1961):

$$C^2S_{l,j} = \frac{n_{p(l,j)}}{2T+1} \quad (1)$$

Here, $n_{p(l,j)}$ is the number of protons for each l,j orbit, and T is the target isospin.

The strength function, $f_{l,j}(E)$ is of the form

$$f_{l,j}(E) = \frac{n_o}{2\pi}\frac{\Gamma(E)}{\left(|E-E_F|-E_{l,j}\right)^2+\Gamma^2(E)/4} \quad (2)$$

where, n_o is the renormalization constant. The Fermi energy E_F is calculated by an empirical formula given by Hisamochi et al. (Hisamochi et al.,1993). The sum rule of the spectroscopic factor and the

centroid energies $(E_{l,j})$ for $j = l \pm 1/2$ shell orbits have been estimated using a BCS calculation (Bardeen et al., 1957). The required single particle energies are calculated following Bohr and Mottelson (Bohr and Mottelson, 1996). The strength function $f_{l,j}(E)$ integrates over the energy integrand dE to unity (Sultana and Rahman, 2021), starting from a certain initial to a final energy of the ejectile, deuterons. The spreading width $\Gamma(E)$ is expressed by a function proposed by Brown and Rho (Brown and Rho, 1981) and also by Mahaux and Sartor (Mahaux and Sartor, 1989 and 1991) as:

$$\Gamma(E) = \frac{\epsilon_0 (E - E_F)^2}{(E - E_F)^2 + E_0^2} + \frac{\epsilon_1 (E - E_F)^2}{(E - E_F)^2 + E_1^2} \quad (3)$$

where, ϵ_0, ϵ_1, $E_{0\,,}$ and E_1 are constants and describe the effects of nuclear damping in the nucleus (Matoba et al., 1995). The estimated values of the constants are taken from Matoba et al. (1995).

Results and Discussion

Double differential cross-sections (DDXs) have been analyzed for the ^{58}Ni(p,d)^{57}Ni reaction at 68 MeV incident proton energy, as shown in Figs. 1-5. The laboratory angles are 25°, 30°, 35°, 45°, and 60° for this work. The data are binned in 500 keV intervals. Experimental and theoretical results are given by the circles and lines, respectively. Three global potentials (Becchetti and Greenlees, 1969; Koning and Delaroche, 2003; Menet et al., 1971) are used here for protons, while for deuteron, an adiabatic potential from Koning and Delaroche (Koning and Delaroche, 2003); those from Becchetti and Greenlees (Becchetti and Greenlees, 1969) and Menet et al. (Menet et al., 1971) based on the proton and neutron potentials were constructed for the DWUCK-4 calculations as shown in Table 1. The solid, dotted, and short-long-dashed lines represent the DDXs for Beccheti and Greenlees (Becchetti and Greenlees, 1969), Koning and Delaroche (Koning and Delaroche, 2003) and Menet et al. (Menet et al., 1971) potentials respectively.

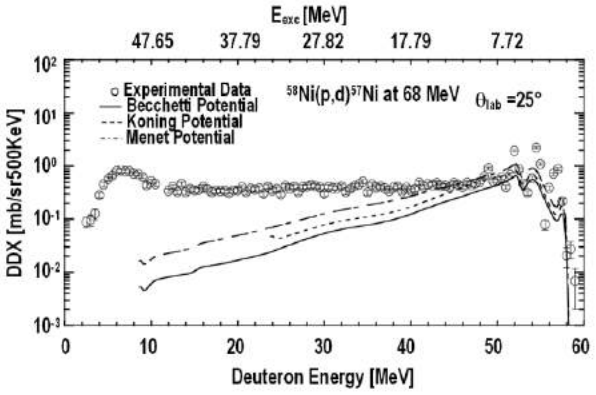

Fig. 1. Double differential cross sections for the ^{58}Ni(p,d)^{57}Ni reaction at 68 MeV for 25° angle.

In Fig. 1, at a 25° angle, the theoretical DDXs are in excellent agreement with the experimental one with Koning and Delaroche (Koning and Delaroche, 2003) potential and those using the Beccheti and Greenlees (Becchetti and Greenlees, 1969) and Menet et al. (Menet et al., 1971) potentials, the theoretical DDXs are in good agreement. The shape of the calculated spectra is in good agreement with experimental ones for all three potentials (Becchetti and Greenlees, 1969; Koning and Delaroche, 2003; Menet et al., 1971) throughout the direct reaction region, i.e., up to ~17.79 MeV excitation energies.

Fig. 2 shows that the calculated DDX spectra are in good agreement with the experimental one using the Koning and Delaroche (Koning and Delaroche, 2003) and Menet et al. (Menet et al., 1971) potentials, both for the peak production and shape at 30° angle. But for Beccheti and Greenlees's (Becchetti and Greenlees, 1969) potential, the calculated DDXs are somewhat underestimated compared with the experimental one.

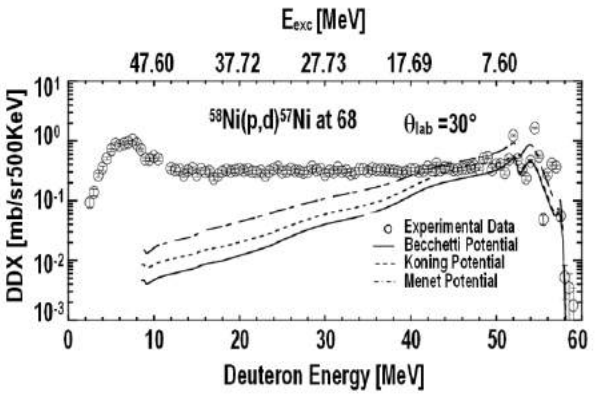

Fig. 2. Double differential cross sections for the ^{58}Ni(p,d)^{57}Ni reaction at 68 MeV for 30° angle.

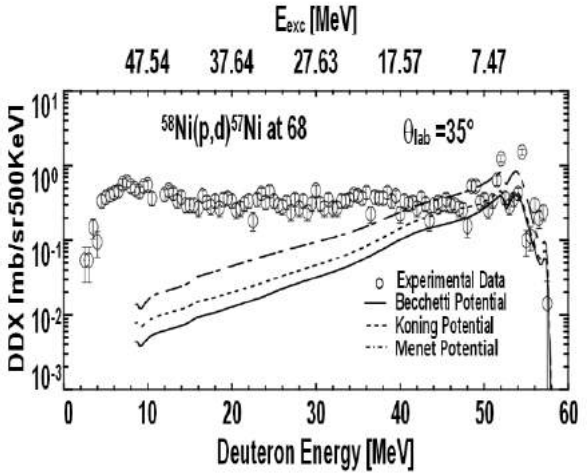

Fig. 3. Double differential cross sections for the ^{58}Ni(p,d)^{57}Ni reaction at 68 MeV for 35° angle.

Fig. 3 shows that the calculated DDX spectra are in very good agreement with the experimental one with Menet et al. (Menet et al., 1971) and Koning and Delaroche (Koning and Delaroche, 2003) potentials, both for the peak production and shape at 35^{o} angle while for Beccheti and Greenlees (Becchetti and Greenlees, 1969) potential, the calculated DDX is a little bit underestimated at higher excitation energies ($\sim 12 - 17.57$ MeV).

It is observed that there is somewhat underestimation of the theoretically calculated DDXs at the peak values of the experimental cross-sections for every angle (25^{o}, 30^{o}, 35^{o}, 45^{o}, and 60^{o}) at the lower excitation energies. This may be due to contributions of some non-pick-up reactions like the multi-step reaction process, which has not been considered in the present calculation.

In Figs. 4 and 5, the shapes of the theoretical DDXs are reproduced well with Menet et al. (Menet et al., 1971) potential as compared with the experimental ones both for 45^{o} and 60^{o} angles, respectively. But, the theoretical DDXs are somewhat underestimated with the Beccheti and Greenlees (Becchetti and Greenlees, 1969) and Koning and Delaroche (Koning and Delaroche, 2003) potentials.

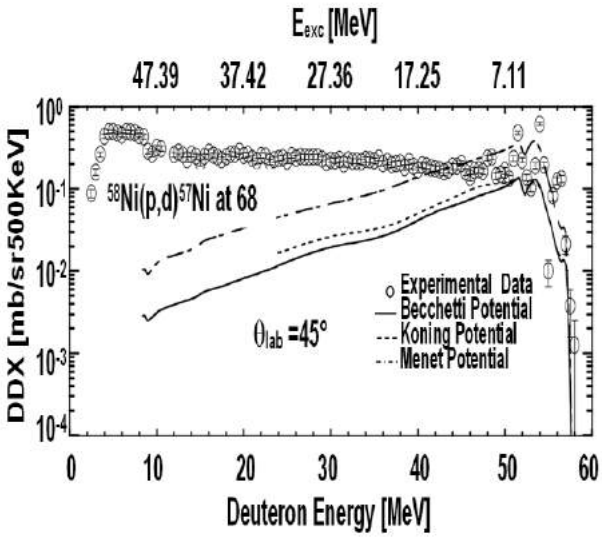

Fig. 4. Double differential cross sections for the ^{58}Ni(p,d)^{57}Ni reaction at 68 MeV for 45° angle.

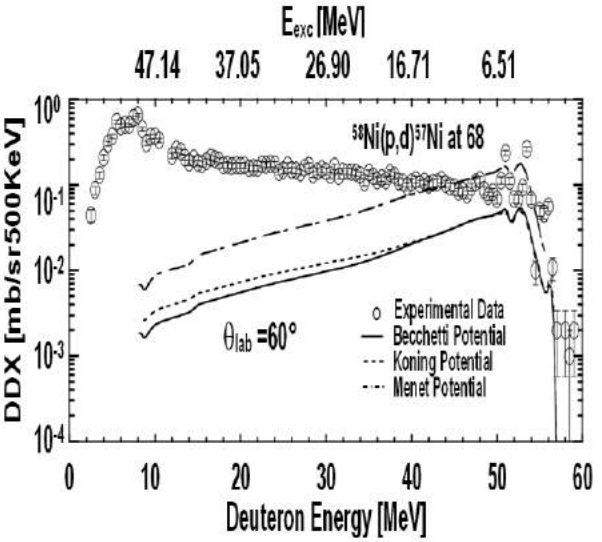

Fig. 5. Double differential cross sections for the ^{58}Ni(p,d)^{57}Ni reaction at 68 MeV for 60° angle.

Generally, the shapes of the continuum spectra are well reproduced, and the absolute values of cross sections are in good agreement with and very close to the experimental data in the direct reaction region. Nevertheless, there is still further scope for improvement by using different optical model potentials for proton and deuteron to overcome the minor discrepancies between theoretical and experimental DDXs in the direct reaction region.

Table 1. Optical model parameters were used in the DWBA calculations for the ^{58}Ni(p,d)^{57}Ni reaction at 68 MeV.

Becchetti and Greenlees potential (Becchetti and Greenlees, 1969)

Particle	V	r	a	r_c	W_v	W_s	r′	a′	V_{so}	r_{so}	a_{so}
	(MeV)	(fm)	(fm)	(fm)	(MeV)	(MeV)	(fm)	(fm)	(MeV)	(fm)	(fm)
Proton	35.96	1.17	0.75	1.25	12.26	0.00	1.32	0.53	6.20	1.01	0.75
Deuteron	a	1.17	0.78	1.25	b	b	1.29	0.58	6.20	1.06	0.75
Neutron	c	1.25	0.65								

[a]$V = 110.3 - 0.64(E_d/2) + 0.4Z/A^{1/3}$ (MeV)

[b]$W_v = 0.44(E_d/2) - 4.26$ (MeV), $Ws = 24.8 - 0.50(E_d/2)$ (MeV), E_d is the deuteron kinetic energy.

[c]Well depth adjusted to fit the separation energy.

Koning and Delaroche potential (Koning and Delaroche, 2003)

Particle	V	r	a	r_c	W_v	W_s	r′	a′	V_{so}	r_{so}	a_{so}
	(MeV)	(fm)	(fm)	(fm)	(MeV)	(MeV)	(fm)	(fm)	(MeV)	(fm)	(fm)
Proton	32.11	1.20	0.67	1.26	7.36	3.11	1.28	0.54	4.51	1.02	0.59
Deuteron	a	1.20	0.67	1.26	a	a	1.28	0.54	a	1.02	0.59
Neutron	b	1.25	0.65								

[a]Adiabatic potentials with those of (Koning and Delaroche, 2003)

[b]Well depth adjusted to fit the separation energy.

Menet potential (Menet et al., 1971)

Particle	V	r	a	r_c	W_v	W_s	r′	a′	V_{so}	r_{so}	a_{so}
	(MeV)	(fm)	(fm)	(fm)	(MeV)	(MeV)	(fm)	(fm)	(MeV)	(fm)	(fm)
Proton	38.74	1.16	0.75	1.25	7.32	1.34	1.37	0.23	6.04	1.06	0.75
Deuteron	a	1.16	0.75	1.25	b	b	1.37	c	6.04	1.06	0.75
Neutron	d	1.25	0.65								

[a]$V = 99.8 - 0.44(E_d/2) + 0.4Z/A^{1/3}$ (MeV)

[b]$W_v = 2.4 + 0.18(E_d/2)$ (MeV), $Ws = 8.40 - 0.10(E_d/2)$ (MeV), E_d is the deuteron kinetic energy.

[c]$a' = 0.74 - 0.008(E_d/2) + 1.0(N-Z)/2A$, [d]Well depth adjusted to fit the separation energy.

For all potentials nonlocality, finite-range parameters and spin-orbit term are shown below:

Particle	Nonlocality parameters (fm)	Finite-range parameter (fm)	Thomas-Fermi spin orbit term
Proton	0.85	0.621	λ= 25
Neutron	0.85	0.621	
Deuteron	0.54		

Conclusions

Nuclear reaction double differential cross sections have been analyzed for the proton-induced reactions on ^{58}Ni at 68 MeV. Three global potentials for proton and deuteron, including the adiabatic potentials for deuteron, are used here to analyze the spectra for the confirmation of the globality of this theoretical model. The calculated spectra show a good agreement with the experimental data both in magnitude and shape. The calculation of theoretical values of spectra without using any arbitrary renormalization of the cross-sections renders this theoretical method more applicable for nuclear data analysis.

Acknowledgment

One of the authors (Dr. S. A. Sultana) is grateful to the Ikeda Laboratory, Department of Applied Quantum Physics and Nuclear Engineering, Kyushu University, Japan, for providing a necessary theoretical base to analyze this work and to JAERI, Japan, for allowing to use the experimental data measured at the TIARA facility.

References

Aramaki F, Syafarudin, Wakabayashi G, Uozumi Y, Ikeda N, Matoba M, Sakae T and Koori N. ^{100}Mo(p,d)^{99}Mo reaction at 50 MeV and direct reaction analysis. In: *Proceedings of the 2002 Symposium on Nuclear Data.* 2002; JAERI-Conf. 2002-006: 178-182.

Bardeen J, Cooper LN and Schrieffer JR. Theory of superconductivity. *Phys. Rev.* 1957; 108(5): 1175-1204.

Becchetti FD, Jr and Greenlees GW. Nucleonnucleus optical-model parameters, A>40, E<50 MeV, *Phys. Rev.* 1969; 18(4): 1190-1209.

Bohr A and Mottelson BR. Nuclear Structure. Volume 1; Single-Particle Motion, Appendix 2D: Model for Strength Function Phenomena. W. A. Benjamin, Inc., New York. 1996; 302-307.

Brown GE and Rho M. The giant Gamow-Teller resonance. *Nucl. Phys. A.* 1981; 372: 397-417.

Crawley GM. Proceeding of the International Symposium on Highly Excited States in Nuclear Reactions, *Osaka, Japan.* 1980; 590-611.

French JB and Macfarlane MH. Isobaric-spin splitting of single-particle resonances. *Nucl. Phys.* 1961; 26: 168-176.

Gales S, Stoyanov Ch and Vdovin AI. Damping of high-lying single-particle modes in heavy nuclei, *Phys. Rep.* 1988; 166 (3): 125-193.

Grudzevich O, Martirosyan J and Yavshits S. Complete files of neutron- and proton-induced nuclear data to 1 GeV for 208Pb target. Proceedings of the International Conference on Nuclear Data for Science and Technology, *EDP Sciences.* 2007; 2: 1213-1215.

Harada M, Watanabe Y, Tanaka Y, Matsuoka Y, Shin K, Meigo S, Takada H, Sasa T, Iwamoto O, Fukahori T, Chiba S and Tanaka S. Light charged-particle production in proton-induced reactions on ^{12}C, ^{27}Al, ^{58}Ni, ^{90}Zr, ^{197}Au, and ^{209}Bi at 42 and 68 MeV. *J. Nucl. Sci. Technol.* (Suppl. 2) 2002; 39: 393-396.

Hisamochi K, Iwamoto O, Kisanuki A, Budihardjo S, Widodo S, Nohtomi A, Uozumi Y, Sakae T, Matoba M, Nakano M, Maki T, Matsuki S and Koori N. Hole strengths and spreading widths observed in reaction at 65 MeV. *Nucl. Phys. A.* 1993; 564: 227-251.

Ignatyuk AV. Statistical theory of nuclear reactions. ICTP-IAEA Joint Workshop on Nuclear Data for Science and Technology: Medical Applications. 2013.

Koning AJ and Delaroche JP. Local and global nucleon optical models from 1 keV to 200 MeV. *Nucl. Phys. A.* 2003; 713: 231-310.

Kunz, P.D., 1974. DWBA code DWUCK- 4, University of Colorado (Unpublished).

Lewis MB. Effects of spreading widths upon the direct nuclear reaction continuum. *Phys. Rev. C.* 1975; 11: 145-153.

Mahaux C and Sartor R. From scattering to very deeply bound neutrons in 208Pb: Extended and improved moment approaches. *Nucl. Phys. A.* 1989; 493: 157-223.

Mahaux C and Sartor R. Single particle motion in nuclei. In: *Advances in Nuclear Physic.* Negele JW, Vogt E. (eds). Vol. 20, Springer, Boston, MA, 1991.

Matoba M, Iwamoto O, Uozumi Y, Sakae T, Koori N, Ohgaki H, Kugimiya H, Ijiri H, Maki T and Nakano M. Fragmentation of neutron-hole strengths in ^{59}Ni observed in the ^{60}Ni (p,d)^{59}Ni reaction at 65 MeV. *Nucl. Phys. A.* 1995; 581: 21-41.

Matoba M, Kurohmaru K, Iwamoto O, Nohtomi A, Uozumi Y, Sakae T, Koori N, Ohgaki H, Ijiri H, Maki T, Nakano M and Sen Gupta HM. (p,d) reaction on ^{62}Ni at 65 MeV. *Phys. Rev. C.* 1996; 53(4): 1792-1803.

Menet JJH, Gross EE, Malanify JJ and Zucker A. Total reaction cross-section measurements for 30-60 MeV protons and the imaginary optical potential. *Phys. Rev. C.* 1971; 4(4): 1114-1129.

Sultana SA and Hossain SM. Analysis of continuum spectra for the ^{58}Ni(p,d)^{57}Ni reaction with direct reaction model. *Nucl. Sci. Appl.,* 2016; 25 (1 & 2): 41-44.

Sultana SA and Imtiaz A. Study of ^{27}Al(p,d)^{26}Al Reaction at 42 MeV. *Nucl. Sci. Appl.,* 2017; 26 (1&2): 29-32.

Sultana SA and Rahman M A. Study of (p,d) reaction on ^{209}Bi at 42 MeV. *J. Bangladesh Acad. Sci.* 2021; 45(2): 197-203.

Sultana SA, Kin T, Wakabayashi G, Uozumi Y, Ikeda N, Watanabe Y and Matoba M. Analysis of continuum spectra for proton induced reactions on ^{27}Al, ^{58}Ni, ^{90}Zr, ^{197}Au and ^{209}Bi at Incident energies 42 and 68 MeV-Direct reaction model analysis. In: *Proceedings of the 2005 Symposium on Nuclear Data, JAEA-Conference.* 2005; 2006-009: 185-189.

Sultana SA, Maki D, Wakabayashi G, Uozumi Y, Ikeda N, Syafarudin, Aramaki F, Kawaguchi T, Matoba M and Sen Gupta HM. The ^{96}Mo(pd)^{95}Mo ^{96}Mo(p→,d)^{95}Mo reaction at 50 MeV. *Phys. Rev. C.* 2004; 70(3): 034612(1)-034612(15).

Sultana SA, Sarker DR, Wakabayashi G, Uozumi Y, Ikeda N and Matoba M. Analysis of ^{197}Au(p,d)^{196}Au reaction with direct reaction model. *Nucl. Sci. Appl.* 2009; 18(1): 24-28.

Sultana SA Syafarudin, Aramaki F, Maki D, Wakabayashi G, Uozumi Y, Ikeda N, Matoba M, Watanabe Y and Sen Gupta HM. Analysis of continuum spectra of (n,d) reactions with direct reaction model. Proceeding of the 2003 Symposium on Nuclear Data of JAERI-Conf. 2004-005, November 27-28, 2003; 133-137.

Sultana SA, Syafarudin, Maki D, Kin T, Wakabayashi G, Uozumi Y, Ikeda N, Watanabe Y, Aramaki F, Matoba M, Kawaguchi T, and Sen Gupta HM. Continuum spectra analysis of (p,d) and (n,d) reactions on Bi in several Tens of MeV energy region. In*: Proceeding of 2004 Symposium on Nuclear Data of JAERI-Conference.* 2005-003, 2004; 143-147.

Sultana SA, Wakabayashi G, Uozumi Y, Ikeda N and Matoba M. Analysis of the 209Bi(n,d)208Pb reaction with direct reaction model. *Nucl. Sci. Appl.* 2010; 19(2): 27-30.

Sultana SA. Continuum spectra in one-nucleon transfer reaction- ^{209}Bi(n,d)^{208}Pb reaction, Ep=41.0-53.5 MeV. *Nucl. Sci. Appl.* 2006; 15(1): 53-57.

Sultana SA. Study of the ^{58}Ni(p,d)^{57}Ni teaction with direct reaction model. *Nucl. Sci. Appl.,* 2017; 26 (1&2): 45-48.

Syafarudin, Aramaki F, Wakabayashi G, Uozumi Y, Ikeda N, Matoba M, Yamaguchi K, Sakae T, Koori N and Maki T. Continuum spectra in one nucleon transfer reactions– (p,d) reactions at medium energy region. *J. Nucl. Sci. Technol.* (Suppl. 2), 2002; 1: 377-380.

U.S. Department of Energy. White Paper on Nuclear Data Needs and Capabilities for Basic Science. Office of Science, US Nuclear Data Program. 2016, August 10-11; 6.

J. Bangladesh Acad. Sci. 46(1); 65-73: June 2022 DOI: 10.3329/jbas.v46i1.60348

Journal of Bangladesh Academy of Sciences

Journal homepage: http://www.bas.org.bd/publications/jbas.html

Research Article

The Sandor-Smarandache function with a prime factor

Abdullah-Al-Kafi Majumdar*, Hary Gunarto[1] and Abul Kalam Ziauddin Ahmed[2]

Yamanote-cho, Beppu-shi, Japan

ARTICLE INFO

Article History

Received: 15 May 2022
Revised: 9 June 2022
Accepted: 12 June 2022

Keywords: Sandor-Smarandache function, Diophantine equation, arithmetic function, prime factor.

ABSTRACT

The Sandor-Smarandache function, denoted by SS(n), is a newly-introduced Smarandache-type arithmetic function. This paper focuses on the functions SS(30p), SS(60p), SS(210p), SS(420p) and SS(840p), where p (≥ 2) is a prime. At the end of the paper, four tables, giving the values of SS(30p), SS(60p), SS(210p) and SS(420p) for the first 200 primes, calculated on a computer, are given.

Introduction

The Sandor-Smarandache function, proposed by Sandor (2001), is denoted by $SS(n)$ and is defined as follows: For $n \geq 7$,

$$SS(n) = max\left\{k : 1 \leq k \leq n-2, n \text{ divides } \binom{n}{k}\right\}, \qquad (1)$$

where by convention,

$$SS(1) = 1, SS(2) = 1, SS(6) = 1. \qquad (2)$$

Let, for $0 \leq k \leq n$,

$$C(n, k) \equiv \binom{n}{k} = \frac{n(n-1)(n-2) \ldots (n-k+1)}{k!}. \qquad (3)$$

Then, the problem of finding $SS(n)$ may be stated as follows: Given an integer n (≥ 7), find the minimum integer k such that $k!$ divides the number $(n-1)(n-2)\ldots(n-k+1)$, where $1 \leq k \leq n-2$. With this minimum k, $SS(n) = n-k$.

Thus, to find $SS(8)$, note that 2! does not divide 7, but $3! = 2\times3$ divides 7×6. Hence, the minimum k such that $k!$ divides 7×6 is 3; consequently, $SS(8) = 8-3 = 5$.

An extensive study of the function was made by Majumdar (2018). Later, the problem was studied, to some extent, by Majumdar (2019), Islam et al. (2021), Majumdar and Ahmed (2021), Islam et al. (2021), and Islam et al. (2022). The following properties are known about $SS(n)$.

Lemma 1: $SS(n) = n-2$ if and only if n (≥ 3) is an odd integer.

Lemma 2: $SS(n) = n-3$ if and only if n (≥ 4) is an even integer, not divisible by 3.

From Lemma 1 and Lemma 2, it follows that $SS(n) \leq n-4$ if n is of the form $n = 6m$, $m \geq 1$ being any integer.

This paper considers functions of the forms $SS(30p)$, $SS(60p)$, and $SS(210p)$, where p is a prime. This is done in the next section. In the analysis of the problem, the following results would be needed.

Lemma 3: Let a, b, and c be any three integers. The linear Diophantine equation $ax + by = c$ has a solution if and only if $d \equiv \gcd(a, b)$ divides c. Moreover, if (x_0, y_0) is a solution, then the general solution is given parametrically by $x = x_0 + (\frac{b}{d})t$, $y = y_0 + (\frac{-a}{d})t$ for any integer t.

Proof: See, for example, Gioia (2001,Theorem 12.2).

Lemma 4: For any integer m (≥ 1), the product of m consecutive integers is divisible by $m!$.

Proof: See Hardy and Wriht (2002, Theorem 74).

*Corresponding author: <aakmajumdar@gmail.com>

[1]APU, Jumonjibaru, Beppu-shi, Japan

[2]World University of Bangladesh, Dhanmondi, Dhaka, Bangladesh

Lemma 3 gives the complete solution of the linear Diophantine equation of the form $ax + by = c$. Recall that a Diophantine equation involves two or more variables for which positive integer solutions are required.

Main results

First, the following result is proved, which gives an explicit form of $SS(30p)$.

Lemma 5: Let $p \geq 2$ be a prime. Then,

$$SS(30p) = \begin{cases} 30p - 4, & if\ \ p = 4s + 3,\ s \geq 0 \\ 30p - 7, & otherwise \end{cases}$$

Proof: Consider the following expression:

$$C(30p, 4) \equiv 30p\left[\frac{(30p-1)(15p-1)(10p-1)}{4}\right].$$

Now, the problem is to find the condition such that the term inside the square bracket is an integer. In other words, the problem is to find the condition on p such that the term inside the square bracket is an integer. Now, p may be of one of the two forms, namely, $p = 4s + 3$ (for some integer $s \geq 0$), and $p = 4t + 1$ (for some integer $t \geq 1$). If $p = 4s + 3$, then

$$15p - 1 = 4(15s + 11),$$

This shows that 4 divides $15p - 1$, so the term inside the square bracket is an integer.

To complete the proof, consider the case when $p = 4t + 1$. Note that, in this case, 4 does not divide $15p - 1$. The expression

$$C(30p, 5) \equiv 30p\left[\frac{(30p-1)(15p-1)(10p-1)(15p-2)}{2\times 5}\right]$$

shows $SS(30p) \neq 30p - 5$ for any prime $p \geq 2$. Also, from the expression for $C(30p, 6)$

$$C(30p, 6) \equiv 30p\left[\frac{(30p-1)(15p-1)(10p-1)(15p-2)(6p-1)}{3\times 4}\right]$$

it follows that $SS(30p) \neq 30p - 6$ for any prime $p \geq 3$. Now, consider the expression

$$C(30p, 7) \equiv$$

$$30p\left[\frac{(30p-1)(15p-1)(10p-1)(15p-2)(6p-1)(5p-1)}{2\times 7}\right].$$

Here, one of the numbers, $15p - 2$ and $15p - 1$, is even, depending on whether $p = 2$ or p is odd. Also, $p \neq 7$ (since by part (1) of the lemma, $SS(210) = 206$). Thus, the term inside the square bracket is an integer by virtue of Lemma 4. All these establish the lemma.

The lemma below finds $SS(60p)$.

Lemma 6: Let $p \geq 2$ be a prime. Then,

$$SS(60p) = \begin{cases} 30p - 6, & if\ \ p = 6s + 5,\ s \geq 0 \\ 60p - 7, & if\ \ p = 6t + 1,\ t \geq 2 \end{cases}$$

Proof: Consider the following expression:

$$C(60p, 4) \equiv 60p\left[\frac{(60p-1)(30p-1)(20p-1)}{4}\right].$$

Clearly, the numerator of the term inside the square bracket is not divisible by 4. Also, the expression

$$C(60p, 5) \equiv 60p\left[\frac{(60p-1)(30p-1)(20p-1)(15p-1)}{5}\right]$$

shows that the term inside the square bracket cannot be an integer. Thus, for any prime p,

$SS(60p) \neq 60p - 4$, $SS(60p) \neq 60p - 5$, Now, consider the expression:

$$C(60p, 6) \equiv 60p\left[\frac{(60p-1)(30p-1)(20p-1)(15p-1)(12p-1)}{6}\right].$$

Note that, p is either of the form $p = 6s + 5$ (for some integer $s \geq 0$), or it is of the form $p = 6t + 1$ (for some integer $t \geq 0$). With $p = 6s + 5$,

$$20p - 1 = 3(40s + 33),$$

so that $20p - 1$ is divisible by 3; also, with this p, $15p - 1$ is even. Thus, the term inside the square bracket is an integer.

Next, consider the following expression:

$$C(60p, 7) \equiv$$

$$60p\left[\frac{(60p-1)(30p-1)(20p-1)(15p-1)(12p-1)(10p-1)}{7}\right].$$

Here, by Lemma 4, the term inside the square bracket is an integer if and only if $p \neq 7$. All these complete the proof of the lemma.

It may be mentioned here that, in Lemma 6, p can be any prime except 7. Thus, Lemma 6 is supplemented by the value $SS(420) = 412$.

The next lemma deals with $SS(210p)$.

Lemma 7: Let $p \geq 2$ be a prime. Then,

$$SS(210p)=\begin{cases}210p-4, & if\ \ p=4s+1,\ s\geq 1\\ 210p-8, & if\ \ p=8t+3,\ t\geq 0\\ 210p-9, & if\ \ p=72u+31,\ u\geq 0\\ & or, if\ \ p=72v+71,\ v\geq 0\\ 210p-11, & otherwise\end{cases}$$

Proof: Consider the expression below:

$$C(210p,4)\equiv 210p\left[\frac{(210p-1)(105p-1)(70p-1)}{4}\right].$$

Note that, if $p=4s+1$, then

$$105p-1=4(105s+26),$$

This shows that $105p-1$ is divisible by 4, so the term inside the square bracket is an integer. This establishes part (1) of the lemma.

Next, let $p=4t+3$. The expression

$$C(210p,5)\equiv$$

$$210p\left[\frac{(210p-1)(105p-1)(70p-1)(105p-2)}{2\times 5}\right]$$

shows that $SS(210p)\neq 210p-5$ for any prime p, from the expression

$$C(210p,6)\equiv$$

$$210p\left[\frac{(210p-1)(105p-1)(70p-1)(105p-2)(42p-1)}{2\times 6}\right]$$

(since 4 divides neither $105p-1$ nor $105p-2$) it follows that $SS(210p)\neq 210p-6$ for any prime p, and the expression

$$C(210p,7)\equiv 210p\left[\frac{(210p-1)(105p-1)(70p-1)}{2\times 7}\times (105p-2)(42p-1)(35p-1)\right]$$

shows that $SS(210p)\neq 210p-7$ for any prime p, since by Lemma 4, the numerator of the term inside the square bracket is not divisible by 7. So, consider

$$C(210p,8)\equiv 210p\left[\frac{(210p-1)(105p-1)(70p-1)}{16}\times (105p-2)(42p-1)(35p-1)(30p-1)\right].$$

If $p=8s+3$, then

$$105p-1=2(420s+157),$$

$$35p-1=8(35s+13),$$

so that, the term inside the square bracket is an integer if $p=8s+3$.

Next, consider the expression:

$$C(210p,9)\equiv 210p\left[\frac{(210p-1)(105p-1)(70p-1)}{8\times 9}\times (105p-2)(42p-1)(35p-1)(30p-1)(105p-4)\right].$$

Now, the problem is to find the condition such that the term inside the square bracket is an integer. Looking at the terms in the numerator, it is clear that, one possibility is that 4 divides $35p-1$ (in which case, $105p-1$ is divisible by 2) and 9 divides $70p-1$. By inspection, it is found that, when $p=72s+31$, then

$$35p-1=4(630s+271),$$

$$70p-1=9(560s+241),$$

so that $(105p-1)(35p-1)(70p-1)$ is divisible by 72. The second possibility is that 36 divides $35p-1$. With $p=72t+71$,

$$35p-1=36(70t+69),$$

so that $(105p-1)(35p-1)$ is divisible by 72. All these prove part (2) of the lemma.

Next, consider the expression below:

$$C(210p,10)\equiv$$

$$210p\left[\frac{(210p-1)(105p-1)(70p-1)(105p-2)}{3\times 5\times 16}\times (42p-1)(35p-1)(30p-1)(105p-4)(70p-3)\right].$$

Here, in order that the term inside the square bracket is an integer, a necessary condition is that $42p-1$ must be divisible by 5. This leads to the Diophantine equation $42p-1=5\alpha$, with the solution $p=5x+3$ ($x\geq 0$) (see Lemma 3). The second condition that must be satisfied is that $35p-1$ must be divisible by 8. Since, $35p-1=175x+104$, it follows that $x=8$, so that $p=40x+3$, which violates part (2) of the lemma.

Finally, consider the following expression for $C(210p,11)$:

$$210p\left[\frac{(210p-1)(105p-1)(70p-1)(105p-2)(42p-1)}{8\times 3\times 11}\times (35p-1)(30p-1)(105p-4)(70p-3)(21p-1)\right].$$

Now, by Lemma 4, $(70p-1)(35p-1)(70p-3)$ is divisible by 3. Also, it may easily be verified that $(105p-1)(35p-1)(21p-1)$ is divisible by 8 if p is either of the form $p=4s+1$ or of the form $p=4t+3$.

Moreover, $p \neq 11$. Hence, the term inside the square bracket is an integer, which was intended to prove.

The lemma below deals with $SS(420p)$.

Lemma 8: Let $p \geq 2$ be a prime. Then

$$SS(420p) = \begin{cases} 420p-6, & if\ p = 6s+5,\ s \geq 0 \\ 420p-8, & if\ p = 8t+1,\ t \neq 3x+2 \\ 420p-9, & if\ p = 18u+13,\ u \neq 4y+2 \\ 420p-10, & if\ p = 40v+29,\ v \neq 3a, v \neq 9b+5 \\ 420p-11, & otherwise \end{cases}$$

Proof: The expressions

$$C(420p, 4) \equiv 420p\left[\frac{(420p-1)(210p-1)(140p-1)}{4}\right],$$

$$C(420p,5) \equiv 420p\left[\frac{(420p-1)(210p-1)(140p-1)(105p-1)}{5}\right],$$

show that, for any prime p,

$$SS(420p) \neq 420p-4,\ SS(420p) \neq 420p-5.$$

So, consider the expression:

$$C(420p, 6) \equiv 420p\left[\frac{(420p-1)(210p-1)(140p-1)(105p-1)(84p-1)}{6}\right].$$

Here so that the term inside the square bracket is an integer, p must be odd, and 3 must divide $140p-1$. Now, the solution of the Diophantine equation $140p - 1 = 3\alpha$ is $p = 3x + 2$. To guarantee that p is odd, x must be odd. Therefore, by writing $x = 2t + 1$, the desired expression of p is obtained.

The expression

$$C(420p,7) \equiv 420p\left[\frac{(420p-1)(210p-1)(140p-1)}{7} \times (105p-1)(84p-1)(70p-1)\right]$$

shows $SS(420p) \neq 420p-7$ for any prime p. So, consider

$$C(420p,8) \equiv 420p\left[\frac{(420p-1)(210p-1)(140p-1)}{8} \times (105p-1)(84p-1)(70p-1)(60p-1)\right].$$

Here, the term inside the square bracket is an integer if and only if 8 divides 105p –1. Thus, p must satisfy the equation $105p - 1 = 8\alpha$, with the solution $p = 8t + 1$ ($t \geq 2$ being any integer). Now, considering the Diophantine equation $8t + 1 = 6a + 5$, using Lemma 3, the solution is found to be $t = 3x + 2$ ($x \geq 0$ being any integer).

Next, consider the expression:

$$C(420p,9) \equiv 420p\left[\frac{(420p-1)(210p-1)(140p-1)}{2\times 9} \times (105p-1)(84p-1)(70p-1)(60p-1)(105p-2)\right].$$

Now, note that, one of $105p-1$ and $105p-2$ is even. Thus, the term inside the square bracket is an integer if and only if 9 divides $70p - 1$. This leads to the Diophantine equation $70p - 1 = 9\alpha$, whose solution is $p = 9x + 4$. In order to guarantee that p is odd, x is replaced by $2u + 1$, to get $p = 18u + 13$. To exclude common values, the Diophantine equations $18u + 13 = 6a + 5$, and $18u + 13 = 8b + 1$ are to be considered. By Lemma 3, the first equation has no solution, while the solution of the second equation is $u = 4x + 2$ ($x \geq 0$ being any integer).

Now, consider the expression:

$$C(420p, 10) \equiv 420p\left[\frac{(420p-1)(210p-1)(140p-1)(105p-1)}{3\times 4\times 5} \times (84p-1)(70p-1)(60p-1)(105p-2)(140p-3)\right].$$

Here, in order that the term inside the square bracket is an integer, the only possibility is that 5 divides $84p-1$ and 4 divides $105p-1$. Thus, for some integers α and β,

$$84p - 1 = 5\alpha,\ 105p - 1 = 4\beta,$$

with the solutions $p = 5x + 4$ and $p = 4y + 1$ respectively. Now, the combined equation is $5x + 4 = 4y + 1$, whose solution is $x = 4z + 1$, so that, finally, $p = 5(4z + 1) + 4 = 20z + 9$. Next, the equation $20z + 9 = 8b + 1$. This shows that z must be even. Therefore, writing $z = 2v + 1$, finally, $p = 20(2v + 1) + 9 = 40v + 29$. Considering the equations $40v + 29 = 6a + 5$ and $40v + 29 = 18c + 13$, the solutions are found to be $v = 3a$ and $v = 9b + 5$ respectively, $a \geq 0$ and $b \geq 0$ being any integers.

Finally, consider the expression:

$$C(420p, 11) \equiv 420p\left[\frac{(420p-1)(210p-1)(140p-1)(105p-1)}{2\times 3\times 11} \times (84p-1)(70p-1)(60p-1)(105p-2)(140p-3)(42p-1)\right].$$

Here, $p \neq 11$. Hence, the term inside the square bracket is an integer.

The lemma below finds $SS(840p)$.

Lemma 9: Let $p \geq 2$ be a prime. Then,

$$SS(840p) = \begin{cases} 840p - 9, & if\ p = 9s + 1,\ s \geq 0 \\ & or,\ p = 9t + 2,\ t \geq 0 \\ 840p - 10, & if\ p = 10s + 7, \\ & s \neq 9x + 3,\ s \neq 9y + 4 \\ 840p - 11, & otherwise \end{cases}$$

Proof: From the expressions of $C(840p, 4)$, $C(840p, 5)$, $C(840p, 6)$, $C(840p, 7)$, and $C(840p, 8)$, it can be seen that, for any prime p,

$SS(840p) \neq 840p - 4$, $SS(840p) \neq 840p - 5$,

$SS(840p) \neq 840p - 6$, $SS(840p) \neq 840p - 7$,

$SS(840p) \neq 840p - 8$.

So, consider the expression

$$C(840p,9) \equiv 840p\left[\frac{(840p-1)(420p-1)(280p-1)}{9} \times (210p-1)(168p-1)(140p-1)(120p-1)(105p-1)\right].$$

Clearly, the term inside the square bracket is an integer if and only if either 9 divides $280p - 1$ or 9 divides $140p - 1$. The resulting equations are $280p - 1 = 9\alpha$ and $140p - 1 = 9\beta$, whose solutions are $p = 9s + 1$ and $p = 9t + 2$ respectively.

Next, consider

$$C(840p, 10) \equiv 840p\left[\frac{(840p-1)(420p-1)(280p-1)(210p-1)}{2\times3\times5} \times (168p-1)(140p-1)(120p-1)(105p-1)(280p-3)\right].$$

Here, so that the term inside the square bracket is an integer, 5 must divide $168p - 1$; moreover, p must be odd. Now, the solution of the Diophantine equation $168p - 1 = 5\alpha$ is $p = 5x + 2$. In order to guarantee that p is odd, x is replaced by $2s + 1$ to get the desired result.

Finally, consider

$$C(840p, 11) \equiv 840p\left[\frac{(840p-1)(420p-1)(280p-1)(210p-1)}{3\times11} \times (168p-1)(140p-1)(120p-1)(105p-1)(280p-3)(84p-1)\right].$$

Here, since $p \neq 11$, it follows that the term inside the square bracket is an integer.

Conclusions

This paper derives the explicit forms of $SS(30p)$, $SS(60p)$, $SS(210p)$ and $SS(420p)$, where p is a prime. It is found that, surprisingly, $SS(30p)$ and $SS(60p)$ behave differently. For example, in $SS(30p)$, the minimum integer k such that $30p$ divides $C(30p, k)$ can be 4 and 7 only (depending on p), while the only possible values of the minimum k in $SS(60p)$ are 6 and 7. Again, in $SS(210p)$ (depending on p), the minimum k can only be one of four possible values, namely, 4, 8, 9, and 11, whereas the minimum k in $SS(420p)$ is five in number, namely, 6, 8, 9, 10, and 11. On the other hand, Lemma 9 shows that, the minimum k in $SS(840p)$ can be only one of three values, namely, $k = 9, 10, 11$.

The accompanying tables give the values of $SS(30p)$, $SS(60p)$, $SS(210p)$, and $SS(420p)$ for the first 200 primes, calculated on a computer, using the formula (3) for the binomial coefficients.

Conflict of interest

The authors declare that there is no conflict of interest regarding the publication of this article.

References

Gioia AA. *The Theory of Numbers*: *An Introduction*, Dover Publications Inc., USA, 2001.

Hardy GH and Wright EM. *An Introduction to the Theory of Numbers*, Oxford Science Publications, 5th Edition, 2002.

Islam SMS and Majumdar AAK. On some values of the Sandor- Smarandache function. *J. Sci. Res.* 2022; 14(1): 45- 65.

Islam SMS and Majumdar AAK. Some results on the Sandor-Smarandache function. *J. Sci. Res.* 2021; 13(1): 73-84.

Islam SMS, Gunarto H and Majumdar AAK. On the Sandor-Smarandache function. *J. Sci. Res.* 2021; 13(2): 439-454.

Majumdar AAK and Ahmed AKZ. A note on the Sandor-Smarandache function. *J. Bangladesh Acad. Sci.* 2021; 45(2): 255-258 (Short Communication).

Majumdar AAK. On some values of the Sandor-Smarandache function. *Ganit*: *J. Bangladesh Math. Soc*. 2019; 39: 15-25.

Majumdar, AAK. *Smarandache Numbers Revisited*, Pons Publishing House, Belgium, 2018.

Sandor J. On a new Smarandache type function, *Smarandache Notions J*. 2001; 12: 247-248.

Table 1. Values of $SS(30p)$, p is a prime

p	SS(n)	p	SS(n)	p	SS(n)	p	SS(n)	p	SS(n)
1	23	173	5183	409	12263	659	19766	941	28223
2	53	179	5366	419	12566	661	19823	947	28406
3	86	181	5423	421	12623	673	20183	953	28583
5	143	191	5726	431	12926	677	20303	967	29006
7	206	193	5783	433	12983	683	20486	971	29126
11	326	197	5903	439	13166	691	20726	977	29303
13	383	199	5966	443	13286	701	21023	983	29486
17	503	211	6326	449	13463	709	21263	991	29726
19	566	223	6686	457	13703	719	21566	997	29903
23	686	227	6806	461	13823	727	21806	1009	30263
29	863	229	6863	463	13886	733	21983	1013	30383
31	926	233	6983	467	14006	739	22166	1019	30566
37	1103	239	7166	479	14366	743	22286	1021	30623
41	1223	241	7223	487	14606	751	22526	1031	30926
43	1286	251	7526	491	14726	757	22703	1033	30983
47	1406	257	7703	499	14966	761	22823	1039	31166
53	1583	263	7886	503	15086	769	23063	1049	31463
59	1766	269	8063	509	15263	773	23183	1051	31526
61	1823	271	8126	521	15623	787	23606	1061	31823
67	2006	277	8303	523	15686	797	23903	1063	31886
71	2126	281	8423	541	16223	809	24263	1069	32063
73	2183	283	8486	547	16406	811	24326	1087	32606
79	2366	293	8783	557	16703	821	24623	1091	32726
83	2486	307	9206	563	16886	823	24686	1093	32783
89	2663	311	9326	569	17063	827	24806	1097	32903
97	2903	313	9383	571	17126	829	24863	1103	33086
101	3023	317	9503	577	17303	839	25166	1109	33263
103	3086	331	9926	587	17606	853	25583	1117	33503
107	3206	337	10103	593	17783	857	25703	1123	33686
109	3263	347	10406	599	17966	859	25766	1129	33863
113	3383	349	10463	601	18023	863	25886	1151	34526
127	3806	353	10583	607	18206	877	26303	1153	34583
131	3926	359	10766	613	18383	881	26423	1163	34886
137	4103	367	11006	617	18503	883	26486	1171	35126
139	4166	373	11183	619	18566	887	26606	1181	35423
149	4463	379	11366	631	18926	907	27206	1187	35606
151	4526	383	11486	641	19223	911	27326	1193	35783
157	4703	389	11663	643	19286	919	27566	1201	36023
163	4886	397	11903	647	19406	929	27863	1213	36383
167	5006	401	12023	653	19583	937	28103	1217	36503

Table 2. Values of $SS(60p)$, p is a prime

p	SS(n)	p	SS(n)	p	SS(n)	p	SS(n)	p	SS(n)
1	53	173	10374	409	24533	659	39534	941	56454
2	113	179	10734	419	25134	661	39653	947	56814
3	173	181	10853	421	25253	673	40373	953	57174
5	294	191	11454	431	25854	677	40614	967	58013
7	412	193	11573	433	25973	683	40974	971	58254
11	654	197	11814	439	26333	691	41453	977	58614
13	773	199	11933	443	26574	701	42054	983	58974
17	1014	211	12653	449	26934	709	42533	991	59453
19	1133	223	13373	457	27413	719	43134	997	59813
23	1374	227	13614	461	27654	727	43613	1009	60533
29	1734	229	13733	463	27773	733	43973	1013	60774
31	1853	233	13974	467	28014	739	44333	1019	61134
37	2213	239	14334	479	28734	743	44574	1021	61253
41	2454	241	14453	487	29213	751	45053	1031	61854
43	2573	251	15054	491	29454	757	45413	1033	61973
47	2814	257	15414	499	29933	761	45654	1039	62333
53	3174	263	15774	503	30174	769	46133	1049	62934
59	3534	269	16134	509	30534	773	46374	1051	63053
61	3653	271	16253	521	31254	787	47213	1061	63654
67	4013	277	16613	523	31373	797	47814	1063	63773
71	4254	281	16854	541	32453	809	48534	1069	64133
73	4373	283	16973	547	32813	811	48653	1087	65213
79	4733	293	17574	557	33414	821	49254	1091	65454
83	4974	307	18413	563	33774	823	49373	1093	65573
89	5334	311	18654	569	34134	827	49614	1097	65814
97	5813	313	18773	571	34253	829	49733	1103	66174
101	6054	317	19014	577	34613	839	50334	1109	66534
103	6173	331	19853	587	35214	853	51173	1117	67013
107	6414	337	20213	593	35574	857	51414	1123	67373
109	6533	347	20814	599	35934	859	51533	1129	67733
113	6774	349	20933	601	36053	863	51774	1151	69054
127	7613	353	21174	607	36413	877	52613	1153	69173
131	7854	359	21534	613	36773	881	52854	1163	69774
137	8214	367	22013	617	37014	883	52973	1171	70253
139	8333	373	22373	619	37133	887	53214	1181	70854
149	8934	379	22733	631	37853	907	54413	1187	71214
151	9053	383	22974	641	38454	911	54654	1193	71574
157	9413	389	23334	643	38573	919	55133	1201	72053
163	9773	397	23813	647	38814	929	55734	1213	72773
167	10014	401	24054	653	39174	937	56213	1217	73014

Table 3 . Values of *SS*(210*p*), *p* is a prime

p	SS(n)	p	SS(n)	p	SS(n)	p	SS(n)	p	SS(n)
1	206	173	36326	409	85886	659	138382	941	197606
2	412	179	37582	419	87982	661	138806	947	198862
3	622	181	38006	421	88406	673	141326	953	200126
5	1046	191	40099	431	90501	677	142166	967	203061
7	1459	193	40526	433	90926	683	143422	971	203902
11	2302	197	41366	439	92179	691	145102	977	205166
13	2726	199	41779	443	93022	701	147206	983	206419
17	3566	211	44302	449	94286	709	148886	991	208099
19	3982	223	46819	457	95966	719	150981	997	209366
23	4819	227	47662	461	96806	727	152659	1009	211886
29	6086	229	48086	463	97221	733	153926	1013	212726
31	6501	233	48926	467	98062	739	155182	1019	213982
37	7766	239	50179	479	100579	743	156019	1021	214406
41	8606	241	50606	487	102259	751	157701	1031	216499
43	9022	251	52702	491	103102	757	158966	1033	216926
47	9859	257	53966	499	104782	761	159806	1039	218181
53	11126	263	55219	503	105621	769	161486	1049	220286
59	12382	269	56486	509	106886	773	162326	1051	220702
61	12806	271	56899	521	109406	787	165262	1061	222806
67	14062	277	58166	523	109822	797	167366	1063	223219
71	14901	281	59006	541	113606	809	169886	1069	224486
73	15326	283	59422	547	114862	811	170302	1087	228259
79	16579	293	61526	557	116966	821	172406	1091	229102
83	17422	307	64462	563	118222	823	172821	1093	229526
89	18686	311	65299	569	119486	827	173662	1097	230366
97	20366	313	65726	571	119902	829	174086	1103	231619
101	21206	317	66566	577	121166	839	176179	1109	232886
103	21621	331	69502	587	123262	853	179126	1117	234566
107	22462	337	70766	593	124526	857	179966	1123	235822
109	22886	347	72862	599	125779	859	180382	1129	237086
113	23726	349	73286	601	126206	863	181221	1151	241701
127	26659	353	74126	607	127461	877	184166	1153	242126
131	27502	359	75381	613	128726	881	185006	1163	244222
137	28766	367	77059	617	129566	883	185422	1171	245902
139	29182	373	78326	619	129982	887	186259	1181	248006
149	31286	379	79582	631	132499	907	190462	1187	249262
151	31699	383	80419	641	134606	911	191299	1193	250526
157	32966	389	81686	643	135022	919	192979	1201	252206
163	34222	397	83366	647	135861	929	195086	1213	254726
167	35059	401	84206	653	137126	937	196766	1217	255566

Table 4 . Values of $SS(420p)$, p is a prime

p	SS(n)	p	SS(n)	p	SS(n)	p	SS(n)	p	SS(n)
1	412	173	72654	409	171772	659	276774	941	395214
2	831	179	75174	419	175974	661	277611	947	397734
3	1249	181	76009	421	176809	673	282652	953	400254
5	2094	191	80214	431	181014	677	284334	967	406131
7	2929	193	81052	433	181852	683	286854	971	407814
11	4614	197	82734	439	184369	691	290209	977	410334
13	5451	199	83569	443	186054	701	294414	983	412854
17	7134	211	88611	449	188574	709	297770	991	416209
19	7969	223	93649	457	191932	719	301974	997	418729
23	9654	227	95334	461	193614	727	305329	1009	423772
29	12174	229	96171	463	194451	733	307851	1013	425454
31	13011	233	97854	467	196134	739	310369	1019	427974
37	15529	239	100374	479	201174	743	312054	1021	428811
41	17214	241	101212	487	204529	751	315411	1031	433014
43	18049	251	105414	491	206214	757	317929	1033	433852
47	19734	257	107934	499	209571	761	319614	1039	436371
53	22254	263	110454	503	211254	769	322972	1049	440574
59	24774	269	112974	509	213774	773	324654	1051	441409
61	25609	271	113809	521	218814	787	330531	1061	445614
67	28131	277	116329	523	219649	797	334734	1063	446449
71	29814	281	118014	541	227209	809	339774	1069	448970
73	30652	283	118851	547	229729	811	340609	1087	456529
79	33169	293	123054	557	233934	821	344814	1091	458214
83	34854	307	128929	563	236454	823	345651	1093	459051
89	37374	311	130614	569	238974	827	347334	1097	460734
97	40732	313	131452	571	239811	829	348170	1103	463254
101	42414	317	133134	577	242332	839	352374	1109	465774
103	43251	331	139009	587	246534	853	358249	1117	469129
107	44934	337	141532	593	249054	857	359934	1123	471649
109	45770	347	145734	599	251574	859	360771	1129	474172
113	47454	349	146570	601	252412	863	362454	1151	483414
127	53329	353	148254	607	254931	877	368331	1153	484252
131	55014	359	150774	613	257449	881	370014	1163	488454
137	57534	367	154129	617	259134	883	370849	1171	491809
139	58371	373	156651	619	259969	887	372534	1181	496014
149	62574	379	159169	631	265009	907	380929	1187	498534
151	63409	383	160854	641	269214	911	382614	1193	501054
157	65931	389	163374	643	270051	919	385969	1201	504412
163	68449	397	166729	647	271734	929	390174	1213	509449
167	70134	401	168414	653	274254	937	393532	1217	511134

J. Bangladesh Acad. Sci. 46(1); 75-83: June 2022 DOI: 10.3329/jbas.v46i1.59693

Journal of Bangladesh Academy of Sciences

Journal homepage: http://www.bas.org.bd/publications/jbas.html

Research Article

Removal of methylene blue and other pollutants from tannery wastewater using chemically modified tannery solid waste

Mohammad Nazmul Hossain[1], Md Didarul Islam[2], Ashiqur Rahaman[3], Mahadi Hasan[4], Meem Muhtasim Mahdi[3], Md. Arafat Hossain[3], Nazma Khatun[*] and Md. Abdul Matin[1]

Atomic Energy Centre, Chattogram, Bangladesh Atomic Energy Commission, Chattogram, Bangladesh

ARTICLE INFO

Article History

Received: 24 May 2022
Revised: 9 June 2022
Accepted: 12 June 2022

Keywords: Biovalorization, Methylene blue, Activated carbon, Chrome shaving dust, Wastewater treatment.

ABSTRACT

The adsorption of methylene blue (MB) was investigated using the prepared activated carbon (AC); obtained by the chemical activation of chrome shaving dust (CSD). Results represented that the increase of particle size and impregnation ratio of AC possessed a proportional effect on the adsorption of MB. AC produced by H_3PO_3, impregnation ratio of 1:6, and mesh size of 40 showed the highest adsorption performance. The removal of other organic and inorganic pollutants from different tannery effluent was found satisfactory like pH, conductivity, turbidity, BOD_5, COD, and Cl^- values are reduced to 5.5-8.48, 73-93%, 76-92%, 80-96%, 71-87% and 84-94%, respectively which are nearly closed to the WHO's standards for industrial effluent to the environment. The microscopic analysis confirmed the smooth and porous surface characteristics of the adsorbent. Hence, CSDAC can be expected to become an effective, low-cost, and suitable adsorbent for both dye and pollutants removal from industrial wastewater.

Introduction

For the last few decades, water pollution has become a global phenomenon that results in the scarcity of fresh water for drinking and carrying out our daily activities smoothly. UNO assumes that by the year 2050, approximately 40% of the world population will face a drinking water shortage if this scenario continues (de Aquim et al., 2010). Hence, the water resource management authorities should give more attention to water conservation and the sustainability of the human race on earth. Rapid industrialization and extensive use of mechanized and chemical appliances in agricultural and household activities have been categorized as the major causes of water pollution. Among industries, paper, pulp, thermal, metal extraction, paints and pigments, textile, and leather generate a significant quantity of color and toxic metal wastes with wastewater that are responsible for both aesthetical and toxicological problems (Anandkumar and Mandal, 2009). The discharged color effluents release a substantial amount of dissolved and suspended solids with a high degree of biochemical and chemical oxygen demand when mixed with groundwater (Etezad and Sadeghi-Kiakhani, 2021). Moreover, these compounds act as interference in water that blocks sunlight penetration, hampers photosynthesis, and show toxicity in some microbial species and carcinogenic effects in the human body (Kasmaei et al., 2020). Therefore, the remediation of dyes from effluents is essential before discharging them into water resources to reduce water pollution. MB is a well-known dye that has extensive applications in several industries. It was first synthesized by Caro and has a wide range of applications in textile coloration, calico-printing, and titration indicators (Dutta, 1990).

[*]Corresponding author: <nazmabaec@gmail.com>

[1]Department of Glass and Ceramic Engineering, Bangladesh University of Engineering and Technology, Dhaka, Bangladesh
[2]Department of Applied Chemistry and Chemical Engineering, University of Dhaka, Dhaka, Bangladesh
[3]Institute of Leather Engineering and Technology, University of Dhaka, Dhaka, Bangladesh
[4]Faculty of Environmental Science and Engineering, Babes-Bolyai University, Cluj-Napoca, Romania

It is a dark green-colored cationic dye and highly soluble in aqueous and alcoholic media. Despite its benefits to industries, MB shows negative symptoms in the human body, such as inhaled respiratory problems, nausea, vomiting, burning sensation, mental confusion, etc., upon swallowing (Wijaya et al., 2020). As a result, the quantity of MB in industrial wastewater should be kept within the permissible limit.

Some wastewater treatment methods have recently been developed to reduce water pollution [viz. Reverse Osmosis (RO), adsorption, ion exchange, chemical coagulation, membrane filtration, etc.]. These techniques are also used to mitigate pollutants from industrial effluents (Thilagavathy and Santhi, 2013). However, adsorption is becoming more popular than all other treatment methods. It is highly efficacious due to the easy removal of various chemicals using activated carbon, nano-magnetic materials, and zeolites (Ebrahimi et al., 2013; Khalid et al., 2018). These materials require high preparation costs and possess less recyclability. Thus, developing low-cost, recyclable, and locally available adsorbents is a prime need for the redemption of different types of toxins from wastewaters.

In the history of human civilization, the leather processing industry is the most ancient and important. Its worldwide importance is due to meet the global market demand for leather. But a huge amount of solid wastes and effluents are produced during the hide/skin processing. According to literature, approximately 750-850 kg of solid wastes in both tanned and un-tanned is generated per ton of hides/skins processing, and the global rate of tannery solid waste generation is 6 million tons per annum (Paul et al., 2013; Andrioli and Gutterres, 2015; Abajihad, 2012; Sundar et al., 2011). These solid wastes have limited applications but can cause many adverse effects on environmental and human health if they are not properly treated. Therefore, valorization of tannery solid waste is important rather than its disposal in landfilling or incineration, and effluent treatment should be monitored properly (Tahiri and de la Guardia, 2009, Hashem and Nur-A-Tomal, 2018, Madhavi et al., 2011; Li et al., 2019).

Regarding these circumstances, we attempted to valorize solid leather shaving waste by converting it into AC through pyrolysis and applying it for MB adsorption and other pollutants removal from tannery effluent. The other objectives included- (1) the study of the effect of impregnation ratio of various chemicals with prepared AC during chemical activation, (2) the study of the nature of chemically modified AC by spectral and microscopic analyses, and (3) the study of the removal capacity of the prepared adsorbent.

Materials and Methods

Preparation of synthetic sample

Analytical grade MB (Fig. 1) was purchased from Sigma-Aldrich, USA, to prepare a standard synthetic solution for batch experiments and a calibration curve for measuring dye removal amount. Stock MB solution (1000 mg/L) was made by dissolving the dye powder into deionized water in a 1000 mL Erlenmeyer flask using a magnetic stirrer at room temperature. Later, a desired intermediate standard solution (i.e., a solution in which the dye concentration was ranged from 50-200 mg/L) was prepared by mixing deionized water properly with the stock solution (methylene blue).

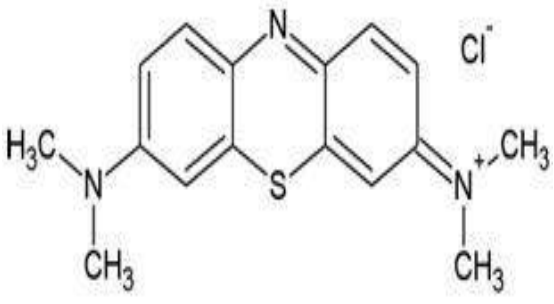

Fig. 1. Chemical structure of methylene blue

Sample collection and characterization

In an airtight polyethylene bag, chrome shaving dust (CSD) was collected from Samina tannery Ltd., at Hemayetpur, Savar, Dhaka. The collected CSD was immediately brought to the laboratory, thoroughly

washed with tap water to remove impurities and sun-dried for a week. The dried CSD was crushed, and then divided into various mesh sizes: 20, 30, and 40 through a sieving machine (Retsch D-42459 HAAN, Germany). Proximate analysis of physical characteristics of CSD was tested by following standard testing methods (FAAS methods equipped with Zeeman background), and the result was shown in Table 1. Finally, the dried CSD powder was stored in the dark at room temperature for further experiment.

Table 1. The characters of analyzed chrome shaving dust (CSD)

Parameter	Value (%)
Proximate analysis (weight, %)	
Water/Moisture content	13.29
Volatile Matter	53.40
Fixed carbon	24.53
Ash	9.56
Ultimate analysis (dry basis weight. %)	
Carbon (C)	54.8
Nitrogen (N)	6.33
Hydrogen (H)	6.54
Cl (Chlorine)	4.32
S (Sulfur)	1.30
Cr (Chromium)	2.76
Si (Silicon)	2.74

Wastewater collection

A sufficient amount of wastewater from different chemical operations of leather processing was obtained from Ruma tannery Ltd., at Hemayetpur, Savar, Dhaka by following Pearson et al. method (Pearson et al., 1987). The spent liquors were collected in labeled, airtight plastic bottles from the discharge point that led to the sewage line. The bottles were previously disinfected by soaking them overnight in 10% HNO_3 solution, washed thoroughly with deionized water to remove the surplus acid, and oven-dried at 80ºC for two (2) hours to avoid any contamination during sample collection. The collected wastewater sample was stored at 3-5ºC in the laboratory upon filtration to prevent further oxidation/hydrolysis.

Adsorbent preparation

Chemical impregnation

The dried CSD sample was chemically impregnated for its surface modification before pyrolysis. CSD of various particle sizes was placed in 250 mL beakers and mixed with standard solutions of H_3PO_3 and $ZnCl_2$ at different ratios. Chemical impregnation was done in an oven at 110ºC for 6 hours. After impregnation, the chemically impregnated leather wastes were transferred into a horizontal tube furnace after loading them inside a ceramic tube for pyrolysis.

Carbonization

The thermal activation of chemically impregnated raw material was conducted at 600ºC for an hour in a pyrolyzer with having 500 mm long quartz tube with a 20 mm internal diameter under an inert atmosphere of nitrogen gas (99.99%) at a rate of 150 cm^3/minute. The temperature was elevated to the desired temperature at a rate of 5ºC/minute, and the temperature was kept constant for a certain time to complete the pyrolysis. After pyrolysis, a certain quantity of char was cooled at room temperature with nitrogen flow and then washed with deionized (DI) water to remove surplus chemicals. Finally, the sample was taken in a beaker, stirred with 250 ml HCl solution for an hour, and thoroughly washed with hot deionized (DI) water until it reached 6-7 pH (neutral).

Batch studies

The adsorption process of MB was carried out in batch mode. 100 ml solution of 200 ppm MB solution was taken on a 250 ml conical flask, treated with 1 gm of AC (various impregnation ratios with different chemical activation), and constantly shaken at a speed of 200 rpm (mechanically) for the desired time at ambient temperature. After the desired time, the mixture was

centrifuged at 5000 rpm for 10 minutes to separate the solid phase. The amount of MB in the solution was determined by a double-beamed Ultra-violet spectrophotometer (Shimadzu, Japan) at 668 nm with respect to the previously prepared calibration curve for minimal error. The calibration curve was reproducible and linear over the concentration range during analysis. Equations 1 and 2 were used to calculate the % removal of MB and adsorbed quantity, respectively.

$$\% \text{ Removal} = \frac{C_i - C_f}{C_i} \times 100 \quad (1)$$

$$\text{Amount absorbed } (q_e) = \frac{(C_i - C_f) \times V}{m} \quad (2)$$

Here, C_i and C_f were the initial concentration of dye solution before treatment and the final concentration of dye solution after treatment. V= volume of the dye solution (mL), and m= mass of AC used as adsorbent (mg/L). Each of the experiment series was further carried out by using the blank solution as control, and the average values of these experiments obtained from duplicate runs were further analyzed and compared.

Analysis of physicochemical properties of wastewater

Several physicochemical parameters like pH, conductivity, turbidity, TDS, BOD_5 and COD values of the wastewater sample were tested by using calibrated machinery as per their standard operating procedure. pH was measured by a digital pH meter, conductivity was estimated by following the electrometric method, turbidity was determined by a turbidity meter and a digitalized potentiometer was used to measure the amount of total dissolved solids in wastewater. BOD and COD were assessed by following the five-day BOD test and open reflux method suggested by Kopp (1979). Each of the physicochemical parameters was tested before and after treatment to evaluate the adsorption efficiency of the developed AC (i.e., generated by activation with H_3PO_4 1:6 impregnated ratio and mesh size 40).

Results and Discussion

Methylene blue (MB) adsorption

In this experiment, chemical activation of three types of AC categorized in three dissimilar mesh sizes (20, 30, and 40) was done by two different chemicals (H_3PO_3 and $ZnCl_2$) at various impregnation ratios (chrome shaving dust: $ZnCl_2/H_3PO_4$= 1:2, 1:4, and 1:6) to evaluate the superior adsorbent for the adsorption of MB from industrial wastewater among them. It was noted that the adsorption of MB was gradually increased with the increase of mesh number of the AC samples (Fig. 2). At the same time, the activation capacity of AC molecules was increased with the increasing quantity of applied chemicals because of the increasing percentage of chemical penetration inside the raw materials. The adsorption capacity of MB was found to increase with the gradual increase of the amount of activating chemicals. The excess contact time of impregnation chemicals char materials played a vital role in such phenomenon. Besides, the adsorption capacity of H_3PO_3 impregnated char was 1.27-1.36 times higher than that of $ZnCl_2$. It indicated that H_3PO_3 impregnated char was superior to $ZnCl_2$ impregnated char for MB adsorption. However, the difference was insignificant, and the chemical activation value was found to be closed as described in the literature (Pereira et al., 2014).

Pollutant reduction

Different types of tannery effluents discharged from different chemical operations of various leather-manufacturing stages were treated with the prepared AC to reduce the amount of both forms of pollutants (i.e., organic and inorganic) for the reduction of water pollution. In situ data analysis of the physicochemical parameters, e.g., pH, conductivity, turbidity, COD, BOD_5, and Cl^-, etc., of the collected wastewater samples, both initial and before treatment, were represented in a tabular form (Table 2).

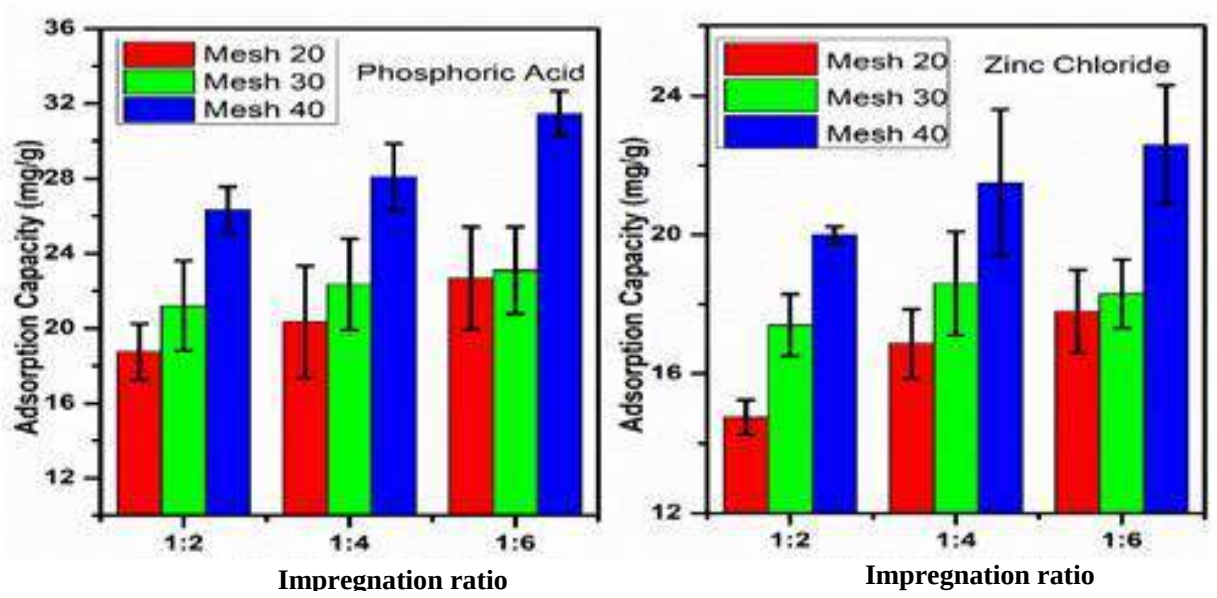

Fig. 2. MB adsorption of different sizes AC impregnated by H_3PO_3 and $ZnCl_2$ at various impregnation ratio

Table 2. The physical properties of raw tannery outflow (before and after treatment)

Effluent	Before treatment						After treatment					
Sample	pH	BOD_5 mg/l	COD mg/l	Conductivity µS/cm	Turbidity NTU	Chloride mg/l	pH	BOD_5 mg/l	COD mg/l	Conductivity µS/cm	Turbidity NTU	Chloride mg/l
Soaking	8.1	2100	4350	1237	990	35.75	6.95	274.05	904	289	215	2
Liming	13.2	5500	9523	1191	550	24.23	7.48	678.15	2136	215	57	4.3
Deliming	7.77	2500	5563	2016	840	22.75	6.97	349.00	1245	385	170	3.5
Bating	7.49	3000	6250	3160	660	78.88	7.4	450.00	1200	5	60	8
Pickling	2.5	1100	2600	1515	1020	16.58	7.06	50.05	321	17.15	253	1.5
Chrome Tanning	2.4	1950	3650	425	1050	12	7.5	112.13	727	6.15	160	0.69
Re-tanning	3.9	2100	4700	415	990	11.58	7.4	405.09	1255	10.9	153	0.5
Fat liquoring	3.62	4100	9500	750	1000	68.5	5.50	734.31	2700	11.17	107	10
Dyeing	4.9	2700	7770	650	900	28.3	6.76	404.19	1542	15.15	228	4.5

From some literature, it was found that the values of pH, COD, BOD, Cl^-, and conductivity in surface water should be 5.5-9, 40 mg/L, 5 mg/L, 250 ppm, 1000 µS/cm, respectively (Thurston et al., 1981; Patil et al., 2012; Environment, 2008; Naubi et al., 2016). From the test results, it was observed that the pH values of each wastewater sample exceeded the threshold limit except for de-liming and bating wastewater before treatment. These values revealed that these wastewaters could bring about adverse effects on both aquatic life and the aquatic environment if they are discharged into the environment without any further treatment. However, the pH values of the wastewater sample were found within the tolerable limit (5.5-8.48).

The values of both COD and BOD_5 of every untreated effluent were beyond the acceptable limit prescribed by WHO. Those effluents were not suitable for any specific reuse, especially in irrigation or agricultural applications. At the same time, those effluents seemed very threatening to the aquatic living beings if they were discharged into the rivers. Besides, the BOD_5 (80-96%), and COD (71-87%) values of these respective wastewater samples were significantly reduced after treatment (Fig. 3) which Conductivity and turbidity are two critical parameters describing water's aesthetic quality. Conductivity narrates the total amount of dissolved matter, and turbidity is an essential indicator in determining the suspended sediment quantity in water. These two parameters were also examined for the collected wastewater samples before and after treatment with activated carbon. It was observed from the analysis (Fig. 3) that a substantial amount of reduction in the values of conductivity (73-93%) and

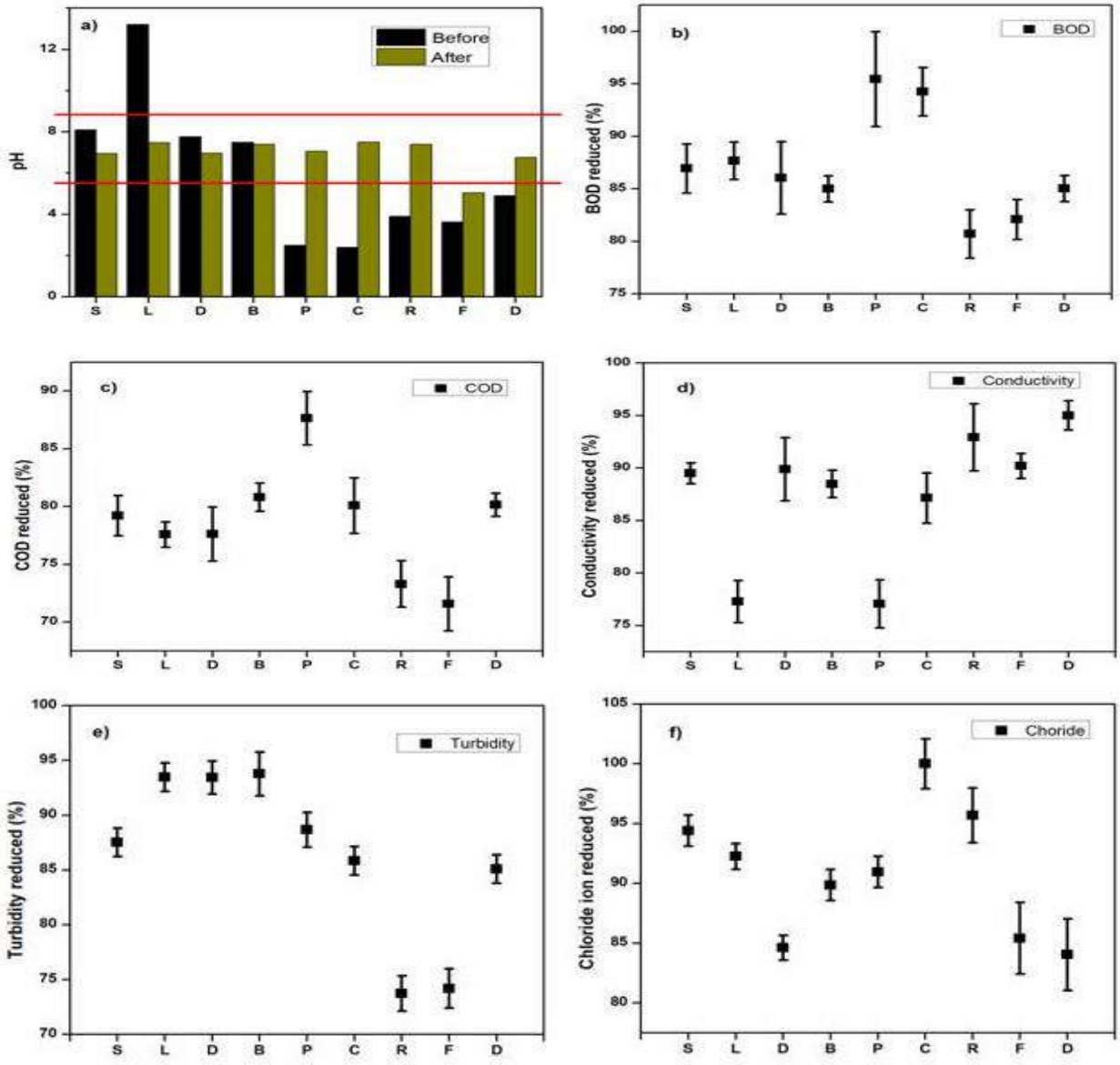

Fig. 3. Decrease all physical parameters of wastewater by using activated carbon where S, L, D, B, P, C, R, F, and D indicate Soaking, Liming, Deliming, Bating, Pickling, Chrome tanning, Re-tanning, Fat liquoring, and Dyeing respectively.

turbidity (76-92%) was obtained in the treated effluents. Most of the values were found closed to the acceptable level recommended by WHO for wastewater released into the environment. Additionally, Cl^{-1} concentration was also remarkably decreased (84-94%) from the effluents.

Microscopic analysis

SEM micrographs of AC samples after MB adsorption are shown in Fig. 4. The micrographs demonstrated AC's smooth surface and porous structure that occurred due to surface modification by phosphoric acid before pyrolysis. The high temperature of pyrolysis causes the reaction of the organic compounds present in CSD with H_3PO_3, and finally, the release of the organic compounds causes pores in the structure. These pores enhance adsorption by offering increased surface area.

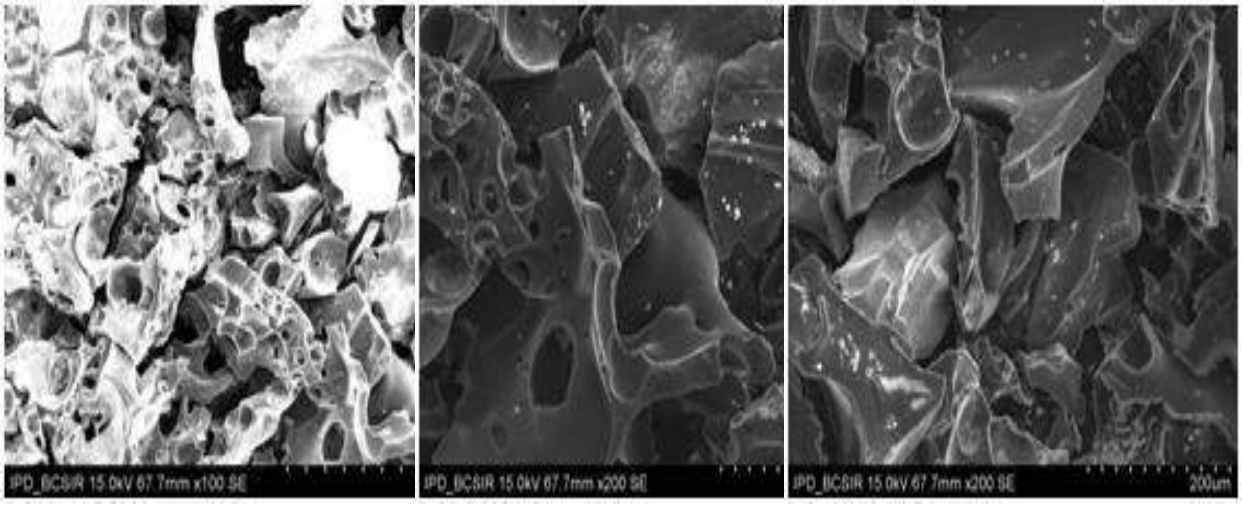

(a) **(b)** **(c)**

Fig. 4. SEM analysis of adsorbent (a) raw CSD (b) CSDAC activated by H_3PO_3 (c) MB adsorbed CSDAC

Conclusion

This research was conducted to evaluate the adsorption effectiveness of prepared AC from leather shaving dust that was mainly attempted to create value addition of solid leather waste along with pollution control. Leather wastes were chemically impregnated using different chemicals at different impregnation ratios before pyrolysis for surface modification to improve their adsorption capacity. Finally, the produced char was used for MB adsorption from an aqueous solution. It has been observed that the chemically impregnated char with phosphoric acid (similar impregnation ratio and similar mesh size) was the superior adsorbent. The adsorption capacity was in a proportional relationship with the impregnation ratio of chemicals and particle size of shaving dust as well. The tested water quality parameters viz. pH, electrical conductivity, turbidity, TDS, chloride, BOD, and COD of the collected effluent samples discharged from each chemical operation during leather manufacturing were also studied. After treatment with AC activated by phosphoric acid, significant amount of pH (5.5-8.48), conductivity (73-93%), turbidity (76-92%), BOD_5 (80-96 %), COD (71-87 %), Cl^- (84-94%) were decreased. From the above outcomes, it can be summarized that AC produced from chrome shaving dust can be a very fruitful adsorbent that can be used for wastewater treatment and a suitable example of a waste recycling system.

Statements and Declarations

Acknowledgments

The authors sincerely thank the Department of Glass and Ceramic Engineering (GCE),

Bangladesh University of Engineering and Technology (BUET), Dhaka, Bangladesh, for providing outstanding laboratory facilities.

Availability of Data and Material

The data in this study are available from the corresponding author on reasonable request.

Funding: There was no funding for this research.

Conflict of Interest: The authors declare that they have no conflict of interest.

References

Abajihad Z. Assessment of tannery solid waste management and characterization, A case of Ethio-Leather Industry Private Limited Company (EliCO), MSc thesis, Addis Ababa University, Ethiopia, 2012; p.53-54.

Anandkumar J and Mandal B. Removal of Cr (VI) from aqueous solution using Bael fruit (*Aegle marmeloscorrea*) shell as an adsorbent. *J. Hazard. Mater*. 2009; 168: 633-640.

Andrioli E and Gutterres M. Evaluation of waste management in tanneries. In: Proceedings of the XXXIII IULTCS Congress, Novo-Hamburgo, Brazil. 2015; 180: 1-9.

de Aquim PM, Gutterres M and Trierweiler J. Assessment of water management in tanneries: State of Rio Grande do Sul case study. *Lume UFRGS*. 2010; p.94.

Dutta SS. An introduction to the principles of leather manufacturing. Indian Leather Technologists Association, Mercantiles Buildings, Lalbazar Street Calcutta-700001, India. 1990; p. 452.

Ebrahimi A, Arami M, Bahrami H and Pajootan E. Fish bone as a low-cost adsorbent for dye removal from wastewater: response surface methodology and classical method. *Environ. Model. Assess.* 2013; 18(6): 12-23.

Environment and Forest, Guide for Assessment of Effluent Treatment Plants. 2008; 1st edi, p. 122.

Etezad SM and Sadeghi-Kiakhani M. Decolorization of malachite green dye solution by bacterial biodegradation. *Prog. Color Colorants Coat.* 2021; 14: 79-87.

Hashem MA and Nur-A-Tomal MS. Tannery solid waste valorization through composite fabrication: A waste-to-wealth approach. *Environ. Prog. Sus. Ener.* 2018; 35(5): 1722-1726.

Kasmaei AS, Rofouei MK, Olya ME and Ahmed S. Kinetic and thermodynamic studies on the reactivity of hydroxyl radicals in wastewater treatment by advanced oxidation processes. *Prog. Color Colorants Coat.* 2020; 13: 1-10.

Khalid R, Aslam Z, Abbas A, Ahmad W, Ramzan N and Shawabkeh R. Adsorptive potential of *Acacia nilotica* based adsorbent for chromium (VI) from an aqueous phase. *Chin. J. Chem. Eng.* 2018; 26(3): 614-622.

Kopp JF. Methods for Chemical Analysis of Water and Wastes. 1978. Environmental Monitoring and Support Laboratory, Office of Research and Development, US Environmental Protection Agency. 1979. p.45-46.

Li Y, Guo R, Lu W and Zhu D. Research progress on resource utilization of leather solid waste. *J. Leat. Sci. Eng*. 2019; 1: 6.

Madhavi J, Srilakshmi J, Rao MVR and Rao KRSS. Efficient leather dehairing by bacterial thermostable protease. *Int. J. Bio-Sci. Bio-Technol.* 2011; 3(1): 11-26.

Naubi I, Zardari NH, Shirazi SM, Ibrahim NFB and Baloo L. Effectiveness of water quality index for monitoring malaysian river water quality. *Pol. J. Environ. Stud.* 2016; 25(1): 231-239.

Patil P, Sawant D and Deshmukh R. Physico-chemical parameters for testing of water-A review. *Int. J. Environ. Sci.* 2012; 3(3): 1194-1205.

Paul HL, Antunes APM, Covington AD, Evans P and Phillips PS. Bangladeshi leather industry: An overview of recent sustainable developments. *Soc. Leat. Technol. Chem.* 2013; 97: 25-32.

Pearson HW, Mara DD and Bartone CR. Guidelines for the minimum evaluation of the performance of full-scale waste stabilization ponds. *Water Res*. 1987; 21(9): 1067-1075.

Pereira RG, Veloso CM, da Silva NM, de Sousa LF, Bonomo RCF, de Souza, AO, da Guarda Souza MO and Fontan RDCI. Preparation of activated carbons from cocoa shells and siriguela seeds using H_3PO_4 and $ZnCl_2$ as activating agents for BSA and α-lactalbumin adsorption. *Fuel pross. technol*. 2014; 126: 476-486.

Sundar VJ, Gnanamani A, Muralidharan C, Chandrababu NK and Mandal AB. Recovery and utilization of proteinous wastes of leather making: a review. *Rev. Environ. Sci. Biotechnol.* 2011; 10: 151-163.

Tahiri S and de la Guardia M. Treatment and valorization of leather industry solid wastes: A review. *J. Am. Leath. Chem. Assoc*. 2009; 104(2): 52-67.

Thilagavathy P and Santhi T**.** Sorption of toxic Cr (VI) from aqueous solutions by using treated *Acacia nilotica* leaf as adsorbent: Single and binary system. *Bio Res.* 2013; 8: 1813-1830.

Thurston RV, Russo RC and Vinogradov G. Ammonia toxicity to fishes. Effect of pH on the toxicity of the unionized ammonia species. *Environ. Sci. technol.* 1981; 15(7): 837-840.

Wijaya R, Andersan G, Santoso SP and Irawaty W. Green reduction of graphene oxide using kaffir lime peel extract (*Citrus hystrix)* and its application as adsorbent for methylene blue. *Sci. Rep*. 2020; 10(1): 667.

J. Bangladesh Acad. Sci. 46(1); 85-99: June 2022 DOI: 10.3329/jbas.v46i1.59177

Journal of Bangladesh Academy of Sciences

Journal homepage: http://www.bas.org.bd/publications/jbas.html

Research Article

Fate of heavy metals in Swarna rice after traditional cooking and submerged fermentation linked to bacterial interactions

Md. Azizul Haque*, Md. Atikur Rahman[1], Jannatul Ferdousi, Md. Bokhtiar Rahman[1] and Abubakar Halilu[2]

Department of Biochemistry and Molecular Biology, Faculty of Agriculture, Hajee Mohammad Danesh Science and Technology University, Dinajpur, Bangladesh

ARTICLE INFO

Article History

Received: 20 April 2022
Revised: 7 May 2022
Accepted: 12 June 2022

Keywords: Heavy metals, Swarna rice, Hazard quotient, Carcinogenic risk, Submerged fermentation (Panta vhat), Lactic acid bacteria

ABSTRACT

This research aimed to assess the concentrations of As, Cd, Cr, Pb, and Zn in Swarna rice (NR) collected from Kaharole, Biral, and Sadar Upazilla of Dinajpur and their reduction by cooking associated submerged fermentation. The levels of As, Cd, Cr, and Zn were lower than the individual metal's safe limit, but the (Pb) concentrations were found at 0.2582, 0.9028, 0.9164, 0.7303, 0.8574, 0.6440, 0.6622 mg/kg in SR02, SR04, SR05, SR06, SR07, SR08, and SR09 of NR samples, respectively, which were higher than the (Pb) safe limit. Notably, the reduced hazard index (HI) was found from the standard limit 1 for all fermented rice (FR) samples and all boiled rice (BR) samples except SR05. Six different *Streptococcus* sp. strains were identified in FR that suggested *Streptococcal* involvement in leaching of HMs during submerged-fermentation. Consequently, compared to NR, hazard index and cumulative carcinogenic risk were declined by several folds in FR.

Introduction

Swarna rice variety is locally cultivated in approximately 46% of the land of Dinajpur in the Aman season (August to November) (Hossain et al., 2013). According to the Bangladesh Bureau of Statistics (BBS), in 2011, Bangladeshi people consumed an average of 416 gm of rice daily (BBS, 2011). Though life expectancy is gradually improving the percentage of people with non-communicable diseases increases yearly. According to the International Diabetes Federation (IDF) report in 2017, 6,926,300 diabetic patients were identified in Bangladesh, of which about 6.9% were adults (IDF, 2017). Over the last decade, the number of diabetic patients has been increasing in the rural areas of Dinajpur, even though they do not carry proper risk factors such as obesity, smoking, genetics, and other factors. Therefore, it is a surprising and common question how and why diabetes is more frequent in this area? Recently, it has been reported that heavy metals (HMs) are involved in the risk factor of type-2 diabetes (Zheng et al., 2018).

Heavy metals (HMs) are accumulated in the human body through drinking water, dermal contact, HMs-contaminated foods, and exposure to dust particles (Zheng et al., 2018). In this regard, cooking rice with a large volume of water (6:1; water: rice) has been documented to reduce inorganic As compared to the general cooking of rice (Raab et al., 2009). It is reported that the rinse cooking of rice with a large volume of water reduced HMs concentrations (Sharafia et al., 2019), but Kathe cooking does not need steaming of rice. Rinse cooking was practiced for a couple of decades, which has changed to Kathe cooking due to technological development. In the last two decades, the mass media have suggested using

*Corresponding author: <helalbmb2016@hstu.ac.bd>

[1]Grassland and Forages Division, National Institute of Animal Science, Rural Development Administration, Cheonan, South Korea
[2]Department of Pharmaceutics and Pharmaceutical Microbiology, Usmanu Danfodiyo University, Sokoto State, Nigeria

the optimum doses of fertilizers and pesticides in the rice fields. Unfortunately, it is yet to be practically executed by the farmers. Consequently, HMs and toxic chemicals are gradually accumulating in the rice. Additionally, local people are ignorant about the rinse cooking of rice.

Panta-Bhat is semi-fermented boiled rice immersed in water overnight (about 12-15 h). It is generally softened due to partial fermentation, which is served to eat in the morning. Although HMs associated with hazardous risks of rice in America, India, Pakistan, Thailand, and China have been reported (Shraim, 2014; Roya and Ali, 2017; Morekian et al., 2013; Naseri et al., 2015), a little research has been conducted on it in some rice cultivars in Bangladesh (Proshad et al., 2019). Until now, HMs-associated hazardous risk in Bangladeshi Swarna rice (Normal rice, NR) has not been studied. Assessing the health risk of highly consumed rice, especially Swarna rice, is imperative exploring a cost-effective cooking approach to reduce HMs from rice is also essential. The investigation of the concentration levels of other HMs in rice grown in the northern part of Bangladesh is highly demanded. The toxicity levels of HMs in cooked rice and HMs abundance in fermented rice are still to be explored.

The study aimed to screen the HMs associated health risk in Swarna rice and to explore a strategy for reducing HMs from rice. First, this study reported the reduction strategy of HMs by rinsed associated Panta-Bhat (submerged fermented rice) preparation, which provides valuable information to rice consumer to be free of hazards from rice.

Materials and Methods

Rice sample collection and preparation

The rice sample was collected during the Aman season (November-January, 2017) from Sundarpur, Poyesh, Dhonigram at Kaharol (25° 47′ 4.942″ N, 88° 35′ 46.593″ E), Tegra, Kajihat, Kanchan at Biral (25° 37′48.139″ N, 88° 33′ 20.75″ E, and Gabura, Kawgaon, Pulhat at Sadar (25° 36′ 36.814″ N, 88° 38′ 59.403″ E) Upazila′s in Dinajpur, Bangladesh. Briefly, 250 gm of rice from each nine samples were sun-dried for 24 h and then de-husked manually. The de-husked rice grains were boiled (rice: distilled water; 1:10) in a water-containing steel saucepan set on an electric cooker. The temperature of the electric cooker was fixed at 160 °C, and cooking was continued for 45 min. To flash out of HMs from Swarna rice, grains were stirred smoothly by the wood spoon every 5 min so that HMs could separate and leach out properly. One-fourth of the boiled water was drained from the saucepan after 15 min of cooking; subsequently, an equal amount of distilled water was added and boiled again. The aforementioned process was repeated three times during the whole cooking. This boiled rice (BR) was allowed for cooling at room temperature; subsequently, 10 gm of rice was collected and stored in the refrigerator for further analysis. The rest of the BR samples were weighed and transferred to a pot containing normal distilled water. The rice was immersed in water (1:2) for 15 h for fermentation at room temperature. This short-time fermented rice is locally called Panta-Bhat. The water liquor from the Panta-Bhat samples was discarded, and then the FR was collected and stored in the refrigerator.

Flame atomic absorption spectrometry (FAAS)

One gram of rice powder from each group (NR, BR, and FR) was digested using a 15 mL ternary solution ($HNO_3/H_2SO_4/ HClO_4$, 5:1:1 v/v) at 80 °C to make the solution transparent. As, Cd, Cr, Pb, and Zn in digested solution were quantified using a flame atomic absorption spectrophotometer (FAAS; 240FS, Agilent, Australia). Before quantifying HMs, the FAAS was calibrated using a standard of the specific metals. The wavelength (λ) was set at 193.7, 228.8, 357.9, 283.3, and 213.9 nm for the standard As, Cd, Cr, Pb, and Zn solutions. The Zn, Cr, and As were analyzed using a hollow cathode lamp (HCL). In contrast, Cd and Pb were analyzed using an electrodeless discharge lamp

(EDL) in the flame atomizer AAS (Tchounwou et al., 2003). The blank reagent and metal-specific standards were considered for each sample in a separate batch to verify the accuracy and precision of the digestion procedure. Briefly, 250 µL of standard solutions of each element were prepared from the stock standard solution (1000 mg/L) in a plastic volumetric flask (25 mL) and made up to the mark with 0.5 N HCL solutions, thus making the intermediate standard solution (10 mg/L). A suitable working solution (control) was prepared for As, Cd, Cr, Pb, Zn as 0.1583, 0.1686, 0.1400, 0.5226, 0.3103 ppm for control 1 and 0.6395, 0.5791, 0.46114, 1.7800, 0.65232 ppm for control 2, respectively and the absorbance of each sample solution was taken.

Statistical analysis

The HMs abundance results were statistically analyzed using variance analysis (ANOVA) and Duncan's multiple range test (DMRT) to determine the significant (ρ<0.05) differences among the group means.

Estimation of daily intake (EDI)

The estimated daily intake (EDI) of As, Pb, Cd, Cr, and Zn from rice consumption was calculated by using the following equation (Hertzberg, 2000):

$$EDI = EF \times ED \times FIR \times Cm / WAB \times Ta$$

Where, EDI=Estimated daily intake (mg/kg/day) of a specific metal; EF=Exposure frequency (365 days/year); ED= Exposure duration (equivalent to a mean lifetime of the Bangladeshi people, i.e., 72 years); FIR=Ingestion rate (g/person/day) of rice (Based on the HIES, FIR was 367); Cm= Metals concentration (mg/kg, dry weight); and Ta= (EF × ED) is the mean exposure time that is 72 years lifetime (Bamuwamye et al., 2015).

Incremental lifetime cancer risk (ILCR) and cumulative carcinogenic risk (CCR)

The probability of cancer risk of heavy metals (As, Pb, Cd, Cr, Zn) from rice consumption was estimated after considering the incremental lifetime cancer risk (ILCR) by using the following equation (Sultana et al., 2017):

$$ILCR = EDI \times CSF$$

Where, EDI represents estimated daily intake (mg/kg/day), and CSF represents cancer slope factor 20. The CSF for As, Pb, Cd, Cr, and Zn is 1.5, 0.0085, 0.38, 0.5, and 0.0 (mg/Kg-day)-1, respectively (OEHHA, 2009). The cumulative carcinogenic risk (CCR) is the sum of ILCR of As, Pb, Cd, Cr, and Zn that was calculated by using the following equation:

$$CCR = ILCRPb + ILCRAs + ILCRCd + ILCRCr + ILCRZn$$

Target hazard quotients (THQ)

The THQ was calculated by the following formula established by the EPA 19:

$$THQ = EF \times FD \times EDI / RfD \times W \times T,$$

Where EF represents the frequency of exposure of a particular HM =365 days/year for rice; FD is the duration of exposure = 72 years, EDI is the estimated daily ingestion (mg/person/day), and RfD is the oral reference dose (mg/Kg/day); W is the average body weight=58 Kg and T is the average exposure time for non-carcinogens (365 days year-1 × 72). The oral approval doses (RfD) were considered as 0.003, 0.0003, 0.001, 0.004and 0.3 mg/kg for Cr, As, Cd, Pb, and Zn, respectively.

Isolation and biochemical characterization of lactic acid bacteria

The liquid portion of fermented rice (Panta vhat) was collected to evaluate the metal scavenging bacteria. The liquid portion was serially diluted using a 10-fold dilution method, and 30-50 µL of diluted sample was spread on the sterilized De Man, Rogosa, and Sharpe agar (MRS) plates. The agar plates were incubated at 30 °C for 48 h in an incubator. The distinct bacterial colonies were picked up from the

MRS agar plates and streaked on MRS agar plates for further purification. A set of purified isolates was stored in 80% glycerol for further analysis. The isolates were biochemically characterized according to the results of oxidase, catalase, methyl red (MR), Voges-Proskauer (VP), triple sugar iron (TSI), citrate utilization (CU), indole, motility indole urease (MIU), and carbohydrates (lactose, maltose, sucrose and dextrose) fermentation tests in aseptic condition (Abdullah-Al-Mamun et al., 2022; Haque et al., 2015a). The activities of the extracellular amylase, pectinase, xylanase, and protease of the isolates were conducted by spreading the bacterial samples with a sterile loop in starch, pectin, xylan, and casein medium that served as the sole carbon source in an aseptic condition as described (Das et al., 2022; Haque et al., 2021). The agar plates were streaked by picking off a loopful colony of 24 h pure culture of the isolates. The culture plates were incubated at 37 °C for 24 h. Finally, the plates (starch, pectin, xylan, casein) were washed with Congo red followed by distilled water, and the hydrolytic zone was observed as described (Das et al., 2022).

Molecular characterization of lactic acid bacteria

The molecular characterization of the isolated bacterial strains was performed based on 16S rRNA gene sequencing analyses. The PCR amplification was carried out in a 200 µL PCR tube containing 25 µL of 2X PCR Master mix solution (Promega Corporation, USA), 27F (5′- AGA GTT TGT TGA TGG CTC AG - 3′) as the forward primer (5.0 µL), and 1492R (5′-GGT TAC CTT GTT ACG ACT T- 3′) as the reverse primer (5.0 µL), template DNA 2.0 µL, and a nuclease-free water 13.0 µL. The following PCR steps were programmed, visualized, purified, and sequenced for gene amplification, (Haque et al., 2021; Das et al., 2022). The query sequence was used to construct a phylogenetic tree using MEGA 7.0 software with the neighbor-joining method (bootstrap 1000x).

Results and Discussion

Level of heavy metal in normal Swarna rice (NR) grain

The FAAS technique determined the levels of free As, Cd, Cr, Pb, and Zn in NR grain, and the results are presented in Table 1. The analysis of five HMs indicated a significant ($\rho<0.05$) difference between nine sample′ highest and lowest levels. The accumulations of HMs in rice grain were ranged from (0.0129−0.01866) mg/kg, (0.0037−0.01723) mg/kg, (0.0043−0.2018) mg/kg, (0.01901−0.9164) mg/kg, (0.02893−0.3542) mg/kg for As, Cd, Cr, Pb and Zn, respectively. The levels of As were 1.26 to 1.47-fold higher in SR02, SR04, SR05, SR06, SR07, SR08, and SR09 samples compared to the SR01 sample, whereas no significant ($\rho<0.05$) differences were observed in As accumulation among the rice samples of SR04, SR06, SR07, and SR09. In contrast, relatively higher levels of As (0.314 mg/kg) were observed in TajMahal rice samples of India (Roya and Ali, 2017). The levels of As should not be exceeded 0.050 mg/kg for a rice consumer who eats 200 g of rice per day, which is equivalent to an exposure of As in drinking water at 10 µg/L (Zhu et al., 2008). In this study, the rice samples SR04 and SR07 accumulated 0.01866 mg/kg As, representing 0.0093 mg/kg of inorganic As (Heikens, 2006). The highest level of As 0.01866 mg/kg was obtained from the SR06 sample, which was approximately 10.7-fold lower than the safe limit of 0.2 (WHO, FAO) and 8.03-fold lower compared to the safe limit of 0.15 mg/kg (National standards of Iran/China). One of the highest levels of As (0.23 mg/kg) in rice samples of the Southwestern part of Bangladesh has been reported by (Rahman et al., 2010), which is almost 12.3-fold higher than the Swarna rice samples SR04, SR06, and SR07. These results suggested that Swarna rice grown in Dinajpur district contains a lower level of As than in the South-western district of Bangladesh.

Table 1. Average concentrations (mean±SEM) mg/kg of heavy metals present in rice were determined using a flame atomic absorption spectrophotometer (FAAS).

HM (mg/kg)	SR01	SR02	SR03	SR04	SR05	SR06	SR07	SR08	SR09
As	0.0129^{e} $\pm5.7\times10^{-5}$	0.0176^{c} $\pm2.88\times10^{-4}$	0.0163^{d} $\pm1.73\times10^{-4}$	0.01866^{a} $\pm2.40\times10^{-4}$	0.01715^{c} $\pm8.68\times10^{-5}$	0.01849^{a} $\pm1.49\times10^{-4}$	0.0186^{a} $\pm2.88\times10^{-4}$	0.0177^{bc} $\pm1.73\times10^{-4}$	0.01823^{ab} $\pm2.18\times10^{-4}$
Cd	0.0120^{c} $\pm2.90\times10^{-4}$	0.01413^{b} $\pm2.05\times10^{-4}$	0.0073^{d} $\pm1.87\times10^{-4}$	0.0074^{d} $\pm1.47\times10^{-4}$	0.00393^{e} $\pm8.54\times10^{-5}$	0.00745^{d} $\pm1.84\times10^{-4}$	0.0037^{e} $\pm2.27\times10^{-4}$	0.0137^{b} $\pm3.18\times10^{-4}$	0.01723^{a} $\pm2.05\times10^{-4}$
Cr	0.0045^{g} $\pm2.51\times10^{-4}$	0.0580^{e} $\pm4.04\times10^{-3}$	0.01933^{f} $\pm2.40\times10^{-4}$	0.0945^{c} $\pm4.84\times10^{-4}$	0.0043^{g} $\pm4.04\times10^{-4}$	0.2018^{a} $\pm2.75\times10^{-3}$	0.0730^{d} $\pm2.64\times10^{-3}$	0.1696^{b} $\pm7.22\times10^{-4}$	0.1675^{b} $\pm1.72\times10^{-3}$
Pb	0.01901^{g} $\pm6.01\times10^{-5}$	0.2582^{e} $\pm7.26\times10^{-4}$	0.0675^{f} $\pm7.55\times10^{-4}$	0.9028^{a} $\pm9.13\times10^{-3}$	0.9164^{a} $\pm5.69\times10^{-3}$	0.7303^{c} $\pm2.90\times10^{-3}$	0.8574^{b} $\pm1.62\times10^{-2}$	0.6440^{d} $\pm6.38\times10^{-3}$	0.6622^{d} $\pm2.18\times10^{-3}$
Zn	0.0451^{d} $\pm3.46\times10^{-4}$	0.08063^{c} $\pm6.12\times10^{-4}$	0.1119^{b} $\pm9.93\times10^{-4}$	0.0716^{c} $\pm6.08\times10^{-4}$	0.02893^{e} $\pm3.93\times10^{-4}$	0.3542^{a} $\pm1.14\times10^{-2}$	0.0470^{d} $\pm8.54\times10^{-4}$	0.0565^{d} $\pm5.68\times10^{-4}$	0.06923^{c} $\pm3.18\times10^{-4}$

Data were presented as mean values ± standard deviation of three independent experiments. According to Duncan's multiple range test, values with different letters are significantly different ($\rho\leq0.05$). SR01: Sundarpur (Kaharole); SR02: Poyesh (Kaharole); SR03: Dhonigram (Kaharole); SR04: Teghra (Biral); SR05: Kajihat (Biral);SR06: Kanchan (Biral); SR 07: Gabura (Sadar); SR08: Kawgaon (Sadar); SR09: Pulhat (Sadar).

Table 1 shows the Cd levels ranged from 0.0037 to 0.17233 mg/kg. The difference between the highest level of Cd in SR09 and the lowest level in SR05 was 4.65-fold. Similar Cd concentrations were found for SR02 and SR08 samples that were about 1.2-fold lower than SR09. The differences among Cd concentrations in SR03, SR04, and SR06 samples were insignificant. It has been noticed that the variations of Cd level depend on the type of agricultural soil, application of phosphate fertilizer, and use of groundwater (Jorhem, 2000). This study also showed the variation in Cd levels which did not exceed the current safe limit of 0.1 mg/kg (FAO/WHO 2011; ISIRI, 2010). The Cd level has been screened in rice in some Asian countries, e.g., Thailand, China, and South Korea, and they were 0.150, 0.0345, and 0.021 mg/kg, respectively. But the higher levels of Cd were found in rice of Koshan-2015 (0.64 mg/kg), Mazandaran-2013 (0.0193 mg/kg), and Shiraz-2010 (0.34 mg/kg) in Iran (Jafari, 2018).

The concentration of Cr in rice samples SR01, SR02, SR03, SR04, SR05, and SR06 were significantly varied except for SR08 and SR09. Rice samples' Cr levels were screened between 0.0045-0.20183 mg/kg. The lowest content of Cr was found in SR01, almost 44.8-fold and 37.5-fold lower than that of samples SR06, and SR08, respectively. In a related study, the Cr levels were determined to be 0.24 mg/kg in Mazandaran-2013 and 0.39 mg/kg in Shiraz-2010 Iranian rice cultivars (Jafari, 2018). In addition, Indian rice contains 0.184 mg/kg Cr, which is lower than the minimum concentration limit (MCL) of 0.2 mg/kg 10. However, the levels of Cr in SR01, SR02, SR03, SR04, SR05, and SR07 Swarna rice samples were lower than in the MCL.

The maximum and minimum concentrations of Pb were statistically significant ($\rho<0.05$) (Table 1). The highest level of Pb was determined in sample SR05, while the lowest was observed in sample SR01. No significant ($\rho<0.05$) difference has been found in Pb accumulation between the samples SR08 and SR09. The Pb level of samples SR01 and SR03 was less than the safe limit (0.2 mg/kg), but the remaining samples SR02, SR04, SR05, SR06, SR07, SR08, and SR09 crossed the Pb safe limit. Therefore, these results revealed that most of the Swarna rice samples exceeded the maximum contaminant level of Pb. The Pb is highly accumulated in rice, and its accumulation level

depends explicitly on the plants' cultivar and ecological and regional distribution. For example, the concentration of Pb (0.64 mg/kg) in some Iranian rice was higher than that of MCLs 13, and similar results have been obtained in (Shraim, 2014) imported rice varieties (Roya and Ali, 2017). In contrast, a moderate level of Pb (0.254 mg/kg) was observed in the Indian rice sample that was higher than the maximum allowable level (Morekian, 2013).

The highest Zn level was obtained in sample SR06, whereas the lowest was in SR05. In Table 1, no significant difference was observed in Zn accumulation among the samples SR02, SR04, and SR09, and between the samples SR07 and SR08. In contrast, a significant difference has been found between the SR01 and other samples. Several reports have provided comparisons regarding the Zn level found in local rice cultivars (Kashian and Fathivand, 2015). In contrast, the highest level of Zn 290 mg/kg and 21.8 mg/kg has been determined in Taiwanese and Thai, respectively (Parengam et al., 2010), higher than the Zn levels in Swarna rice of Bangladesh. In a related study, Proshad et al. (2019) found the higher concentrations of HMs in rice samples cultivated in industrially polluted areas in Tangail district, Bangladesh. Therefore, we assumed that the difference in HMs levels in rice in South-Asian countries could be associated with spatial distribution, application of agrochemicals, and industrial activities.

Table 2. Correlation matrix (Pearson) for heavy metals in Swarna rice grown in Dinajpur, Bangladesh.

The right upper part is a significant level, and the left lower is the correlation coefficient. *Correlation is significant at the 0.05 level (2-tailed)

Table 2. Correlation matrix (Pearson) for heavy metals in Swarna rice grown in Dinajpur, Bangladesh.

	As	Cd	Cr	Pb	Zn
As		0.69	0.081	0.017	0.49
Cd	-0.152		0.32	0.29	0.77
Cr	0.609	0.369		0.25	0.11
Pb	0.759*	-0.39	0.42		0.88
Zn	0.264	-0.112	0.56	0.05	

A correlation (Pearson) of HMs found in Swarna rice was analyzed and presented in Table 2.

The regional distributions, along with HMs influences, were raised by a PCA biplot analysis. In the correlation biplot, the variables very close to each other and located in the same quadrant indicated a strong positive correlation. The F1 and F2 showed a 76.43% variation, in which F1 contributed 28.46% and F2 contributed 47.97% (Fig. 1).

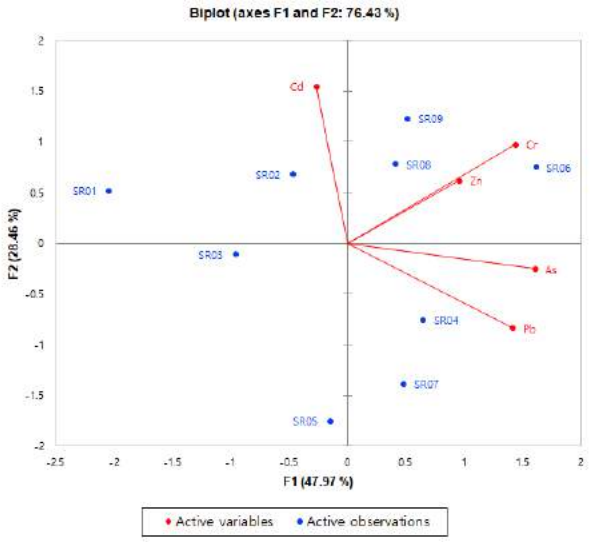

Fig. 1. Principal component analysis of heavy metals in Swarna rice. The biplot show the correlations among the five heavy metals (As, Cd, Cr, Pb, and Zn) and nine studied areas (SR01 to SR09).

A significant ρ<0.05) positive correlation existed between the As and Pb but was negative in the case of Cd. Such spatial correlation among the HMs was not surprising because of its association with the variation of soil pH and organic matters. However, the selected variables with spatial correlations may help divide the zones for different agricultural management.

Leaching of HMs from rice in different processing conditions

A comparative study was performed to determine the HM content in regular Swarna rice (NR), boiled rice (BR), and fermented rice (FR). The As, Cd, Cr, Pb, and Zn levels in three conditions, NR, BR, and FR, were measured and presented in Fig. 3. Five samples (SR01 to SR05) for each condition were considered representative studies. The results dealt with a significant ρ<0.05) reduction of As in samples SR01 to SR05 of BR and FR (Fig. 2A). In particular, compared to NR samples, As

levels were reduced by 7.16-, 2.31-,6.27-, 4.53-, and 7.43-fold in BR, whereas 11.7-, 7.33-, 9.05-, 5.8-, and 10.0-fold in FR samples. As seen in Fig. 2B, the level of Cd was significantly reduced in BR and FR of SR01, SR02, and SR03 samples. However, the reduction of Cd was more prominent in FR than in BR. The Cr levels declined 3.75-, 4.86-, 6.63-, 1.94-, and 1.05-fold for BR, whereas 5.45-, 7.42-, 9.12-, 2.11-, and 3.54-fold for FR compared to NR. The level of Cr was significantly reduced for FR in the case of all five rice samples, as seen in Fig. 2C. No significant reduction of Cr has been found in samples SR02, SR03, and SR05 for FR and BR. But, the Cr level declined by 0.94-, 1.036-, 6.89-, and 1.95-fold for BR and 1.25-, 17.6-, 8.39-, and 2.7-fold for FR of SR01, SR02, SR03, and SR05 samples, respectively.

In Fig. 2D, the level of Pb was significantly declined in all samples of BR and FR compared to NR. The level of Pb was downturned by 2.97-, 40.3-, 25.0-, 2.14-, 1.12-folds in BR, and 14.6-, 58.61-, 45-, 2.5-, 1.78-folds in FR of the above five samples (SR01 to SR05). Like Pb, an almost similar trend of reduction of Zn level was found in SR01 to SR05 samples (Fig. 2E). The above results clarify that HMs in rice samples were substantially purged by boiling and fermentation.

Several studies have indicated the influence of cooking on HMs concentrations. For instance, As level declined from 3.5 to 6.0% in cooked rice compared to uncooked rice (Zhuang et al., 2016). It is reported that the reduction of inorganic arsenic is positively influenced by the volume of water, amount of rice, and flash out of boiled water during rice cooking (Carey et al., 2015). Most of the current rice cooking systems (electronic-based) are not up to the mark regarding his removal. In this auto-cooking system, a significant amount of total water is absorbed by the rice, and a small amount is evaporated (Sengupta et al., 2006; Torres-escribano et al., 2008). As a result, a marginal amount of HMs is removed from rice. Consequently, the concentrations of HMs did not decline in rice while microwave ovens were used for rice cooking (Zhuang et al., 2016). In contrast, traditional cooking in South-East Asian countries is more convenient and effective for reducing HMs from rice. In manual cooking, flashing out of excess boiled water after a certain time was one of the key factors for reducing HMs from rice; local people were completely habituated to this cooking system, though they were not well-known concerning the HMs concentration reduction strategies. Several studies reported that inorganic As was reduced in cooked rice compared to raw rice (Torres-escribano et al.,2008; Jane and Shen, 1993), which is agreed with the present study results.

The cooking process led to the discharge of some molecules like amylose, amylopectin, protein, and fat (Yang et al., 2016). Carey et al. (2015) reported that leaching of HMs occurred during cooking rice with a greater volume of water. Therefore, we hypothesized that the free HMs linked with proteins due to the binding nature of HMs, allowing the leaching of HMs during continuous cooking concurrently. The manual draining of excess boiled water from the rice panel's upper layer helps reduce the HMs concentration.

Reduction of HMs by rice fermentation

Long time fermentation of rice leads to the breakdown of the original structure of rice. Therefore, fermentation of rice was performed for 15 h (short duration) at room temperature to maintain the eating suitability and native structure of rice. As seen in Fig. 3, the levels of HMs were significantly reduced after 15 h of fermentation of cooked rice. We tried to understand how HMs was purged during short time fermentation. Though no prior bacterial inoculation and sterile deionized water were used during the cooking and fermentation process, the rice became soft. As a consequence of this observation, including some additional microbial experiments, we identified six different strains of *Streptococcus* from the fermented rice liquor (Table 3). Molecular characterization of HSTU-1 to HSTU-8 bacterial strains was performed by 16S rRNA gene sequencing.

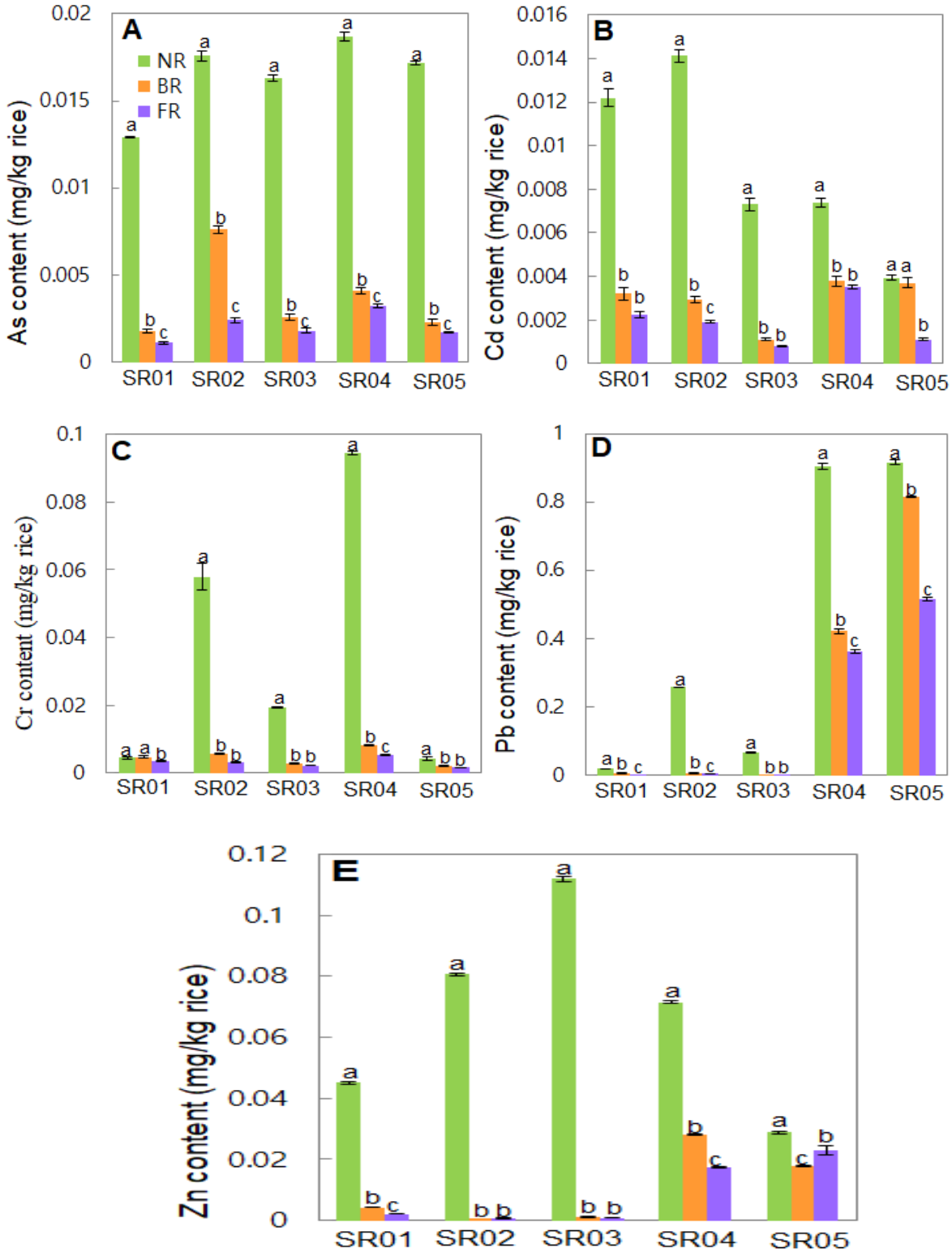

Fig. 2. A comparison of heavy metals in Swarna normal rice (NR), boiled rice (BR), and fermented rice (FR). According to Duncan's multiple range tests, different letters above the error bars indicate a statistically significant difference ($\rho \leq 0.05$).

Table 3. Biochemical characterization of six LAB isolates from fermented rice liquor.

Biochemical tests	***Streptococcus* sp. HSTU-1**	***Streptococcus* sp. HSTU-3**	***Streptococcus* sp. HSTU-4**	***Streptococcus* sp. HSTU-6**	***Streptococcus* sp. HSTU-7**	***Streptococcus* sp. HSTU-8**
Catalase test	-	-	-	-	-	-
Oxidase test	-	-	-	-	-	-
Methyl Red test	+	-	+	+	+	+
Voges-Proskauer (VP) test	-	-	-	-	-	-
Triple sugar iron test	+	+	+	+	+	+
Citrate utilization test	-	-	-	-	-	-
Motility indole urease test	+	+	+	+	+	+
Mortality	+	+	+	+	+	+
Indole test	-	-	-	-	-	-
Fermentation of maltose	-	+	+	-	-	-
Fermentation of sucrose	-	+	-	-	+	-
Fermentation of lactose	-	-	-	-	+	+
Fermentation of dextrose	+	-	-	-	-	-
Cellulase	-	-	-	-	-	-
Xylanase	+	+	+	+	+	+
Amylase	-	+	+	-	-	+
Pectinase	-	-	-	-	-	-
Protease	+	+	-	+	-	+

All strains showed xylanase activities but not cellulase and pectinase (Table 3). HSTU-3 and HSTU-4 showed amylase activity, and HSTU-1, HSTU-6, and HSTU-8 showed protease activity. The PCR bands of the 16S rRNA gene showed approximately 1.4 kb sizes in the agarose gel electrophoresis (Fig. 3A). Moreover, the DNA sequencing results of the 16S rRNA gene after nucleotide BLAST homology analysis revealed that the strains were 99% related to *Streptococcus infantarius* and other species. Therefore, based on phylogeny, the isolates were named *Streptococcus sp.* strain HSTU-1 to *Streptococcus sp.* strain HSTU-8. The strains were different from each other according to their alignment results. The phylogenetic tree construction revealed that the strains belonged to lactic acid bacteria and especially were closer to the *Lactococcus* sp. (Fig. 3B).

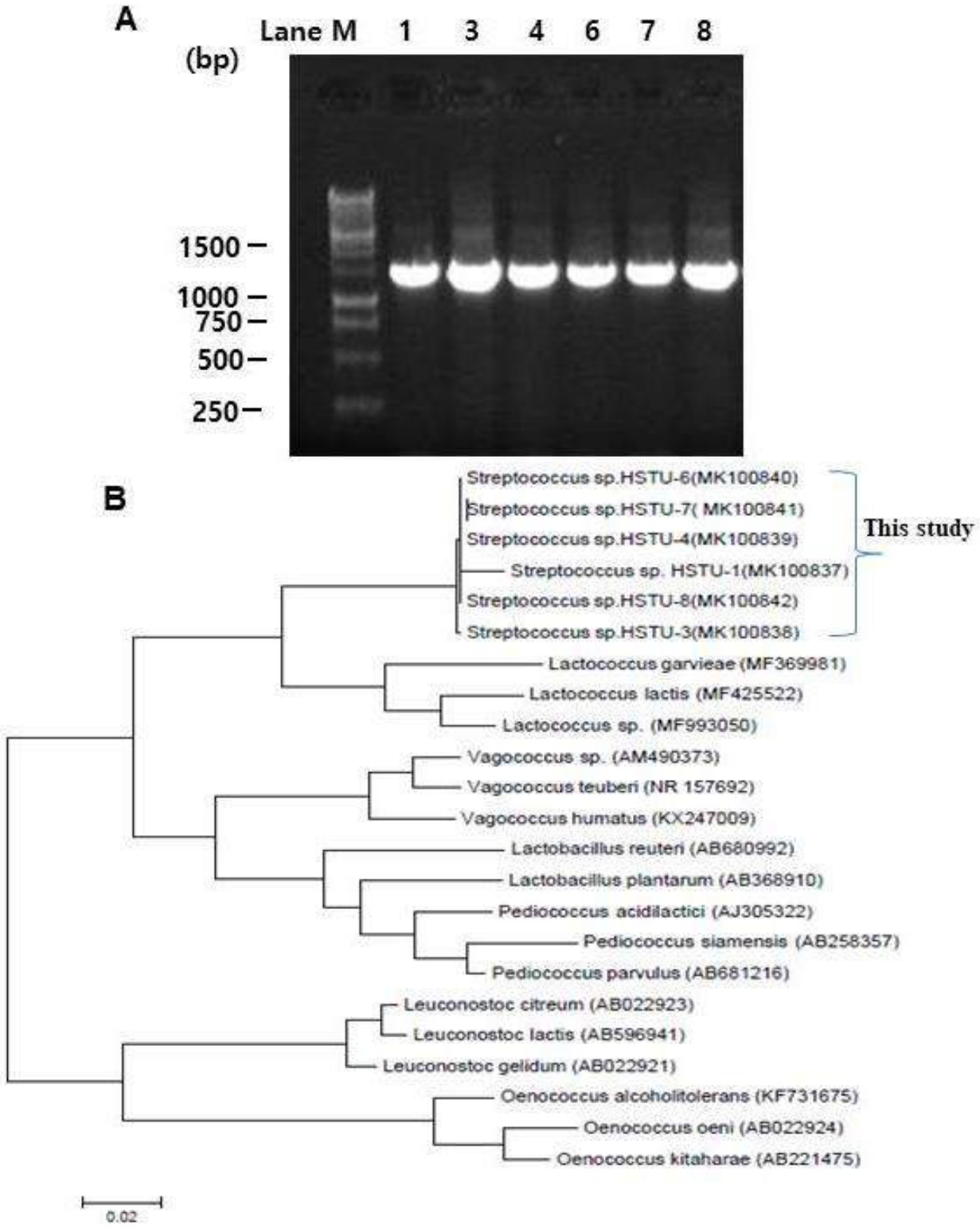

Fig. 3. Molecular identification of lactic acid bacteria (LAB) growing in fermented rice (FR). A) Polymerase chain reaction product bands of LAB isolates from the liquor of FR, B) Phylogenetic tree was constructed using a software MEGA8 using the neighbor-joining method.

The strains HSTU-3 and HSTU-7 were involved in sucrose fermentation, while the rest were not. In addition, the other sugars were randomly fermented by the strains. However, all six *Streptococcus sp.* together secret xylanase, protease, and amylase enzymes (Table 3), which suggests that the rice was further softened and de-agglomerated during fermentation due to the unwinding of the helical structure of starch by the action of those enzymes. As a consequence, the HMs were leached out into the water. In addition, the *Streptococcus* sp. was capable of fermenting maltose, sucrose, lactose, and dextrose (Table 3), which suggested that the sugar residues were perfectly metabolized during fermentation. A group of Lactic acid bacteria, including *viridescens* MYU205, *L. Plantarum*, and *L. fermentum* ME3, is known to be involved in the removal of Pb and Cd (Haltunnen et al., 2007; Kinoshita et al., 2013). Moreover, a combined application of *L. Plantarum* and *P. pantosaceus* strains (2:1 v/v) ratio was used in the highly Cd impregnated (0.647 mg/kg) rice powder for the fermentation to reduce the level of Cd (Fu et al., 2015). Therefore, the above findings indicated that the generation of *Streptococcus* sp. HSTU strains were involved in rice fermentation along with reducing HMs from rice.

Target hazard quotient (THQ) and hazard index (HI)

The HM-specific THQ and the total THQ of five HMs were presented as HI of a particular rice sample (Fig. 5). The HI is an indicator that helps determine the potential exposure of HMs in our studied samples. The Pb level indicated its highest exposure, followed by As and Cr in SR04, SR05, SR06, SR07, SR08, and SR09 samples compared to all other metals (Fig. 4A). The HI level indicated that rice samples of Kaharole (SR01, SR02, and SR03) were free from hazardous risk, but the rice samples of Sadar (SR07, SR08, and SR09) and Biral (SR04, SR05, and SR06) were not free from risk of hazards. In this regard, we reduced the potential health risk by boiling and fermentation. Consequently, BR and FR samples SR01 to SR05 were provided a lower value of HI than the NR samples (Fig. 4B). In particular, the four samples (SR01 to SR04) showed HI lowers than 1, while the SR05 sample was greater than 1. It is important that the samples SR01, SR02, and SR03 showed HI less than 0.2. The lower value of HI was found in both BR and FR samples, but a noticeable reduction (HI<0.1) was observed in samples FR samples (Fig. 4C).

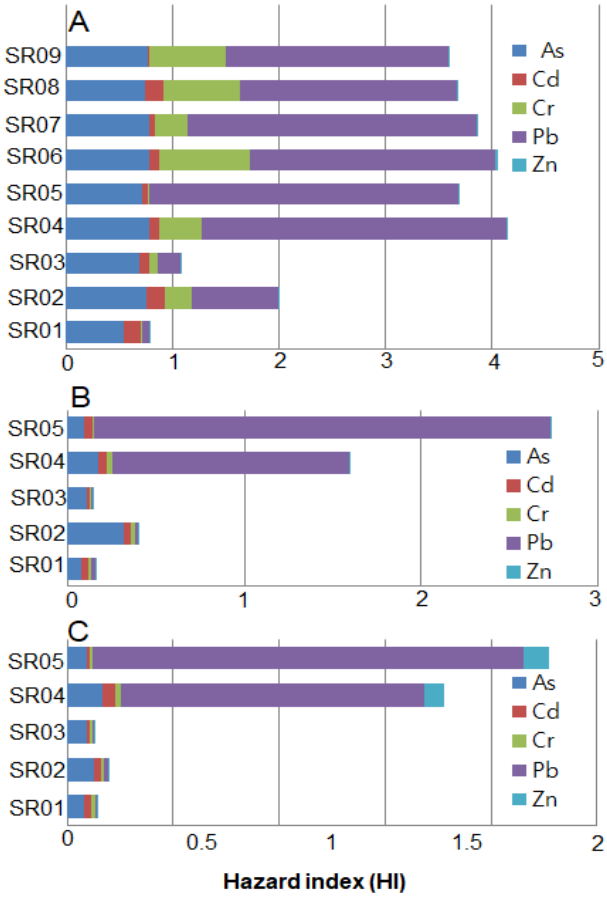

Fig. 4. The hazard index (HI) of Swarna rice samples of Dinajpur, Bangladesh. The numerically presented on each figure's left side indicates the sample number. The HI of the Swarna normal rice (A), boiled rice (B), and fermented rice (FR), respectively.

It could have happened due to the step-wise reduction of HMs during fermentation that caused the reduction of non-carcinogenic risk (HI) reduction in all five FR samples. A comparative heat map was constructed using the THQ results of rice samples. Heat map analysis revealed that the highest THQ was obtained from As, followed by Pb Cr, Cd, and Zn in NR samples (Fig. 5). The least THQ was observed for the Zn in almost all NR samples.

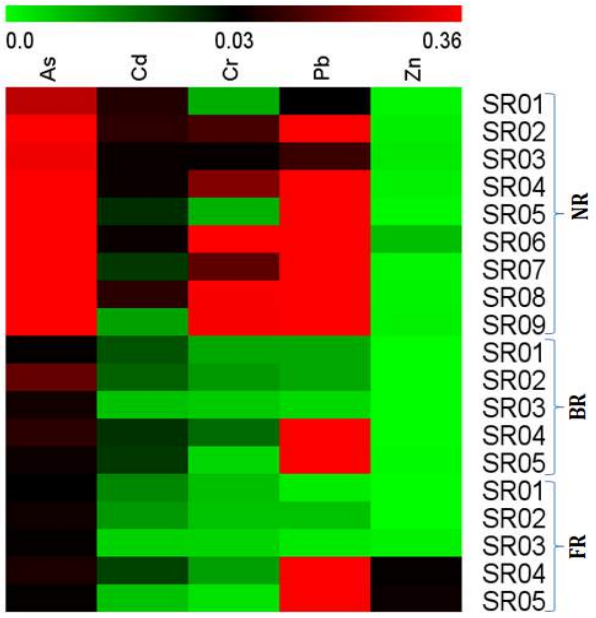

Fig. 5. Target hazard quotient (THQ) of heavy metal in rice, presented by hierarchical clustering analysis. The color ranges from green to red, indicating for the lowest to the highest heavy metal toxicity. Each row of colored boxes is representative of a single sample, and each metal is represented using a single column (indicated).

However, a considerable reduction in THQ level was observed for all HMs in BR samples, followed by FR. Although the Pb concentration was reduced in BR and FR, the highest THQ value was observed in heat map analysis due to the higher concentration of Pb compared to the other HMs. This result suggests that people of the Biral and Sadar area should return to their traditional rice-cooking system, which may provide better options for reducing HMs from rice. Suppose it is possible to consume boiling rice followed by partial fermentation from three meals per day. In that case, the carcinogenic hazard along with the risk associated with diabetes, pancreatitis, kidney disease, and hypertension might be avoided.

Incremental lifetime cancer risk (ILCR) and cumulative carcinogenic risk (CCR)

The ILCR and CCR for the NR, BR, and FR were presented in Table 4. The As, Cd, Cr, and Pb levels were higher than the safe limit (10-4 to 10-6) of ILCR and CCR for the NR sample recommended by USEPA (2002). In contrast, no carcinogenic risk was observed for Zn because the cancer slope factor (CSF) of Zn was constant at zero. Consequently, we calculated ILCR for BR and FR, where the ILCR values of HMs were declined in samples SR01 to SR05 compared to the NR. However, less ILCR has been observed in most BR and FR samples. The CCR of SR01, SR02, SR03, SR04, and SR05 was declined by 4.1-, 4.13-, 6.54-, 5.6-, 2.88-folds in BR, and 5.34, 10.54-, 9.10-, 7.22-, 4.55-folds in FR, respectively. ILCR reduction was due to the special cooking followed by fermentation of rice. Unfortunately, the over-consumption (367 gm/day) of rice was almost 3.33-fold higher than the Iranian people (Naseri et al., 2015), causing the greater risk levels of CCR in this study.

Conclusion

We have explored a straightforward and consumer-friendly cooking-based fermentation approach for reducing HMs-associated health risks for rice consumption. This study assessed HMs from rice samples in different conditions (NR, BR, and FR) and health risk-associated indices ILCR, CCR, and THQ. The results suggest that the rice grown in Kaharole contains a minor concentration of As, Cd, Cr, and Pb than the rice of Biral and Sadar Dinajpur, Bangladesh. In the case of all NR samples, the levels of As, Cd, Cr, and Zn were under the safe limit except Pb. However, the As, Cd, Cr, and Pb levels were dramatically reduced for BR and FR samples. The HI of the boiled rice followed by partial fermentation was below the safe limit 1. Our study provided the molecular-microbial evidence on rice fermentation and HMs reduction from rice. It also suggests that rice fermentation would be a practical approach for purging HMs from rice. This study hypothesized that HMs associated with hazardous risk could be reduced by:

1. Increasing the traditional rinsed rice cooking process instead of auto-rice cooking.
2. By reducing rice consumption per meal.
3. By motivating people to eat partially fermented rice e.g. Panta-Bhat.

Table 4. Incremental liftime cancer risk (ILCR) and cumulative carcinogenic risk CCR) for normal, boiled, and fermented rice.

Normal rice

Metals	SRO1	SRO2	SRO3	SRO4	SRO5	SRO6	SRO7	SRO8	SRO9
As	0.123	0.17	0.15	0.176	0.162	0.17	0.176	0.17	0.17
Cd	0.029	0.034	0.017	0.0178	0.0094	0.01778	0.00889	0.033	0.042
Cr	0.014	0.18	0.06	0.23	0.014	0.64	0.23	0.54	0.53
Pb	0.000462	0.01388	0.00363	0.0485	0.0493	0.0393	0.0462	0.0347	0.0356
Zn	0.0	0.0	0.0	0.0	0.0	0.0	0.0	0.0	0.0
CCR	0.1659540	0.400776	0.23683	0.54188	0.23453	0.87055	0.462554	0.772045	0.77950

Boiled rice

Metals	SRO1	SRO2	SRO3	SRO4	SRO5
As	0.0171	0.072	0.025	0.039	0.022
Cd	0.0077	0.0069	0.0026	0.009	0.0089
Cr	0.0152	0.0177	0.0088	0.026	0.0069
Pb	0.00034	0.00034	0.000145	0.0227	0.0438
Zn	0.0	0.0	0.0	0.0	0.0
CCR	0.040305	0.09713	0.03624	0.09664	0.08142
Fermented rice					
As	0.0144	0.0228	0.0171	0.0304	0.016
Cd	0.0053	0.0046	0.0019	0.0084	0.0026
Cr	0.0114	0.01044	0.0073	0.0167	0.0050
Pb	0.000069	0.00024	0.000080	0.0195	0.028
Zn	0.0	0.0	0.0	0.0	0.0
CCR	0.031	0.038	0.026	0.075	0.0515

The level from 10^{-4} to 10^{-6} is acceptable/permissible limits, higher than this value of ILCR, and CCR is carcinogenic.

Acknowledgment

The authors thank the Institute of Research and Training (IRT), Hajee Mohammad Danesh Science and Technology University (HSTU), Dinajpur, Bangladesh, for financial support.

Conflicts of Interest

The authors declare that they have no conflicts of interest regarding the publication of this article.

Author's contribution

Haque MA: Conceptualization, fund acquisition, writing and editing, Rahman MA: Writing and editing, analysis; Ferdousi J: experiments, writing; Halilu A: Metals Experiments and analysis; Rahman B; Microbial experiments.

References

Abdullah-Al-Mamun M, Hossain MS, Debnath GC, Sultana S, Rahman A, Hasan Z, Das SR, Ashik MA, Prodhan MY, Aktar S, Cho KM and Haque MA. Unveiling lignocellulolytic trait of a goat omasum inhabitant *Klebsiella variicola* strain HSTU-AAM51 in light of biochemical and genome analyses. *Braz. J. Microbiol.* 2022; 53(1): 99-130.

Bamuwamye M, Ogwok P and Tumuhairwe V. Cancer and non-cancer risks associated with heavy metal exposures from street foods : evaluation of roasted meats in an urban setting. *Journal of Environment Pollution and Human Health.* 2015; 3(2): 24-30.

BBS. Stattistical Year Book of Bangladesh-2011. Bangladesh Bureau of Statistics. Statistics and Informatics Division. Ministry of Planning. 2011

Carey M, Jiujin X, Farias JG and Meharg AA. Rethinking rice preparation for highly efficient removal of inorganic arsenic using percolating cooking water. *PLoS One*. 2015; 10(7): e0131608.

Das SR, Haque MA, Akbor MA, Abdullah-Al-Mamun M, Debnath GC, Hossain MS, Hasan Z, Rahman A, Islam MA, Hossain MA, Yesmin S, Nahar MNN and Cho KM. Organophosphorus insecticides mineralizing endophytic and rhizospheric soil bacterial consortium infuence eggplant growth-promotion. *Arch. Microbiol*. 2022; 204: 199.

FAO/WHO: Joint FAO/WHO food standards programme, codex committee on contaminations in food (FAO/WHO), 2011, fifth session, Netherlands.

Fu L, Liao L, Liu Y and Wu W. Optimization of fermentation process of removal of cadmium in rice powder using lactic acid bacteria. *Nongye Gongcheng Xuebao/Transaction of the Chinese Society of Agricultural Engineering*. 2015; 31: 319-326.

Halttunen T, Salminen S and Tahvonen R. Rapid removal of lead and cadmium from water by specific lactic acid bacteria. *Int. J. Food. Microbiol*. 2007; 114(1) 30-35.

Haque A, Hwan J and Man K. Endophytic bacterial diversity in Korean kimchi made of Chinese cabbage leaves and their antimicrobial activity against pathogens. *Food Control.* 2015a; 56: 24-33

Haque A, Man K, Nath D, Keun M and Dae H. A potential cellulose microfibril swelling enzyme isolated from *Bacillus* sp. AY8 enhances cellulose hydrolysis. *Process Biochem.* 2015b; 50: 807-8015.

Haque MA, Ashik MA, Aktar S, Akter MS, Halilu A, Haque MA, Islam MR, Abdullah-Al-Mamun M, Nahar MNN, Das SR, Das KC, Ahmed I, Manir MS, Islam MK and Shahadat MRB. Rapid deconstruction of cotton, coir, areca, and banana fibers recalcitrant structure using a bacterial consortium with enhanced saccharifcation. *Waste Biomass Valori.* 2021; 12(7): 4001-4018.

Heikens A. Arsenic contamination of irrigation water, soil and crops in Bangladesh: Risk implications for sustainable agriculture and food safety in Asia. FAO. 2006.

Hertzberg, R. Supplementary guidance for conducting health risk assessment of chemical mixtures. ESPEA. 2000.

Hossain M, Jaim WMH, Alam MS and Rahman AM. Rice biodiversity in Bangladesh: Adoption, diffusion and disappearance of varieties. A statistical report from farm survey in 2005. BRAC Research and Evaluation Division, Dhaka, Bangladesh. 2013.

ISIRI (Institute of Standards and Industrial Research of Iran: ISIRI 12968. Food and feed-maximum limit of heavy metals (1st edi.), Tehran, Iran, ISIRI Pres, 2010, p.210.

IDF (International Diabetes Federation: IDF Diabetes Atlas, 8th edition, 2017.

Jafari A, Kamarehie B, Ghaderpoori M, Khoshnamvand N, and Birjandi M. The concentration data of heavy metals in Iranian grown and imported rice and human health hazard assessment. *Data Br.* 2018;16: 453-459.

Jane J and Shen JJ. Internal structure of the potato starch granule revealed by chemical gelatinization. *Carbohydr. Res.* 1993; 247: 279-290.

Jorhem L. Determination of metals in foods by atomic absorption Spectrometry after dry ashing : NMKL collaborative study. *J. AOAC Int.* 2000; 83(5)

Kashian S and Fathivand AA. Estimated daily intake of Fe, Cu, Ca and Zn through common cereals in Tehran, Iran. *Food Chem.* 2015; 176: 193-196.

Kinoshita H, Sohma Y, Ohtake F, Ishida M, Kawai Y, Kitazawa H, Saito T and Kimura K. Biosoption of heavy metals by Lactic acid bacteria and identification of mercury binding protein. *Res. Microbiol.* 2013; 164: 701-709.

Morekian R, Mirlohi M, Azadbakht L and Maracy MR. Heavy metal distribution frequency in Iranian and imported rice varieties marketed in central Iran, Yazd, 2012. *Int. J. Env. Health. Eng.* 2013; 2: 1-5.

Naseri M, Vazirzadeh A, Kazemi R and Zaheri F. Concentration of some heavy metals in rice types available in Shiraz market and human health risk assesment. *Food Chem.* 2015; 175: 243-248.

OEHHA, 2009. Air toxics hot spots program technical support document for cancer potencies. Appendix B. Chemical-specific Summaries of the Information Used to Derive Unit Risk and Cancer Potency Values. Updated 2011.

Parengam M, Judprasong K, Srianujata S and Jittinandana S. Study of nutrients and toxic minerals in rice and legumes by instrumental neutron activation analysis and graphite furnace atomic absorption spectrophotometry. *J. Food Compos. Anal.* 2010; 23: 340-345.

Proshad R, Kormoker T, Islam MS, and Chandra K (2019). Potential health risk of heavy metals via consumption of rice and vegetables grown in the industrial areas of Bangladesh, *Hum. Ecol. Risk Assess.* 2019; 26, 921-943.

Raab A, Baskaran C and Meharg AA. Cooking rice in a high water to rice ratio reduces inorganic arsenic content. *J. Environ. Monit.* 2009; 11: 41-44.

Rahman MS, Abdul M and Miah M. Arsenic concentrations in groundwater , soils, and irrigated rice in Southwestern Bangladesh. *Commun. Soil Sci. Plant Anal.* 2010; 41(16): 37-41.

Roya AQ and Ali MS. Heavy metals in rice samples on the Torbat- Heidarieh market, Iran. *Food Addit. Contam. Part B Surveill*. 2017; 10: 59-63.

Sengupta MK, Hossain MA, Mukherjee A, Ahamed S, Das B, Nayak B, Pal A and Chakrabarti D. Arsenic burden of cooked rice: Traditional and modern methods. *Food Chem. Toxicol.* 2006; 44(11): 1823-1829.

Sharafia K, Yunesiana M, Nodehia RN, Mahvia AH, Pirsaheb M and Nazmara S. The reduction of toxic metals of various rice types by different preparation and cooking processes-Human health risk assessment in Tehran households, Iran. *Food Chem.* 2019; 15(280): 294-302.

Shraim, A. M. Rice is a potential dietary source of not only arsenic but also other toxic elements like lead and chromium. *Arab. J. Chem.* 2014; 10(2), S3434-S344

Sultana MS, Rana S, Yamazaki S, Aono T and Yoshida S. Health risk assessment for carcinogenic and non-carcinogenic heavy metal exposures from vegetables and fruits of Bangladesh. *Cogent Environ. Sci.* 2017; 166: 1-17.

Tchounwou PB, Ayensu WK, Ninashvili N and Sutton D. Environmental exposure to mercury and its toxicopathologic implications for public health. *Environ Toxicol.* 2003; 149-175.

Torres-escribano S, Leal M, Vélez D, Agroquímica Ide and Csic DA. Total and inorganic arsenic concentrations in rice sold in Spain, effect of cooking, and risk assessments. *Environ. Sci. Technol.* 2008, 3867-3872.

Yang L, Sun YH, Liu Y, Mao Q, You LX, Hou JM and Ashraf MA. Effects of leached amylose and amylopectin in rice cooking liquidon texture and structure of cooked rice. *Braz. Arch. Biol. Technol.* 2016; 59: e16160504.

Zheng T, Liu S, Bai Y, Cheng N, Buka S, Yang A, Shi K, Zhang X, Li Y, Xu S, Zhang B and Wise J. Current understanding of the relationship between metal exposures and risk of type 2 diabetes. *Curre. Res. Diabetes & Obes. J.* 2018; 7: 169-171.

Zhuang P, Zhang C, Li Y, Zou B, Mo H, Wu K, Wu J and Li Z. Assessment of influences of cooking on cadmium and arsenic bioaccessibility in rice, using an in vitro physiologically-based extraction test. *Food Chem.* 2016; 15(213): 206-214.

Zhu YG, Williams PN and Meharg AA. Exposure to inorganic arsenic from rice: a global health issue? *Environ. Pollut.* 2008; 154(2): 169-171

J. Bangladesh Acad. Sci. 46(1); 101-115: June 2022 DOI: 10.3329/jbas.v46i1.59791

Journal of Bangladesh Academy of Sciences

Journal homepage: http://www.bas.org.bd/publications/jbas.html

Research Article

Goal programming approach for multi-objective optimization to the transportation problem in uncertain environment using fuzzy non-linear membership functions

Md. Musa Miah*, Abdur Rashid[1], Aminur Rahman Khan[1] and Md. Sharif Uddin[1]

Department of Mathematics, Mawlana Bhashani Science and Technology University, Santosh, Tangail, Bangladesh

ARTICLE INFO

Article History

Received: 22 May 2022
Revised: 14 June 2022
Accepted: 15 June 2022

Keywords: Transportation problem, Uncertain parameters, Non-linear membership functions, Compromise solution.

ABSTRACT

The ultimate goal of the decision maker (DM) is to take right decisions to optimize the profit or loss of the organization when the parameters of the transportation problem are ambiguous because of some uncontrollable effects. In this paper, mathematical models are proposed using fuzzy non-linear membership functions and the inverse uncertain normal distribution has been used to eliminate the uncertainty in the parameters which will help the DM to find a compromise solution of the uncertain multi-objective transportation problem (UMOTP) and to achieve the desired goals for a chosen level of confidence for the uncertain parameters. The compromise solutions of the uncertain multi-objective transportation problem are presented to obtain the DM satisfaction if the problem becomes achievable for this preferred confidence level of the parameters. Numerical illustration is given where Linear Programming Problems (LPPs) are resolved with LINGO and the graphs are designed with the help of MATLAB 18.00.

Introduction

When the aspiration level to each of the objectives in a Multiobjective Transportation Problem (MOTP) is identified, the fuzzy objectives turned as fuzzy goal programming. These fuzzy goals are then can be characterized by the fuzzy membership functions. In the present paper, goals of the DM for the specific objectives are considered as the goal to achieve. MOTP is a very distinctive variety of linear programming problem (LPP) where the restraints are equality or inequality form and the purposes are varying from each other. The primal simplex method in transportation problem was used by (Dantzing, 1963). All the proposed methods to solve MOTP breed a set of compromise solution. The Goal programming technique with the priority along with various situations such as environmental constraints, organizational goal and bureaucratic decision structures and many more has a vast use to solve different problems involving multiple objectives. (Zadeh, 1965), (Bellman and Zadeh, 1970) gave a brief description about a new technique for decision making in a fuzzy situation. (Lee and Moore, 1973) optimize the TP with numerous objectives applying the goal programming concept. (Zimmermann, 1978) applied the fuzzy programming and linear programming concept with numerous objective functions with some fuzzy membership function to solve MOTP. The converted ordinary values of the uncertain parameters were calculated using uncertain normal distribution proposed by (Liu, 2008), (Liu, 2010), (Liu, 2009(b)). (Wahed and Lee 2006), together with the concept of fuzzy membership function, formulate a LPP that develop the uncertain measure theorem. (Hasan 2017) uses fuzzy TOPSIS for a perfect choice that can reduces the cost and sufferings of the DM. (Hasan 2015) developed an algorithm to ensure the quickest flow of material at the lowest cost.

*Corresponding author: <mmusa@mbstu.ac.bd>

[1]Department of Mathematics, Jahangirnagar University, Savar, Dhaka, Bangladesh

Table 1. Related Research and their Contributions

References	Objective Functions			Uncertain Supply	Uncertain Demand	Using Fuzzy Logic	Goal Programming
	Uncertain TP Cost	Uncertai n Profit	Uncertain Damage cost				
Anukokila et al (2017)	–	–	–	–	–	√	√
Bit et al. (1993)	√	√	–	–	–	√	–
Bit et al. (1992)	–	–	–	–	–	–	√
Cadenas and Verdegay (2000)	–	–	–	–	–	√	–
Liu (2008)	√	–	√	–	–	–	–
Das et al. (1999)	√	√	√	–	–	–	–
Wahed (2001)	–	–	–	–	–	√	√
Maity and Roy (2015)	–	–	–	√	√	–	–
Roy and Midya (1988)	√	–	–	–	–	√	–
Surapati and Roy (2008)	–	–	–	–	–	√	√
Shenh and Yao (2012)	√	–	√	–	–	–	–
Zangiabadi and Maleki (2007)	–	–	–	–	–	–	√
Jagtap and Kawale (2017)	–	–	–	–	–	–	√
Wahed and Lee (2006)	–	–	–	–	–	√	√
Wahed and Abo-Sinna (2001)	–	–	–	–	–	√	√
Gupta and Kumar (2012)	–	–	–	–	–	√	–
Delgado et al. (1989)	–	–	–	–	–	√	–
Kaur and Kumar (2011)	–	–	–	–	–	–	√
This study	√	√	√	√	√	√	√

From the literature review and the interpretations provided in Table 1, it can be seen that some gap attained in model development for MOTP in uncertain environment using fuzzy goal programming. In the present research, we have work hard to remove this gap by extending the work of (Wahed and Lee, 2006) combining the uncertainty not only in the objective functions but also in all parameters which will be very helpful for the DM regarding decision making in very uncertain situation. The notable executions of the designed study are shortened as follows:

- Fuzzy goal programming is implemented to an uncertain parameter problem.
- Uncertain MOTP is changed applying the uncertain normal distribution concept.
- DM's confidence levels are in consideration
- Non-linear membership functions of fuzzy programming approach are used to model the algorithm.

Nomenclature

Notations	Descriptions
x_{ij}	Transporting amount from i^{th} origin to j^{th} destination
C_{ij}	Cost parameter in unit price for i^{th} origin to j^{th} destination
a_i	Supply parameters
b_j	Demand parameters
$\hbar$	Uncertain variable
$\Re$	Uncertain distribution
ϕ	Normal uncertain distribution
Ω	Uncertain measure function
e	Expected value of the parameter
σ	Standard deviation
ω	Confidence level
η	Satisfaction level of the DM
d_i^+	Positive deviation or over achievement from i^{th} goal
d_i^-	Negative deviation or under achievement from i^{th} goal
$\mu_k(Z^k)$	Linear membership function for the k^{th} objective
β_{ij}	Uncertain distribution for cost
θ_i	Uncertain distribution for demand
ψ_j	Uncertain distribution for supply
G^k	Desired goal of k[th] objective
Z^k	Objective of the k[th] goal
L_k	Lower bound of the k[th] objective
U_k	Upper bound of the k[th] objective

Materials and Methods

If C_{ij} is the per unit transportation cost from i^{th} origin to j^{th} destination and x_{ij} is the unknown quantity to be shifted from the i^{th} origin to j^{th} destination then the original transportation model is written as:

$$\left.\begin{aligned} &\text{Minimize} \ : Z(x) = \sum_{i=1}^{m}\sum_{j=1}^{n} C_{ij}x_{ij}. \\ &\text{Subject to :} \\ &\sum_{j=1}^{n} x_{ij} \le a_i, \quad i = 1, 2, 3, \ldots\ldots\ldots\ldots, m \\ &\sum_{i=1}^{m} x_{ij} \ge b_j, \quad j = 1, 2, 3, \ldots\ldots\ldots\ldots, n \\ &\forall\ x_{ij} \ge 0, \quad i = 1,2,\ldots m; \quad j = 1,2,\ldots, n \end{aligned}\right\} \ldots(1)$$

And the feasibility condition is $\sum_{i=1}^{m} a_i \ge \sum_{j=i}^{n} b_j$.

Where $a_1, a_2, \ldots, a_m$ are the m sources (origins) and $b_1, b_2, \ldots, b_n$ are the n destinations (demands) Taking the multiple objective idea, the original model can be written as follows:

$$\left.\begin{aligned} &\text{Minimize} \ : Z(x) = \sum_{i=1}^{m}\sum_{j=1}^{n} C_{ij}^{k}x_{ij}. \\ &\text{Subject to :} \\ &\sum_{j=1}^{n} x_{ij} \le a_i, \quad i = 1, 2, 3, \ldots\ldots\ldots\ldots, m \\ &\sum_{i=1}^{m} x_{ij} \ge b_j, \quad j = 1, 2, 3, \ldots\ldots\ldots\ldots, n \\ &\forall\ x_{ij} \ge 0, \quad i = 1,2,\ldots, m; \quad j = 1,2,\ldots, n \end{aligned}\right\} \ldots(2)$$

feasibility condition $\sum_{i=1}^{m} a_i \ge \sum_{j=i}^{n} b_j$, where C_{ij}^k is the unit cost for transporting from i^{th} origin to j^{th} destination , $a_i\ (i = 1,2,\ldots\ldots, m)$ is the supply and $b_j (j = 1,2,\ldots\ldots, n)$ is the demand parameter for the $k^{th}\ (k = 1,2,\ldots\ldots, K)$ objective function of the MOTP.

Introducing inverse measure theorem, equation (2) can be written as follows:

$$\left.\begin{aligned}&\text{Max/Min}: Z^k(x)=\sum_{i=1}^{m}\sum_{j=1}^{n}\left[\Omega\left(C_{ij}^k\right)\geq\alpha_{ij}\right]x_{ij}.\\&\text{Subject to}:\\&\Omega\left(\sum_{j=1}^{n}x_{ij}\leq a_i\right)\geq\gamma_i \quad i=1,2,3,.....,m\\&\Omega\left(\sum_{i=1}^{m}x_{ij}\geq b_j\right)\geq\delta_j, \quad j=1,2,3,.....,n\\&\forall\ x_{ij}\geq 0, \quad i=1,2,.....m; \quad j=1,2.....,n\end{aligned}\right\}..(3)$$

The inverse normal uncertainty distribution of Normal uncertain variable $N(e,\sigma)$ is defined as $\Re^{-1}(x)=e+\frac{\sqrt{3}\sigma}{\pi}\ln\left(\frac{\omega}{1-\omega}\right)$,where' $\ln$ 'denotes natural logarithm and ω is the confidence level of the DM. Considering the uncertainty distributions β_{ij}, θ_i and ψ_j for cost C_{ij} $(i=1,2,.....,m;\ j=1,2,.....,n)$, demand $a_i(i=1,2,.....,m)$ and supply parameters $b_j(j=1,2,.....,n)$ respectively, the inverse measure shows the following results:

$\Omega\left(C_{ij}^k\right)\geq\alpha_{ij}\approx C_{ij}^k\geq\beta_{ij}^{-1}(1-\alpha_{ij})$;

$\Omega\left(\sum_{j=1}^{n}x_{ij}\leq a_i\right)\geq\gamma_i\Rightarrow\sum_{j=1}^{n}x_{ij}\leq\Re_i^{-1}(1-\gamma_i)$ and

$\Omega\left(\sum_{i=1}^{m}x_{ij}\geq b_j\right)\geq\delta_j$ is reduced to $\sum_{i=1}^{m}x_{ij}\leq\psi_j^{-1}\delta_j$.

Then equation (3) is reduced as follows:

$$\left.\begin{aligned}&\text{Max/Min}: Z^k(x)=\sum_{i=1}^{m}\sum_{j=1}^{n}\left[\beta_{ij}^{-1}(1-\alpha_{ij})\right]x_{ij}.\\&\text{Subject to}:\\&\sum_{j=1}^{n}x_{ij}\leq\theta_i^{-1}(1-\gamma_i), \quad i=1,2,3,.....,m\\&\sum_{i=1}^{m}x_{ij}\leq\psi_j^{-1}\delta_j, \quad j=1,2,3,.....,n\\&\forall\ x_{ij}\geq 0, \quad i=1,2,...m; \quad j=1,2,.....,n\end{aligned}\right\}...(4)$$

Model for Non-linear Membership Function

Step 1: Obtain the crisp values of the parameters using normal uncertain distribution.

Step 2: Construct the given MOTP for uncertain parameters to an ordinary TP using the crisp number obtained from step 1.

Step 3: Single objective TP are solved ignoring all others objectives.

Step 4: Define non-linear membership function $\mu(Z^k)$ for the k^{th} objective function.

Step 5: Change the fuzzy model obtained in **Step** 4, as follows:

$$\left.\begin{aligned}&\text{Maximize} \quad \xi\\&\text{Subject to}\\&\xi\leq\mu\left(Z^k\right)\\&\sum_{j=1}^{n}X_{ij}\leq a_i, i=1,2,3,.....m\\&\sum_{i=1}^{m}X_{ij}\geq b_j, j=1,2,3,.....,n\\&\xi\geq 0, \quad X_{ij}\geq 0, i=1,2,...,m;\\&j=1,2,..,n\end{aligned}\right\}...(5)$$

Step 6: Advance Step 5 as a goal programming problem as follows:

$$\left.\begin{aligned}&\text{Maximize} \quad \xi\\&\text{Subject to}\\&\xi\leq\mu\left(Z^k\right)\\&\sum_{j=1}^{n}X_{ij}\leq a_i, \quad i=1,2,3,...,m\\&\sum_{i=1}^{m}X_{ij}\geq b_j, \quad j=1,2,3,...,n\\&\mathrm{Z^k(x)-d_k^+ + d_k^- = G^k},\\&\mathrm{k=1,2,3,.....,K}\\&\xi\geq 0, \quad X_{ij}\geq 0,\\&i=1,2,.....m; j=1,2,.....,n\end{aligned}\right\}....(6)$$

Step 7: Solve the model in **Step** 6.

Step 8: Reveal the feasible solution to the DM. If DM satisfies, go to **Step** 9; otherwise, go through **Step** 1 to **Step** 7.

Step 9: Stop.

For the computational algorithm, a flow chart is presented in Fig.1.

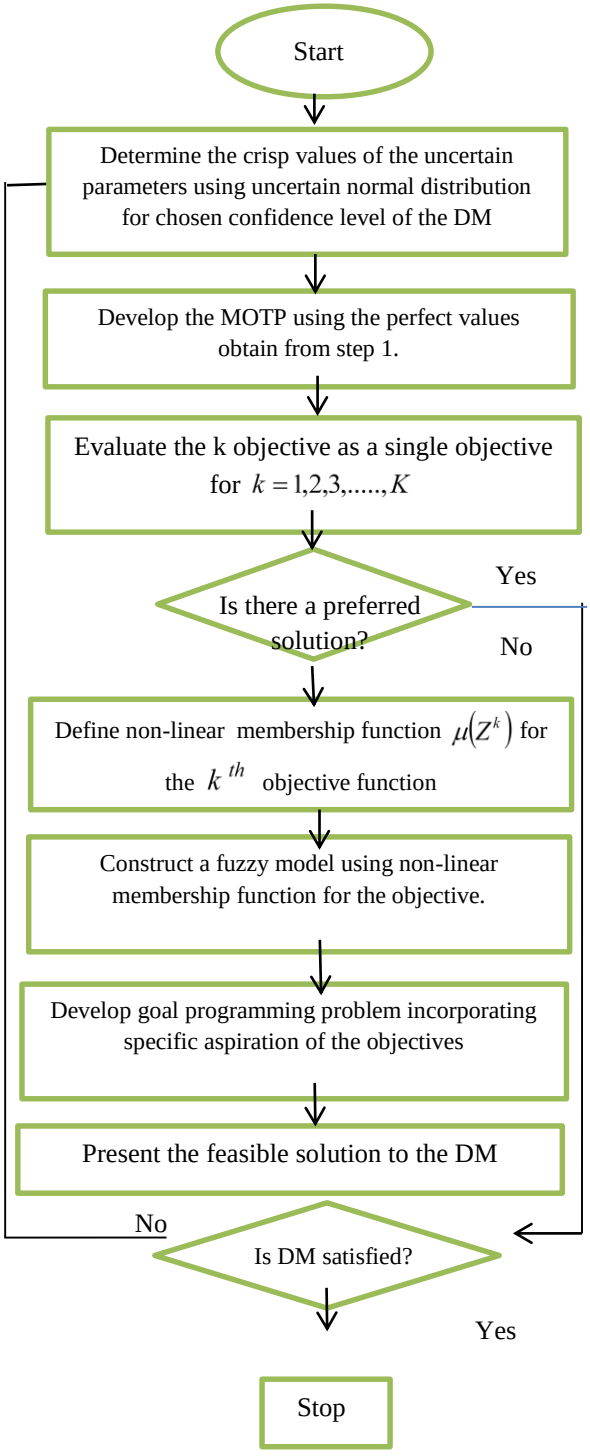

Fig. 1. Flow chart of the proposed model for goal programming using non-linear membership functions

Results and Discussions

To testify the feasibility of the proposed model, consider a MOTP with the uncertainty in transportation cost, profit, damage cost due to delay or early supply. Demand and supply in the market are also considered as uncertain. The DM wants to deliver the goods from three sources S_1, S_2, S_3 to four destination points D_1, D_2, D_3, D_4 and optimize the objectives as:

(i) The transportation cost must be from \$3000 to \$3500 (Z^1)

(ii) Profit will be not more \$1200 (Z^2) and not less than \$900

(iii) Damage cost have to be in between \$700 to \$1000 (Z^3)

The data tables of this example are taken from Uddin et al., 2021) and (Maity et al., 2016):

Table 2. Data for uncertain transportation cost C_{ij}^1

	D_1	D_2	D_3	D_4
S_1	$(20,2)$	$(18,2)$	$(22,3)$	$(24,3)$
S_2	$(10,1)$	$(12,2)$	$(15,3)$	$(13,1)$
S_3	$(22,3)$	$(20,3)$	$(24,2)$	$(23,2)$

Table 3. Data for uncertain profit C_{ij}^2

	D_1	D_2	D_3	D_4
S_1	$(5,1)$	$(6,1.5)$	$(4,1)$	$(3,0.5)$
S_2	$(6,1)$	$(5,1.5)$	$(5,0.5)$	$(4,1)$
S_3	$(9,1)$	$(8,1.5)$	$(8,2)$	$(10,2)$

Table 4. Data for uncertain damage cost C_{ij}^3

	D_1	D_2	D_3	D_4
S_1	$(4,1)$	$(4,1)$	$(3,1)$	$(5,2)$
S_2	$(3,1)$	$(6,1)$	$(4,1)$	$(4,1)$
S_3	$(4,1.5)$	$(3,1)$	$(4,1)$	$(5,1.5)$

Table 5. Data for uncertain demand

b_1	b_2	b_3	b_4
$(40,3)$	$(36,4)$	$(35,5)$	$(40,3)$

Table 6. Data for uncertain supply

a_1	a_2	a_3
$(55,4)$	$(60,5)$	$(70,4)$

Mathematical Illustration using Exponential Membership Function (EMF)

Using the inverse uncertain distribution with confidence level $\omega = 0.78$ Tables 2, 3, 4, 5 and 6 reduced to Tables 7, 8, 9, 10 and 11 respectively.

Table 7. Crisp value for transportation cost C_{ij}^1 for confidence level $\omega = 0.78$

	D_1	D_2	D_3	D_4
S_2	10.70	13.40	17.10	13.70
S_3	24.10	22.10	25.40	24.40

Table 8. Crisp value for profit C_{ij}^2 for confidence level

	D_1	D_2	D_3	D_4
S_1	5.70	7.05	4.70	3.35
S_2	6.70	6.05	5.35	4.70
S_3	9.70	9.05	9.40	11.40

Table 9. Crisp value for damage cost C_{ij}^3 for confidence level $\omega = 0.78$

	D_1	D_2	D_3	D_4
S_1	4.70	4.70	3.87	6.40
S_2	3.70	6.70	4.70	4.70
S_3	5.05	3.70	4.70	6.05

Table 10. Crisp value for demand for confidence level $\omega = 0.78$

b_1	b_2	b_3	b_4
42.1	38.8	38.5	42.1

Table 11. Crisp value for supply for confidence level $\omega = 0.78$

a_1	a_2	a_3
52.2	56.5	67.2

In this present problem, the goal of the DM is the transportation cost must be from \$3000 to \$3500, profit will be no more \$1200 and no less than \$900 and the damage cost have to be in between \$700 to \$1000 (Z^3).

Therefore, the membership functions are:

$$\mu_1\left(Z^1(x)\right) = \frac{3500 - Z^1(x)}{3500 - 3000},$$

$$\mu_2\left(Z^2(x)\right) = \frac{1200 - Z^2(x)}{1200 - 900}, \text{ and}$$

$$\mu_3\left(Z^3(x)\right) = \frac{1000 - Z^3(x)}{1000 - 700}.$$

Let η be the satisfaction level of the DM, Then from model (6), we have the following LPPs: Max Subject to:

$$Z^1 = 21.4x_{11} + 19.4x_{12} + 24.1x_{13} + 26.1x_{14} + 10.7x_{21} + 13.4x_{22} + 17.1x_{23} + 13.7x_{24} + 24.1x_{31} + 22.1x_{32} + 25.4x_{33} + 24.4x_{34}$$

$$Z^2 = 5.7x_{11} + 7.05x_{12} + 4.7x_{13} + 3.35x_{14} + 6.7x_{21} + 6.05x_{22} + 5.35x_{23} + 4.7x_{24} + 9.7x_{31} + 9.05x_{32} + 9.4x_{33} + 11.4x_{34}$$

$$Z^3 = 4.7x_{11} + 4.7x_{12} + 3.7x_{13} + 6.4x_{14} + 3.7x_{21} + 6.7x_{22} + 4.7x_{23} + 4.7x_{24} + 5.05x_{31} + 3.7x_{32} + 4.7x_{33} + 6.05x_{34}$$

$$\exp\left(\frac{-Z^1 + 3500}{500}\right) \geq 0.63\xi + 0.37$$

$$\exp\left(\frac{-Z^2 + 1200}{200}\right) \geq 0.63\xi + 0.37$$

$$\exp\left(\frac{-Z^3 + 1000}{200}\right) \geq 0.63\xi + 0.37$$

$$21.4x_{11} + 19.4x_{12} + 24.1x_{13} + 26.1x_{14} + 10.7x_{21} + 13.4x_{22} + 17.1x_{23} + 13.7x_{24} + 24.1x_{31} + 22.1x_{32} + 25.4x_{33} + 24.4x_{34} + d_1^- - d_1^+ = 3000$$

$$5.7x_{11} + 7.05x_{12} + 4.7x_{13} + 3.35x_{14} + 6.7x_{21} + 6.05x_{22} + 5.35x_{23} + 4.7x_{24} + 9.7x_{31} + 9.05x_{32} + 9.4x_{33} + 11.4x_{34} + d_1^- - d_1^+ = 900$$

$$4.7x_{11} + 4.7x_{12} + 3.7x_{13} + 6.4x_{14} + 3.7x_{21} + 6.7x_{22} + 4.7x_{23} + 4.7x_{24} + 5.05x_{31} + 3.7x_{32} + 4.7x_{33} + 6.05x_{34} + d_1^- - d_1^+ = 700$$

$$x_{11} + x_{12} + x_{13} + x_{14} \le 52.2$$
$$x_{21} + x_{22} + x_{23} + x_{24} \le 56.5$$
$$x_{31} + x_{32} + x_{33} + x_{34} \le 67.2$$
$$x_{11} + x_{21} + x_{31} \ge 42.1$$
$$x_{12} + x_{22} + x_{32} \ge 38.8$$
$$x_{13} + x_{23} + x_{33} \ge 38.5$$
$$x_{14} + x_{24} + x_{34} \ge 42.1$$

$x_{ij} \ge 0$ for all intger i,j. Using LINGO software, the optimal compromise solution is obtained as follows:

$x_{11} = 5.93,\quad x_{12} = 38.80,\quad x_{13} = 7.469,\quad x_{14} = 0,$
$x_{21} = 36.170,\quad x_{22} = 0,\quad x_{23} = 0,\quad x_{24} = 20.330,$
$x_{31} = 0.00,\quad x_{32} = 0,\quad x_{33} = 31.03,\quad x_{34} = 30,$
$d_1^- = 470.926,\ d_2^+ = 7.787,\ d_3^- = 255.20,$
$\eta = 0.7021,\ Z^1 = 3030.30,\quad Z^2 = 1207.80,$
$Z^3 = 744.80$

The overall satisfaction of the DM for confidence level $\omega = 0.78$ is $\xi = 0.9394$, which indicates 93.94%. Table 12, represents the values of the satisfaction level of the DM, values of the objectives and deviation from the desired goal corresponding to several confidence levels.

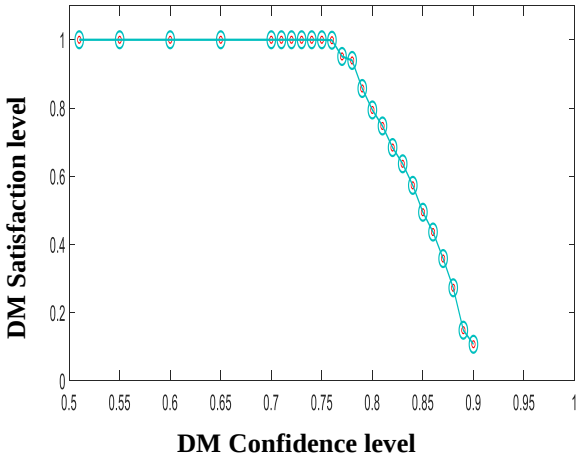

Fig. 2. Satisfaction level versus Confidence level of goal programming using exponential membership function.

From Fig. 2, it observed that, using exponential membership function, the DM's level of satisfaction is at pick level 0.51 to 0.76 because the entire desired DM goal is being met in that region**.** Table 12, for confidence level point from the confidence 0.77, objective for maximizing profit have shown insignificant over achievement from the goal and that is why DM satisfaction level undertakes from that point and incessantly declines until arriving at the poorest satisfaction level 10.76% for the confidence level 0.90. The infeasibility of the problem occurs for the confidence level 0.00 to 0.50 and 0.91 to onwards.

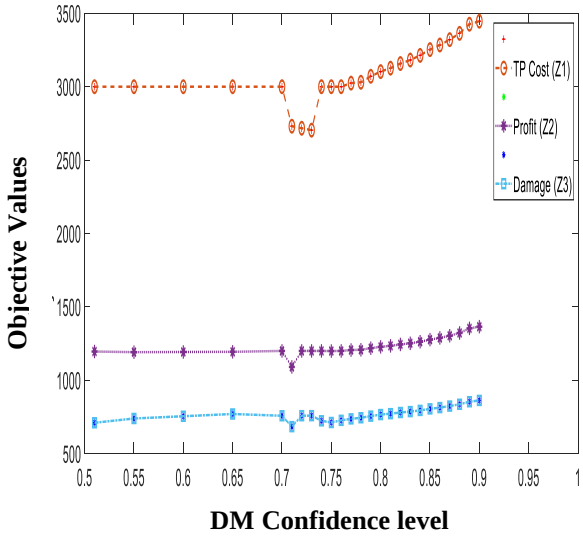

Fig. 3. Objective values versus Confidence level of goal programming using exponential membership function.

Fig. 3 shows that the profit and cost due to damage are rise when the confidence level surges only exception at 0.71 whereas the TP cost deceases from the confidence level 0.70 to 0.75 after unveiling a stability from the confidence level 0.50 to 0.70 and then it gradually increases until the confidence level 0.90. Moreover, from Table 12, we can declare that profit becomes under achievement from the confidence level 0.76 and that is why the DM's satisfaction level decreasing from its height desired level 100%.

Table 12. Computational results using exponential membership function in accordance to different confidence levels

ω (DM Confidence Level)	η (DM Satisfaction Level)	Objective Values			Deviations from Goal (Positive or Negative)						Satisfaction (%)	Feasible Solution (FS)/No-feasible Solution (No-FS)
		Z^1 Not More 3500 (TP Cost)	Z^2 Not More 1200 (Profit)	Z^3 Not more 1000 (Damage Cost)	d_1^+	d_1^-	d_2^+	d_2^-	d_3^+	d_3^-		
0.00-0.50	--	--	--	--	--	--	--	--	--	--	--	No-FS
0.51	1.000	3000.00	1195.91	710.52	--	500.00	--	4.09	--	289.47	100%	FS
0.55	1.000	3000.00	1191.63	739.72	--	500.00	--	8.37	--	260.28	100%	FS
0.60	1.000	3000.00	1192.85	755.08	--	500.00	--	7.15	--	244.92	100%	FS
0.65	1.000	3000.00	1193.94	770.43	--	500.00	--	6.06	--	229.56	100%	FS
0.70	1.000	3000.00	1200.00	758.34	--	500.00	--	0.00	--	241.66	100%	FS
0.71	1.000	2730.9	1091.00	684.21	--	500.00	--	109.0	--	315.8	100%	FS
0.72	1.000	2716.94	1200.00	758.81	--	783.06	--	0.00	--	241.19	100%	FS
0.73	1.000	2704.00	1200.00	759.00	--	796.00	--	0.00	--	241.00	100%	FS
0.74	1.000	3000.00	1200.00	724.00	--	500.00	--	0.00	--	275.98	100%	FS
0.75	1.000	3000.00	1199.33	712.45	--	500.00	--	0.67	--	287.54	100%	FS
0.76	0.9987	3000.00	1200.00	727.27	--	500.00	--	0.00	--	272.72	99.87%	FS
0.77	0.9511	3024.41	1206.24	737.16	--	475.58	6.25	--	--	262.84	95.11%	FS
0.78	0.9394	3030.30	1207.80	744.80	--	470.	7.80	--	--	255.2	93.94%	FS
0.79	0.8572	3071.00	1218.85	756.00	--	429.00	17.1	--	--	244.00	85.72%	FS
0.80	0.7943	3102.83	1227.75	766.58	--	397.17	27.7	--	--	233.41	79.43%	FS
0.81	0.7474	3126.29	1234.66	772.53	--	373.70	34.6	--	--	227.47	74.74%	FS
0.82	0.6841	3157.92	1244.37	780.51	--	342.07	44.3	--	--	219.48	68.41%	FS
0.83	0.6365	3181.73	1252.00	786.60	--	318.26	52.0	--	--	313.39	63.65%	FS
0.84	0.5733	3213.34	1262.61	794.82	--	286.65	62.6	--	--	205.17	57.33%	FS
0.85	0.4945	3252.71	1276.97	805.31	--	248.52	76.6	--	--	194.67	49.45%	FS
0.86	0.4365	3284.17	1288.65	813.91	--	215.82	88.6	--	--	186.08	43.65%	FS
0.87	0.3588	3320.58	1303.48	824.32	--	179.41	103.4	--	--	175.67	35.88%	FS
0.88	0.2731	3363.43	1322.47	836.61	--	136.56	122.4	--	--	163.38	27.31%	FS
0.89	0.1488	3425.58	1353.67	854.00	--	74.42	153.6	--	--	146.00	14.88%	FS
0.90	0.1076	3446.17	1365.19	862.91	--	55.05	165.1	--	--	137.08	10.76%	FS
0.91-1.00	---	---	---	---	--	---	---	---	--	---	---	No-FS

'---'indicates not applicable

Mathematical Illustration for Hyperbolic Membership Function (HMF)

Using the inverse uncertain distribution with confidence level $\omega = 0.75$ Table 2, 3, 4, 5 and 6 changes to Table 13, 14, 15, 16 and 17 respectively as follows:

Table 13. Crisp value for transportation cost C_{ij}^1 for confidence level

	D_1	D_2	D_3	D_4
S_1	21.22	19.22	23.83	25.83
S_2	10.61	13.22	16.83	13.61
S_3	23.83	21.83	25.22	24.22

Table 14. Crisp value for profit C_{ij}^2 for confidence level $\omega = 0.75$

	D_1	D_2	D_3	D_4
S_1	5.61	6.92	4.61	3.31
S_2	6.61	5.92	5.31	4.61
S_3	9.61	8.92	9.92	11.22

Table 15. Crisp value for damage cost C_{ij}^3 for confidence level $\omega = 0.75$

	D_1	D_2	D_3	D_4
S_1	4.61	4.61	3.61	6.22
S_2	3.61	6.61	4.61	4.61
S_3	4.92	3.61	4.61	5.92

Table 16. Crisp value for demand for confidence level $\omega = 0.75$

b_1	b_2	b_3	b_4
41.8	38.4	38.05	41.83

Table 17. Crisp value for supply for confidence level $\omega = 0.75$

a_1	a_2	a_3
52.6	57	67.56

Here we set the goal that the transportation cost must be in between \$3000 and \$3500, profit will be no more \$1200 and no less than \$900 and the damagecost have to be from \$700 to \$1000 (Z^3). Using this goals, the membership functions have the following from:

$$\mu_1(Z^1(x)) = \frac{3500 - Z^1(x)}{3500 - 3000},$$

$$\mu_2(Z^2(x)) = \frac{1200 - Z^2(x)}{1200 - 900} \text{ ,and}$$

$$\mu_3(Z^3(x)) = \frac{1000 - Z^3(x)}{1000 - 700}.$$

Let η be the satisfaction level of the DM, then from equation (6), using hyperbolic membership function, we have the following LPPs: Max ξ Subject to:

$$Z^1 = 21.22x_{11} + 19.22x_{12} + 23.83x_{13} + 25.83x_{14} + 10.61x_{21} + 13.22x_{22} + 16.83x_{23} + 13.61x_{24} + 23.83x_{31} + 21.83x_{32} + 25.22x_{33} + 24.22x_{34}$$

$$Z^2 = 5.616x_{11} + 6.92x_{12} + 4.61x_{13} + 3.31x_{14} + 6.61x_{21} + 5.92x_{22} + 5.31x_{23} + 4.61x_{24} + 9.61x_{31} + 8.92x_{32} + 9.22x_{33} + 11.22x_{34}$$

$$Z^3 = 4.61x_{11} + 4.61x_{12} + 3.61x_{13} + 6.22x_{14} + 3.61x_{21} + 6.61x_{22} + 4.61x_{23} + 4.61x_{24} + 4.92x_{31} + 3.61x_{32} + 4.61x_{33} + 5.92x_{34}$$

$$Z^1\left(\frac{6}{500}\right) + \xi \le \left(\frac{3}{500}\right)(3500 + 3000)$$

$$Z^2\left(\frac{6}{200}\right) + \xi \le \left(\frac{3}{200}\right)(1200 + 1000)$$

$$Z^3\left(\frac{6}{200}\right) + \xi \le \left(\frac{3}{200}\right)(1000 + 800)$$

$$Z^1 + d_1^- - d_1^+ = 3000 \quad Z^2 + d_1^- - d_1^+ = 900$$

$$Z^3 + d_1^- - d_1^+ = 700$$

$$x_{11} + x_{12} + x_{13} + x_{14} \le 52.56$$

$$x_{21} + x_{22} + x_{23} + x_{24} \le 56.95$$

$$x_{31} + x_{32} + x_{33} + x_{34} \le 67.56$$

$$x_{11} + x_{21} + x_{31} \ge 41.83$$

$$x_{12} + x_{22} + x_{32} \ge 38.44$$

$$x_{13} + x_{23} + x_{33} \ge 38.05$$

$$x_{14} + x_{24} + x_{34} \ge 41.83$$

$$x_{ij} \ge 0 \text{ for all intger } i,j.$$

Using LINGO software, the optimal compromise solution can be decorated as follows:

$x_{11} = 26.71,\quad x_{12} = 19.865,\quad x_{13} = 5.985,$
$x_{14} = 0,\ x_{21} = 15.12,\ x_{22} = 0.00,\ x_{23} = 0.00,$
$x_{24} = 41.83,\quad x_{31} = 0.00,\ x_{32} = 18.575,$
$x_{33} = 32.065,\ x_{34} = 0.00,\quad d_1^- = 464.885,$
$d_2^- = 130.992, d_3^- = 301.388,\quad \eta = 0.9297,$
$Z^1 = 3035.115, Z^2 = 1069.008, Z^3 = 698.611$

The overall satisfaction of the DM for confidence level $\omega = 0.75$ is $\xi = 0.9297$, which indicates 92.97%. Table 18, represents the satisfaction level of the DM, the targeted values and the deviation from the intended goal.

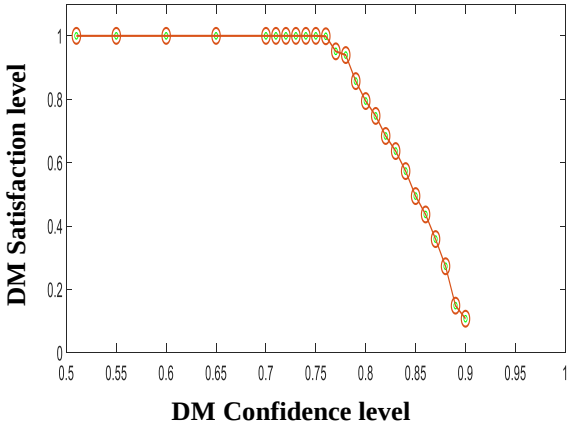

Fig. 4. Satisfaction level versus Confidence level of goal programming using hyperbolic membership function.

Fig. 4 present the satisfaction level of the DM using HMF configuring 100% from the confidence level 0.51 to 0.74 because all the desired goal of the DM is satisfied within this region and then continuously decreases from the confidence level 0.75 until arriving at the worst satisfaction level 64.18% 0.80. The infeasibility of the problem occurs for the confidence level 0.00 to 0.50 and 0.80 to onwards.

Fig. 5 revels that the objective values of Z^2 and Z^3 increase when the confidence level increases only exception at 0.73 where Z^1 have a very tiny deceases

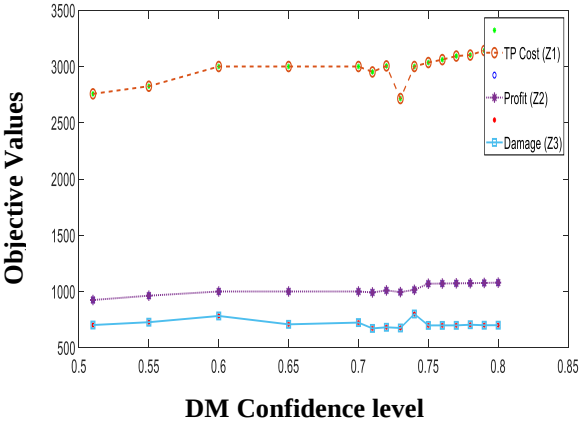

Fig. 5. Objective values versus Confidence level of goal programming using hyperbolic membership function.

and immediate gradually increases until the confidence level 0.80. Moreover, from table 18, it observed that the objective values become under achievement from the confidence level 0.75 and that is why the DM's satisfaction level decreasing from its height desired level 100%.

Comparative Results Obtain from Different Non-linear Membership Functions.

From the previous discussions, it is clear that there are slight differences in the objective values and the satisfaction level of the decision maker for the reporting membership functions corresponding to the DM choices. In the Table 19 below, we will have an explicit overview of the information gather from the previous calculation.

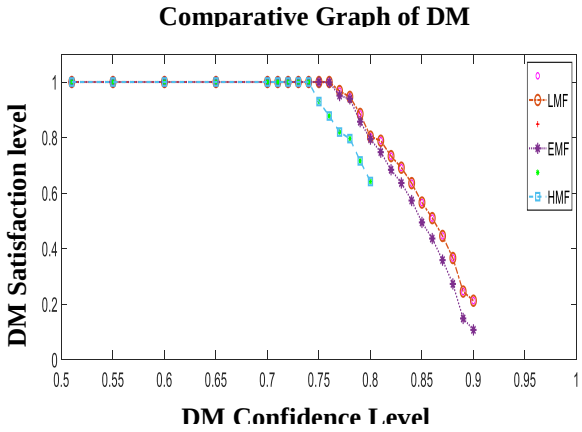

Fig. 6. Comparative graph of DM confidence level versus DM Satisfaction level of goal programming.

Table 18. Computational results using hyperbolic membership function in accordance to different confidence levels.

ω (DM Confidence Level)	ξ (DM Satisfaction Level)	Objective Values			Deviations from Goal (Positive or Negative)						Satisfaction (%)	Feasible Solution (FS)/No feasible Solution (No-FS)
		Z^1 Not More 3500 (TP Cost)	Z^2 Not More 1200 (Profit)	Z^3 NotMore 1000 (Damage Cost)	d_1^+	d_1^-	d_2^+	d_2^-	d_3^+	d_3^-		
0.00-0.50	---	---	---	---	---	---	---	---	--	---	---	No-FS
0.51	1.000	2756.94	924.37	702.00	---	743.05	---	275.62	---	298.10	100%	FS
0.55	1.000	2824.73	962.69	727.00	---	675.26	---	237.30	---	273.00	100%	FS
0.60	1.000	3000.00	1000.00	782.55	---	500.00	---	200.00	---	217.45	100%	FS
0.65	1.000	3000.00	1000.00	708.04	---	500.00	---	200.00	---	291.95	100%	FS
0.70	1.000	3000.00	1000.00	723.57	---	500.00	---	200.00	---	276.42	100%	FS
0.71	1.000	2951.74	991.50	671.80	---	548.25	---	208.50	---	328.20	100%	FS
0.72	1.000	3005.49	1009.61	681.82	---	494.51	---	190.39	---	318.17	100%	FS
0.73	1.000	2715.27	994.64	675.71	---	784.73	---	205.36	---	324.28	100%	FS
0.74	1.000	3000.00	1014.71	800.00	---	500.00	---	185.28	---	200.00	100%	FS
0.75	0.9297	3035.11	1069.00	698.61	---	464.88	---	131.00	---	301.38	92.97%	FS
0.76	0.8776	3061.16	1070.74	698.76	---	438.83	---	129.25	---	301.24	87.76%	FS
0.77	0.8198	3090.07	1072.67	698.90	---	409.93	---	127.32	---	301.09	81.98%	FS
0.78	0.7962	3101.87	1073.45	704.65	---	398.12	---	126.54	---	295.34	79.62%	FS
0.79	0.7159	3142.02	1076.13	700.00	---	357.97	---	123.86	---	300.00	71.59%	FS
0.80	0.6418	3179.10	1078.60	700.37	---	320.89	---	121.39		299.63	64.18%	FS
0.81-1.00	---	---	---	---	---	---	---	---	--	---	---	No-FS

'---'indicates not applicable

Table 19. Comparative results of the membership functions for different confidence level of the decision maker.

Hyperbolic Membership Function (HMF)					Exponential Membership Function (EMF)					DM Confidence Level
Z^1	Z^2	Z^3	Satisfaction level (100%)	Feasible / No-feasible Solution	Z^1	Z^2	Z^3	Satisfaction level (100%)	Feasible / No-feasible Sol.	
3000.00	1000.00	723.57	100%	Feasible Sol.	3000.00	1200.00	758.34	100%	FS.	0.70
2951.74	991.50	671.80	100%	Feasible Sol.	2730.9	1091.00	684.21	100%	FS.	0.71
3005.49	1009.61	681.82	100%	Feasible Sol.	2716.94	1200.00	758.81	100%	FS.	0.72
2715.27	994.64	675.71	100%	Feasible Sol.	2704.00	1200.00	759.00	100%	FS.	0.73
3000.00	1014.71	800.00	100%	Feasible Sol.	3000.00	1200.00	724.00	100%	FS.	0.74
3035.11	1069.00	698.61	92.97%	Feasible Sol.	3000.00	1199.33	712.45	100%	FS.	0.75
3061.16	1070.74	698.76	87.76%	Feasible Sol.	3000.00	1200.00	727.27	99.87%	FS.	0.76
3090.07	1072.67	698.90	81.98%	Feasible Sol.	3024.41	1206.24	737.16	95.11%	FS.	0.77
3101.87	1073.45	704.65	79.62%	Feasible Sol.	3030.30	1207.80	744.80	93.94%	FS.	0.78
3142.02	1076.13	700.00	71.59%	Feasible Sol.	3071.00	1218.85	756.00	85.72%	FS.	0.79
3179.10	1078.600	700.37	64.18%	Feasible Sol.	3102.83	1227.75	766.58	79.43%	FS.	0.80
---	---	---	---	No Feasible Sol.	3126.29	1234.66	772.53	74.74%	No FS.	0.81
---	---	---	---	No Feasible Sol.	3157.92	1244.37	780.51	68.41%	No FS.	0.82
---	---	---	---	No Feasible Sol.	3181.73	1252.00	786.60	63.65%	No FS.	0.83
---	---	---	---	No Feasible Sol.	3213.34	1262.61	794.82	57.33%	No FS.	0.84
---	---	---	---	No Feasible Sol.	3252.71	1276.97	805.31	49.45%	No FS.	0.85

'---'indicates not applicable

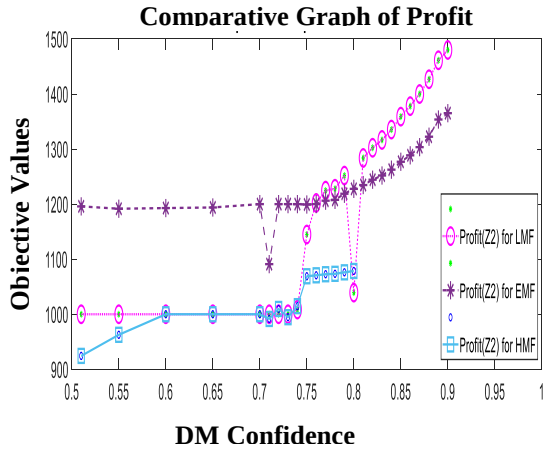

Fig. 7. Comparative graph of Objective values versus DM confidence level of goal programming for TP cost.

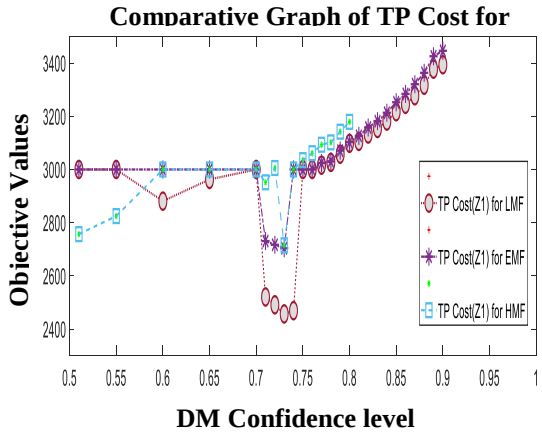

Fig. 8. Comparative graph of Objective values versus DM confidence level of goal programming for profit.

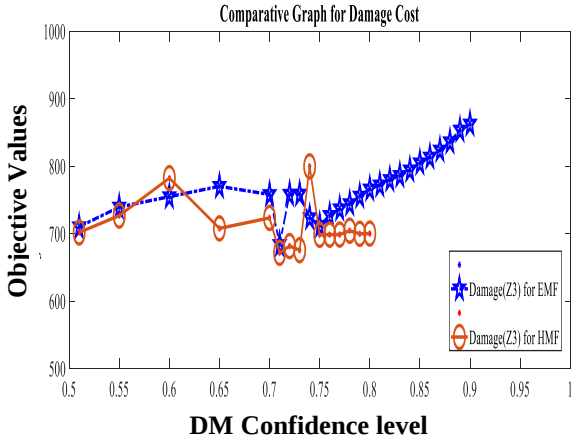

Fig. 9. Comparative graph of Objective values versus DM confidence level of goal programming for damage cost.

From the graphs presented in Figs. 6 to 9, we have a very specific observations of various parameters of the goal programming transportation problem in uncertain environment using fuzzy membership functions. Fig. 6 reveals the satisfaction level of the decision maker for various confidence level using the fuzzy membership functions, linear, exponential and hyperbolic. It is clear from the graph that the satisfaction of DM in all three cases, is height for the confidence level 0.51 to 0.75 and then continuously decreases from the confidence level 0.75 until arriving at the worst satisfaction level 10.16% at 0.90.

Fig. 7 unwrapped the transportation cost against the confidence level for the fuzzy membership functions. All the three function have shown almost same pattern throughout the region except 0.70 to 0.75. The linear membership function has shown more fluctuation regarding the objective value other than two in the area 0.72 to 0.74 whereas the others have same oscillation on that region. All the three membership function have shown the increasing behavior of TP cost from 0.75 to onwards.

Fig. 8 and Fig. 9 have shown some anomaly regarding the profit and damage cost for the chosen confidence level of the DM but have similar increasing pattern visible from 0.80 to onwards.

Conclusion

In this research, uncertain MOTP has been investigated based on the method presented in this paper. The uncertain parameters were resolved by uncertain normal distribution. MOTP in uncertain parameters using the fuzzy non-linear membership functions with their mathematical algorithms have shown with applicability of these algorithms by a heuristic example of same data table with a variety of confidence level of the DM for each case. Sometime the problem becomes infeasible for a chosen confidence level due to the violation of the feasibility condition of the transportation problem. The satisfactions in percent of the decision maker are obtained for a chosen confidence level that is accumulated in listed tables. From the comparative results, we see that the satisfactions level of the

DM using hyperbolic membership function has shown multiple time 100% in a region but solution is not feasible for a large scale of confidence level. On the other hand, the objective values using exponential membership functions are more considerable than that hyperbolic.

Acknowledgment

Authors are very much thankful to the anonymous reviewers for their constructive comments and suggestions. This project was supported by the research cell of Mawlana Bhashani Science and Technology University under the research grand number RG-3631108.

Declarations

The contents of the paper were not published before or submitted for publication in any other journal and all the co-authors have given their consent for the article to be considered by the Editorial Board for publication in the Journal of Bangladesh Academy of Sciences.

Conflicting interests

The authors declare that there are no conflicts of interest.

References

Anukokila P, Radhakrishnan B and Rajeshwari M. Multi-objective transportation problem by using goal programming approach. *Intl. J. Pure Appl. Math.* 2017; 117(11): 393-403.

Bellman R and Zadeh LA. Decision making in a fuzzy environment. *Manag. Sci.* 1970; 17(B): 141-164.

Bit AK and Alam SS. An additive fuzzy programming model for multi-objective transportation problem. *Fuzzy Sets Syst.* 1993; 57: 313-319.

Bit AK, Biswal MP and Alam SS. Fuzzy programming approach to multicriteria decision making transportation problem. *Fuzzy Sets Syst.* 1992; 50: 135-141.

Cadenas JM and Verdegay JL. Using ranking functions in multi-objective fuzzy linear programming. *Fuzzy sets syst.* 2000; 111 (1): 47-53.

Dantzing GB. *Linear Programming and Extensions.* Princeton University Press, 1963.

Das SK, Goswami A and Alam SS. Multi-objective transportation problem with interval cost, source and destination parameters. *Eur. J. Oper. Res.* 1999; 117: 100-112.

Delgado M, Verdegay JL and Vila MA. A general model for fuzzy linear programming *Fuzzy Sets syst.* 1989; 29(1): 21-29.

Gupta A and Kumar A. A new method for solving linear multi-objective transportation problems with fuzzy parameters. *Appl. Math. Model.* 2012; 36: 1421-1430.

Hasan M, Khan AR, Gosh N and Uddin MS. On development of algorithm to design layout in faculty layout planning problems. *J. Phys. Sci.* 2015; 20: 35-42.

Hasan M, Hossain S, Ahmed MK and Uddin MS. Sustainable way of choosing effective electronic devices using fuzzy TOPSIS method. *Am. Sci. Res. J. Eng. Tech. Sci. (ASRJETS)*; 2017; 35: 342-351.

Jagtap KB and Kawale SV. Optimizing transportation problem with multi-objective by hierarchical order goal programming model. *Global J. Pure App. Math.;* 2017*;* 13(9): 5333-5339.

Kaur L and Kumar A. A new method for solving fuzzy transportation problems using ranking function. *Appl. Math. Model.* 2011; 35: 5652-5661.

Lee SM and Moore LJ. Optimizing transportation problems with multiple objectives. *AIEE Trans.* 1973; 5: 333-338.

Liu B. Fuzzy Process, Hybrid process and uncertain process. *J. Unc. Syst.* 2008; 2(1): 3-16.

Liu B. Some research problems in uncertainty theory. *J. Unc. Syst.;* 2009(b); 3(1): 3-10.

Liu B. Uncertainty theory: A branch of mathematics for modeling human uncertainty. In: Studies in computational Intelligence, vol. 300, *Springer, Berlin*, Heidelberg, 2010. pp.1-79.

Maity G and Roy SK. Solving a multi-objective transportation problem with nonlinear cost and multi-choice demand. *Int. J. Manag. Sci.* 2015; 11(1): 1-9.

Maity G, Roy SK and Verdegay JL. Multi-objective transportation problem with cost reliability under uncertain environment. *Int. J. Comput. Intell. Syst.*, 2016; 9(5): 839-849.

Roy SK and Midya S. An improvement of Goyal's modified VAM for the unbalanced transportation problem. *J. Oper. Res. Socl.* 1988; 39: 609-610.

Sheng Y and Yao K. A transportation model with uncertain costs and demands, *Int. J. Inf.* 2012; 15(8): 1-7.

Surapati P and Roy TK. Multi-objective transportation model with fuzzy parameters: Priority based fuzzy goal programming approach. J. Tran. Sys. Engin. Info. Tech.; 2008; 8: 40-48.

Uddin MS, Miah MM**,** Khan MA and Arjani AA. Goal programming tactic for multi-objective transportation problem using fuzzy linear membership function. *Alex. Eng. J.* 2021; 60: 2525-2533.

Wahed WF and Abo-Sinna MA. A hybrid fuzzy-goal programming approach to multiple objective decision making problems. *Fuzzy Sets Syst.* 2001; 119: 71-85.

Wahed WF and Lee SM. Interactive fuzzy goal programming for multi-objective transportation problem. *Omega*, 2006; 34: 158-166.

Wahed WF. A multi-objective transportation problem under fuzziness; *Fuzzy Sets Syst.* 2001; 117: 27-33.

Zadeh LA. Fuzzy sets, *Inf. Cont.* 1965; 8: 338-353

Zangiabadi M and Maleki HR. Fuzzy goal programming for multi-objective transportation problem. *J. App. Math. Comput.* 2007; 24(12): 449-460.

Zimmermann HJ. Fuzzy programming and linear programming with several objective functions. *Fuzzy Sets Syst.* 1978; 1: 45- 55.

J. Bangladesh Acad. Sci. 46(1); 117-128: June 2022 DOI: 10.3329/jbas.v46i1.60443

Journal of Bangladesh Academy of Sciences

Journal homepage: http://www.bas.org.bd/publications/jbas.html

Research Article

Comparison of different blood biomarkers of cervical cancer patients with control subjects

N. M. Abdullah Al Mamun, Salwa Abdul Quyyum, Kohereen Bashar[1], Yearul Kabir, Mustafizur Rahman and M M Towhidul Islam[*]

Department of Biochemistry and Molecular Biology, University of Dhaka

ARTICLE INFO

Article History

Received: 4 June 2022
Revised: 20 June 2022
Accepted: 22 June 2022

Keywords: Cervical cancer, Oxidant-antioxidant balance, Biomarker, Cholesterol/phospholipid ratio, Osmotic fragility

ABSTRACT

Cervical cancer shows a high prevalence among Bangladeshi women. Reports indicated that oxidant-antioxidant balance plays a role in cervical cancer pathogenesis. Therefore, this study explores the change of different blood-derived enzymes, antioxidants, and biomarkers to understand the oxidative stress status of Bangladeshi cervical cancer patients. A clinician recruited the case and control participants for the study based on histopathologic reports. No significant difference was observed in the random blood glucose level, blood pressure, total cholesterol, triglycerides (TGs), HDL cholesterol, LDL cholesterol, and total protein levels in case participants compared to age and sex-matched control subjects. However, serum albumin, vitamins like alpha-tocopherol and ascorbic acid, antioxidant enzymes like SOD, and catalase levels significantly decreased in patients compared to controls. Other parameters, like, ALT, AST, ALP, phospholipid hydroperoxide, TBARS, protein carbonyl content, serum nitric oxide, cholesterol/phospholipid ratio (C/P) of erythrocyte and osmotic fragility were significantly increased in the case subjects compared to control. All of these reflect an oxidant-antioxidant imbalance in this setting. Thus, this study provides a detailed profile of the oxidant-antioxidant levels of the Bangladeshi cervical cancer patients, which revealed that the compromised antioxidant system in cervical cancer patients is associated with damage to various biomolecules and ultimately impairs cellular functions.

Introduction

Cervical cancer is the fourth most common carcinoma among women worldwide. Less-developed countries experience a very high prevalence of cancer, where 87% of the world's cervical cancer occurs (Ferlay et al., 2015). Over 2.7 million people died were between the ages of 25 and 64 worldwide, of which 2.4 million deaths reported in developing areas and 0.3 million in developed countries (Yang et al., 2004; Castle and Pierz, 2019). In Bangladesh, the rate is also very high. It is the second most common cancer amongst Bangladeshi women, with an estimated 11,956 incidents and 6582 deaths in 2012 (Islam et al., 2018). Current evidence indicates that the leading cause of cervical cancer is cervical infection with certain types of Human Papilloma Virus (HPV), transmitted sexually (Kjaer et al., 2001). Besides, many data have recently been published supporting the fact that oxidative stress plays a significant role in aggravating the pathogenesis of cervical cancer (Ebrahimi et al., 2019). Moreover, a severe imbalance was observed during the oxidative stress between the production of reactive species and antioxidant defenses, leading to potential tissue damage and carcinogenesis

[*]Corresponding author: <towhidbmb@du.ac.bd>

[1]Comilla Medical College, Comilla

(Rani et al., 2016). Oxidative stress is persistent during aerobic metabolism when highly reactive free radicals-ROS (Reactive Oxygen Species) and RNS (Reactive Nitrogen Species) such as superoxide, hydroxyl radical, nitric oxide, and hydrogen peroxide are continuously produced and cause oxidative damage to DNA, carbohydrates, proteins, and lipids. This leads to fragmentation and cross-linking cellular macromolecules (Rani et al., 2016; Kruk and Aboul-Enein, 2017). It also modulates the function of cancer cells, such as cell proliferation, alterations in cellular sensitivity to anticancer agents, invasion, and metastasis by increasing mutations, and genetic instability (Zelenka et al., 2018; Wang et al., 2018; Saha et al., 2017).

Over the past several decades, numerous studies have examined the relationship between oxidative stress status with cervical neoplasia and cancer risk (Castle and Giuliano, 2003; Tong et al., 2015; Cruz-Gregorio et al., 2018). ROS are essential contributors linking environmental toxicity to the multistage carcinogenic process. These oxidants can be generated in response to both endogenous and exogenous stimuli. To counter balance ROS-mediated injury, an endogenous antioxidant defense system exists. The antioxidant system consists of enzymatic and non-enzymatic components (Rani et al., 2016). Superoxide dismutase (SOD) and catalase are the antioxidant enzymes among those components. SOD protects by catalyzing the dismutation of superoxide radicals to H_2O_2. Increased lipid peroxidation occurs due to decreased SOD levels, resulting in deformation and rigidness of cells (Islam et al., 2019; Bairova et al., 2014). Another enzyme, catalase, prevents the cell membrane from being damaged by detoxifying H_2O_2 to water and molecular oxygen. It is one of the ways by which catalase protects erythrocytes from oxidative stress (He et al., 2017). The decreased level of catalase is linked with the low detoxification of oxidants in cancer. However, when oxidation exceeds the control mechanisms, oxidative stress begins. Chronic and cumulative oxidative stress induces deleterious modifications to various macromolecular components, such as DNA, lipids, and proteins (Glorieux and Calderon, 2017). Recent studies showed decreased antioxidant concentrations and increased oxidative stress in cervical cancer (Cruz-Gregorio et al., 2018). Moreover, the cervical cancer cell line shows that ascorbic acid has potential in the treatment of cervical cancer by inhibiting critical steps in cancer development and spread (Mane et al., 2016; Blaszczak et al., 2019). Protective effects were also observed for vitamins A, C, and E and beta-carotene (Jain et al., 2017). Therefore, the purpose of the present study is to evaluate the antioxidant status in cervical cancer patients by estimating different serum biomarkers in addition to the level of nitrite, antioxidant enzymes, and structural integrity of erythrocytes, since oxidative stress is considered to play a major role along with HPV in the progression of cervical cancer.

Materials and Methods

This case-control study was carried out in the Department of Biochemistry and Molecular Biology of Dhaka University, involving 60 Bangladeshi participants. Participants were distributed equally among the control- and patient-group based on the inclusion and exclusion criteria of the study. The study was explained to all the participants to get written consent. An expert clinician confirmed the patients using the acetic acid test of the cervix (VIA) in the clinic of Gynecological Oncology, Department of National Institute of Cancer Research and Hospital (NIRCH), Mohakhali, Dhaka. Moreover, participants were informed about their rights to withdraw their involvement from the study at any time. Study subjects completed a structured questionnaire about their age, age at the time of marriage, no. of children, medical, residential, occupational, and family history of chronic diseases, along with other details. At the same time, 30 healthy female subjects from the same

socioeconomic status, having no history of smoking, alcoholism, or carcinoma, were recruited as controls. Ethical Review Committee of the Department of Biochemistry and Molecular Biology, University of Dhaka, approved the study and all the participants provided written informed consent before participation.

Blood samples from the cervical cancer patients and the control subjects were collected under protocols approved by the Department of Biochemistry and Molecular Biology, University of Dhaka. About 5 mL of venous blood was drawn from each individual using a disposable syringe with the help of a trained person, following all aseptic precautions. Blood was maintained with EDTA for erythrocyte membrane preparation and without EDTA for serum preparation and osmotic fragility test. The drawn blood was transported to the laboratory using an icebox and then centrifuged for 10 minutes at 3,000 rpm. The serum was collected from the centrifuged tube carefully with a Pasteur pipette. The samples were either analyzed on the same collection day or stored at -20° C until further use.

All the methods were standardized first, and standard graphs were obtained. Random Blood glucose was determined by the glucose oxidase (GOD) method according to the protocol provided by the reagent kit of Linear chemicals, Spain. Alanine aminotransferase (ALT), Aspartate aminotransferase (AST), and ALP (Alkaline Phosphatase) were determined by the reagent kit of Randox, UK. Serum total protein was determined by a modification of the Lowry technique (Okutucu et al., 2007). In the modified method, the protein binds to copper in an alkaline medium and produces Cu^{++}. This catalyzes the oxidation of aromatic amino acids by reducing phosphomolybdotungstate to heteropolymolybdanum blue, which predominantly depends upon the tyrosine and tryptophan protein content. In another protocol, albumin reacts with the anionic Bromocresol green (BCG) and produces a green color, which is measured at 546 nm (Duly et al., 2003). Furthermore, serum carbonyl groups were measured using a reaction with dinitrophenylhydrazine (DNPH), forming of stable hydrazone products and measuring the absorbance at 370 nm (Colombo et al., 2016). Total cholesterol and triglyceride were determined according to the protocol provided by Linear Chemicals Limited, Spain. HDL- and LDL- cholesterol were determined according to the protocol supplied by the Erba diagnostics Mannheim GmbH, Germany, and Friedword's formula, respectively. The thiobarbiturate reactive substances (TBARS) were determined by the method of Yagi (1998). Serum lipid peroxide was measured by precipitating lipoproteins with trichloroacetic acid and boiled with thiobarbituric acid, which reacted with malondialdehyde to develop pink color, which was quantified at 535 nm (Dasgupta and Klein, 2014). Phospholipid hydroperoxide was determined by a colorimetric method based on the oxidation of ferrous to ferric ions in the presence of xylenol orange. Serum vitamin A and vitamin E were measured simultaneously by the high-pressure liquid chromatography (HPLC) method. Acetonitrile and methanol (88:12) were used as mobile phase, Nucleosil C18; 5µ, 4.6 X 250 mm column, and UV detector (absorbance at 292 nm for both retinol and tocopherol) were used. 50 µL sample was injected, the flow rate was 1.0 mL/min, temperature was ambient, and sensitivity was 0.0005. Serum ascorbic acid was measured by reacting with dinitrophenylhydrazine. The level of serum nitrite (NO_2^-) was determined by the reduction of nitrate by copper-cadmium alloy, followed by color development with Griess reagent (sulfanilamide and N-naphthylethyl enediamine) in an acidic medium according to the method of Sastry et al. (2002). The activity of serum SOD was determined by using of either ferricytochrome c, an electron-carrying protein containing one heme group found in mitochondria of all aerobic organisms, or nitro blue tetrazolium according to the method described by Beyer and Fridovich (1987). The serum catalase level was determined by the breakdown of hydrogen peroxide by the action of catalase and the measurement of the ultraviolet absorption of peroxide according to the method of Beers and Sizer (1952). Erythrocyte membrane cholesterol was determined by the method

of Allain et al. (1974). According to this method, cholesterol esters were hydrolyzed to free cholesterol by cholesterol ester hydrolase. The free cholesterol produced was oxidized by cholesterol oxidase to cholest-4-en-3-one with the simultaneous production of hydrogen peroxide, which oxidatively couples with 4-amino antipyrine and phenol in the presence of peroxidase to yield a chromogen with maximum absorption at 500 nm. Erythrocyte membrane phospholipid was determined by the method of Bartlett, where phosphorus reaction mixture was heated in the presence of strong sulfuric acid, and absorption was taken at 830 nm (Bartlett, 1959). Erythrocyte membrane protein was determined by Folin phenol reagent after alkaline copper treatment according to the method of Lowry (Nayak et al., 2008). Osmotic fragility was determined using whole blood by the method of Parpart et al. (1947) and Layton and Roper (2016). The degree of resistance of red cells to a decrease in salt content has long been used as a measure of their viability and clinically as diagnostic characteristics. When any red cell reaches the hemolytic volume, the hemoglobin of that cell diffuses to equilibrium, usually without rupturing the plasma membrane of the cell (Toepfner et al., 2018).

Data obtained from the experiments were analyzed using the GraphPad Prism version 6.0 and Microsoft Excel 2007. Data are expressed as mean ± SEM. The student's t-test was used for statistical analysis. p-value <0.05 was considered a statistically significant.

Results

In this case-control study, 30 female subjects were enrolled as the patient (case) who was diagnosed as cervical cancer positive with pap smear tests (Shlay et al., 1998), and 30 age-matched control subjects with no history of cervical cancer. Interestingly, when we analyzed the average age at which they got married, we have found that the patient group married at a significantly earlier age (case vs. control, 17 vs. 23 years, $p<0.05$) compared to the control subjects, which indicates marriage age could be a potential risk factor for cervical cancer (Table 1).

Table 1. Characteristics of the study subjects

Parameters		Control (n=25)	Patient (n=25)
Age (GM in years)		49	52
Marriage Age (in years)		23	17 *
Married life (in years)		27	34 *
No. of Children		2	4*
Systolic BP (mmHg)		110	104
Diastolic BP (mmHg)		70	65
Random blood glucose (mg/dL)		132.07	113.14
Educational Level	Illiterate	6	12
	Primary	9	7
	Secondary	7	4
	Above secondary	3	2

GM means Geometric Mean, ns means non-significant, *p<0.05.

Moreover, the duration of marriage life also a significantly impacts cancer prognosis. Table 1 showed that the patient group has a significantly longer marriage life compared to the control (case vs. control, 34 vs. 27 years, $p<0.05$). Additionally, the patient group experienced a significantly higher number of childbirths than the control group (case vs. control, 4 vs. 2 children, $p<0.05$). However, no differences were found in the blood pressure level, random blood glucose level, or educational status with the disease outcome between the two groups (Table 1). When fasting blood lipid profiles were analyzed, it was found that both the case and control groups have similar lipid profiles, where total cholesterol levels were (135.5±15.56 vs. 122.4±27.29 mg/dL, $p=0.69$), triglycerides levels were (113.9±15.29 vs. 102.6±29.76 mg/dL, $p=0.74$), HDL cholesterol (34.60±1.50 vs. 31.6±3.17 mg/dL, $p=0.42$), and LDL cholesterol levels were (78.2±11.77 vs. 49.61±3.93 mg/dL, $p=0.051$) case vs. control, respectively (Table 2). The blood levels of enzymes (ALP, ALT, and AST) were significantly ($p<0.05$) higher in the cervical cancer subjects compared to the control subjects (1361.0±15.4 vs. 895.3±7.6 U/L, 2646.0±4.3 vs. 1723.0±7.1 U/L, and 1340.0±21.9 vs. 910.9±6.5 U/L, respectively) (Table 2).

Table 2. Lipid profiles and serum enzymes in control and cervical cancer subjects (n=5).

Parameters	Control	Patient
Cholesterol mg/dL	135.5±15.56	122.4±27.29
Triglycerides mg/dL	113.9±15.29	102.6±29.76
HDL Cholesterol mg/dL	34.60±1.50	31.6±3.17
LDL Cholesterol mg/dL	78.2±11.77	49.61±3.93
Alkaline phosphatase U/L	1361.0±15.4	895.3±7.6*
Alanine transaminase U/L	2646.0±4.3	1723.0±7.1*
Aspartate transaminase U/L	1340.0±21.9	910.9±6.5*

The data are expressed as mean±SEM. *Differences were considered significant at p<0.05.

In similar experiments, different redox parameters of the blood were analyzed, where the case group differs significantly from the control. The case group had phospholipid hydroxide at a level of 4.1±0.08 vs. 2.3±0.07 nmol/ml in the control group, which was significantly different, p<0.05. The levels of TBARS were also significantly different in case vs. control (2.70±0.29 vs. 1.1±0.13 nmol/ml, respectively, p<0.05). Similarly, protein carbonyl contents were significantly higher (0.23±0.02 nmol/mg of protein) in case subjects vs. (0.14±0.01 nmol/mg of protein) control subjects (Fig. 1).

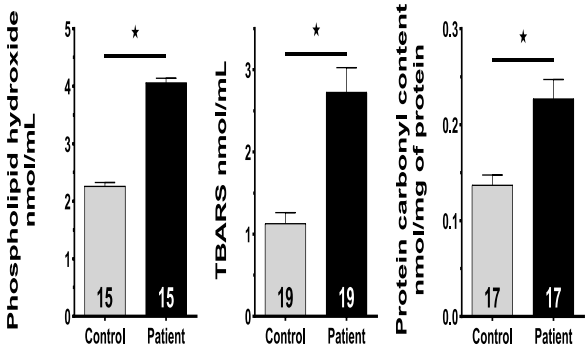

Fig. 1. Redox status in control and cervical cancer subjects. The number inside the bars indicates the number of participants. *indicates statistically significant differences at p<0.05.

Total protein content, albumin, and globulin levels were also analyzed on the blood samples and found that the total protein level (42.2±2.45 vs. 42.6±1.91 g/L, p=0.90) and globulin levels (29.3±3.39 vs. 24.9± 1.80 g/L, p=0.28) were comparable between the case and control groups, whereas the blood albumin level was significantly lower in the case group compared to the control group (18.9±1.20 vs. 24.5±1.52 g/L, p<0.05) (case vs. control, respectively; Fig. 2).

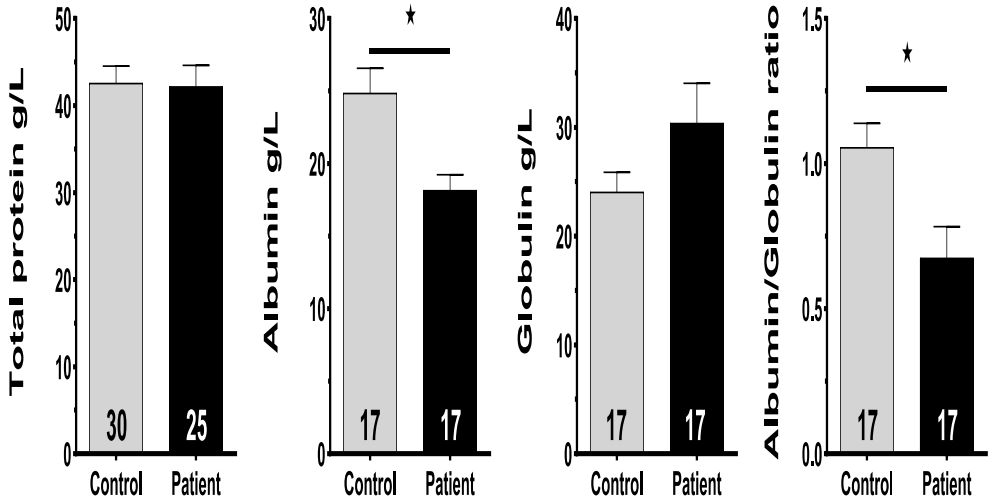

Fig. 2. Blood levels of proteins in control and cervical cancer subjects. The number inside the bars indicates the number of participants. *indicates statistically significant differences at p<0.05.

When levels of different vitamins were analyzed in the blood, it was found that the case group had significantly lower levels of ascorbic acid (0.78±0.12 vs. 1.50±0.12 mg/dL, p<0.05), retinol (38.0±5.04 vs. 62.2±2.76 g/mL, p<0.05) and alpha-tocopherol (6.3±0.85 vs. 14.1±1.90 g/mL, p<0.05) (case vs. control, respectively; Fig. 3).

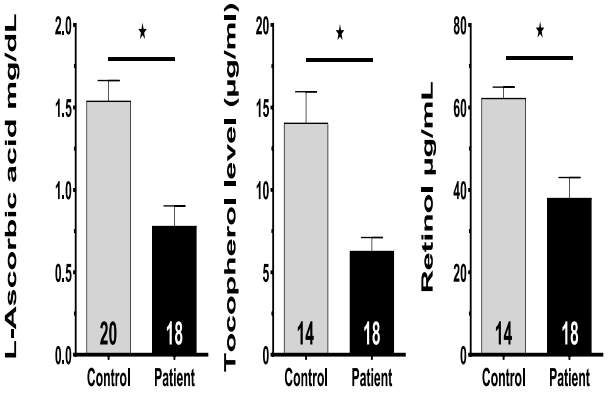

Fig. 3. Vitamin levels in control and cervical cancer subjects. The number inside the bars indicates the number of participants. *indicates statistically significant differences p<0.05.

The blood maintains a different antioxidant system to control the redox status of the body. When serum nitrate, superoxide dismutase (SOD) and catalase levels were analyzed, it was found that serum nitrate was 5.6±0.09 vs. 3.0±0.05 µmol/L, p<0.05, SOD was 4.1±0.09 vs. 10.30±0.74 units/mL, p<0.05 and catalase was 0.93±0.04 vs. 10.3±0.49 units/mL, p<0.05 (case vs. control, respectively; Table 3). Significantly increased cholesterol and decreased phospholipid in the erythrocyte membrane of the case subjects were observed compared to the control (Table 4). Besides, a significant increase in the C/P ratio was observed in the case subjects compared to the control subjects (Table 4).

Table 3. Level of nitrite and antioxidant enzymes in the blood of control and case participants. (n=30).

Parameters	Control	Patient
Nitrite (µmol/L)	3.0± 0.05	5.6 ± 0.09*
SOD (units/mL)	10.30±0.74	4.1±0.09*
Catalase (units/mL)	10.30±0.49	0.93±0.04*

The data are expressed as mean±SEM. *Differences were considered significant at p< 0.05.

Table 4. Cholesterol, phospholipid content, and C/P ratio of erythrocyte membrane in control and cervical cancer samples (n=30).

Parameters	Control	Patient
Cholesterol (µg/mg protein)	212.2±11.0	277.8±8.18*
Phospholipid (µg/mg protein)	593.5±30.42	221.9±12.10*
C/P ratio	0.35±0.01	0.54±0.01*

The data are expressed as mean±SEM. *Differences were considered significant with p< 0.05.

It indicates that the fluidity of the RBC was significantly decreased in case subjects. Moreover, when fragility was considered, it was found that the erythrocytes of cervical cancer patients were more fragile than the control subjects. When the osmotic pressure-induced RBC fragility was tested, a rightward shift of the fragility curve, meaning more hemolysis, in cervical cancer patients was observed compared to the control subjects (Fig.4).

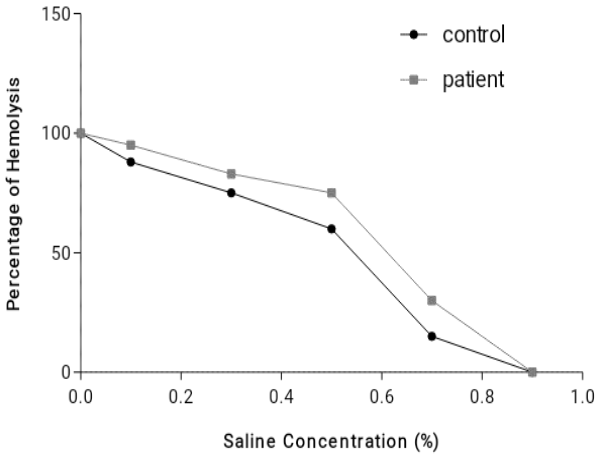

Fig. 4. Red blood cell fragility in control and cervical cancer subjects. Each dot indicates the mean value of at least 5 samples.

Discussion

It is now a well-established concept that oxidative stress has a pathogenic effect and plays a crucial role in developing many diseased conditions, including cancer, neurological diseases, and cardiovascular diseases (Halliwell and Gutteridge, 2015). The pathogens are

initiated due to inadequate performance of the antioxidant defense mechanism and cause constant damage to the cellular macromolecules, which ultimately leads to alteration of cellular physiology (Cruz-Gregorio et al., 2018; Devi et al., 2000).

Altered biochemical and nutritional parameters levels were found in cervical cancer patients (Orr et al., 1985). When we compared blood glucose or blood pressure, it was found that both the study groups had similar patterns. Although scientists believe that hyperglycemia is strongly associated with a poor prognosis of cervical cancer, the high prevalence of diabetes and hypertension in this country may be the reason for similar blood glucose and blood pressure patterns in these study groups. Interestingly, significantly higher levels of triglycerides and lower total cholesterol levels were observed in previous cervical cancer patients (Preetha et al., 2016). Ray et al. showed, on the other hand, lower levels of all lipid fractions (Ray et al., 1997). However, in our study, both the cervical cancer patients and control subjects had comparable lipid profiles (Table 2). Moreover, different serum enzymes like aspartate transaminase (AST), alanine transaminase (ALT), and alkaline phosphatase (ALP) activity were reported to be higher in the circulation of cervical cancer patients (Manju et al., 2002). Similarly, in our study, ALT, AST, and ALP levels of the cervical cancer patient group were significantly increased compared to the control group. This may be because carcinogenic agents alter cellular growth, leading to various biochemical changes in the blood (Chougule et al., 2008).

Lipid peroxidation appears to be a significant cause of human's endogenous DNA damage that may contribute significantly to cancer (Gentile et al., 2017). Among the peroxidation end products of membranous polyunsaturated fatty acids, Malonaldehyde (MDA) was reported as mutagenic in bacterial and mammalian cells and carcinogenic in rats (Niedernhofer et al., 2003). MDA reacts with thiobarbituric acid (TBA) to form a fluorescent red adduct and can be used as an indicator of oxidative stress (Marnett, 2000; Balas et al., 2011). Several studies showed thiobarbituric acid reactive substance (TBARS) levels were significantly higher in the cervical cancer patient group than in control (Kolanjiappan et al., 2002; Chiou and Hu, 1999; Manju et al., 2002; Kim et al.; 2003; Jelić et al., 2018; Balasubramaniyan et al., 1994). Moreover, myeloperoxidases and lipid peroxide-modified proteins were also increased in gynecological malignancies (Song and Santanam, 2001). In the present study, we reported similar findings where cervical cancer patients have significantly higher levels of phospholipid hydroperoxide, and TBARS compared to control subjects.

Protein profiling data showed no significant difference in the levels of total protein. Still, serum albumin level was significantly decreased, whereas serum globulin increased in cervical cancer patients. It has already been reported that reduced serum albumin ratio is associated with malnutrition. In contrast, an increased globulin level means the severity of the inflammatory response, which results in the cardinal features of cancer cachexia (Chi et al., 2018). The reason might be that albumin sequesters copper and other toxic transition metals to detoxify them and protects against cellular damage. Interestingly, these cancer patients had lower albumin to globulin ratio than the control. Yoshino et al. reported that low albumin to globulin ratio high globulin levels are associated with poor survival of cervical cancer patients (Yoshino et al., 2019). Moreover, a high protein carbonyl level produced due to excess ROS indicates higher oxidative stress in these cervical cancer patients. Because all the amino acid residues of a protein can be modified by $OH\cdot$ and O_2^-, which increases the formation of carbonyl groups in proteins (Shrivastava et al., 2019). In the presence of O_2^-, a high amount of peroxyl radicals and peroxides (protein peroxidation) might be formed to oxidize proteins and other targets.

In addition to increased oxidative stress, a decrease in antioxidant concentrations were also noted in cervical cancer (Palan et al., 2004; Jiang et al., 2013). For example, an increase in ascorbic acid, concentration has the potential for the treatment of cervical cancer by inhibiting cell proliferation (MTT assay), modulation of matrix metalloproteinases (MMP-2 and MMP-9) expression (gelatinase zymography), and cancer cell invasive potential (Matrigel) in cancer development and spread (Roomi et al., 2006). Similarly, in this study, it was found that cervical cancer patients have significantly decreased vitamin A, E, and C levels compared to the control group.

Nitric oxide (NO•) is an abundant radical in the biological system. It is generated during arginine to citrulline metabolism, catalyzed by nitric oxide synthases (NOSs) (Ghafourifar and Cadenas, 2005). When reacting with water, NO• also produces nitrate (NO_3-) and nitrite (NO_2-). NO•, at its lower concentration, plays an important role in the host defense system and homeostasis at a lower concentration. However, when produced at higher concentrations for a prolonged time, NO• exhibits tumorigenic effects either by the formation of carcinogenic N-nitroso compounds, direct deamination of DNA bases, or oxidation of DNA after the formation of peroxynitrite and hydroxyl radicals (Hogg et al., 1996; Liu and Hotchkiss, 1995; Sowjanya et al., 2016). Thus, an altered level of NO• can induce DNA damage when the antioxidant defense system is not functioning properly (Liu and Hotchkiss, 1995; Shrivastava et al., 2019). Antioxidant enzymes can scavenge these radicals and provide direct protection from the radical-mediated damages. However, a decreased level of SOD and catalase activity, as found in the study, cannot handle all the ROS and a high magnitude of oxidative stress that may form in cervical cancer patients.

Moreover, an increased C/P ratio in this study indicates the loss of erythrocyte fluidity in cervical cancer patients. Probably this is due to the alteration in its lipid composition (Kolanjiappan et al., 2002). A membrane's cholesterol and phospholipid content determine its fluidity (Shinitzky and Inbar, 1976; Johnson and Robinson, 1979). Increased cholesterol is a critical factor in fluidity reduction that distorts the membrane structure and might interfere with many cellular functions. In addition to the oxidative damage, this abnormal membrane structure might also be responsible, to some extent, for its increased osmotic fragility. It makes the RBC more sensitive to changing the osmotic pressure. Since it helps to determine the integrity, membrane permeability, and alterations of erythrocytes, measurement of osmotic fragility was applied previously to diagnose diseases and analytic studies (Kumar et al., 2008). All these fit together very well with the findings of this study, where excess lipid peroxidation of the erythrocyte membrane leads to decreased resistance to hemolysis.

Conclusions

From the above discussion, it is clear that the presence of cervical cancer a significantly impacts different biochemical parameters of the human body. The present study, thus, demonstrated that the antioxidant system is compromised in cervical cancer patients more than in control groups and affects cellular function and integrity. These routine biochemical parameters can be used in the early diagnosis of cervical cancer, which will be low-cost and widely available.

- **Funding:** Not applicable
- **Acknowledgements:** The authors are grateful to the Department of Biochemistry and Molecular Biology, University of Dhaka; and University Grants Commission, Bangladesh for their support throughout the study.
- **Conflict of interest:** On behalf of all authors, the corresponding author states that there is no conflict of interest.

References

Allain CC, Poon LS, Chan CSG, Richmond W and Fu PC. Enzymatic determination of total serum cholesterol. *Clin. Chem*. 1974; 20: 470-475.

Bairova TA, Kolesnikov SI, Kolesnikova LI, Pervushina OA, Darenskaya MA and Grebenkina LA. Lipid peroxidation and mitochondrial superoxide dismutase-2 gene in adolescents with essential hypertension. *Bull. Exp. Biol. Med*. 2014; 158: 181-184.

Balas VI, Verginadis II, Geromichalos GD, Kourkoumelis N, Male L, Hursthouse MB, Repana KH, Yiannaki E, Charalabopoulos K and Bakas T. Synthesis, structural characterization and biological studies of the triphenyltin (IV) complex with 2-thiobarbituric acid. *Eur. J. Med. Chem*. 2011; 46: 2835-2844.

Balasubramaniyan N, Subramanian S and Govindasamy S. Status of antioxidant systems in human carcinoma of uterine cervix. *Cancer Lett*. 1994; 87: 187-192.

Bartlett GR. Phosphorus assay in column chromatography. *J. Biol. Chem*. 1959; 234: 466-468.

Beers RF and Sizer IW. A spectrophotometric method for measuring the breakdown of hydrogen peroxide by catalase. *J. Biol. Chem*. 1952; 195: 133-140.

Beyer Jr WF and Fridovich I. Assaying for superoxide dismutase activity: some large consequences of minor changes in conditions. *Anal. Biochem*. 1987; 161: 559-566.

Blaszczak W, Barczak W, Masternak J, Kopczyński P, Zhitkovich A and Rubiś B. Vitamin C as a modulator of the response to cancer therapy. *Molecules*, 2019; 24(3): 453.

Castle PE and Giuliano AR. Chapter 4: Genital tract infections, cervical inflammation, and antioxidant nutrients-assessing their roles as human papillomavirus cofactors. *Jnci. Monogr*. 2003; 29-34

Castle PE and Pierz A. (At Least) Once in her lifetime: global cervical cancer prevention. *Obstet. Gynecol. Clin. North Am.* 2019; 46: 107-123.

Chi J, Xie Q, Jia J, Liu X, Sun J, Chen J and Yi L. Prognostic value of albumin/globulin ratio in survival and lymph node metastasis in patients with cancer: A systematic review and meta-analysis. *J. Cancer*, 2018; 9: 2341-2348.

Chiou J-F and Hu M-L. Elevated lipid peroxidation and disturbed antioxidant enzyme activities in plasma and erythrocytes of patients with uterine cervicitis and myoma. *Clin. Biochem*. 1999; 32: 189-192.

Chougule A, Hussain S and Agarwal DP. Prognostic and diagnostic value of serum pseudocholinesterase, serum aspartate transaminase, and serum alinine transaminase in malignancies treated by radiotherapy. *J. Cancer. Res. Ther*. 2008; 4: 21.

Colombo G, Clerici M, Garavaglia ME, Giustarini D, Rossi R, Milzani A and Dalle-Donne I. A step-by-step protocol for assaying protein carbonylation in biological samples. *J. Chromatogr. B. Analyt. Technol. Biomed. Life. Sci*. 2016; 1019: 178-190

Cruz-Gregorio A, Manzo-Merino J and Lizano M. Cellular redox, cancer and human papillomavirus. *Virus Res*. 2018; 246: 35-45

Dasgupta A and Klein K. Antioxidants in food, vitamins and supplements: prevention and treatment of disease. *Academic Press*. 2014.

Devi GS, Prasad MH, Saraswathi I, Raghu D, Rao DN and Reddy PP. Free radical's antioxidant enzymes and lipid peroxidation in different types of leukemias. *Clin. Chim. Acta.* 2000; 293: 53-62.

Duly EB, Grimason S, Grimason P, Barnes G and Trinick TR. Measurement of serum albumin by capillary zone electrophoresis, bromocresol green, bromocresol purple, and immunoassay methods. *J. Clin. Pathol.* 2003; 56: 780-781.

Ebrahimi S, Soltani A and Hashemy SI. Oxidative stress in cervical cancer pathogenesis and resistance to therapy. *J. Cell Biochem.* 2019; 120(5); 6868-6877.

Ferlay J, Soerjomataram I, Dikshit R, Eser S, Mathers C, Rebelo M, Parkin DM, Forman D and Bray F. Cancer incidence and mortality worldwide: sources, methods and major patterns in GLOBOCAN 2012. *Int. J. cancer*. 2015; 136: E359-E386.

Gentile F, Arcaro A, Pizzimenti S, Daga M, Cetrangolo GP, Dianzani C, Lepore A, Graf M, Ames PRJ and Barrera G. DNA damage by lipid peroxidation products: implications in cancer, inflammation and autoimmunity. *AIMS Genet.* 2017; 4: 103-137.

Ghafourifar P and Cadenas E. Mitochondrial nitric oxide synthase. *Trends. Pharmacol. Sci*. 2005; 26: 190-195.

Glorieux C and Calderon PB. Catalase, a remarkable enzyme: targeting the oldest antioxidant enzyme to find a new cancer treatment approach. *Biol. Chem*. 2017; 398(10):1095-1108.

Halliwell B and Gutteridge JMC. *Free Radicals in Biology and Medicine*. 5th Edition, Oxford University Press, New York, USA, 2015.

He L, He T, Farrar S, Ji L, Liu T and Ma X. Antioxidants maintain cellular redox homeostasis by elimination of reactive oxygen species. *Cell Physiol. Biochem.* 2017; 44: 532-553.

Hogg N, Singh RJ and Kalyanaraman B. The role of glutathione in the transport and catabolism of nitric oxide. *FEBS Lett.* 1996; 382: 223-228.

Islam JY, Khatun F, Alam A, Sultana F, Bhuiyan A, Alam N, Reichenbach L, Marions L, Rahman M and Nahar Q. Knowledge of cervical cancer and HPV vaccine in Bangladeshi women: a population based, cross-sectional study. *BMC Womens Health*, 2018; 18(1):15.

Islam MO, Bacchetti T and Ferretti G. Alterations of antioxidant enzymes and biomarkers of nitro-oxidative stress in tissues of bladder cancer. *Oxid. Med. Cell. Longev*. 2019: 2019: 2730896.

Jain A, Tiwari A, Verma A and Jain SK. Vitamins for cancer prevention and treatment: An insight. *Curr. Mol. Med*. 2017; 17: 321-340.

Jelić M, Mandić A, Kladar N, Sudji J, Božin B and Srdjenović B. Lipid peroxidation, antioxidative defense and level of 8-hydroxy-2deoxyguanosine in cervical cancer patients. *J. Med. Biochem*. 2018; 37: 336-345.

Jiang B, Xiao S, Khan MA and Xue M. Defective antioxidant systems in cervical cancer. *Tumour Biol.* 2013; 34: 2003-2009.

Johnson SM and Robinson R. The composition and fluidity of normal and leukaemic or lymphomatous lymphocyte plasma membranes in mouse and man. *Biochim. Biophys. Acta. (BBA)-Biomembranes*, 1979; 558: 282-295.

Kim SY, Kim JW, Ko YS, Koo JE, Chung HY and Lee-Kim YC. Changes in lipid peroxidation and antioxidant trace elements in serum of women with cervical intraepithelial neoplasia and invasive cancer. *Nutr. Cancer*. 2003; 47: 126-130.

Kjaer SK, Chackerian B, Van Den Brule AJC, Svare EI, Paull G, Walbomers JMM, Schiller JT, Bock JE, Sherman ME and Lowy DR. High-risk human papillomavirus is sexually transmitted: evidence from a follow-up study of virgins starting sexual activity (intercourse). *Cancer Epidemiol. Biomarkers Prev.* 2001; 10(2): 101-106.

Kolanjiappan K, Manoharan S and Kayalvizhi M. Measurement of erythrocyte lipids, lipid peroxidation, antioxidants and osmotic fragility in cervical cancer patients. *Clin. Chim. Acta*, 2002; 326: 143-149.

Kolanjiappan K, Manoharan S and Kayalvizhi M. Measurement of erythrocyte lipids, lipid peroxidation, antioxidants and osmotic fragility in

cervical cancer patients. *Clin. Chim. Acta*, 2002; 326: 143-149.

Kruk J and Aboul-Enein HY. Reactive oxygen and nitrogen species in carcinogenesis: Implications of oxidative stress on the progression and development of several cancer types. *Med. Chem*. 2017; 17: 904-919.

Kumar B, Koul S, Khandrika L, Meacham RB and Koul HK. Oxidative stress is inherent in prostate cancer cells and is required for aggressive phenotype. *Cancer Res.* 2008; 68:1777-1785.

Layton M and Roper D. 12 - Investigation of the hereditary haemolytic anaemias: Membrane and enzyme abnormalities. In: *Dacie and Lewis Practical Haematology*, Chapter 12, Bain BJ, Bates I, Laffan MABT-D, eds., Elsevier, 2016; p. 228-253.

Liu RH, Hotchkiss JH. Potential genotoxicity of chronically elevated nitric oxide: a review. *Mutat. Res. Genet. Toxicol.* 1995; 339: 73-89.

Mane SD, Thoh M, Sharma D, Sandur SK and Naidu KA. Ascorbyl stearate promotes apoptosis through intrinsic mitochondrial pathway in hela cancer cells. *Anticancer Res*. 2016; 36: 6409-6417

Manju V, Balasubramanian V and Nalini N. Oxidative stress and tumor markers in cervical cancer patients. *J. Biochem. Mol. Biol. Biophys*. 2002; 6: 387-390.

Manju V, Sailaja JK and Nalini N. Circulating lipid peroxidation and antioxidant status in cervical cancer patients: a case-control study. *Clin Biochem*. 2002; 35: 621-625.

Marnett LJ. Oxyradicals and DNA damage. *Carcinogenesis*, 2000; 21: 361-370.

Nayak BS, Beharry VY, Armoogam S, Nancoo M, Ramadhin K, Ramesar K, Ramnarine C, Singh A, Singh A, Nwachi KU, Teelucksing S, Mathura R and Roberts L. Determination of RBC membrane and serum lipid composition in Trinidadian type II diabetics with and without nephropathy. *Vasc. Health Risk. Manag.* 2008; 4: 893-899.

Niedernhofer LJ, Daniels JS, Rouzer CA, Greene RE and Marnett LJ. Malondialdehyde, a product of lipid peroxidation, is mutagenic in human cells. *J. Biol. Chem*. 2003; 278: 31426-31433.

Okutucu B, Dinçer A, Habib O and Zihnioglu F. Comparison of five methods for determination of total plasma protein concentration. *J. Biochem. Biophys. Methods*, 2007; 70: 709-711.

Orr Jr JW, Wilson K, Bodiford C, Cornwell A, Soong SJ, Honea KL, Hatch KD and Shingleton HM. Nutritional status of patients with untreated cervical cancer: I. Biochemical and immunologic assessment. *Am. J. Obstet. Gynecol*. 1985; 151: 625-631.

Palan PR, Woodall AL, Anderson PS and Mikhail MS. α-Tocopherol and α-tocopheryl quinone levels in cervical intraepithelial neoplasia and cervical cancer. *Am. J. Obstet. Gynecol*. 2004; 190: 1407-1410.

Parpart AK, Lorenz PB, Parpart ER, Gregg JR and Chase AM. The osmotic resistance (fragility) of human red cells. *J. Clin. Invest.* 1947; 26: 636-638.

Preetha A, Banerjee R and Huilgol N. Surface activity, lipid profiles and their implications in cervical cancer. *J. Cancer. Res. Ther*. 2016; 1: 180-186.

Rani V, Deep G, Singh RK, Palle K and Yadav UCS. Oxidative stress and metabolic disorders: Pathogenesis and therapeutic strategies. *Life Sci.* 2016; 148:183-193

Ray A, Sharma BK, Bahadur AK, Pasha ST, Bhadola P and Murthy NS. Serum lipid profile and its relationship with host immunity in carcinomas of the breast and uterine cervix. *Tumori*, 1997; 83: 943-947.

Roomi MW, Ivanov V, Kalinovsky T, Niedzwiecki A and Rath M. Suppression of human cervical cancer cell lines Hela and DoTc2 4510 by a mixture of lysine, proline, ascorbic acid, and green tea extract. *Int. J. Gynecol. Cancer*, 2006; 16: 1241-1247.

Saha SK, Lee S Bin, Won J, Choi HY, Kim K, Yang G-M, Dayem A and Cho S-G. Correlation between oxidative stress, nutrition, and cancer initiation. *Int. J. Mol. Sci.* 2017; 18(7): 1544.

Sastry KVH, Moudgal RP, Mohan J, Tyagi JS and Rao G. Spectrophotometric determination of serum nitrite and nitrate by copper–cadmium alloy. *Anal. Biochem*. 2002; 306: 79-82.

Shinitzky M and Inbar M. Microviscosity parameters and protein mobility in biological membranes. Biochim. Biophys. *Acta. (BBA)-Biomembranes*. 1976; 433: 133-149.

Shlay JC, McGill WL, Masloboeva HA and Douglas JM. Pap smear screening in an urban STD clinic. Yield of screening and predictors of abnormalities. *Sex Transm. Dis.* 1998; 25: 468-475.

Shrivastava A, Aggarwal LM, Mishra SP, Khanna HD, Shahi UP and Pradhan S. Free radicals and antioxidants in normal versus cancerous cells-An overview. Indian. *J. Biochem. Biophys*. 2019; 56: 7-19.

Song M and Santanam N. Increased myeloperoxidase and lipid peroxide-modified protein in gynecological malignancies. *Antioxid. Redox Signal.* 2001; 3: 1139-1146.

Sowjanya AP, Rao M, Vedantham H, Kalpana B, Poli UR, Marks MA and Sujatha M. Correlation of plasma nitrite/nitrate levels and inducible nitric oxide gene expression among women with cervical abnormalities and cancer. *Nitric oxide. Biol. Chem.* 2016; 52: 21-28.

Toepfner N, Herold C, Otto O, Rosendahl P, Jacobi A, Kräter M, Stächele J, Menschner L, Herbig M, Ciuffreda L, Ranford-Cartwright L, Grzybek M, Coskun Ü, Reithuber E, Garriss G, Mellroth P, Henriques-Normark B, Tregay N, Suttorp M, Bornhäuser M, Chilvers ER, Berner R and Guck J. Detection of human disease conditions by single-cell morph rheological phenotyping of blood. *eLife*. 2018; 7: e29213.

Tong L, Chuang C-C, Wu S and Zuo L. Reactive oxygen species in redox cancer therapy. *Cancer Lett*. 2015; 367: 18-25.

Wang X, Huang X and Zhang Y. Involvement of human papillomaviruses in cervical cancer. *Front. Microbiol.* 2018; 9: 2896.

Yagi K. Simple procedure for specific assay of lipid hydroperoxides in serum or plasma. Methods Mol. Biol. 1998; 108: 107-110.

Yang BH, Bray FI, Parkin DM, Sellors JW and Zhang Z. Cervical cancer as a priority for prevention in different world regions: an evaluation using years of life lost. *Int. J. Cancer.* 2004; 109: 418-424.

Yoshino Y, Taguchi A, Shimizuguchi T, Nakajima Y, Takao M, Kashiyama T, Furusawa A, Kino N and Yasugi T. A low albumin to globulin ratio with a high serum globulin level is a prognostic marker for poor survival in cervical cancer patients treated with radiation based therapy. *Int J. Gynecol. Cancer*. 2019; 29: 17-22.

Zelenka J, Koncošová M and Ruml T. Targeting of stress response pathways in the prevention and treatment of cancer. *Biotechnol. Adv*. 2018; 36: 583-602.

J. Bangladesh Acad. Sci. Volume 46, Issue 1, June 2022

BANGLADESH ACADEMY OF SCIENCES

Acknowledgment to Reviewers

The editorial board of the ***Journal of Bangladesh Academy of Sciences*** volumes 44 (June & December issues), 45 (June & December issues), and 46 (June issue) (2019-2022) extends their gratitude and appreciation to the following reviewers whose comments and criticism ensured the quality of the articles published in this journal.

Contributing Reviewers

Department of Applied Mathematics, University of Dhaka
Prof. Dr. A.B.M. Shahadat Hossain

Department of Biochemistry and Molecular Biology, University of Chittagong
Prof. Dr. Md. Atiar Rahman

Department of Biochemistry and Molecular Biology, University of Dhaka
Prof. Dr. Haseena Khan
Prof. Dr. Yearul Kabir
Prof. Dr. Md. Enamul Haque
Prof. Dr. Hossain Uddin Shekhar
Prof. Dr. Md. Rakibul Islam

Department of Botany, University of Rajshahi
Prof. Dr. Golam Kabir

Department of Chemistry, University of Chittagong
Prof. Dr. S. M. Abe Kawsar

Department of Chemistry, University of Dhaka
Prof. Dr. Md. Muhibur Rahman
Prof. Dr. Amir Hussain Khan
Prof Dr. Mohammad Yousuf Ali Mollah

Department of Chemistry, Jahangirnagar University
Prof. Dr. Rabiul Islam

Department of Chemical Engineering, Bangladesh University of Engineering and Technology (BUET)
Prof. Dr. Md. Shahinoor Islam

Department of Chemistry, Shahjalal University of Science and Technology
Prof. Dr Mohammad Abul Hasnat

Department of Electrical and Computer Engineering, North-South University, Dhaka
Dr. Mahdy Rahman Chowdhury

Department of Electrical and Electronic Engineering, Bangladesh University of Engineering and Technology (BUET)
Prof. Dr. Rezwan Khan
Prof. Dr. Kamrul Hasan

Department of Genetic Engineering and Biotechnology, University of Dhaka
Prof. Dr. Mohammed Nazmul Ahsan
Prof. Dr. A.B.M. Md. Khademul Islam

INSTRUCTION FOR AUTHORS

The Journal of Bangladesh Academy of Sciences is published twice a year in June and December. Original research articles, review articles, and short communications of high standards of all branches of Science and Technology are considered for publication in this journal. Review articles are generally by invited authors; however, the Editor welcomes suggestions of potential topics and potential authors.

The following instructions must be followed while preparing the manuscript intended for publication in this journal:

1. **Research Article:** Manuscripts should be concise and consistent with the style of the journal. The manuscript must be typed using Times New Roman font, size 12 on A4 size page, and wide (1 inch) margins on all four sides. The main text must be typed in a two-column format with 1.5 spacing, and for full papers, it should not exceed 10-20 typed pages, including figures, tables, and references. In general, an article may contain the following sub-titles in sequence: **Title, Abstract, Keywords, Introduction, Materials and Methods, Results and Discussion, Acknowledgement (**if any), and **References.**

A. Title: The first page of the paper, the title page, should have the title and the names of the authors. The title should be brief and specific. Abbreviations and formulae should be avoided where possible. The next line in italics should be the authors' affiliation addresses (where the actual work was done) below the names. Indicate all affiliations with a lowercase superscript letter immediately after the author's name and in front of the appropriate address. The corresponding author, along with email address, should be indicated at the footnote with a proper asterisk.

B. The second page should carry the Title of the paper, Abstract, and Keywords. Author(s) name must not be typed on this page.

(i) Abstract: It should not exceed 150 words and should briefly state the purpose of the research, the significant results, and meaningful conclusions. Nonstandard or uncommon abbreviations should be avoided, but if essential, they must be defined at their first mention in the abstract itself.

(ii) Keywords: Immediately after the abstract, provide a maximum of 6 keywords.

C. The next pages (a maximum of 15 printed pages), will contain the main text of the paper.

(i) Introduction: It should be concise and relevant to the objectives of the study. The importance of the research work described should be pointed out. An appropriate review of the current literature should be made to identify the frontier of existing knowledge and point out the need for further work. The knowledge contributed to the study should be mentioned.

(ii) Materials and Methods: Materials used should be mentioned precisely along with their sources and any pre-treatment undertaken.

The description of methods must be brief but clear enough to enable a reader to reproduce the results. References must be considered sufficient for methods described in earlier publications: only relevant modifications should be described.

It is recommended that authors use the nomenclature and symbols adopted by IUPAC document UIFII (S.U.N. 65-3) 1965, symbols, units, and nomenclature in Physics or by IUPAC Manual of Physiochemical symbols, Terminology and similarly for other disciplines.

(iii) Results and Discussion: This section should include descriptions of results obtained with the help of figures, tables, graphs, and photographs as may be necessary. Tables should have a descriptive title. Large and cumbersome tables should be avoided. Figures and graphs should be prepared and should be properly labelled with bold solid lines such that no further size reduction will be necessary. The paper should contain a minimum number of **Tables, Graphs,** and **Figures.** The same data should not be depicted using both tables and figures. The photographs are to be submitted in JPEG format.

The discussion should include thorough analysis and interpretation of results, and comparison with existing relevant published results, if any, and self-evaluation of the new knowledge contributed, avoiding extensive citations and discussion of published literature.

(iv) Conclusions

The study's main conclusions may be presented in a short Conclusions section, which may stand alone or form a part of the Results and Discussion section.

(v) Acknowledgment: The following support for the research work should be acknowledged:

- Funding by any agency;
- The use of instruments in a laboratory other than those of the authors;
- Individual's help during the research (e.g., providing an interpretation of results, language help, writing assistance, or proofreading, etc.).

(vi) Author contributions

For transparency, we encourage authors to submit an author contribution statement outlining each author's contributions to the paper. The authors should have participated sufficiently in the work to take public responsibility for appropriate portions of the content.

(vii) References and Text Citations:

In the text, references should be cited within brackets quoting the first author's surname followed by et al. if necessary and the year of publication in the appropriate place, e.g. (Bhuiyan, 2020), Khan et al. (2021) or (Khan et al., 2021). In the case of only two authors, surnames of both need to be mentioned, e.g., (Khan and Rahman, 2021). A semi colon should separate two or more references when putting within the same bracket. At the end of the manuscript, references should be listed and arranged alphabetically according to the first author's surname according to the style described below:

(a) Journal article:

In each reference, names of all authors' will have to be given in the same style, e.g., surname followed by initials, lumped together without using a full stop. The names will be followed by the full title of the article and the journal's abbreviated title (in italics). The year of publication will be given next, followed by volume number (issue number) and page ranges. For abbreviations of the names of journals, authors are advised to follow the *World List of Scientific Periodicals.* For online publications, the URL address must be given. Note: Please list ALL authors' names in the list of references, do not use (et al.). **Examples:**

Islam S. The Induced Morphological and Root Anatomical Changes in Lentil. *J. Bangladesh Acad. Sci.* 2019; 43(2):107-112.

James BD and Bennett DA. Causes and Patterns of Dementia: An Update in the Era of Redefining Alzheimer's Disease. *Annu. Rev. Public Health;* 2019; 40: 65-84.

Moniruzzaman M, Khatoon R and Qamruzzaman AKM. Influence of Plant growth Regulators on Vegetative Growth, Sex Expression and Yield of Summer Bottle Gourd. *Bangladesh J. Agril. Res*. 2019; 44(4): 577-590.

(b) Book or Chapter in a Book:

The place and name of the publisher, year of publication, will have to be given in addition to the name of the author(s), the title of the book (in italics), edition number (if not first), and the number of pages. In the case of an article or chapter in a book or proceedings of a conference, author(s) name and the title of the article or chapter will be followed by the title of the book (in italics), the names of the editors of the book, edition number (if not first), the place and name of the publisher, year of publication and page or page numbers of chapter. **Examples:**

Book:

Carlson BM. *Human embryology and developmental biology*. 4th ed. St. Louis: Mosby; 2009. p.541.

Cassese A, Acquaviva G, Fan M and Whiting A. *International criminal law: cases and commentary*. Oxford University Press; 2011, p. 600.

Chapter in an edited book:

Muhammad HFL and Dickinson KM. Nutrients, energy values and health impact of conventional beverages, Chapter 3. In: *The Science of Beverages, Volume 12: Nutrients in Beverages*, Grumezescu AM, Holban AM, eds., Elsevier Science; 2019; p. 77-109.

Balsam KF, Martell CR, Jones KP, Safren SA. Affirmative cognitive behavior therapy with sexual and gender minority people. In: *Culturally responsible cognitive behavior therapy: Practice and supervision*, Iwamasa GY, Hays PA,eds., 2nd edition, American Psychological Association. 2019; p. 287-314.

(c) Proceedings of a Conference:

Luca J and Tarricone P. Does emotional intelligence affect successful teamwork? In: *Meeting at the Crossroads*, Kennedy G, Keppell M, McNaught C, eds., Proceedings of the 18th Annual Conference of the Australasian Society for Computers in Learning in Tertiary Education, 2001 Dec 9-12; Melbourne: Biomedical Multimedia Unit, The University of Melbourne; 2001. p. 367-76.

(d) Reports:

Bangladesh Bureau of Statistics (BBS). Population census - 2011. Preliminary report. Bangladesh Bureau of Statistics, Ministry of Planning, Dhaka, 2011.

Rowe IL and Carson NE. *Medical manpower in Victoria. East Bentleigh (AU)*: Monash University, Department of Community Practice; 1981. p. 35. Report No.: 4.

2. **Short communication:** Important research findings that may initiate further research in the relevant field may be published in the form of a short communication. This should not exceed three printed pages (900 words), including Graphs, Tables, and Figures. The presentation should be continuous and paragraphed, i.e., without headings like Introduction, Materials, and Methods, etc. A short communication paper should have an **Abstract** containing the gist of the article and should not exceed 60 words, followed by **Keywords.**

3. **Declarations:** While submitting, the corresponding **a**uthor will have to make a declaration mentioning the laboratory/laboratories in which the work was carried out and certifying that the contents of the paper were not published before or submitted for publication in any other journal and that all the co-authors have given their consent for the article to be considered by the Editorial Board for publication in the Journal of Bangladesh Academy of Sciences.

Declaration of conflicting interests

The corresponding author must provide a formal conflict of interest statement for all authors disclosing any financial and personal relationships with other people or organizations that could inappropriately influence (bias) their work. If no conflict exists, please state that 'The author(s) declare(s) that they have no conflicts of interest regarding the publication of this article.'

4. The manuscript should be submitted in pdf or MS Word or LaTex files through online at www.bas.org.bd/publications/jbas.html. Equations generated by using Math Type or Math ML should be incorporated in the text.

   Soft copies of manuscripts with tables, graphs, illustrations, and photographs placed correctly in a printable format are to be submitted. Authors wishing to publish coloured schemes/diagrams/ sketches/photographs in their papers need to pay for the printing charges of one format. This will be charged only after the acceptance of the manuscripts for publication in the JBAS.

   The manuscript submitted should also contain a separate list of tables, figures, illustrations, photographs, and sketches with appropriate captions.

5. Electronic versions of final galley proofs will be sent to authors. No alteration in the title or additions in the text is desirable at this stage.

6. All correspondence for publication should be made on www.bas.org.bd/publications/jbas.html to the **Editor, Journal of Bangladesh Academy of Sciences, National Museum of Science and Technology, Agargaon, Dhaka 1207.**

N.B.: No paper will be accepted for publication if it does not conform to the style specified for the journal and approved by the Editorial Board, which has the authority to accept or reject the manuscript of a paper submitted without showing any reason.